

**Universidade de Évora - Instituto de Investigação e Formação Avançada**

Programa de Doutoramento em Biologia

Tese de Doutoramento

**Benthic biodiversity and bottom-up effects based on food web attributes in response to sediment condition in Sado estuary (SW Coast, Portugal)**

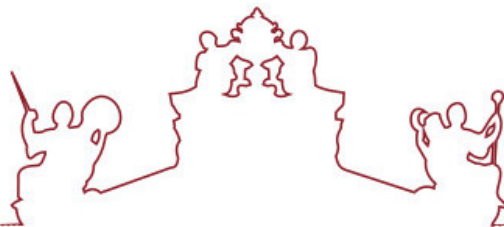
Soraia Vanessa Teixeira de Aguiar Vieira

Orientador(es) | Cláudia Vicente

Cristina Barrocas Dias

Helena Adão

Évora 2025



**Universidade de Évora - Instituto de Investigação e Formação Avançada**

**Programa de Doutoramento em Biologia**

Tese de Doutoramento

**Benthic biodiversity and bottom-up effects based on food web attributes in response to sediment condition in Sado estuary (SW Coast, Portugal)**

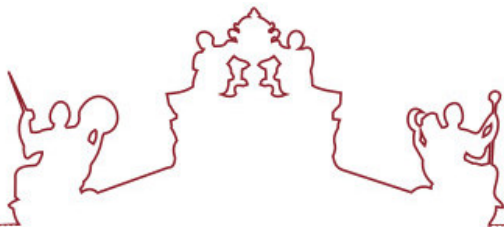
Soraia Vanessa Teixeira de Aguiar Vieira

Orientador(es) | Cláudia Vicente

Cristina Barrocas Dias

Helena Adão

Évora 2025



A tese de doutoramento foi objeto de apreciação e discussão pública pelo seguinte júri nomeado pelo Diretor do Instituto de Investigação e Formação Avançada:

Presidente | António Mira (Universidade de Évora)

Vogais | Helena Adão (Universidade de Évora) (Orientador)  
Joana Isabel do Espírito Santo Robalo (ISPA - Instituto Universitário de Ciências Psicológicas, Sociais e da Vida)  
José Lino Vieira de Oliveira Costa (Universidade de Lisboa - Faculdade de Ciências)  
Margarida Espada (Universidade de Évora)  
Sofia dos Santos da Rocha Costa (Universidade do Minho)

Évora 2025





UNIVERSIDADE  
DE ÉVORA



MARE

centro de  
ciências do mar  
e do ambiente



AQUATIC RESEARCH NETwork



REPÚBLICA  
PORTUGUESA



## ACKNOWLEDGEMENTS

First and foremost, I would like to express my deepest gratitude to my supervisors. To **Helena Adão**, for challenging me to board on this incredible journey that was my PhD. For allowing me to be part of an original and ambitious project like D4Ss, which aimed to evaluate and analyze benthic trophic webs. This project provided the scientific groundwork for my PhD research. She not only enabled me to develop various skills by expanding my knowledge through high-level scientific approaches but also continuously encouraged and facilitated my participation in complementary training courses and international conferences. These experiences significantly contributed to my scientific development, improving my performance and helping me establish and expand connections with other scientific institutions. She also played a key role in my pedagogical growth, allowing me to present my work in undergraduate and master's classes, as well as in workshops. Additionally, she supported my involvement in mentoring in the curricular unit of PCB II, Bachelor's Degree in Biology and master's and ERASMUS+ TRAINEESHIP students. Her knowledge transfer in Marine Nematology, a field still underdeveloped in Portugal, enabled me to acquire a unique skillset.

To **Cláudia Vicente**, my supervisor in the microbiology component (particularly in omics), I extend my sincere appreciation for helping me consolidate my knowledge of advanced molecular techniques. She accompanied me from laboratory activities to the complex analysis of sequencing-generated metadata. Her unwavering dedication and availability throughout every stage of my research were invaluable and greatly contributed to my progress.

**Cristina Dias** also played a crucial role in carrying out the laboratory work at Hercules, particularly in the analysis of stable isotopes, where I also had the essential support of **Anne-France Maurer** in processing the generated data. This component was consistently and attentively guided by **Cristina Dias**, through whom I was able to deepen my expertise in advanced chemical analysis.

Beyond my supervisors, I must also express my gratitude to researcher **Kasia Sroczynska** for all her work in the study of trophic webs. Her essential support in sampling, sample processing, isotope data analysis, and trophic chain interpretation was invaluable.

I would also like to highlight and thank all those who collaborated in the sampling campaigns, especially **Jordana Branco**, **Margarida Espada**, **João Balsa** and **Mélanie Costa**. My extracurricular internship students, **Inês Pessoa** and **Beatriz Ferreira**,

deserve special recognition for being my right hand in processing nematode community samples—a highly demanding and time-consuming task.

To the **Nemalab team**, who have always been incredibly supportive and encouraging, I extend my appreciation, with a special mention to **Margarida Espada** for her valuable academic advice. **Mélanie Costa** for all moments that she advised and support me.

I would like to thank **the Fundação para a Ciência e a Tecnologia** (FCT) for the financial support provided by the PhD grant (2021.06804.BD).

Finally, to my **family and friends**, who have been by my side through all the highs and lows that come with the challenging journey of completing a PhD—thank you for your unwavering support and belief in me.



## ABSTRACT

Studies that concurrently assess diversity patterns and interactions among benthic organisms remain scarce. This research aims to investigate how benthic community diversity influences trophic interactions and the structure of benthic food webs, providing fundamental knowledge to support the development of new approaches for assessing Descriptors 1, 4 and 6 (Marine Strategy Framework Directive).

Spatial-temporal patterns of benthic bacterial and nematode communities in response to sediment conditions were analysed at three sampling sites in Sado estuary (Portugal) using 16S metagenomic and morphological identification, respectively. Both communities exhibited comparable responses to environmental variables, although nematodes were more sensitive to site-specific variations than bacteria. The co-occurrence of specific taxa suggests potential interactions these communities most likely influenced by local anthropogenic activities, emphasizing their value as effective ecological indicators.

Benthic food webs were analyzed through stable isotope ratios  $\delta^{13}\text{C}$  and  $\delta^{15}\text{N}$  of macrobenthic organisms and their potential food sources. Isotopic metrics were combined with multivariate methods to identify food web indicators. Trophic structure, aligned with the benthic diversity, revealed a clear spatial pattern driven by sediment grain size, organic matter content, and primary production. "Navigator" and "Gambia" sites exhibited simpler food webs, consistent with organic enrichment, dominance of anaerobic bacteria, and prevalence of opportunistic nematode genera. Temporal variability of both food webs was driven by differences in the resources. In contrast, "Tróia" food webs were more complex, with a high diversity of consumers and efficient resource exploitation. Overall, spatial differences were more pronounced than temporal trends, although food web complexity increased over time at 'Navigator' and 'Gambia'. The 'Tróia' food web exhibited only minor temporal variation, reflecting subtle changes in resource use. This study introduces a novel approach integrating benthic diversity and trophic interactions to assess estuarine habitat condition, supporting Blue Economy activities, habitat recovery, and sustainable coastal management.

**Keywords:** Nematode assemblages; Bacterial communities; Benthic food webs; Marine Strategy Framework Directive; Descriptor 4.



Biodiversidade e os efeitos “bottom-up” na cadeia trófica bentónica estuarina  
em resposta a diferentes condições dos sedimentos (Estuário do Sado,  
Portugal)

## RESUMO

Estudos que avaliem simultaneamente padrões de diversidade e interações entre organismos bentónicos para compreensão do funcionamento dos ecossistemas são raros. Este estudo investigou o efeito da diversidade das comunidades bentónicas nas interações tróficas, promovendo novas abordagens para avaliar os Descritores 1, 4 e 6 da Diretiva-Quadro Estratégia Marinha.

A distribuição espacial e temporal das comunidades bentónicas bacterianas e de nemátodes em resposta às condições sedimentares foi analisada em três locais do estuário do Sado (Portugal), através da metagenómica 16S e identificação morfológica, respetivamente. Embora as comunidades respondessem de forma semelhante às condições do sedimento, as comunidades de nemátodes mostraram-se mais sensíveis às variações locais. Verificou-se a coocorrência de taxa específicos sugerindo potenciais interações entre bactérias e nemátodes possivelmente influenciado pelos efeitos antropogénicos e evidenciando o seu valor como indicadores ecológicos.

As cadeias tróficas bentónicas foram analisadas através da medição de isótopos estáveis -  $\delta^{13}\text{C}$  e  $\delta^{15}\text{N}$  - de organismos macrobentónicos e fontes alimentares. As razões isotópicas, combinadas com métodos multivariados, permitiram identificar indicadores tróficos. As topologias tróficas refletiram os padrões de diversidade bentónica, sendo fortemente influenciados pela granulometria, matéria orgânica e produção primária. Os locais “Navigator” e “Gambia” apresentaram cadeias tróficas simples, associadas ao enriquecimento orgânico, elevada prevalência de bactérias anaeróbicas e géneros oportunistas de nemátodes. A variabilidade temporal resultou das diferenças no uso de recursos. Em oposição, as cadeias tróficas de “Tróia” mostraram-se mais complexas, com maior diversidade de consumidores e uso eficiente dos recursos disponíveis. Os padrões temporais foram menos evidentes do que os espaciais, embora a complexidade trófica em “Navigator” e “Gambia” tenha aumentado ao longo do tempo. Cadeias tróficas de “Tróia” mostraram ligeira variabilidade sazonal associada às mudanças no uso dos recursos. Este estudo propõe uma abordagem inovadora para avaliar ecossistemas, integrando diversidade bentónica e interações tróficas, recuperação de habitats, apoiando Economia Azul.

**Palavras-chave:** Comunidades de nemátodes; Comunidades de Bactérias; Cadeias tróficas bentónicas; Diretiva Quadro Estratégia Marinha; Descritor 4.



# CONTENTS

ACKNOWLEDGEMENTS .....	I
ABSTRACT.....	IV
RESUMO .....	VI
LIST OF FIGURES.....	XII
LIST OF TABLES .....	XVIII
CHAPTER 1 - GENERAL INTRODUCTION.....	1
1.1 Assessing the functional integrity of benthic estuarine ecosystems based on community-level interactions and energy transfer .....	2
1.2 The role of benthic habitats in the functional integrity of estuarine ecosystems ...	3
1.2.1 Benthic organisms as good ecological indicators of ecosystem functioning and sediment condition .....	4
1.2.2 Ecological roles and interactions of benthic nematodes .....	7
1.2.3 Structuring factors shaping the diversity and distribution patterns of benthic communities .....	8
1.3 Food webs contributions to assess the Good Environmental Status (GES) of the ecosystem .....	10
1.3.1 Spatial and temporal variability of the food web structures .....	11
1.3.2 Estuarine food webs main structuring factors and their patterns .....	12
1.4 PhD project conceptualization .....	12
Study Area .....	14
1.5 References .....	17
CHAPTER 2 - DISTRIBUTION PATTERNS OF BENTHIC BACTERIA AND NEMATODE COMMUNITIES IN ESTUARINE SEDIMENTS .....	30
2.1 Abstract .....	31
2.2 Introduction.....	32
2.3 Material and Methods .....	33
2.3.1 Study area and sampling design .....	33
2.3.2 Sediment physicochemical processing.....	35
2.3.3 Sample processing of benthic communities .....	35
2.3.4 Statistical analyses .....	36
2.4 Results.....	38
2.4.1 Environmental variables .....	38
2.4.2 Sequencing statistics, diversity, and richness estimations.....	39
2.4.3 Bacterial composition, abundance across sites .....	40
2.4.4 Density and structural diversity of nematode assemblages .....	41

2.4.5 Structural diversity, trophic composition and functional diversity .....	43
2.4.6 Environmental variables influencing the spatial patterns of bacterial and nematodes assemblages .....	44
2.5 Discussion .....	46
2.6 Concluding remarks .....	48
2.7 References .....	48
Supplementary information of Chapter 2 .....	56
Appendix A - Figures .....	56
Appendix B - Tables.....	58
<b>CHAPTER 3 - ASSESSING SPATIAL AND TEMPORAL PATTERNS OF BENTHIC BACTERIAL COMMUNITIES IN RESPONSE TO DIFFERENT SEDIMENT CONDITIONS .....</b>	<b>62</b>
3.1 Abstract .....	63
3.2 Introduction.....	64
3.1 Material and Methods .....	66
3.1.1 Study area and sampling design .....	66
3.1.2 Sediment sample processing.....	67
3.1.3 Total DNA extraction of sediment and amplicon sequencing.....	67
3.1.4 Bioinformatics analyses and data availability .....	68
3.1.5 Data analysis .....	69
3.2 Results.....	70
3.2.1 Physical-chemical characterization of Sado estuary sediments .....	70
3.2.2 Bacterial community composition and diversity.....	72
3.2.3 Spatial and temporal patterns of bacterial communities.....	75
3.2.4 Environmental variables influencing the patterns of bacterial communities.....	77
3.3 Discussion .....	80
3.4 Concluding remarks .....	83
3.5 References .....	84
Supplementary information of Chapter 3 .....	93
Appendix A – Figures and Tables.....	93
<b>CHAPTER 4 - FOOD WEB ATTRIBUTES TO ASSESS SPATIAL-TEMPORAL DYNAMICS IN ESTUARINE BENTHIC ECOSYSTEM .....</b>	<b>99</b>
4.1 Abstract .....	100
4.2 Introduction.....	102
4.2.1 Study conceptualization and hypothesis .....	103
4.3 Material and Methods .....	107

4.3.1 Study area.....	107
4.3.2 Sampling design .....	108
4.3.3 Sediment biogeochemistry and environmental parameters .....	108
4.3.4 Sample collection for stable isotope analysis .....	109
4.3.5 Sample processing in the lab.....	109
4.3.6 Stable isotope analysis .....	110
4.3.7 Data analysis .....	110
<b>4.4 Results.....</b>	<b>112</b>
4.4.1 Biogeochemical and environmental characteristics of the study sites .....	112
4.4.2 Spatial variation of the benthic food web structure.....	114
4.4.3 Temporal variation of the benthic food web structure .....	119
<b>4.5 Discussion .....</b>	<b>123</b>
4.5.1 Spatial variation of the benthic food web structure.....	123
4.5.2 Temporal variation of the benthic food web structure .....	124
<b>4.6 Concluding remarks .....</b>	<b>126</b>
<b>4.7 References .....</b>	<b>126</b>
<b>Supplementary information of chapter 4.....</b>	<b>134</b>
Appendix A – Figures and tables .....	134
<b>CHAPTER 5 - SPATIAL AND TEMPORAL DISTRIBUTION PATTERNS OF THE ESTUARINE NEMATODE ASSEMBLAGES AND THEIR RELATIONSHIP WITH BENTHIC BACTERIA COMMUNITIES.....</b>	<b>151</b>
5.1 Abstract .....	152
5.2 Introduction.....	153
5.3 Material and Methods .....	154
5.3.1 Study area and sampling design .....	154
5.3.2 Sampling and sample treatment.....	156
5.3.3 Data analysis .....	156
5.4 Results.....	158
5.4.1 Environmental variables .....	158
5.4.2 Nematode assemblages: density, structural and functional diversity.....	159
5.4.2 Spatial and temporal distribution patterns of nematode assemblages.....	168
5.4.3 Environmental variables vs nematode communities .....	170
5.5 Discussion .....	171
5.5.1 Does nematode assemblages and benthic bacterial communities provide similar ecological responses to the sediment condition? .....	171
5.6 Concluding remarks .....	174

5.7 References .....	174
Supplementary information of chapter 5.....	182
CHAPTER 6 - GENERAL DISCUSSION .....	193
6.1 General Discussion.....	194
6.2 Conclusions.....	198
6.3 References .....	200

## LIST OF FIGURES

### CHAPTER 1

---

<b>Figure 1.</b> Distribution patterns of benthic communities mediated by oxygen availability through sediment depth (adapted by Jessen et al., (2017)).....	5
<b>Figure 2.</b> Benthic nematodes genera: <b>a)</b> <i>Desmodora</i> (200x); <b>b)</b> <i>Enoploides</i> head and buccal structure (600x); <b>c)</b> <i>Pterygonema</i> (200x); <b>d)</b> <i>Pterygonema</i> head and buccal structure (600x) (images taken on Olympus BX50 light microscope and cell software D Olympus, Japan).....	6
<b>Figure 3.</b> Nematode-bacteria symbiotic strategy forming a viscous shield in their cuticle against sulphides toxicity. Nematodes from the families Stilbonematinae, Desmodoridae and Sulfur-oxidizing bacteria <i>Candidatus Thiosymbion</i> . (Ott et al., 2004).....	7
<b>Figure 4.</b> Graphical concept of the PhD project representing the sediment trophic state, biological interactions mediating biogeochemical processes and implications in the benthic trophic webs and energy pathways base on bottom-up effects.....	13
<b>Figure 5.</b> Abiotic and biotic interactions in response to different sediment conditions: implications for energy pathways and ecosystem functioning. (H1): Hypothesis 1 and (H2) Hypothesis 2 and Hypothesis 3 (H3).....	15
<b>Figure 6.</b> Sampling design to assess the spatial and temporal variability of the benthic communities in Sado estuary (Chapter 3, 4 and 5): 3 sampling sites (Navigator, Gambia and Tróia) 4 sampling occasions (winter 2019 (win19) and 2020 (win20); summer 2020 (Sum 20) and 2021 (Sum 21)) .....	15

### CHAPTER 2

---

<b>Figure 1.</b> Sado estuary located at Southwest of Portugal (38° 31' 14" N, 8° 53' 32" W). The selected sampling sites: Navigator (38.487033, -8.795686) (grey circle), highly industrialized area; Moinho (38.528101, -8.802995) (orange circle) with high organic inputs and Tróia (38.417317, -8.816433) (green circle) with coarser sediment. Moinho and Tróia are situated in a protected area.....	34
<b>Figure 2.</b> PCA plot based on Euclidian distances, according to environmental variables measured (Organic Matter: OM, gravel, Fine Fraction: FF, Total Nitrogen: TN and Salinity: sal) at each sampling site: Navigator, Moinho and Tróia, PC1 73,6%; PC2 22%.....	39
<b>Figure 3.</b> Bar plot displays the relative abundance of OTUs (%). Representing the top 10 most abundant Phylum in each site Moinho; Navigator and Tróia, the other relative frequencies are collapsed into the Others category.....	40
<b>Figure 4.</b> Bar plot displays the relative density (%) of the top 10 most abundant of nematodes genera in each sampling site Moinho, Navigator and Tróia, the other relative frequencies are collapsed into the Others category.....	41

<b>Figure 5 (A).</b> Constrained redundancy analysis displaying contributions of environmental factors to bacterial composition (RDA1= 56% and RDA2 = 8%). The species that are displayed in the graph have a goodness of fit higher than 0.4 .....	44
<b>Figure 5 (B).</b> Constrained redundancy analysis displaying contributions of environmental factors to nematode assemblages (RDA1= 25.5% and RDA2 = 28.5%). The species that are displayed in the graph have a goodness of fit higher than 0.2.....	45
<b>Figure A.1</b> Rarefaction curve of reads clustered in OTUs each sampling site Moinho (MOIR1-R3), Navigator (NAVR1-R3) and Tróia (TROIAR1-R3). .....	56
<b>Figure A.2</b> Heatmap of the top 10 of most abundant orders represented in the bacterial communities of each site Moinho (MOIR1-R3); Navigator (NAVR1-R3) and Tróia (TROIAR1-R3) and were sorted by Bray Curtis similarity.....	57
<b>Figure A.3</b> Heatmap showing the density at Genus-level of nematode communities in each site Moinho (MOIR1-R3); Navigator (NAVR1-R3) and Tróia (TROIAR1-R3) and were sorted by Bray Curtis similarity.....	58

## CHAPTER 3

---

<b>Figure 1.</b> Sado estuary located at southwest of Portugal (38° 31' 14" N, 8° 53' 32" W). The selected sampling sites: Navigator (38.486502, -8.795191) (grey circle), highly industrialized area; Gambia (38.537263, -8.742584) (orange circle) with high organic inputs from aquacultures; Tróia (38.461421, -8.857838) located at mouth of estuary (adapted from Vieira et al., 2024) .....	66
<b>Figure 2.</b> Principal component analysis (PCA) biplot based on scaled environmental and biogeochemical variables measured for the three sampling sites in Sado estuary, colored by estuary “confidence” convex type. Variable's vectors are colored based on their contributions to the principal components (gradient colors and transparency of vectors varying between 6 and 12 is result of cos2 index that classify the variable vectors by their quality and contribution (“contrib”), with the color red representing highest contributions, yellow intermediate and blue representing lowest contributions. The dots represent the cluster centroids for group variables.....	71
<b>Figure 3.</b> Relative abundance of the amplicon sequence variants (ASVs) of the most representative orders (n=15) in each sampling site (Gambia, Navigator and Tróia, n=12) across all sampling occasions. The X-axis is the relative abundance from 0 to 1, which corresponds to 0 -100 %. The “Other” represent the less abundant orders. ....	72
<b>Figure 4.</b> Heatmap plot of the relative abundance of the ASVs, based on Bray-Curtis dissimilarity, of the most representative families (n= 15) of each site (Navigator, Gambia and Tróia) across the sampling occasions winter 2019 (WIN19), summer 2020 (SUM20), winter 2020 (WIN20) and summer 21 (SUM21).....	73
<b>Figure 5.</b> Principal component analysis (PCoA) plot based on Bray-Curtis dissimilarity, according to ASVs relative abundance of all taxa obtained in each “site”. PCoA1 = 37.17 % and PCoA2 =6.69 %. The vectors are the most representative taxa of the variability observed in bacterial communities. The vectors are represented by the ASVs sequences that correspond to a family taxon: ASV1390	

( <i>Syntrophobacteriales</i> ), ASV6270 ( <i>Chromatiaceae</i> ), ASV4279 ( <i>Flavobacteriaceae</i> ), ASV5726 ( <i>Kiloniellaceae</i> ) and ASV 7599( <i>Woeseiaceae</i> ).....	76
<b>Figure 6.</b> Heatmap presenting the Spearman correlation between top 10 most abundant families, (transformed by centered log ratio-transformed (CLT) and all representative environmental variables: <b>a</b> ) sediment variables (organic matter (OM), gravel, clay, total carbon (CT), chlorophyll a and phaeopigments ratio (chla_phaeo), carbonate of calcium ( $\text{CaCO}_3$ ) and sand); and <b>b</b> ) Metals (Sr, Pb, U, Ba, Be, and Hg). In both, the “Abun.” is bacterial community abundance and “Prev.” is prevalence of the Top10 families. The green square corresponds to the dominant taxa vs constrained variables of Navigator and Gambia sites and the blue square represents Tróia dominant taxa vs constrained variable.....	78
<b>Figure 7.</b> RDA Constrained redundancy analysis displaying contributions of environmental variables for the distribution of bacterial communities filtered at family level: <b>a</b> ) bacterial communities constrained by sediment variables: OM, chla_phaeo, $\text{CaCO}_3$ and sand (RDA1 = 39.3 % and RDA2 = 5.9%); and <b>b</b> ) bacterial communities constrained by metals contents (Hg, Sr, U, Be and Ba) (RDA1 = 36.0 % and RDA2 = 1.5%). The vectors are the constrained variables, the main contributors for distribution of the data. ....	80
<b>Figure. A.1</b> Rarefaction curve of ASVs reads from each sampling site Navigator, Gambia and Tróia.....	93

## CHAPTER 4

---

<b>Figure 1.</b> Sado estuary located at southwest of Portugal ( $38^{\circ} 31' 14''$ N, $8^{\circ} 53' 32''$ W). The selected sampling sites: Navigator (38.486502, -8.795191), highly industrialized area; Gambia (38.537263, -8.742584) with high organic inputs from aquacultures; Tróia (38.461421, -8.857838) located at mouth of estuary.....	107
<b>Figure 2.</b> Principal component analysis (PCA) biplot based on scaled environmental and biogeochemical variables measured at three study sites in Sado estuary, coloured by estuary “confidence” convex type. Variable’s vectors are presented based on their contributions to the principal components (gradient colours and transparency of vectors) with red representing high contributions, yellow intermediate and blue representing very low contributions. The dots represent the cluster centroids for group variables. ....	113
<b>Figure 3.</b> Plots with all sites pooled per sampling occasions (winter 2019 and 2020 and summer 2020 and 2021). In the x-axis and y-axis are the isotopic signatures of carbon ( $\delta^{13}\text{C}$ ) and nitrogen ( $\delta^{15}\text{N}$ ), respectively. The convex hull volume represented by the yellow, green, and purple areas, correspond to Navigator, Gambia and Tróia, respectively. The Feeding guilds (FG) are represented by geometric shapes.....	114
<b>Figure 4.</b> Principal component analysis (PCA) biplot based on scaled metrics ( <i>CR</i> , <i>NR</i> , <i>TA</i> , <i>Iric</i> , <i>Idiv</i> and <i>Omniv_car</i> ) used to characterize the food web structure analyzed at three study sites (Navigator, Gambia and Tróia in Sado estuary, coloured by estuary “confidence” convex type. Variable’s vectors are presented based on their contributions to the principal components (gradient colors and transparency of vectors) with gray representing high contributions, yellow intermediate and blue	

representing very low contributions. The dots represent the cluster centroids for group variables. .... 117

**Figure 5.** Isotopic overlap metrics in a two-dimensional isotopic space (d13C and d15N), between two sites across the 4 sampling occasions (win19, sum20, win20 and sum21). *i*) Navigator vs Gambia (blue and red, respectively); *ii*) Navigator vs Tróia (blue and red, respectively); *iii*) Gambia vs Tróia (blue and red, respectively). Isotopic overlap metrics were measured using the isotopic richness of the two sites (i.e., convex hull volume represented by the red and blue areas, respectively) and the volume of isotopic space they shared. Isotopic similarity is the ratio between the volume shared (purple area). Isotopic nestedness is the ratio between the volume shared and the volume of the smallest convex hull (in blue). Isotopic overlap on each stable isotope axis is showed by the overlap of the colored segments representing range of scaled values for each site. .... 118

**Figure 6.** Isotopic overlap metrics in a two-dimensional isotopic space (13C and 15N), between seasons: win19 vs sum20 / win20/ sum21; win20 vs sum20/ sum21 and sum20 vs sum21 in each site. **a**) Navigator; **b**) Gambia and **c**) Tróia. Isotopic overlap metrics were measured using the isotopic richness of the two sites (i.e., convex hull volume represented by the red and blue areas, respectively) and the volume of isotopic space they shared (i.e., volume of their intersection, delimited by the purple line). Isotopic similarity is the ratio between the volume shared (purple area) and the volume of the union of the two convex hulls. Isotopic nestedness is the ratio between the volume shared and the volume of the smallest convex hull (in blue). Isotopic overlap on each stable isotope axis is shown by the overlap of the colored segments representing a range of values for each site. .... 121

**Figure 7.** Principal component analysis (PCA) biplot based on scaled metrics (CR, NR, TA, Irac, Idiv, Max TP and Omniv\_car) used to characterize the food web structures analyzed across 4 seasons (win19, sum20, win20 and sum21) in Sado estuary, coloured by estuary “confidence” convex type. Variable's vectors are presented based on their contributions to the principal components (gradient colours and transparency of vectors) with grey representing high contributions, yellow intermediate and blue representing very low contributions. The dots represent the cluster centroids for group variables. .... 122

**Figure A.1.** Biplots of carbon ( $\delta^{13}\text{C}$ ) and nitrogen ( $\delta^{15}\text{N}$ ) isotopic signatures (representing mean and standard deviation) for each taxon with colors depicting different FG (Feeding Guild) assignment (according to Fauvel 1927; Hayward & Ryland, 1995), at three study sites for (A) win19, (B) sum20, (C) win20 and (D) sum21. Convex hull areas are drawn only for consumers (shaded area) and represent total area in the biplot occupied by all the consumers. .... 137

## CHAPTER 5

**Figure 1.** Sado estuary located at southwest of Portugal ( $38^{\circ} 31' 14'' \text{N}$ ,  $8^{\circ} 53' 32'' \text{W}$ ). The selected sampling sites: Navigator (38.486502, -8.795191) (grey circle), highly industrialized area; Gambia (38.537263, -8.742584) (orange circle) with high organic inputs from aquacultures; Tróia (38.461421, -8.857838) located at mouth of estuary (adapted from Vieira et al., 2024a). .... 155

**Figure 2.** Principal component analysis (PCA) biplot based on scaled environmental and biogeochemical variables measured in sediment samples from 3 sampling sites in Sado estuary during 4 distinct sampling occasions, colored by estuary “confidence” convex type. Variable’s vectors are presented based on their contributions to the principal components (gradient colors and transparency of vectors varying between 6 and 12 is result of cos2 index that classify the variable vectors by their quality and contribution (“contrib”), with grey representing high contributions, yellow intermediate and blue representing very low contributions. The dots represent the cluster centroids for group variables, adapted from Vieira et al., (2025)..... 159

**Figure 3.** Bar plot displays the relative density (%) of the top 10 most abundant of nematodes genera in each sampling site Gambia, Navigator and Tróia, across all sampling occasions (win19, sum20, win20 and sum21). The other relative frequencies are collapsed into the “Others” category..... 166

**Figure 4.** Principal component analysis (PCoA) plot based on Bray-Curtis dissimilarity, according to nematode relative density of all genera obtained for: **a**) “site” (Gambia, Navigator and Tróia) and **b**) “sampling occasions” (win19, sum20, win 20 and sum 21). The two first axes represent 51.2 % of the total variation (PCoA1 = 45.24 % and PCoA2 = 6.03 %). The vectors are the most representative genera of the variability observed in nematode communities..... 169

**Figure 5.** RDA Constrained redundancy analysis displaying contributions of environmental variables for the distribution of nematode communities filtered at genera level: Sand, CaCO<sub>3</sub>, Li, OM, NT, chla\_phaeo, Hg and Sr (RDA1 = 29.5% and RDA2 = 3%). The vectors are the constrained variables and the taxa that are the main contributors for distribution of the communities..... 170



## LIST OF TABLES

### CHAPTER 2

---

<b>Table 1.</b> Mean $\pm$ standard error (SE), n=3 of Alpha diversity descriptors (Observed OTUs, Chao1, Shannon, Simpson and Pielou's Evenness) calculated for the bacterial communities from each sampling site: Moinho (MOI), Navigator (NAV), Tróia (TROIA).....	39
<b>Table 2.</b> One-way PERMANOVA test, Beta-diversity of bacterial communities, between "Sites" (3 level fixed) for all variables analysed, (p=0.007), n=3. ....	40
<b>Table 3.</b> Mean density $\pm$ standard error (SE), n=3, of the nematode genera (number of individuals per 10 cm <sup>-2</sup> ), at each sampling site (Moinho, Navigator and Tróia). Trophic group (TG) and c-p value of each genera included. Only the most abundant genera are included in this table.....	42
<b>Table 4.</b> Mean $\pm$ standard error (SE), n=3 of diversity descriptors of nematode assemblages (S) genera, (d) Margalef, (H) Shannon (logo based); (ITD <sup>-1</sup> ) reciprocal Index Trophic Diversity and (MI) Maturity Index). from each sampling site: Moinho (MOI), Navigator (NAV), Tróia (TROIA). .....	43
<b>Table B.1</b> Mean $\pm$ SE, n=3, of the environment parameters measured in sediments from each sampling site - Moinho (MOI), Navigator (NAV) and Tróia (TROIA). Granulometric parameters (%) are Gravel, Sand and Fine fraction (FF). The elemental analysis (w%) are organic matter (OM), Total Nitrogen and Carbon (TN and TC). Sal: salinity.....	58
<b>Table B.2</b> Kruskal-Wallis test: bacterial communities alpha diversity significance between groups (Moinho, Navigator, Tróia), p<0.05. ....	59
<b>Table B.3</b> SIMPER summarized table of the bacterial and nematode communities, with the genera that most contributed for (dis)similarities (%), within and between sites (Moinho, Navigator and Tróia). ....	59
<b>Table B.4</b> One- way PERMANOVA test of nematodes assemblages, with "Sites" (3 level fixed) for all variables analysed. Bold values represent significant differences between sites (NAV, MOI, TROIA), (p≤0.05). ....	60

### CHAPTER 3

---

<b>Table 1.</b> Alpha diversity significance between groups, for each site (Gambia, Navigator and Tróia) using Kruskal-Wallis test. Bold values represent significant differences between sites. The replicates n=12 assume the 3 replicates in each sampling occasion (n=4). Significant levels considered: p ≤ 0.05 (*), p ≤ 0.01 (**) and p ≤ 0.001 (***) H: Kruskal-Wallis statistic; p-value significance level; q-value false discovery rate (FDR).....	74
---	----

<b>Table 2.</b> Two-way PERMANOVA test, Beta-diversity of bacterial communities, between "Sites" (si) (3 level, fixed) and across "sampling occasions" (sa) (4 levels, random) for all variables analyzed. Bold values represent significant differences between sites (Navigator, Gambia and Tróia). Significant levels considered p ≤ 0.05 (*), p ≤ 0.01	
--	--

(**) and $p \leq 0.001$ (***) . Res: residual; df: Degrees of freedom; SS: Sum square; MS: Mean Square; Pseudo-F: Friedman test; P(perm) p-value from permutation test; Unique perms: Unique permutations; P(MC): p-value (Monte Carlo).....	75
<b>Table A.1</b> Mean $\pm$ SE, n=3 of the raw data of the environmental and biogeochemical parameters measured in each site (Navigator, Gambia and Tróia), across the 4 sampling occasions (winter 2019 and 2020, summer 2020 and 2021). Granulometric parameters (expressed in %) are clay, sand and gravel. The elemental composition (expressed in weight %) are organic matter (OM), Total Nitrogen and Carbon (NT and CT), pigments measured (expressed in mg/g) are chlorophyl a (chl <sub>a</sub> ) and phaeopigment (Phaeo) the quality of organic matter “freshness” was calculated the ratio of both pigments, chlorophyl a/ phaeopigment (chl <sub>a</sub> _phaeo). The instant variables measured <i>in situ</i> were Temperature (°C), Salinity, Oxygen (mg/L) and pH. (adapted from Vieira et al., 2024).....	94
<b>Table A.2</b> Mean $\pm$ SE (n=3), metal concentrations measured in sediment samples from each site (Navigator, Gambia and Tróia) across 4 sampling occasions (Winter 2019 and 2020, Summer 2020 and 2021). The analyzed metals were Li, Sr, Mn, Ni, Cr, Be, U, Ba, Co, Cu, Zn, As, Pb and Hg (expressed in mg/kg), (adapted from Vieira et al., 2024). .....	95
<b>Table A.3</b> Mean $\pm$ SE, (n=3) of alpha diversity descriptors (Observed ASVs, Chao1, se.Chao1 (standard error of Chao1), Abundance-based coverage estimator (ACE), se.ACE (standard error of ACE), Shannon (H), Effective numbers for Shannon ( $H1=\exp(H')$ ), Simpson (D) and Inverse Simpson index (InvSimpson)) calculated for each sampling site (Navigator, Gambia and Tróia) across 4 sampling occasions (Winter 2019 and 2020, Summer 2020 and 2021). .....	96
<b>Table A.4:</b> Permutation test for RDA under reduced model. Number of permutations: 999. Model: rda(formula = bio_family ~ Sr + Be + U + Ba + Hg, data = env_metal). Biologic data is the abundance ASVs filtered in family level. Level significance $p<0.05$ for the selected variables. Df: Degrees of freedom, F: F-test, Pr(>F): p-value (***) $<0.0001$ . .....	97

## CHAPTER 4

<b>Table 1</b> Summary of the selected metrics in relation to the hypothesis tested in this study (H1–H4). Along with each metric name and hypothesis, the spatial and temporal scale, how the metric is measured, and the ecological meaning of the metrics are presented. .....	105
<b>Table 2.</b> Food web isotopic and diversity metrics calculated for each community sampled in three sampling sites (Navigator, Gambia and Tróia) of Sado Estuary across 4 sampling occasions (win19, sum20, win20 and sum21). Isotopic and diversity metrics: Carbon Range (CR); Nitrogen Range (NR); Total Area (TA); Maximum Trophic Position (Max TP); Isotopic Richness (Iric); Isotopic divergence (Idiv), Isotopic dispersion (IDis), Isotopic evenness (IEve), Isotopic uniqueness (IUni), Carnivorous percentage (car_perc) and omnivores and carnivorous ratio (omniv_car). .....	115

<b>Table A.1.</b> Mean $\pm$ SE of C and N isotopes measured from the consumers, Feeding Guild (FG), consumer level. From each site Navigator (NAV), Tróia (TROI) and Gambia (GAM) and across all seasons (winter 19, summer 20, winter 20 and summer 21).....	138
<b>Table A.2.</b> Mean $\pm$ SE, n=3 of the environment and biogeochemical parameters measured in each site (Navigator, Gambia and Tróia), across the 4 seasons (win19, sum20, win20 and sum21). Granulometric parameters (%) are Clay_per, Sand_per, Gravel_per. The elemental analysis (w%) are organic matter (OM_per), Total Nitrogen and Carbon (N_total_per and C_total_per), pigments measured (mg.g $^{-1}$ ) are Chlorophyl a (Chla_mg.g $^{-1}$ ) and Phaeopigment (Phaeo_mg.g $^{-1}$ ) the freshness calculated by the ratio between Chla and Phaeo pigments (Chla_phaeo). Metals concentration (mg/kg) Li, Sr, Mn, Ni, Cr, Be, U, Ba, Co, Cu, Zn, As, Pb and Hg. Instant variables, measured in each site Temperature (Temp) °C, Salinity (Sal), Oxygen (O2) mg/L and pH.....	145
<b>Table A.3.</b> Results for a two-way factorial ANOVA of isotopic and diversity metrics, calculated for each community sampled at three sites (Navigator, Gambia and Tróia) of Sado Estuary, along 4 seasons (win19, sum20, win20 and sum21). ANOVA test and Tukey's post-hoc multiple comparisons were performed considering the significance levels of p<0.05 (*) and p<0.001 (**). ....	147

## CHAPTER 5

---

<b>Table 1:</b> Two-way PERMANOVA test, between "Sites" (3 level fixed) and across "sampling occasion" (4 level, random) for all analyzed variables, (nematode Density, Diversity and Richness metrics (N) number of individuals, (S)number of Taxa, (d) Margalef, (J') Pielou's evenness, (H') Shannon, Simpson and ecological strategies metrics: Trophic composition, (ITD-1) Trophic diversity index and (MI) Maturity index. Bold values highlight significant effects and interactions (p < 0.05). Monte Carlo test P(MC) set for 9000 permutations, (p < 0.05(*), p<0.001(**) and p<0.001(***)). ....	161
--	-----

<b>Table 2:</b> Mean $\pm$ SE n=9, of the diversity descriptors in 3 sites (Navigator, Gâmbia and Tróia), during 4 sampling occasions (winter 19, summer 20, winter 20 and summer 21): Diversity and Richness metrics (N) number of individuals, (S)number of Taxa, (d) Margalef, (J') Pielou's evenness, (H') Shannon, Simpson and ecological strategies metrics: Trophic composition, (ITD-1) Trophic diversity index and (MI) Maturity index. ....	167
---	-----

<b>Table S1:</b> Mean $\pm$ SE. n=3 of the environment and biogeochemical parameters measured in each site (Navigator, Gambia and Tróia). across the 4 seasons (win19, sum20, win20 and sum21). Granulometric parameters (%) are Clay_per, Sand_per, Gravel_per. The elemental analysis (w%) are organic matter (OM_per). Total Nitrogen and Carbon (N_total_per and C_total_per). pigments measured (mg.g $^{-1}$ ) are Chlorophyl a (Chla_mg.g $^{-1}$ ) and Phaeopigment (Phaeo_mg.g $^{-1}$ ) the freshness calculated by the ratio between Chla and Phaeo pigments (Chla_phaeo). Metals concentration (mg/kg) Li, Sr, Mn, Ni, Cr, Be, U, Ba, Co, Cu, Zn, As, Pb and Hg. Instant variables, measured in each site Temperature (Temp) °C, Salinity (Sal), Oxygen (O2) mg/L and pH.....	182
---	-----

<b>Table 3:</b> Mean density $\pm$ standard error (SE) of all nematode genera (number of individuals per 10 cm <sup>2</sup> ) each site (Navigator, Gambia and Tróia) and sampling occasion (winter 19, summer 20, winter 20 and summer 21).....	184
<b>Table S4:</b> SIMPER summarized table of nematode communities, with the genera that most contributed for (dis)similarities (%), <b>a</b> ) between sites (Navigator, Gambia and Tróia).and <b>b</b> ) across 4 sampling occasions (winter 19, summer 20, winter 20, summer 21).....	190



## **CHAPTER 1 - GENERAL INTRODUCTION**

## 1.1 Assessing the functional integrity of benthic estuarine ecosystems based on community-level interactions and energy transfer

Estuaries are one of the most dynamic aquatic systems, where the freshwater and seawater mix, which favors nutrient inputs and multiple physical-chemical reactions. Nutrient enrichment makes them one of the most productive ecosystems in the world, with a great diversity of habitats, many of which support various human activities (Elliot & Quintino, 2007). However, the overloading of nutrients and organic matter, mostly from terrestrial sources, increases productivity and oxygen consumption rates, leading to eutrophication (Elliott & McLusky, 2002). Despite of being intensely disturbed by anthropogenic activities, these habitats can provide various ecosystem services, such as food, maintenance of water quality, and recover from disturbances (Liquete et al., 2016). The rapid growth of opportunistic species and the uncontrolled development of economic activities, suggest that estuaries will lose several unique habitats (Kennish, 2002). Given the rapid loss of these environments, the current concern is to improve environmental management practices to ensure the sustainability of the ecosystem services (Schratzberger & Somerfield, 2020).

Several indicators were developed, related with ecosystem structure (e.g. diversity, species composition, abundance) and functional aspects to measure ecosystem activities (e.g. productivity, nutrient cycling, ecosystem metabolism). Together, these indicators provided valuable insights into ecosystem health (Elliott & Quintino, 2007), although the concept of ecosystem-based management remains a challenging goal. Biological indicators have focused on only one group of organisms or community, lacking the interaction component to assess the ecosystem complexity (Rombouts et al., 2013; Terborgh, 2015; Fraser et al., 2017).

Biodiversity is a fundamental component that sustains estuarine and marine ecosystem services, supporting food resources, maintaining water quality, and enabling recovery from disturbances (Liquete et al., 2016). Aquatic management must support all the biological parts that ensure the functional component of ecosystems and maintain biodiversity at all levels, preserving the integrity and stability of ecosystems (Fraser et al., 2017). Directives to regulate and protect the marine environments were implemented in Europe, with the main propose of unifying common commitments for marine management practices and establishing criteria to evaluate the ecosystems status. With the implementation of the Marine Strategy Framework Directive (**MSFD**), the main challenge is to provide scientific knowledge to assess the ecological status of marine environment and ensure its protection across Europe (Rombouts et al., 2013). **MSFD** covers a wide range of ecosystem components and pressures through eleven

quantitative descriptors, all aimed at achieving “Good Environmental Status” (**GES**) of marine ecosystems (MSFD; 2008/56/EC). The descriptors are based on specific pressures, and all represent an impact to biodiversity. The descriptors - **D1 - Biodiversity, D4 - food-webs and D6 - seafloor integrity** - are considered the “*biodiversity group*” crucial for monitoring plans, to ensure the biodiversity prevalence and occurrence of habitats. The **D4** is highlighted as the most difficult to implement due to significant lack of knowledge on functional aspects of marine food webs related with the high dynamic and complex interactions (Rogers et al., 2010; Rombouts et al., 2013). Functional aspects, such as species interactions and energy transfer, are constantly changing, making it challenging to define and implement a single condition that represents “**GES**” (Bohan et al., 2017; Bush et al., 2019).

The functional integrity of aquatic ecosystems is based on ecological responses resulting from multiple and complex interactions between organisms that mediate the energy transfer to higher trophic levels (Schratzberger & Somerfield, 2020; Ridall & Ingels, 2021). To assess the effectiveness of these processes, it is crucial to quantify this energy transfer by analyzing the ecological regulation of species diversity through resource-based (**bottom-up**) and predator-based (**top-down**) pathways (Terborgh, 2015). Until now, the current indicators under **D4** have been focused on the well-studied pelagic habitats or economically significant groups like fish and birds, overlooking benthic habitats and ecosystem processes that are key for detecting environmental disturbances, especially at the base of the food web (Rogers et al., 2010). Benthic food webs differ from their pelagic and terrestrial counterparts by supporting higher degrees of omnivory and connectivity, becoming a promising approach to effectively detect changes in the energy pathways (Campanyà-Llovet et al., 2017).

## 1.2 The role of benthic habitats in the functional integrity of estuarine ecosystems

**Benthic habitats** represent the largest ecosystem on Earth in spatial coverage and are predominantly composed of microorganisms and metazoans. These organisms dominate the benthic biomass and are primary mediators of several ecosystem processes and interactions (Schratzberger & Ingels, 2018). One of the most productive areas in estuaries is the **intertidal flat areas**, accessible during low-tide periods, which are known to be model areas for assessing various ecological issues that affect ecosystem health (Kaiser et al., 2011; Schratzberger & Somerfield, 2020). Sediments are structured along different environmental gradients and various regulatory processes such as food production, pollutant degradation, nutrients recycling, and mediation of

energy flows that promote ecosystem functioning and contribute to human well-being (Schratzberger & Ingels, 2018).

### *1.2.1 Benthic organisms as good ecological indicators of ecosystem functioning and sediment condition*

**Interstitial benthic organisms** that live within sediments' spaces, exhibit limited reduced mobility, rendering them particularly vulnerable to environmental changes (Bonaglia et al., 2014; Schratzberger & Ingels, 2018). This rapid response to environmental stressors makes them powerful bioindicators for evaluating sediment quality status (Schratzberger & Somerfield, 2020). The community's integrity, structure (e.g., diversity, trophic levels), and dynamics (e.g., robustness, resilience), reflect significantly on the quality and provision of the ecosystem services (Schratzberger & Ingels, 2018). **Benthic microorganisms** are the primary facilitators of biogeochemical processes, including organic matter processing (Wang et al., 2020), which have direct implications on sediment trophic conditions (Baker et al., 2015; Trevathan-Tackett et al., 2019). Due to their high efficiency in energy capture, they are more prone to establish symbiotic relationships with other organisms, such as invertebrates (e.g., sponges, tunicates, and corals) (Peixoto et al., 2017) and **benthic nematodes** (Bellec et al., 2019; Ott et al., 2004). The chemoautotrophy of these organisms is dominant in estuarine sediments, driven by the oxidation of reduced inorganic compounds such as hydrogen sulfide ( $H_2S$ ) or methane ( $CH_4$ ), which is a result of organic matter degradation and mineralization (Marshall et al., 2021; Petersen and Yuen, 2021). Sediment organic enrichment is common and stimulates the growth of a wide range of organisms; however, excessive organic input may negatively impact benthic communities, by inducing hypoxic or anoxic conditions (Balsamo et al., 2012; Steyaert et al., 2007).

Vertical patterns observed in benthic communities are generally associated with oxygen gradients, which regulate the distribution of nutrients and biological interactions (Broman et al., 2020). As oxygen levels gradually decline with depth, anaerobic processes become prevalent, and several microorganisms use inorganic sulfur and other compounds (e.g. Mg and Fe) to support their metabolism (Figure 1) (Wasmund et al., 2017; Jensen et al. 2017; Broman et al., 2020).

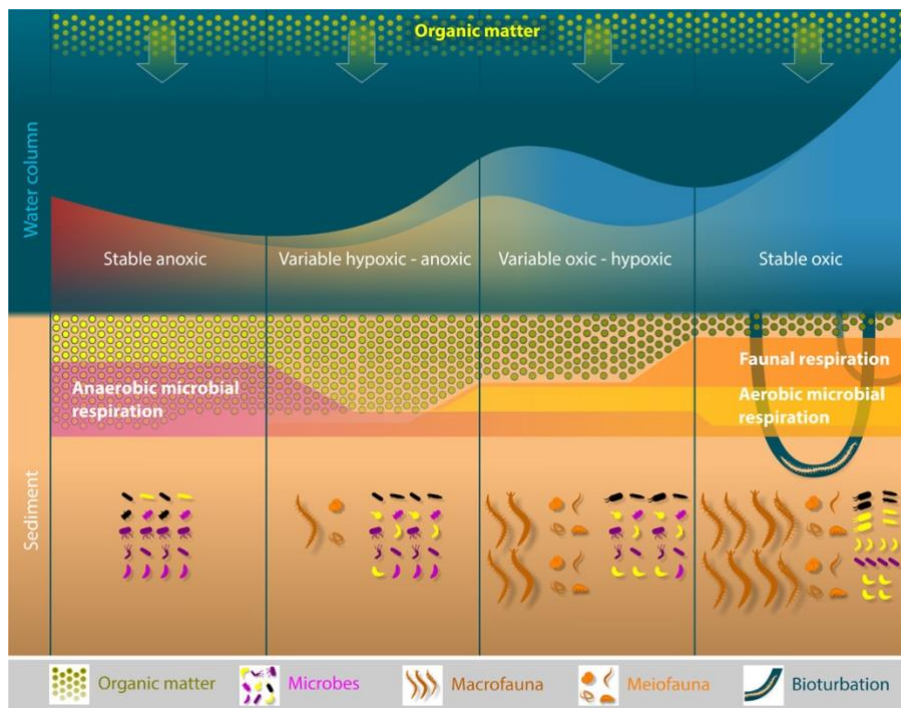


**Figure 1.** Distribution patterns of benthic communities mediated by oxygen availability through sediment depth (adapted by Jessen et al., (2017)).

In several environments, **microbial communities** have proven to be very sensitive to natural and anthropogenic pressures, modifying the diversity patterns and function (Jessen et al., 2017; Zhao et al., 2019). The composition and metabolic activities of these communities are directly influenced by physical-chemical changes in the sediment, making them highly reactive to local and global pressures (Buongiorno et al., 2019; Jokanovic et al., 2021; Rocca et al., 2019). The short generation times, high functional diversity, and phenotypic plasticity allow their fast response to the surrounding changes, and thus are suggested **good indicators** of current sediment conditions. Nevertheless, these microbial benthic communities remain relatively under-explored (Pawlowski et al., 2021). In addition, these microorganisms, as mediators of energy transfer, establish several interactions with other benthic organisms (e.g., nematodes), increasing the efficiency of energy transfer within the ecosystem (Bonaglia et al., 2014; De Mesel et al., 2006; Nascimento et al., 2012). These contributions reinforce the potential of using bacteria in monitoring actions to assess ecosystem health. They are relatively easy to sample and display rapid response to environmental changes, thereby potentially simplifying the monitoring efforts (Pawlowski et al., 2021; Lalzar et al., 2023). Recent advances in environmental genomics have significantly improved biodiversity assessment, providing a holistic view of the ecosystems by predicting shifts in biological communities in response to climate changes (Nigel G. Yoccoz, 2012; Jensen et al., 2022; Pawlowski et al., 2021). The use of next generation sequencing (**NGS**) for amplicon-

based metagenomics to assess bacteria diversity patterns (e.g., 16S rRNA gene) further endorse this taxon as a powerful tool to evaluate sediment quality (Nawaz et al., 2018; Mahamound et al., 2018; Stoeck et al., 2018). Understanding the taxonomic basis of metabolic skills helps us to accurately predict the functional changes and the sustainability of biogeochemical processes (Laiolo et al., 2024). As a result, bacteria started to be a key component in monitoring programs for assessing marine environment status (Borja et al., 2006; Chen et al., 2021).

**Meiofauna** is a **benthic group** of small-sized organisms (< 1mm) that share the sediment habitat with the microorganisms. Opposite to macrofauna (>1mm), meiofauna organisms complete their life cycle within sediment and can be found in a wide variety of habitats (such as deep sea, estuaries, lakes, as well as tropical reefs, cold seeps and polar ice) (Semprucci et al., 2014; Panieri et al., 2023; Vanreusel et al., 2010; Zeppilli et al., 2018), showing a high degree of specificity in the selection of the environment (Semprucci et al., 2022).



**Figure 2.** Benthic nematodes genera: **a)** *Desmodora* (200x); **b)** *Enoploides* head and buccal structure (600x); **c)** *Pterygonema* (200x); **d)** *Pterygonema* head and buccal structure (600x) (images taken on Olympus BX50 light microscope and cell software D Olympus, Japan).

**Nematodes** (Figure 2) are the most diverse and abundant of all meiofaunal metazoans in aquatic systems, and have been used to assess the environmental ecological condition in several marine habitats (Ridall & Ingels 2021; Sroczynska et al., 2021). They exist even in heavily polluted/disturbed areas, as one of the few taxa to persist (Giere, 2019; Ridall & Ingels 2021). The composition and distribution of nematode communities are closely linked to the physicochemical characteristics of sediments, even minor spatial scale differences can lead to substantial shifts in communities' structure (Gallucci et al., 2008; Adão, 2020). Nematodes adjust their biological traits (e.g., biomass, length, weight) based on site-specific conditions, being good ecological indicators of the habitat condition (Patrício et al., 2012; Sroczynska et al., 2021).

### 1.2.2 Ecological roles and interactions of benthic nematodes

In benthic environments, **nematodes** are considered well adapted to extreme conditions being connected to sediment microbiome (Schratzberger & Ingels, 2018; Rzeznik-Orignac et al., 2018; Schuelke et al., 2018; Zeppilli et al., 2018). During organic matter degradation, sulfate-reducing bacteria oxidize organic compounds ( $\text{CH}_4$ ) using sulfate ( $\text{SO}_4^{2-}$ ) to produce hydrogen sulfide ( $\text{H}_2\text{S}$ ), a compound that is extremely toxic for other organisms (Ott et al., 2004). Some nematode species protect themselves from sulfides by forming a viscous shield in their cuticle, while others live in symbiosis with sulfide-oxidizing bacteria (e.g. *Candidatus Thiosymbion*) benefiting from a protective shield to avoid the sulfide toxicity (Figure 3) (Steyaert et al., 2007; Broman et al., 2020; Zimmermann et al., 2016).

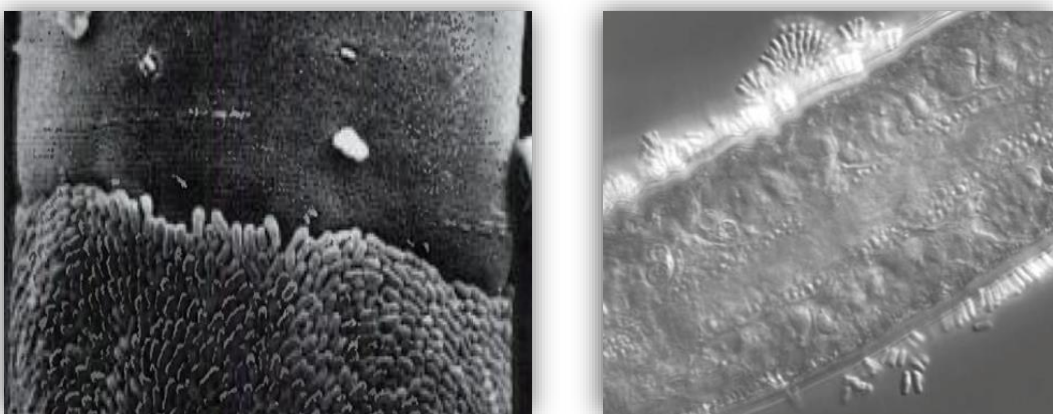


**Figure 3.** Nematode-bacteria symbiotic strategy forming a viscous shield in their cuticle against sulphides toxicity. Nematodes from the families Stilbonematinae, Desmodoridae and Sulfur-oxidizing bacteria *Candidatus Thiosymbion*. (Ott et al., 2004).

Microorganisms associated with the gut lining of nematodes have also been discovered, which can convert organic carbon in energy that is accessible to nematodes (e.g. protein and polysaccharide) (Musat et al., 2007; Bayer et al., 2009; Derycke et al., 2016). Recent studies at hydrothermal vents also support this idea of symbiotic associations observing interactions between nematodes and sulphur-oxidizing bacteria (*Campylobacterota* and *Gammaprobacteria*) (Bellec et al., 2020). This highlights the idea that extreme environments favour positive associations, such as bacteria-nematodes, which are directly related to energy transformation and tolerance to toxicity conditions. On the contrary, the presence of nematodes in sediments has been shown to enhance bacterial biomass, and promote organic matter mineralization and denitrification processes (Bonaglia et al., 2014; Nascimento et al., 2012). Nematode activity associated with **bioturbation** has also been considered essential for regulating biogeochemical processes by stimulating microbial activity (Kristensen et al., 2012; Bonaglia & Nascimento, 2023). Bioturbation alters the porosity and permeability of superficial sediment layers, forming vertical conveyors to transport several solutes (e.g., oxygen ( $O_2$ ), nitrate ( $NO_3^-$ ) and ammonium ( $NH_4^+$ ), modifying the depleted conditions of the surrounding environment (Bonaglia & Nascimento, 2023). During the burrowing activities, nematodes secrete extracellular polymeric substance (**EPS**) biofilms to attach the eggs and stabilise the sediments (Coull, 1999), often used by microbes as a nutrient source (D'Hondt et al., 2018; Moens et al., 2005). The biofilms act as an interacting matrix secreted by nematodes, diatoms, and bacteria for substrate attachment, locomotion, protection against desiccation and carbon overflow (D'Hondt et al., 2018; Gerbersdorf et al., 2009).

**Nematodes** also provide **important trophic links** between macro- and microbenthos, as consume microorganisms while serving as food sources for macrofauna organisms (Gee, 1989; Coull, 1990, 1999). Studies addressing the interactions between organisms (e.g., bacteria and archaea, nematodes, macrobenthos) in response to environmental variations remain scarce. Few studies only focus on a single taxonomic group (Bianchelli et al., 2018; Jokanovic et al., 2021; Wang et al., 2020). Thus, is essential to understand the patterns of diversity and distribution within benthic communities, in particular species coexistence and co-dependency (Lalzar et al., 2023).

### 1.2.3 Structuring factors shaping the diversity and distribution patterns of benthic communities

**Environmental heterogeneity** in estuaries occurs at several scales in space and time influencing the distribution and composition of benthic communities. The **abiotic**

**factors** that determine the estuary typology are the same as those that shape benthic communities. Salinity is among the most structuring factors affecting the diversity of benthic species. Which directly influence the nutrient availability (Adão et al., 2009; Alves et al., 2009). The variability of this factor challenges the tolerance of many organisms, especially in mudflat habitats, which increases with salinity concentration, such as microfauna (Zhang et al., 2006; Zhu et al., 2018) meiofauna (Soetaert et al., 1994; Adão et al., 2009) and macrofauna (Wolf et al., 2009). The hydrodynamic activity and low-tide exposure are also structuring factors, especially in the intertidal zone, favoring the horizontal distribution patterns (zonation) and vertical stratification (Steyaert et al., 2001; Kaiser et al., 2011). For example, nematodes and invertebrates actively move within sediments to avoid desiccation and extreme salinity variations that occur at the sediment surface (Steyaert et al., 2001; Giere, 2009). Moreover, the heterogeneity of benthic habitats is also related to the physical and chemical composition of sediment (e.g., grain size, organic matter, and oxygen concentration) (Bianchelli et al., 2018; Moens & Beninger, 2018), atmospheric events (e.g., wind, rain, temperature, and light), and impacts of human activities (e.g., pollutions, dredging) (Sahaean et al., 2017; Schratzberger & Somerfield, 2020). Another important driver of benthic communities' distribution and diversity patterns are the food sources and their quality (Campanyà-Llovet et al., 2017). In estuaries, organic matter represents an important energy source, derived from multiple origins and primary producers (e.g., microphytobenthos, cyanobacteria, and heterotrophic bacteria) being able to sustain all trophic levels (Moens et al., 2005; Vafeiadou et al., 2013; Van der Heijden et al., 2018). The influence of organic matter on benthic communities is mainly related to multiple interactions with other environmental variables, e.g., hydrodynamic activities, and sediments type, which contribute to increase the diversity of habitat-specific conditions (Schratzberger and Somerfield, 2020). Biotic interactions (e.g. predator-prey competition) are also regulated by abiotic stressors, altering energy flows (Moens & Beninger, 2018). In these habitats, benthic trophic dynamics are influenced not only by the availability of inorganic nutrients driven by primary production, but also by the supply rates and sources of the organic matter (Bianchelli et al., 2020). Until now, the mechanisms by which **benthic communities control the bottom-up interactions** that potentially support fundamental processes and energy flows remain poorly understood (Hooper et al., 2005).

### 1.3 Food webs contributions to assess the Good Environmental Status (GES) of the ecosystem

The main concern about biodiversity loss is not only related to species loss, but also to the consequences on ecosystem functioning. Assessing ecosystem health based only on patterns of community richness and composition, without considering **energy flows** and **species interactions**, does not provide a global and accurate picture of how ecosystems function (Thompson et al., 2012). Food webs analysis provides a broad snapshot of **ecosystem functioning**, characterizing energy flows through a complex network of interconnected organisms that support essential ecological processes (Begon et al., 2006). However, constructing food webs can be highly complex and difficult to predict due to multiple trophic levels, species interactions (e.g., predation, competition, mutualism), and indirect effects (Thompson et al., 2007). To better assess food webs, ecologists started to link trophic positions with feeding behaviors, diets, and energy transfer interactions, describing a position or space occupied by the organism as its **trophic niche** (Post, 2002). However, niche occupancy goes beyond the concept of trophic position as it is directly dependent on the resource use (e.g., organisms can be at the same trophic level and feed on different prey types), describing distinct **niche sizes** (Layman et al., 2007b).

Initially, food webs were constructed based on organisms' stomach contents, providing brief and incomplete information on niche occupancy, limited to organisms' size (Cortes & Preti, 2000; Post, 2002). The **Stable Isotope Analysis (SIA)** overcome these limitations, improving the concept of food web assessment, considering all trophic levels regardless organisms' size, temporal variability, and potential turnover rates of adjacent metabolic processes (Kortsch et al., 2021). This novel multi-dimensional approach for estimating the food web structure based on **stable isotope ratios of nitrogen ( $\delta^{15}\text{N}$ )** and **carbon ( $\delta^{13}\text{C}$ )** provided a high-quality insight into the organism's trophic niche construction (Post, 2002). This allowed inferences about the food sources and trophic variability within a community (Nelson et al., 2015). Later, with the development of **quantitative metrics** to assess isotopic data reflecting community-wide facets, it becomes possible to quantify the **structural responses at community level** (e.g. ecological niches, resource partitioning, and potential competition among species) (Layman et al., 2007a). Statistical comparisons of individual communities using **descriptive metrics** (Layman et al., 2007a) become limited in providing a broader perspective of ecosystem functioning. The metrics were reformulated within a **Bayesian framework** to address uncertainties derived from sampling processes and overcome biased information related to sample size differences. This provided a robust comparison

among data sets with different sample sizes (Jackson et al., 2011). However, the exact contribution of food sources in the food web structure was unclear. Thus, **mixing models** were explored to estimate each source's dietary contribution to a consumer, revolutionizing our understanding of how food sources impact diets by quantifying the extent of specialization and omnivory (Jackson et al., 2017), which became useful to detect **trophic shifts**, standardize **food webs models** and assess the effect of disturbances. Although mixing models showed limitations, their success depends on the number of potential sources sampled and the accuracy of taxonomic identification (Philips et al., 2014). Therefore, ecologists began to use different metrics simultaneously to understand trophic interactions and food sources contributions to the food webs complexity patterns.

### 1.3.1 *Spatial and temporal variability of the food web structures*

Food webs are extremely dynamic in space and time and understanding how respond to ecosystem changes is highly challenging, mostly because traditional metrics are unable to provide quantitative measures of **resource changes** and rarely consider physical environmental factors (McCann & Rooney, 2009). Thus, it become important to include spatial (Vander Zanden & Rasmussen 1999) and temporal variations in isotopic values to capture the factors that directly influence the habitat condition and food availability (Cabana & Rasmussen, 1996). Food web structure changes over different temporal scales, influenced by shifts in abiotic factors (e.g., temperature, organic matter) and biotic processes (e.g., migrations, population dynamics) (Thompson et al., 2012; Bergamino et al., 2015). These variations can shape species diversity, interactions and energy flows, resulting in dynamic and site-specific food webs (Dézerald et al., 2018). Several statistical tools and metrics have been developed to summarize **community-wide isotopic data**, providing **quantitative measures of trophic structure** and **complexity** at the ecosystem level (Layman et al., 2007a; Jackson et al., 2011). Applying a Bayesian approach to these metrics allowed comparisons of trophic structure across ecosystems and over time (Jackson et al. 2012).

Examining **patterns of  $\delta^{15}\text{N}$**  and  **$\delta^{13}\text{C}$** , ecologists are able to quantify several **food web attributes**, including **trophic length**, **niche overlap**, **trophic diversity**, and **redundancy**. This approach provided a comprehensive understanding of energy flow and resource distribution among species (Jackson et al., 2011). But although these metrics mainly reflected **community-wide trophic structure** based on species diversity, there is no consideration about the functional aspects. To complement the existing metrics, a set of four isotopic **diversity metrics (isotopic divergence, dispersion, evenness, and uniqueness)** were developed. These metrics allow to quantify multiple

facets of functional diversity of the community in a multidimensional isotopic space based on functional traits (Cucherousset & Villéger, 2015), which become useful to accurately identify the communities' responses to several types of disturbances.

### 1.3.2 *Estuarine food webs main structuring factors and their patterns*

**Estuarine food webs** are complex and dynamic, shaped by various environmental and biological factors (Vinagre et al., 2017; Young et al., 2021). The spatial and temporal patterns of these food webs have just recently started to be investigated (Liu et al., 2020, Szczepanek et al., 2021; Ziolkowska and Sokolowski, 2022). These studies highlighted the significant influence of seasonally and spatially regulated organic matter inputs, primary productivity, and physical and environmental variables on food webs.

**Benthic organisms** are crucial for capturing the spatial and temporal variability of estuarine food web structures, reflecting diverse patterns of trophic relationships (Donázar-Aramendía et al., 2019; Szczepanek et al., 2021). This is strongly related to their small body size and fast turnover rates which allows them to respond rapidly to the spatial-temporal variations of nutrients and organic matter inputs within the estuary (Kortsch et al., 2018; Liu et al., 2020; Szczepanek et al., 2021). In estuarine benthic food webs, diverse trophic pathways can occur due to high variability in **trophic guild diversity** and the **available resources**, which are particularly abundant in estuarine environments (Hoffman et al., 2015). Benthic organisms are mainly **opportunistic feeders**, yet distinct trophic groups respond differently to quality parameters, suggesting that food quality can significantly alter **benthic trophic structure** (Campanyà-Llovet et al., 2017).

Most marine food web studies focus on pelagic rather than benthic ecosystems, creating a knowledge gap and a disentanglement within food web structures. Benthic consumers already proved to play a crucial role in the connectivity between estuaries and adjacent ecosystems, utilizing subsidies of terrestrial and marine origin (Dias et al., 2023), serving as excellent models for studying the importance of energy pathways across different locations within an estuary.

## 1.4 PhD project conceptualization

Estuarine and coastal ecosystems are considered among the most productive ecosystems, even though highly disturbed by various environmental pressures. The functional integrity of these systems is driven by complex interactions between organisms, which play a crucial role in transferring energy to higher trophic levels. As a result, food webs become a key component to include in the **MSFD**, being recognized

as the function **descriptor 4 (D4)**. The implementation of this descriptor remains challenging due to the **lack of significant information** to evaluate and identify one definitive condition that represents “**GES**”. To date, indicators developed under **D4** have focused mainly on well-studied pelagic habitats, **overlooking benthic habitats** that are essential for detecting environmental disturbances and drawing energy pathways. Despite their potential role as mediators of **fundamental processes** and **energy flows**, little is known about how benthic communities **shape bottom-up interactions** (Figure 4).

Assessing the **energy transferred** to higher trophic levels requires studying the **diversity patterns of benthic communities**, as multiple interactions occur during biogeochemical processes. Furthermore, the interaction among communities and their responses to varying habitat conditions remain poorly understood, limiting our full comprehension of their role in energy pathways. **Nematodes and bacteria** have been proven to be **good indicators** of fundamental processes, responding rapidly to different habitat conditions. Evaluating their responses to different sediment conditions can provide new insights into how environmental changes affect the interactions within benthic communities, impacting other trophic levels and the entire benthic food web (Figure 4).

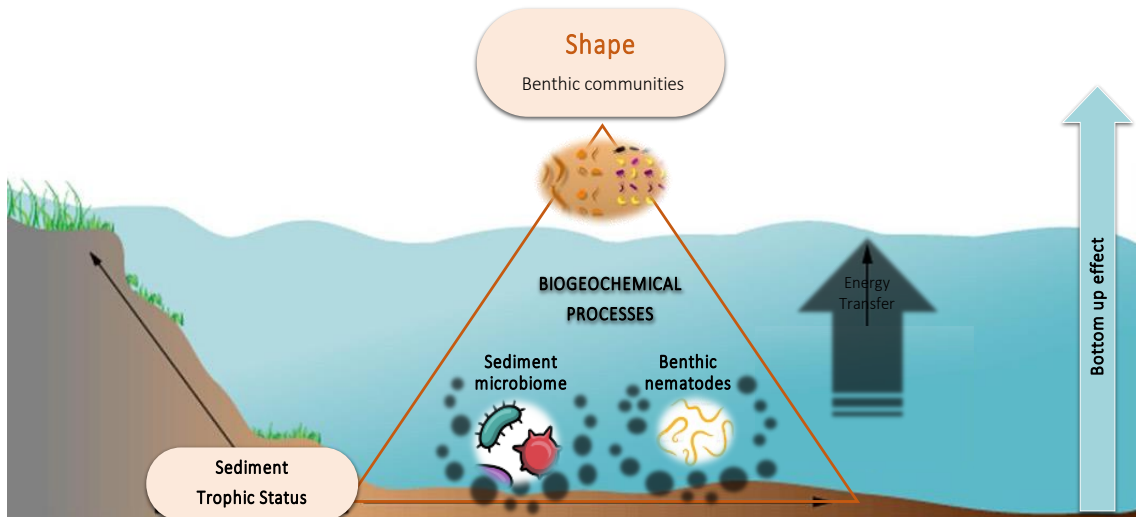


**Figure 4.** Graphical concept of the PhD project representing the sediment trophic state, biological interactions mediating biogeochemical processes and implications in the benthic trophic webs and energy pathways base on bottom-up effects.

Given the existing knowledge gaps regarding how benthic food webs influence energy pathways and the estuarine ecosystem functioning, this PhD project aimed to address the following scientific questions:

**How will different sediment conditions shape the:**

- a) **composition and distribution patterns** of benthic communities?
- b) **interactions** within benthic communities?
- c) **trophic levels** and the entire **benthic food web**?

**Study Area**

The Sado estuary, on the south-west coast of Portugal, is surrounded by extensive urban and industrial areas with many polluting activities (e.g., Lisnave shipyard, Navigator paper mill, and rice paddies). In contrast, parts of the estuary are environmentally protected, highlighting the importance of ecological conservation and biomonitoring. The estuary provides essential habitats for a wide range of species, including migratory birds, fish, and invertebrates. The salt marshes, mudflats, and intertidal zones provide important breeding and feeding grounds for many organisms. In addition, the estuary supports several activities that exploit some areas that are considered nurseries for fish and oysters.

Changes in **sediment trophic conditions** can influence the **abundance and diversity patterns** of benthic communities of Sado estuary, directly affecting **trophic interactions** and the **energy transferred** to higher trophic levels (bottom-up effect) (Figure 4). The following hypothesis was initially proposed (Figure 5):

**H1:** Bacterial and nematode communities will respond equally to different sediment conditions in Sado's Estuary, presenting similar spatial-temporal distribution patterns;

**H2:** The decrease in food availability/quality alters carbon sources, increasing small opportunistic species and reducing the number of specialist species and top predators;

**H3:** The reduction of the energy transfer to higher trophic levels leads to overall simplification of the benthic food webs.

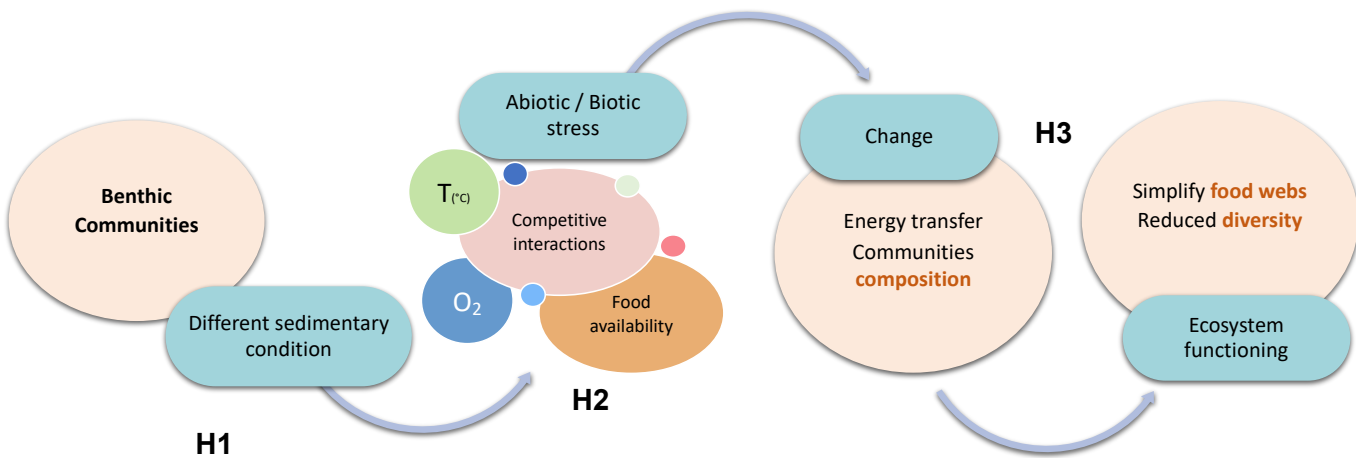


**Figure 5.** Abiotic and biotic interactions in response to different sediment conditions: implications for energy pathways and ecosystem functioning. (H1) Hypothesis 1 and (H2) Hypothesis 2 and Hypothesis 3 (H3).

To test the hypotheses, **three sampling sites** were selected considering **different biogeochemical properties, anthropogenic influences, and hydrodynamic activity**:

**Chapter 2:** “Tróia” sandy sediments, with an intermediate level of OM (a different site from the other “Tróia” site mentioned in **chapters 3, 4 and 5**); “Moinho” muddy sediments with high levels of OM at the inner part of the estuary and “Navigator” sandy sediments with low levels of OM and influenced by the paper mill.

**Chapters 3, 4 and 5:** “Tróia” sandy sediments located in a protected area at the mouth of the estuary, with low level of OM; “Gambia” intermediate level of OM, influenced by aquaculture activities and “Navigator” high levels OM, influenced by the paper mill. All samples were collected simultaneously during **four different occasions** (Figure 6) presenting different environmental conditions (winter 2019 and 2020; summer 2020 and 2021).

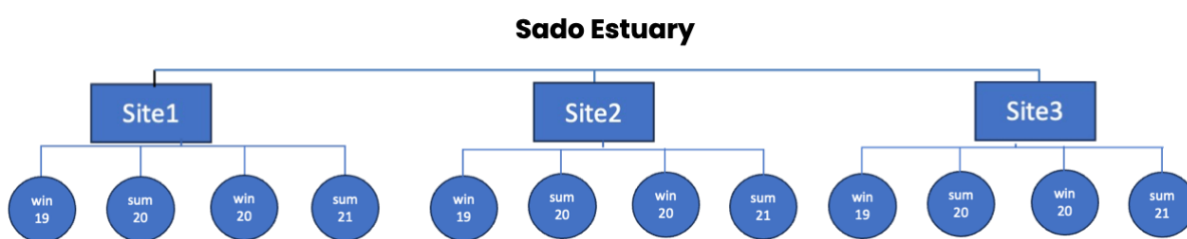


**Figure 6.** Sampling design to assess the spatial and temporal variability of the benthic communities in Sado estuary (Chapter 3, 4 and 5): 3 sampling sites (Navigator, Gambia and Tróia) 4 sampling occasions (winter 2019 (win19) and 2020 (win20); summer 2020 (Sum 20) and 2021 (Sum 21)).

Sediment was collected to analyse: a) biogeochemical composition, b) nematode assemblage, c) bacterial communities; d) trophic composition; e) food sources. Environmental parameters were measured *in situ* (e.g. salinity, oxygen, temperature and pH). This sampling strategy was supported by the D4Ss project (Food-web approaches to assess the functional benthic ecosystem interactions for Marine and Coastal management under the MSFD), which initiated the framework for studying benthic trophic interactions in the Sado estuary.

The **main goals** of this project were:

- I. Investigate how the **bottom-up processes** can modulate the marine benthic food webs;
- II. Assess how different sediment conditions affect **nematode and bacteria communities' structure** (abundance and diversity) and the **trophic pathways** (stable isotopic signatures) of the benthic food webs.
- III. Develop **high-throughput tools** or **methodologies** to complement the routine framework assessments of the **D4** and other associated directives **D1**(biodiversity) **D6** (seafloor integrity) within the **MSFD**.

To achieve these goals the following **objectives** were performed:

1. Analyze the **spatial distribution patterns** of bacterial and nematode communities using 16S amplicon metagenomic and morphological identification, respectively, and assess both communities' responses to different sediment conditions in each site, (**Chapter 2**);
2. Detailed analyze of the bacterial communities **spatial and temporal patterns**, using 16S metagenomic approach to describe their composition, potential metabolic pathways and assess bacterial communities' responses to different sediment conditions (**Chapter 3**);
3. Investigate the **spatial and temporal patterns** of nematode assemblages using morphological identification and relate the distribution patterns of both communities, bacterial and nematode and potential implications for benthic trophic food webs (**Chapter 5**);
4. Analyze **spatial and temporal patterns** of trophic web structures using stable isotopic analysis ( $\delta^{15}\text{N}$  and  $\delta^{13}\text{C}$ ) to evaluate bottom-up effects based on food web attributes (**Chapter 4**).
5. Examine and **integrate the results** to provide methodologies to assess the Descriptor 4 and associated descriptors of the biodiversity theme (**D1, D4 and D6**) of MSFD (**Chapter 6**).

## 1.5 References

Adão, H. (2022). Metazoan meiofauna: Benthic assemblages for sustainable marine and estuarine ecosystems. In Leal Filho, W., Azul, A. M., Brandli, L., Lange Salvia, A., & Wall, T. (Eds.), *Life below water. Encyclopedia of the UN Sustainable Development Goals*. Springer, Cham. [https://doi.org/10.1007/978-3-319-98536-7\\_41](https://doi.org/10.1007/978-3-319-98536-7_41)

Adão, H., Alves, A. S., Patrício, J., Neto, J. M., Costa, M. J., & Marques, J. C. (2009). Spatial distribution of subtidal Nematoda communities along the salinity gradient in southern European estuaries. *Acta Oecologica*, 35, 287–300. <https://doi.org/10.1016/j.actao.2008.11.007>

Alves AS, Adão H, Patrício J, et al (2009) Spatial distribution of subtidal meiobenthos along estuarine gradients in two southern european estuaries (Portugal). *J Mar Biol Assoc United Kingdom* 89:1529–1540. <https://doi.org/10.1017/S0025315409000691>

Baker, B. J., Lazar, C. S., Teske, A. P., & Dick, G. J. (2015). Genomic resolution of linkages in carbon, nitrogen, and sulfur cycling among widespread estuary sediment bacteria. *Microbiome*. <https://doi.org/10.1186/s40168-015-0077-6>

Balsamo, M., Semprucci, F., Frontalini, F., & Coccioni, R. (2012). Meiofauna as a tool for marine ecosystem biomonitoring. *Marine Ecosystems*.

Bayer, C., Heindl, N. R., Rinke, C., Lücker, S., Ott, J. A., & Bulgheresi, S. (2009). Molecular characterization of the symbionts associated with marine nematodes of the genus *Robbea*. *Environmental Microbiology Reports*, 1(2), 136–144. <https://doi.org/10.1111/j.1758-2229.2009.00019.x>

Begon, M., Townsend, C. R., & Harper, J. L. (2006). Ecology: From individuals to ecosystems (4th ed.). Blackwell Publishing.

Bellec, L., Bonavita, M. A. C., Hourdez, S., et al. (2019). Chemosynthetic ectosymbionts associated with a shallow-water marine nematode. *Scientific Reports*, 9, 7019. <https://doi.org/10.1038/s41598-019-43517-8>

Bellec, L., Cambon-Bonavita, M. A., Durand, L., Aube, J., Gayet, N., Sandulli, R., Brandily, C., & Zeppilli, D. (2020). Microbial communities of the shallow-water hydrothermal vent near Naples, Italy, and chemosynthetic symbionts associated

with a free-living marine nematode. *Frontiers in Microbiology*, 11, 2023. <https://doi.org/10.3389/fmicb.2020.02023>

Bergamino, L., & Richoux, N. B. (2015). Spatial and temporal changes in estuarine food web structure: Differential contributions of marsh grass detritus. *Estuaries and Coasts*, 38, 367–382. <https://doi.org/10.1007/s12237-014-9814-5>

Bianchelli, S., Pusceddu, A., Buschi, E., & Danovaro, R. (2018). Nematode biodiversity and benthic trophic state are simple tools for the assessment of the environmental quality in coastal marine ecosystems. *Ecological Indicators*, 95, 270–287. <https://doi.org/10.1016/j.ecolind.2018.07.032>

Bianchelli, S., Nizzoli, D., Bartoli, M., Viaroli, P., Rastelli, E., & Pusceddu, A. (2020). Sedimentary organic matter, prokaryotes, and meiofauna across a river-lagoon-sea gradient. *Diversity*, 12(5), 189. <https://doi.org/10.3390/d12050189>

Bohan, D. A., Vacher, C., Tamaddoni-Nezhad, A., Raybould, A., Dumbrell, A. J., & Woodward, G. (2017). Next-generation global biomonitoring: Large-scale, automated reconstruction of ecological networks. *Trends in Ecology & Evolution*. <https://doi.org/10.1016/j.tree.2017.03.001>

Bonaglia, S., Nascimento, F. J. A., Bartoli, M., Klawonn, I., & Brüchert, V. (2014). Meiofauna increases bacterial denitrification in marine sediments. *Nature Communications*, 5, 5133. <https://doi.org/10.1038/ncomms6133>

Bonaglia, S., Hedberg, J., Marzocchi, U., Iburg, S., Glud, R. N., & Nascimento, F. J. A. (2020). Meiofauna improve oxygenation and accelerate sulfide removal in the seasonally hypoxic seabed. *Marine Environmental Research*, 159. <https://doi.org/10.1016/j.marenvres.2020.104968>

Bonaglia, S., Nascimento, F.J.A. (2023). Meiofauna Shaping Biogeochemical Processes. In: Giere, O., Schratzberger, M. (eds) New Horizons in Meiofauna Research. Springer, Cham. [https://doi.org/10.1007/978-3-031-21622-0\\_2](https://doi.org/10.1007/978-3-031-21622-0_2)

Borja, Á., Galparsoro, I., Solaun, O., Muxika, I., Tello, M. E., Uriarte, A., & Valencia, V. (2006). The European Water Framework Directive and the DPSIR: A methodological approach to assess the risk of failing to achieve good ecological status. *Estuarine, Coastal and Shelf Science*, 66(1–2), 84–96. <https://doi.org/10.1016/j.ecss.2005.07.021>

Broman, E., Bonaglia, S., Holovachov, O., Marzocchi, U., Hall, P. O. J., & Nascimento, F. J. A. (2020). Uncovering diversity and metabolic spectrum of animals in dead zone sediments. *Communications Biology*, 3, 1–12. <https://doi.org/10.1038/s42003-020-0822-7>

Buongiorno JHerbert LC, Wehrmann LM, Michaud AB, Laufer K, Røy H, Jørgensen BB, Szynkiewicz A, Faia A, Yeager KM, Schindler K & Lloyd KG. (2019). Complex Microbial Communities Drive Iron and Sulfur Cycling in Arctic Fjord Sediments. *Appl Environ Microbiol* 85:e00949-19. <https://doi.org/10.1128/AEM.00949-19>

Bush, A., Compson, Z. G., Monk, W. A., Porter, T. M., Steeves, R., Emilson, E., Gagne, N., Hajibabaei, M., Roy, M., & Baird, D. J. (2019). Studying ecosystems with DNA metabarcoding: Lessons from biomonitoring of aquatic macroinvertebrates. *Frontiers in Ecology and Evolution*. <https://doi.org/10.3389/fevo.2019.00434>

Cabana, G., & Rasmussen, J. B. (1996). Comparison of aquatic food chains using nitrogen isotopes. *Proceedings of the National Academy of Sciences*, 93(20), 10844–10847. <https://doi.org/10.1073/pnas.93.20.10844>

Campanyà-Llovet, N., Snelgrove, V. R. P., & Parrish, C. C. (2017). Rethinking the importance of food quality in marine benthic food webs. *Progress in Oceanography*, 156, 240–251. <https://doi.org/10.1016/j.pocean.2017.07.006>

Cortés, E., & Preti, A. (2000). Evaluation of dietary studies of the shortfin mako shark (*Isurus oxyrinchus*) based on analysis of stomach contents and stable isotopes. *Journal of Fish Biology*, 56(1), 1173–1182.

Coull, B. C. (1990). Are members of the meiofauna food for higher trophic levels? *Transactions of the American Microscopical Society*, 109, 233–246.

Coull, B. C. (1999). Role of meiofauna in estuarine soft-bottom habitats. *Australian Journal of Ecology*, 24, 327–343.

Cucherousset, J., & Villéger, S. (2015). Quantifying the multiple facets of isotopic diversity: New metrics for stable isotope ecology. *Ecological Indicators*, 56, 152–160. <https://doi.org/10.1016/j.ecolind.2015.03.032>

D'Hondt, A. S., Stock, W., Blommaert, L., Moens, T., & Sabbe, K. (2018). Nematodes stimulate biomass accumulation in a multispecies diatom biofilm. *Marine*

*Environmental Research*, 140, 78–89.  
<https://doi.org/10.1016/j.marenvres.2018.06.005>

De Mesel, I., Derycke, S., Swings, J., Vincx, M., & Moens, T. (2006). Role of nematodes in decomposition processes: Does within-trophic group diversity matter? *Marine Ecology Progress Series*, 321, 157–166. <https://doi.org/10.3354/meps321157>

Derycke, S., De Meester, N., Rigaux, A., Creer, S., Bik, H., Thomas, W. K., & Moens, T. (2016). Coexisting cryptic species of the *Litoditis marina* complex (Nematoda) show differential resource use and have distinct microbiomes with high intraspecific variability. *Molecular Ecology*, 25, 2093–2110.  
<https://doi.org/10.1111/mec.13597>

Dézerald, O., D. S. Srivastava, R. Cérégino, J. F. Carrias, B. Corbara, V. F. Farjalla, et al., (2018). Functional traits and environmental conditions predict community isotopic niches and energy pathways across spatial scales. *Functional Ecology* 32: 2423–2434. doi: 10.1007/s00227-013-2238-0

Dias E., Morais P., Antunes C. & Hoffman C. J., (2023). The benthic food web connects the estuarine habitat mosaic to adjacent ecosystems. *Food Webs*, 35, e00282  
<https://doi.org/10.1016/j.fooweb.2023.e00282>

Elliott, M. & McLusky, D.S. (2002). The need for definitions in understanding estuaries. *Estuarine, Coastal and Shelf Science* 55: 815–827.

Elliott, M. & Quintino, V., (2007). The Estuarine Quality Paradox, Environmental Homeostasis and the difficulty of detecting anthropogenic stress in naturally stressed areas. *Mar. Pollut. Bull.* 54, 640–645.  
<https://doi.org/10.1016/j.marpolbul.2007.02.003>

Fraser, M.W., Short, J., Kendrick, G., McLean, D., Keesing, J., Byrne, M., Caley, M.J., Clarke, D., Davis, A.R., Erftemeijer, P.L.A., Field, S., Gustin-Craig, S., Huisman, J., Keough, M., Lavery, P.S., Masini, R., McMahon, K., Mengersen, K., Rasheed, M., Statton, J., Stoddart, J. & Wu, P., (2017). Effects of dredging on critical ecological processes for marine invertebrates, seagrasses and macroalgae, and the potential for management with environmental windows using Western Australia as a case study. *Ecol. Indic.*  
<https://doi.org/10.1016/j.ecolind.2017.03.026>

Gallucci F., Moens T., Vanreusel A. & Fonseca G., (2008). Active colonization of disturbed sediments by deep-sea nematodes: evidence for the patch mosaic model. *Mar Ecol Prog Ser* 367:173–183

Gee, J., (1989). An ecological and economic review of meiofauna as food for fish. *Zoological journal of the Linnean Society* 96: 243-261.

Gerbersdorf, S.U., Westrich, B. & Paterson, D.M., (2009). Microbial extracellular polymeric substances (EPS) in fresh water sediments. *Microb. Ecol.* 58, 334–349. <https://doi.org/10.1007/s00248-009-9498-8>

Giere, O. (2009) Meiobenthology: the microscopic motile fauna of aquatic sediments. Springer Science & Business Media, Berlin.

Giere, O. (2019). Pollution and Meiofauna—Old Topics, New Hazards. In: Perspectives in Meiobenthology. SpringerBriefs in Biology. Springer, Cham. [https://doi.org/10.1007/978-3-030-13966-7\\_3](https://doi.org/10.1007/978-3-030-13966-7_3)

Hoffman, J.C., Kelly, J.R., Peterson, G.S. et al., (2015). Landscape-Scale Food Webs of Fish Nursery Habitat Along a River-Coast Mixing Zone. *Estuaries and Coasts*, 38, 1335–1349 (2015). <https://doi.org/10.1007/s12237-014-9880-8>

Hooper, D.U., Chapin, F.S., Ewel, J.J., Hector, A., Inchausti, P., Lavorel, S., Lawton, J.H., Lodge, D.M., Loreau, M., Naeem, S., Schmid, B., Setälä, H., Symstad, A.J., Vandermeer, J. & Wardle, D.A., (2005). Effects of biodiversity on ecosystem functioning: A consensus of current knowledge. *Ecol. Monogr.* 75, 3–35. <https://doi.org/10.1890/04-0922>

Jackson A.L., Inger R., Parnell A.C. & Bearhop S., (2011). Comparing isotopic niche widths among and within communities: SIBER – Stable Isotope Bayesian Ellipses in R. *Journal of Animal Ecology* 2011, 80, 595–602. <https://doi.org/10.1111/j.1365-2656.2011.01806.x>

Jackson M.C., Evangelista C., Zhao T., Lecerf A., Britton J.R. & Cucherousset J., (2017). Between-lake variation in the trophic ecology of an invasive crayfish. *Freshwater Biology*, 62, 1501-1510. <https://doi.org/10.1111/fwb.12957>

Jackson MC, Donohue I, Jackson AL, Britton JR, Harper DM & Grey J., (2012). Population-Level Metrics of Trophic Structure Based on Stable Isotopes and Their Application to Invasion Ecology. *PLoS ONE* 7(2): e31757. <https://doi.org/10.1371/journal.pone.0031757>

Jessen, G.L., Lichtschlag, A., Ramette, A., Pantoja, S., Rossel, P.E., Schubert, C.J., Struck, U. & Boetius, A., (2017). Hypoxia causes preservation of labile organic matter and changes seafloor microbial community composition (Black Sea). *Sci. Adv.* 3, e1601897. <https://doi.org/10.1126/sciadv.1601897>

Jokanovi S, Kajan K, Perovi S, Ivani M, Maci V & Orlic S., (2021). Anthropogenic influence on the environmental health along Montenegro coast based on the bacterial and chemical characterization. *Environmental Pollution* 271, 116383. <https://doi.org/10.1016/j.envpol.2020.116383>

Jokanovic S. et al., (2021). Anthropogenic influence on the environmental health along Montenegro coast based on the bacterial and chemical characterization. *Environmental Pollution* 271, 116383. <https://doi.org/10.1016/j.envpol.2020.116383>

Kaiser, M.J., Attrill, M.J., Jennings, S., Thomas, D.N., & Barnes, D.K., (2011). Marine ecology: processes, systems, and impacts. *Oxford University Press, Oxford*.

Kennish J.M., (2002). Environmental threats and environmental future of estuaries. *Environmental Conservation* 29 (1): 78–107, *Foundation for Environmental Conservation*, DOI:10.1017/S0376892902000061

Kortsch S, Frelat R, Pecuchet L, et al., (2021). Disentangling temporal food web dynamics facilitates understanding of ecosystem functioning. *J Anim Ecol.* 90: 1205–1216. <https://doi.org/10.1111/1365-2656.13447>

Kristensen E, Penha-Lopes G, Delefosse M, Valdemarsen T, Quintana CO & Banta GT., (2012). What is bioturbation? The need for a precise definition for fauna in aquatic sciences. *Mar Ecol Prog Ser* 446:285-302. <https://doi.org/10.3354/meps09506>

Laiolo E, Alam I, Uludag M, Jamil T, Agusti S, Gojobori T, Acinas SG, Gasol JM & Duarte CM. (2024). Metagenomic probing toward an atlas of the taxonomic and metabolic foundations of the global ocean genome. *Front Sci* (2024) 1:1038696. doi: 10.3389/fsci.2023.1038696

Lalzar M, Zvi-Kedem T, Kroin Y, Martinez S, Tchernov D & Meron D. (2023). Sediment Microbiota as a Proxy of Environmental Health: Discovering Inter- and Intrakingdom Dynamics along the Eastern Mediterranean Continental Shelf. *Microbiol Spectr* 11:e02242-22. <https://doi.org/10.1128/spectrum.02242-22>

Layman, C. A., Arrington, D. A., Montana, C. G., & Post, D. M. (2007a). Can stable isotope ratios provide for community-wide measures of trophic structure? *Ecology*, 88(1), 42–48.

Layman, C. A., Quattrochi, J. P., Peyer, C. M., & Allgeier, J. E. (2007b). Niche width collapse in a resilient top predator following ecosystem fragmentation. *Ecology Letters*, 10(10), 937–944.

Liquete C, Cid N, Lanzanova D, Grizzetti B & Reynaud A., (2016). Perspectives on the link between ecosystem services and biodiversity: the assessment of the nursery function. *Ecol Indic* 63:249–257. <https://doi.org/10.1016/j.ecolind.2015.11.058>

Liu, Q., Yia, Y., Hou, C., Wua, X. & Song, J., (2020). Response of trophic structure and isotopic niches of the food web to flow regime in the Yellow River estuary. *Mar. Geol.* 430 (2020), 106329 <https://doi.org/10.1016/j.margeo.2020.106329>.

Mahamound A, Lyautey E, Bonnneau C, Dabrin A. & Pesce S., (2018). Environmental concentrations of Copper, alone or in mixture with Arsenic, can impact river sediment microbial community structure and functions. *Sec. Microbiotechnology*, Vol 9 – 2018 <https://doi.org/10.3389/fmicb.2018.01852>

Marshall, A., Longmore, A., Phillips, L., Tang, C., Hayden, H., Heidelberg, K. & Mele, P., (2021). Nitrogen cycling in coastal sediment microbial communities with seasonally variable benthic nutrient fluxes. *Aquat. Microb. Ecol.* 86, 1–19. <https://doi.org/10.3354/ame01954>

McCann K. S. & Rooney N., (2009). The more food webs change, the more they stay the same. *Phil. Trans. R. Soc.* B3641789–1801. <https://doi.org/10.1098/rstb.2008.0273>

Moens, T., Bouillon, S. & Gallucci, F., (2005). Dual stable isotope abundances unravel trophic position of estuarine nematodes. *J. Mar. Biol. Assoc. U. K.* 85, 1401–1407. <https://doi.org/10.1017/S0025315405012580>

Moens, T. & Beninger, P.G. (2018). Meiofauna: An Inconspicuous but Important Player in Mudflat Ecology. In: Beninger, P. (eds) Mudflat Ecology. *Aquatic Ecology Series*, vol 7. Springer, Cham. [https://doi.org/10.1007/978-3-319-99194-8\\_5](https://doi.org/10.1007/978-3-319-99194-8_5)

Musat, N., Giere, O., Gieseke, A., Thiermann, F., Amann, R. & Dubilier, N., (2007). Brief report Molecular and morphological characterization of the association between

bacterial endosymbionts and the marine nematode *Astomonema* sp. from the Bahamas. <https://doi.org/10.1111/j.1462-2920.2006.01232.x>

Nascimento, F.J.A., Näslund, J. & Elmgren, R., (2012). Meiofauna enhances organic matter mineralization in soft sediment ecosystems. *Limnol. Oceanogr.* 57, 338–346. <https://doi.org/10.4319/lo.2012.57.1.0338>.

Nawaz A., Witoon Purahong W., Lehmann R., Herrmann M., Totsche U.K., Küsel K., Wubet T. & Buscot F., 2018. First insights into the living groundwater mycobiome of the terrestrial biogeosphere. *Water Res.*, 145, pp. 50-61, [10.1016/j.watres.2018.07.067](https://doi.org/10.1016/j.watres.2018.07.067)

Nelson J.A., Deegan L. & Garrett R., (2015). Drivers of spatial and temporal variability in estuarine food webs. *Mar Ecol Prog Ser* 533:67-77. <https://doi.org/10.3354/meps11389>

Nigel G. Yoccoz. (2012). The future of environmental DNA in ecology. *Molecular Ecology* 21, 2031–2038. <https://doi.org/10.1111/j.1365-294X.2012.05505.x>

Ott, J., Bright, M. & Bulgheresi, S.V., (2004). Symbioses between Marine Nematodes and Sulfur-oxidizing Chemoautotrophic Bacteria, *Symbiosis*.

Patrício, J. et al., (2012). Do nematode and macrofauna assemblages provide similar ecological assessment information? *Ecol. Indic.* 14, 124–137. <https://doi.org/10.1016/j.ecolind.2011.06.027>

Pawlowski J., Bonin A., Boyer F., Cordier T. & Taberlet P., (2021). Environmental DNA for biomonitoring. *Mol Ecol*. 2021 Jul;30(13):2931-2936. doi: 10.1111/mec.16023. Epub 2021 Jun 27. PMID: 34176165; PMCID: PMC8451586.

Peixoto, R.S., Rosado, P.M., Leite, D.C. de A., Rosado, A.S. & Bourne, D.G., (2017). Beneficial microorganisms for corals (BMC): Proposed mechanisms for coral health and resilience. *Front. Microbiol.* <https://doi.org/10.3389/fmicb.2017.00341>

Petersen, J.M. & Yuen, B., (2021). The Symbiotic “All-Rounders”: Partnerships between Marine Animals and Chemosynthetic Nitrogen-Fixing Bacteria. *Appl. Environ. Microbiol.* 87, 1–16. <https://doi.org/10.1128/AEM.02129-20>

Post, D. M. (2002). Using stable isotopes to estimate trophic position: Models, methods, and assumptions. *Ecology*, 83(3), 703–718.

Ridall, A. & Ingels, J., (2021). Suitability of free-living marine nematodes as bioindicators: status and future considerations. *Front. Mar. Sci.* 863. <https://doi.org/10.3389/FMARS.2021.685327>

Rocca D. J. et al. (2019). The Microbiome Stress Project: Toward a Global Meta-Analysis of Environmental Stressors and Their Effects on Microbial Communities. *Sec. Microbiotechnology* Vol. 9 - 2018. <https://doi.org/10.3389/fmicb.2018.03272>

Rogers, S., et al., (2010). Marine Strategy Framework Directive-Task Group 4 Report Food Webs. European Commission Joint Research Centre, ICES.

Rombouts, I., Beaugrand G., Fizzala X., Gaill F., Greenstreet S.P.R., Lamare S., Le Loc'h F., McQuatters-Gollop A., Mialet B., Niquil N., Percelay J., Renaud F., Rossberg A. G. & Féral J. P., (2013). Food web indicators under the Marine Strategy Framework Directive: from complexity to simplicity? *Ecol. Ind.* 29, 246-25. <https://doi.org/10.1016/j.ecolind.2012.12.021>

Rzeznik-Orignac J., Puisay A., Derelle E., Peru E., Le Bris N. & Galand P.E. (2018). Co-occurring nematodes and bacteria in submarine canyon sediments. *PeerJ* 6:e5396 <https://doi.org/10.7717/peerj.5396>

Schratzberger, M. & Ingels, J., (2018). Meiofauna matters: the roles of meiofauna in benthic ecosystems. *J. Exp. Mar. Biol. Ecol.* 502, 12–25. <https://doi.org/10.1016/j.jembe.2017.01.007>

Schratzberger, M. & Somerfield, P.J., (2020). Effects of widespread human disturbances in the marine environment suggest a new agenda for meiofauna research is needed. *Sci. Total Environ.* 728, 138435.

Semprucci, F. & Balsamo, M., (2014). Free-Living marine nematodes as bioindicators: past, present and future perspectives. *Trends Environ. Sci.* 17–36

Soetaert K., Vincx M., Wittoeck J., Tulkens M. & Van Gansbeke D., (1994). Spatial patterns of Westerschelde meiobenthos. *Estuar Coast Shelf Sci* 39:367–388

Sroczynska, K., Chainho, P., Vieira, S. & Adão, H., (2021). What makes a better indicator? Taxonomic vs functional response of nematodes to estuarine gradient. *Ecol. Indicat.* 121, 107113 <https://doi.org/10.1016/j.ecolind.2020.107113>

Steyaert, M., Herman, P.M.J., Moens, T., Widdows, J. & Vincx, M., (2001). Tidal migration of nematodes on an estuarine tidal flat (the Molenplaat, Schelde Estuary, SW Netherlands). *Marine Ecology Progress Series* 224: 299-304.

Steyaert, M., Moodley, L., Nadong, T., Moens, T., Soetaert, K. & Vincx, M., (2007). Responses of intertidal nematodes to short-term anoxic events. *J. Exp. Mar. Bio. Ecol.* 345, 175–184. <https://doi.org/10.1016/j.jembe.2007.03.001>

Stoeck T., Larissa Frühe L., Forster D., Cordier T., Martins M.I.C. & Pawlowski J., (2018). Environmental DNA metabarcoding of benthic bacterial communities indicates the benthic footprint of salmon aquaculture. *Mar. Pollut. Bull.*, 127, pp. 139-149.

Szczepanek, M., Silberberger, M.J., Koziorowska-Makuch, K., Nobili, E. & Kedra, M., (2021). The response of coastal macrobenthic food-web structure to seasonal and regional variability in organic matter properties. *Ecol. Ind.* 132, 108326 <https://doi.org/10.1016/j.ecolind.2021.108326>.

Terborgh, J.W., (2015). Toward a trophic theory of species diversity. *Proc. Natl. Acad. Sci. U. S. A.* <https://doi.org/10.1073/pnas.1501070112>

Thompson M.R., Hemberg M., Starzomski M. B. & Shurin B. J., (2007). Trophic levels and trophic tangles: the prevalence of omnivory in real food webs. *Ecology*, 88, 3, 612-617. <https://doi.org/10.1890/05-1454>

Thompson, R. M., Brose, U., Dunne, J. A., Hall, R. O., Hladyz, S., Kitching, R. L., Martinez, N. D., Rantala, H., Romanuk, T. N., Stouffer, D. B., & Tylianakis, J. M. (2012). Food webs: Reconciling the structure and function of biodiversity. *Trends in Ecology & Evolution*, 27, 689— 697.

Trevathan-Tackett, S.M., Sherman, C.D.H., Huggett, M.J., Campbell, A.H., Laverock, B., Hurtado-McCormick, V., Seymour, J.R., Firl, A., Messer, L.F., Ainsworth, T.D., Negandhi, K.L., Daffonchio, D., Egan, S., Engelen, A.H., Fusi, M., Thomas, T., Vann, L., Hernandez-Agreda, A., Gan, H.M., Marzinelli, E.M., Steinberg, P.D., Hardtke, L. & Macreadie, P.I., (2019). A horizon scan of priorities for coastal marine microbiome research. *Nat. Ecol. Evol.* 3, 1509–1520. <https://doi.org/10.1038/s41559-019-0999-7>

Vafeiadou A. M., Materatski P., Adão H., Troch M. & Moens T., (2013). Food sources of macrobenthos in an estuarine seagrass habitat (*Zostera noltii*) as revealed by dual stable isotope signatures. *Mar Biol*, 160:2517–2523.

Van der Heijden, L.H., Rzeznik-Orignac, J., Asmus, R.M., Fichet, D., Bréret, M., Kadel, P., Beaugeard, L., Asmus, H. & Lebreton, B., (2018). How do food sources drive meiofauna community structure in soft-bottom coastal food webs? *Mar. Biol.* 165. <https://doi.org/10.1007/s00227-018-3419-7>

Vander Zanden, M. J. & J. B. Rasmussen, (1999). Primary consumer d13C and d15N and the trophic position of aquatic consumers. *Ecology* 80:1395–1404

Vanreusel, A.; Fonseca, G.; Danovaro, R.; da Silva, M.C.; Esteves, A.M.; Ferrero, T.; Gad, G.; Galtsova, V.; Gambi, M.C.; Fonsêca-Genevois, V.G.; et al., (2010). The contribution of deep-sea macrohabitat heterogeneity to global nematode diversity. *Mar. Ecol.* 2010, 31, 6–20.

Vinagre C., Costa M. J. & Dunne A. J., (2017). Effect of spatial scale on the network properties of estuarine food webs. *Ecological Complexity*, 29, 87-92. <https://doi.org/10.1016/j.ecocom.2017.01.004>

Wang, W., Tao, J., Liu, H., Li, P., Chen, S., Wang, P. & Zhang, C., (2020). Contrasting bacterial and archaeal distributions reflecting different geochemical processes in a sediment core from the Pearl River Estuary. *Amb. Express* 10, 1–14. <https://doi.org/10.1186/s13568-020-0950-y>

Wang, W., Tao, J., Liu, H., Li, P., Chen, S., Wang, P. & Zhang, C., (2020). Contrasting bacterial and archaeal distributions reflecting different geochemical processes in a sediment core from the Pearl River Estuary. *Amb. Express* 10, 1–14. <https://doi.org/10.1186/s13568-020-0950-y>

Wasmund K, Mußmann M, & Loy A. (2017). The life sulfuric: microbial ecology of sulfur cycling in marine sediments. *Environmental Microbiology Reports* (2017) 9(4), 323–344, doi: 10.1111/1758-2229.12538

Wolf B., Kiel E., Hagge A., Krieg H-J. & Feld K.C., (2009). Using the salinity preferences of benthic macroinvertebrates to classify running waters in brackish marshes in Germany. *Ecological Indicator*, 9, 5, 837-847. <https://doi.org/10.1016/j.ecolind.2008.10.005>

Young, M., Howe, E., O'Rear, T., Berridge, K. & Moyle, P., (2021). Food Web Fuel Differs Across Habitats and Seasons of a Tidal Freshwater Estuary. *Estuar. Coasts* 44, 286–301. <https://doi.org/10.1007/s12237-020-00762-9>.

Zeppilli, D., Leduc, D., Fontanier, C., Fontaneto, D., Fuchs, S., Gooday, A. J., Goineau, A., et al., (2018). Characteristics of meiofauna in extreme marine ecosystems: A review. *Marine Biodiversity*. <https://doi.org/10.1007/s12526-017-0815-z>

Zhang, Y., Jiao, N., Cottrell, M.T. & Kirchman, D.L., (2006). Contribution of major bacterial groups to bacterial biomass production along a salinity gradient in the South China Sea. *Aquat. Microb. Ecol.* 43, 233–241. <https://doi.org/10.3354/ame043233>

Zhao Y. et al., (2019). Bioremediation of contaminated urban river sediment with methanol stimulation: Metabolic processes accompanied with microbial community changes. *Science of the Total Environment* 653 (2019) 649–657. <https://doi.org/10.1016/j.scitotenv.2018.10.396>

Zhu, P., Wang, Y., Shi, T., Zhang, X., Huang, G. & Gong, J., (2018). Intertidal zonation affects diversity and functional potentials of bacteria in surface sediments: A case study of the Golden Bay mangrove, China. *Appl. Soil Ecol.* 130, 159–168. <https://doi.org/10.1016/j.apsoil.2018.06.003>

Zimmermann, J., Wentrup, C., Sadowski, M., Blazejak, A., Gruber-Vodicka, H.R., Kleiner, M., Ott, J.A., Cronholm, B., De Wit, P., Erséus, C. & Dubilier, N., (2016). Closely coupled evolutionary history of ecto-and endosymbionts from two distantly related animal phyla. *Mol. Ecol.* 25, 3203–3223. <https://doi.org/10.1111/mec.13554>



## **CHAPTER 2 - DISTRIBUTION PATTERNS OF BENTHIC BACTERIA AND NEMATODE COMMUNITIES IN ESTUARINE SEDIMENTS**

Published in Estuarine, Coastal and Shelf Science (2023)

<https://doi.org/10.1016/j.ecss.2023.108448>

## 2.1 Abstract

Benthic organisms are crucial in the regulation of the ecosystem functions. The interactions between benthic nematodes and sediment bacteria across divergent environmental conditions are poorly understood. The main goal of this study was to understand the spatial distribution patterns and diversity of benthic bacterial communities and nematode assemblages of the intertidal sediments in three sampling sites (Navigator, Tróia and Moinho) along Sado Estuary (SW, Portugal). Bacterial communities were described using a 16S metagenomic approach, while nematode assemblages were characterized using morphological identification. Overall, bacterial and nematode communities presented significant diversity between sites ( $p<0.05$ ), which is primarily related with the environmental variables (e.g., organic matter and percentage of gravel). The spatial distribution of bacterial communities was in accordance with the ecological conditions of three selected sites at a larger scale than nematode assemblages. Previously described as good ecological indicators, nematode assemblages were separated at sampling site level, suggesting that their response is driven by within site specific factors at a smaller scale. Hence, the present study set a fundamental ground for future research on functional interactions between bacteria and nematodes.

**Keywords:** Benthic nematodes, 16S rRNA amplicon sequencing, bacterial communities, Sado Estuary

## 2.2 Introduction

Estuarine and coastal benthic ecosystems represent one of the major sources of essential services for human well-being (Bonaglia *et al.*, 2014; Schratzberger *et al.*, 2018). They play a crucial role in regulating fundamental ecosystem functions such as: food production, degradation and distribution of pollutants, recycling of nutrients and transfer energy through higher trophic levels (Schratzberger *et al.*, 2018). These functions are mediated by intra and interspecific interactions between organisms that support the functional integrity of the benthic ecosystems (Schratzberger *et al.*, 2020).

Benthic nematodes are the most abundant taxon of metazoan meiofauna, representing 50-90% of total meiofauna abundance (Semprucci *et al.*, 2014) and are considered an important tool to assess the effects of natural and anthropogenic disturbances in marine and estuarine sediments (Ridall *et al.*, 2021). These organisms also play important roles in several ecosystem processes, being involved in complex relationships with microbial communities (Bonaglia *et al.*, 2014; Nascimento *et al.*, 2012; Derycke *et al.*, 2016). The trophic composition of the nematode assemblages has been characterized by the morphological diversity of the buccal cavity providing feeding preferences or morphologic restrictions by ingesting certain type of food (e.g., bacteria or detritus). Under adverse environmental conditions, these assemblages can present a high trophic plasticity adopting generalist feeding behaviour (Nascimento *et al.*, 2012; Derycke *et al.*, 2016). Furthermore, nematode activities related with bioturbation, extracellular polymeric substances (EPS) production and grazing have been proved to be important contributors to stimulate the bacterial development and growth (Moens *et al.*, 2005; De Mesel *et al.*, 2006; D'Hondt *et al.*, 2018). Nematodes are thus important mediators of energy transfer to higher trophic levels (Moens *et al.*, 2005; De Mesel *et al.*, 2006; D'Hondt *et al.*, 2018; Vafeiadou *et al.*, 2013), while sediment microbes are the primary facilitators of biogeochemical processes, such as carbon remineralization and sulphate reduction (Hargrave *et al.*, 2008; Wang *et al.*, 2020). A strong interconnection between nematode-microbe communities is well recognized, the presence of nematodes enhances bacterial metabolic activities, while bacteria provide physiological adaptations to nematodes under hypoxic and anoxic conditions (Bayer *et al.*, 2009; Nascimento *et al.*, 2012; Broman *et al.*, 2020).

Assessing ecosystem conditions become one of the major concerns over the past two decades. Majority of the studies have been focused on the analysis of a single domain distribution patterns and relate with ecosystem environmental parameters (Materatski *et al.*, 2015; Branco *et al.*, 2018; Bulseco *et al.*, 2020). However, such approach does not consider the interaction between organisms belonging to different

domains, thereby limiting the assessment of the functional component of the ecosystem. Besides the existence of the above-mentioned associations between bacteria and nematodes, it is still largely unknown how both groups interact in the context of community distributional patterns and most importantly if exists any congruence between both groups in their response to ecological conditions. Applying the novel high performance methodological approaches such as 16S metagenomics to analyse the sediment bacterial diversity provide the possibility to develop essential understanding of the connection between benthic organisms. The main goal of this study was to understand the relation between the spatial distribution patterns and diversity of benthic bacterial and nematode communities of the intertidal sediments in Sado Estuary in Portugal. The diversity patterns were investigated using: *i*) a 16S metagenomic approach for bacterial communities' assessment; and *ii*) a morphological approach for the characterization of nematode assemblages. The sediment biogeochemical conditions were analysed to assess the ecological conditions at each sampling site. Drawing from above it is hypothesized that spatial distribution of both communities will follow a close pattern, both responding to the environmental conditions of the sampling sites in Sado's Estuary.

## 2.3 Material and Methods

### 2.3.1 Study area and sampling design

The Sado Estuary is the second largest estuarine system in Portugal, with an area of approximately 240 km<sup>2</sup>, being one of the most important wetlands in Europe (Bettencourt *et al.*, 2003) (Fig. 1). The intertidal areas comprise approximately 78 km<sup>2</sup>, of which 30% are salt marshes and intertidal flats (Caeiro *et al.*, 2005). Sado estuary has a semi-diurnal mesotidal system with tidal amplitude varying between 0.6 m and 1.6 m during spring and neap tides, respectively. The salinity gradient ranges between 0.75 at upstream to 35.34 at downstream (Sroczyńska *et al.* 2021), and it is influenced by the Sado's river flow (annual mean of 40m<sup>3</sup>s<sup>-1</sup>) changing with seasonal and inter-annual conditions and temperature can range from 10 to 26°C (Bettencourt *et al.*, 2003).

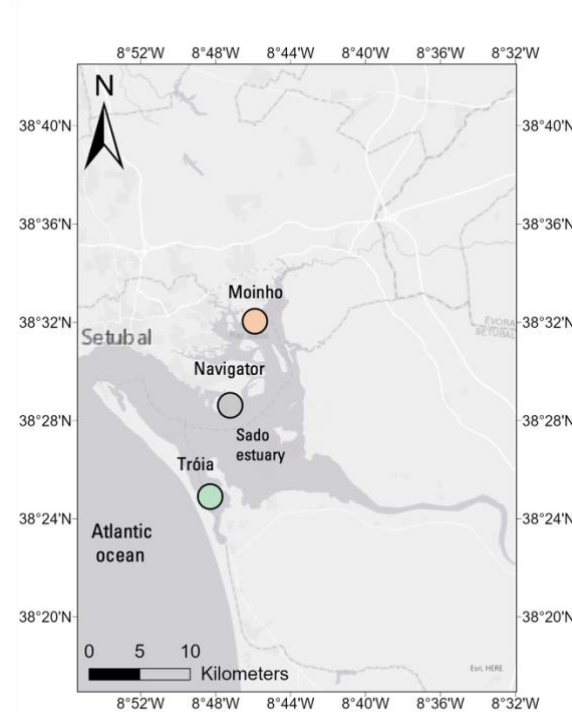


**Figure 1.** Sado estuary located at Southwest of Portugal ( $38^{\circ} 31' 14''$  N,  $8^{\circ} 53' 32''$  W). The selected sampling sites: Navigator (38.487033, -8.795686) (grey circle), highly industrialized area; Moinho (38.528101, -8.802995) (orange circle) with high organic inputs and Tróia (38.417317, -8.816433) (green circle) with coarser sediment. Moinho and Tróia are situated in a protected area.

The sampling sites were selected based on the expected differences in environmental conditions of the sediments according to water hydrodynamics within the Estuary (high/low water residence time), salinity gradient and the type of neighbouring anthropogenic activities (Caeiro *et al.*, 2005; Kennedy *et al.*, 2005; Sroczyńska *et al.*, 2021). Based on above-mentioned criteria three “Sampling Sites” were selected (Fig. 1): (1) Navigator Site located in the proximity of industrial area, dominated by fine sand, clay and high organic contents (Caeiro *et al.*, 2005); (2) Moinho Site is located within the borders of the Sado’s Nature Reserve, affected by the surrounding aquaculture activities with the predominance of clay-fine sediments (Kennedy *et al.*, 2005); (3) Tróia Site is located close to the Estuary mouth, is directly exposed to the main estuary channel, with high water exchange rate and high proportion of sand (Sroczyńska *et al.*, 2021).

Samples were collected between January and February of 2019 at each sampling site during neap low tide. At each site, three sediment samples were randomly collected for community analysis (nematode, n=3; bacteria, n=3) and for sediment physical-chemical analysis (n=3).

### 2.3.2 *Sediment physicochemical processing*

The characterization of sediment samples included the analyses of total organic matter (OM) (%), granulometry, and elemental analysis (C and N), according to Costa *et al.* (2011). The sediment OM content (derived from the total combustible C content) was determined from the organic loss-on-ignition after burning samples at 400 °C for 3h. Gravel (>2mm), sand (2-0.063mm) and fine fraction (FF) (<0.063mm) were determined by hydraulic sieving following disaggregation with pyrophosphate (Costa *et al.*, 2011). For elemental analyses, each sediment sample was first dried (60 °C) to constant weight and subsequently grinded on a planetary micro mill Pulverisette 7 Classic Line from Fritsch. About 1,5 - 2,3 mg of grinded and combusted samples were placed in tin capsules (3,2 x 4 mm) and run in a TruSpec® Micro CHNS elemental analyser (Version 2.72) from LECO, for the simultaneous analysis of total C (TC) and N (TN), as described in (Teixeira *et al.*, 2020). The independent infrared detectors detect the C content and the thermal conductivity detection system, the N content. The results are expressed as weight percentage (wt.%). The relative precision calculated from repeated measurement of samples and standards was 0.05%. In each sampling site, the salinity (SAL) of the sediment interstitial water was measured *in situ* using a VWR pHenomenal ® MU 600 H.

### 2.3.3 *Sample processing of benthic communities*

#### 2.3.3.1 *Total DNA extraction of sediment and amplicon sequencing*

Samples were taken from sediment surface at 10 cm depth into a sterilized 50-mL Falcon Tube (Ø 30mm), snap-freezed in dry ice and transported into the lab, where were stored at -80°C until DNA extraction. Total DNA extraction from 0.25 g of the sediment (surface between 0-3 cm) was conducted under sterile conditions, using the DNeasy® PowerSoil® kit (QIAGEN, Hilden, Germany) following the manufacturer's instructions. For cell lysis, samples were homogenized in a Precellys 24 Tissue Homogenizer (Bertin Instruments) for a total of 6 min under the program 2x 20s at 5000 rpm. The quality and quantity of total DNA was analysed through NanoDropTM2000 Spectrophotometer (Thermo Fisher) and Qubit4® fluorometer (Thermo Fisher Scientific). The presence of amplifiable DNA was confirmed by amplicon amplification with primers flanking the V4 region of 16S rRNA (515F–806R) (Caporaso *et al.*, 2012). A total of 9 samples were selected and sent for sequencing on Illumina MiSeq 2x 250bp (Illumina, Inc. San Diego, CA, USA) for INVIEW Microbiome at EUROFINS Genomics (Cologne, Germany). The protocol for preparation of the 16S rRNA gene library is detailed in 16S Metagenomic Sequencing Library Preparation Reference guide Part#15044223 Rev.B.

### 2.3.3.2 Bioinformatics analyses and data availability

Raw Illumina data was demultiplexed and quality-filtered using the defaults parameters of QIIME2 (Bolyen *et al.*, 2019). Single-end read data were denoised using DADA2 plugin (Callahan *et al.*, 2016), that discarded biased reads (e.g., chimeras, singlettons) and determined the amplicon sequence variants (ASVs). Further, ASVs were clustered into Operational Taxonomic Units (OTUs) at 97% similarity using VSEARCH open-reference OTU picking strategy against the SILVA v138 reference database (Quast *et al.*, 2013). Representative sequences were assigned taxonomy using a trained Naïve Bayes classifier (SILVA 138) (Bokulich *et al.*, 2021) for V3-V4 hyper variable region from 16S rRNA. The resulting OTUs table was filtered to keep only features with a total abundance over 10. OTUs classified as chloroplast, mitochondria, eukaryote, archaea, and unassigned were also removed. Filtered OTUs table was rarefied at 14000 sequences per sample, the lowest sequencing depth (Appendix A, Fig. A.1). Raw data supporting our results have been deposited into the NCBI SRA repository under the Bioproject PRJNA680980 and accessions SRR13151077-13151079 (NAV), SRR13165305-13165307 (TRO), and SRR13165323- SRR13165325 (MOI).

### 2.3.3.3 Nematode assemblages

Nematode samples were collected by forcing a hand core (3.8 cm inner diameter) to a depth of 3 cm into sediment. Each replicate was fixed in a 4% buffered formalin. Each sample was first rinsed on a 1000 µm mesh sieve and then on a 38 µm mesh sieve. Nematodes were extracted from sediment using LUDOX HS-40 colloidal silica at specific gravity 1.18 g cm<sup>-3</sup> (Heip *et al.*, 1985). Nematodes were counted using a stereomicroscope Leica M205 (100x magnification) and a counting dish. From each replicate, a random set of 120 nematodes was picked, transferred through a graded series of glycerol-ethanol solutions, stored in anhydrous glycerol, and mounted on slides for further identification (Vincx, 1996). Based on morphological characters, each nematode was identified until genus level (Olympus BX50 light microscope and cell software D Olympus, Japan). Taxonomic identification until genera, that is considered a level with good resolution in communities' assessment (Warwick *et al.*, 1998) and was made using pictorial keys (Warwick *et al.*, 1998; Platt & Warwick, 1983), and online identification keys/literature available in the Nemys database (Bezerra *et al.*, 2021).

### 2.3.4 Statistical analyses

The statistical analyses of the nematode assemblages and environmental data was performed using the PRIMER v6 software package (Clarke & Warwick, 2001) with

permutational analysis of variance (PERMANOVA) add-on package (Anderson *et al.*, 2008). Statistical analyses of 16S rRNA metagenomics was performed in Quantitative Insights into Microbial Ecology (QIIME2, version 2020.8) (Bolyen *et al.*, 2019) and phyloseq R package (McMurdie & Holmes, 2013).

#### 2.3.4.1 Environmental factors

To explore the multidimensional patterns of the environmental data, environmental matrix was analysed using Principal Component Analysis (PCA). The resemblance matrix was based on Euclidean distances and checked for uniform distribution, when necessary, the data was log (X+1) transformed and normalized (subtracting the mean and dividing by the standard deviation, for each variable) (Clarke and Warwick, 2001). The high correlated variables were selected and removed from the analysis.

#### 2.3.4.2 Bacterial and Nematode Communities

Bacterial communities  $\alpha$ - and  $\beta$ -diversity indexes were calculated with q2-diversity plugin. For  $\alpha$ -diversity analysis, several metrics were determined: Observed OTUs, Chao1, Shannon, Simpson, and Pielou's Evenness. To detect significant differences of  $\alpha$ -diversity indices between sites, Kruskal-Wallis tests were performed,  $p<0.05$ . To detect significant differences of  $\beta$ -diversity index was performed one-way PERMANOVA,  $p<0.05$ .

To assess the diversity of nematode assemblages, Margalef's richness Index (d) (Margalef, 1958) and Shannon Wiener diversity ( $H_0$ ) (Shannon & Weaver, 1963) were determined. To evaluate the trophic composition, each nematode genus was assigned to one of the four feeding groups based on mouth morphology, as follows: selective (1A) and non-selective (1B) deposit feeders, epigrowth feeders (2A) and omnivores/predators (2B) (Wieser, 1953). Based on the above-mentioned feeding-type classification, the reciprocal trophic diversity index ( $ITD^{-1}$ ) was calculated to ascertain higher trophic diversity (Heip *et al.*, 1985). The Maturity index (MI) was utilised as a life strategy measure, in which nematode genera were assigned to a colonizer/persister scale ( $c-p$  scale) varying between 1 (colonizers) and 5 (persisters) (Bongers *et al.*, 1990; Bongers *et al.*, 1991). One-way PERMANOVA analysis was performed to detect significant differences between nematode assemblages from each site, using the following design: fixed factor "Site" with 3 levels "Moinho"; "Navigator"; "Tróia", applying Bray-Curtis similarity matrix (Clarke & Warwick, 2001) with the significant level,  $p<0.05$ . The same statistical test was performed for all diversity and functional descriptors to detect

significant differences ( $p<0.05$ ) in the composition of the assemblages between “Sites”. Data dispersions were inspected with PERMDISP and nematode density data were square root transformed. Within both communities, the relative contribution of each taxon to the (dis)similarities between sites was calculated using the Bray Curtis method, SIMPER two-way crossover similarity percentage analysis (100% cut-off percentage).

#### *2.3.4.3 Environmental factors influencing the both communities*

Redundancy Analysis (RDA) was conducted to test linear combinations of the environmental variables that best explain the variation of the bacteria and nematode communities’ patterns. The response dataset consisted of Hellinger-transformed relative bacteria (observed OTUs with taxonomy assignment, corresponding to the 20 most abundant taxa) matrix, nematode genera abundance matrix (Legendre *et al.*, 2001) and explanatory environmental data. Variation inflation factors (VIF) were calculated to check for linear dependencies and to ensure that only variables with small VIFs (<10) were included. These were: “OM”, “Gravel”, “FF”, “SAL”, “Sand”, “TC” and “TN”. “TN” was removed from the analysis due to high (>95%) correlation with “TC”. All the variables were transformed using arcsine square root transformation, except for “TC” and salinity that was log10 transformed. A forward selection procedure, using function “ordiR2step()” was utilised to select only significant variables ( $p<0.05$ ). RDA analysis was performed in R (Legendre *et al.*, 2001) using “vegan” and “BiodiversityR” packages (Kindt and Coe, 2005). To test the correlation between both ordinations (bacteria and nematodes) it was performed Procrustean test. Procrustean test measures the degree of concordance between two or more datasets having different characteristics and if statistically significant, two datasets reflect in the same way the processes that determine their association (Peres-Neto and Jackson, 2001).

## **2.4 Results**

### *2.4.1 Environmental variables*

The environmental variables measured in sediment revealed three distinct sampling sites (Table B.1). Moinho sediment was predominantly characterized by the highest mean values (%) of Gravel ( $2.27 \pm 0.61$ ), FF ( $80.9 \pm 2.2$ ), OM ( $11.1 \pm 0.3$ ), TC ( $1.46 \pm 0.02$ ) and TN ( $0.16 \pm 0.002$ ), while sediments from Tróia and Navigator presented the highest values of Sand ( $79.0 \pm 7.2$  and  $78.6 \pm 2.1$ , respectively) and SAL ( $35.2 \pm 0.5$  and  $34.7 \pm 0.13$ , respectively) (Appendix B, Table B.1). These results were supported with a clear separation in the PCA (Principal Component Analysis) (PC1: 73,6% and PC2

22%) (Fig. 2). Moinho site was associated with high sediment OM content, FF and total TN, while Navigator and Tróia sites were associated with high SAL and %Gravel, respectively.

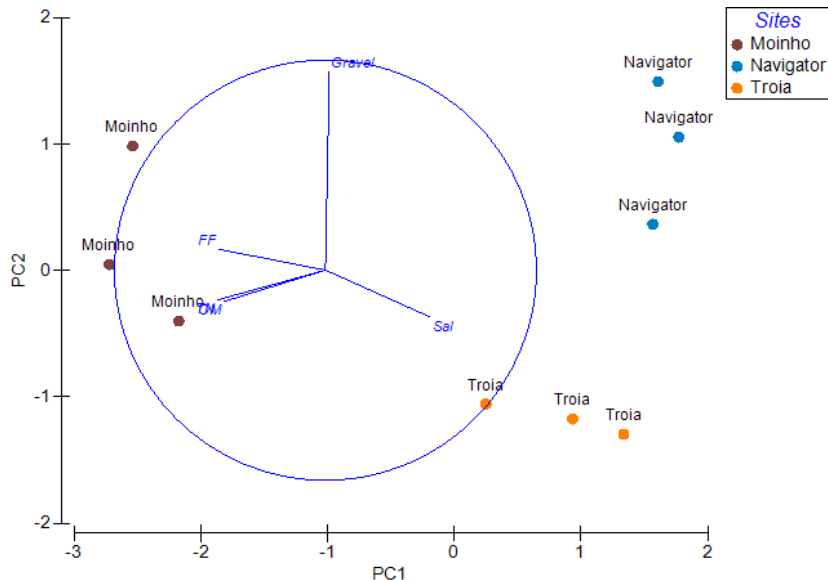


**Figure 2.** PCA plot based on Euclidian distances, according to environmental variables measured (Organic Matter: OM, gravel, Fine Fraction: FF, Total Nitrogen: TN and Salinity: sal) at each sampling site: Navigator, Moinho and Tróia, PC1 73,6%; PC2 22%.

#### 2.4.2 Sequencing statistics, diversity, and richness estimations

Illumina sequencing of the 9 sediment samples (Navigator, NAVR1-R3; Tróia, TROIAR1-R3; and Moinho, MOIR1-R3) yielded a total of 435.781 sequence reads, out of which 175.796 high-quality V3-V4 16S rRNA sequence reads were clustered into 1.683 OTUs. For each sample, 14000 reads were considered for further analysis after rarefaction (Appendix A, Fig. A.1). The estimated bacterial richness (Chao 1) ranged between  $608.2 \pm 46.1$  at Moinho and  $670.3 \pm 33.7$  at Navigator (Table 1).

**Table 1.** Mean  $\pm$  standard error (SE), n=3 of Alpha diversity descriptors (Observed OTUs, Chao1, Shannon, Simpson and Pielou's Evenness) calculated for the bacterial communities from each sampling site: Moinho (MOI), Navigator (NAV), Tróia (TROI).

	<b>Observed</b>	<b>Chao1</b>	<b>Shannon</b>	<b>Simpson</b>	<b>Pielou's Evenness</b>
MOI	$453.3 \pm 30.5$	$608.2 \pm 46.1$	$8.6 \pm 0.1$	$0.9 \pm 0.1$	$0.93 \pm 0.0006$
NAV	$498.6 \pm 30.1$	$670.3 \pm 33.7$	$8.7 \pm 0.1$	$0.9 \pm 0.1$	$0.93 \pm 0.004$
TROI	$455.3 \pm 43.3$	$616.1 \pm 63$	$8.6 \pm 0.1$	$0.9 \pm 0.1$	$0.93 \pm 0.001$

While the diversity and evenness were similar between sites, no significant differences were obtained ( $p=0.670$ ) in accordance with Kruskal-Wallis test (Appendix

B, Table B.2). In terms of  $\beta$ -diversity, significant differences in bacterial composition (PERMANOVA,  $p=0.007$ ) were obtained between sampling sites (Table 2).

**Table 2.** One-way PERMANOVA test, Beta-diversity of bacterial communities, between "Sites" (3 level fixed) for all variables analysed, ( $p=0.007$ ),  $n=3$ .

	<i>Degree of freedom</i>	<i>Sum squares</i>	<i>Mean square</i>	<i>Pseudo-F</i>	<i>P(perm)</i>	<i>Unique perms</i>	<i>P(MC)</i>
<i>Bacterial abundance</i>	2	1108.3	554.13	1.7106	<b>0.007</b>	280	0.0983
	6	1943.7	323.95				
	8	3052					

#### 2.4.3 Bacterial composition, abundance across sites

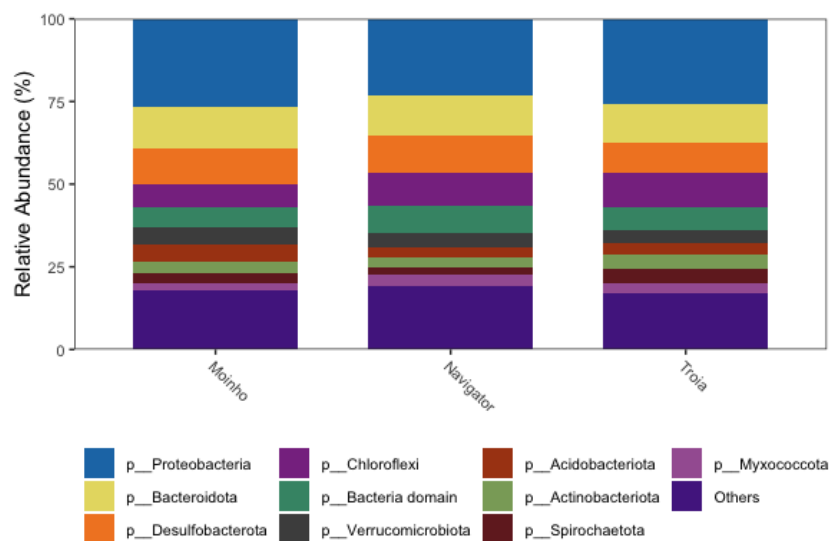


**Figure 3.** Bar plot displays the relative abundance of OTUs (%). Representing the top 10 most abundant Phylum in each site Moinho; Navigator and Tróia, the other relative frequencies are collapsed into the Others category.

Bacterial communities from all sites were composed by 53 phyla from which 18 phyla were the most representative, accounting for more than 90% of the taxa with more than 1% of the communities' total abundance (Fig. 3). The most relative abundant phyla were: *Pseudomonadota* (38-42%), *Desulfobacterota* (20-23%), *Chloroflexota* (5-9%), *Bacteroidota* (5-6%) and *Acidobacteriota* (2%). In all sampling sites the *Steroidobacterales*, *Desulfobacterales* and *Desulfobulbales* were the most relative abundant orders (Appendix A, Fig. A.2), which were represented by high relative abundance of the families *Woeseiaceae*, *Desulfobulbaceae* and *Desulfosarcinaceae* and genera *Woeseia* and *Sva0081\_sediment\_group*. The bacterial community of the Moinho was distinguished from the others by the different relative abundance of common

taxa and the genera *Sva1033* (3.6-3.7%), *B2M28* (1.9-2.8%) and *Candidatus Thiobios* (1.6-2.5%). While the Navigator community is distinguished from the others by the prevalence of the phylum *Cyanobacteria* which is exclusively represented by *Pleurocapsa\_PCC-7319* genus (0-4%) (*Xenococcaceae*). Tróia's bacterial community was distinguished from the others by the different relative abundance of common taxa and the genera *SEEP-SRB1* (1.7-2.6%), *SBR1031* (1.8-3.7%) and *Sva1033* (2.7-3.6%). The SIMPER analysis showed that *Woeseia*, *Sva0081\_sediment\_group* and *Sva1033* (Similarity  $\geq 68\%$ ) contributed the most for the similarity within the three sampling sites. Moreover, the great contributors for the major dissimilarities between sites were the genera *SEEP-SRB1* and *SBR1031* (Moinho vs Tróia, dissimilarity 29.94%), *Pleurocapsa\_PCC-7319*, *Myxosarcina\_GII* and *Cyanobacterium\_CLg1* from the order *Cyanobacteriales* (Moinho vs Navigator and Navigator vs Tróia, dissimilarity 34-36%) (Appendix B, Table B.3).

#### 2.4.4 Density and structural diversity of nematode assemblages

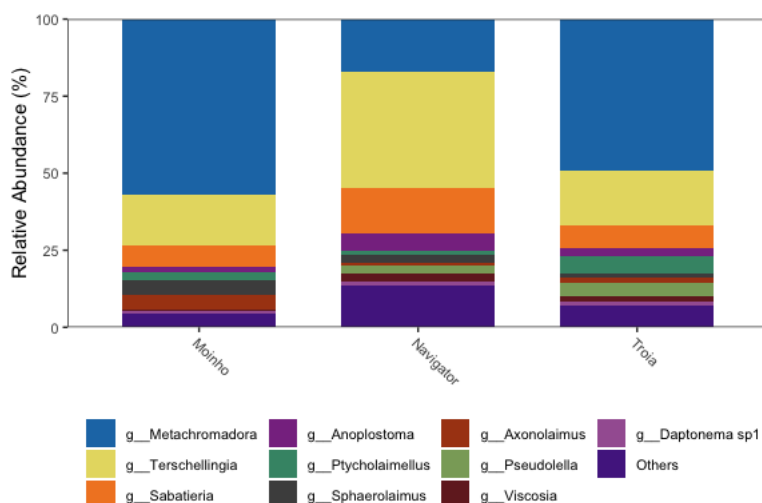


**Figure 4.** Bar plot displays the relative density (%) of the top 10 most abundant of nematodes genera in each sampling site Moinho, Navigator and Tróia, the other relative frequencies are collapsed into the Others category.

Overall, the nematode density varied between 2706.3 and 13466.9 individuals per 10 cm<sup>-2</sup> (Table 3). The nematode assemblages of Moinho site registered the mean density ( $13466.9 \pm 1631.1$  ind. 10 cm<sup>-2</sup>), whilst the lowest mean density was obtained at Navigator sampling site ( $2706.4 \pm 1092$  ind. 10 cm<sup>-2</sup>). PERMANOVA analysis for the nematode density revealed significant differences between "Sites",  $p= 0.012$  (Appendix B, Table B.4). The nematode assemblages of all sites were represented by the predominance of the orders Chromadorida, Monhysterida and Enoplida accounting for

more than 80% of the total relative density. All assemblages were composed by the families Linhomoeidae, Desmodoridae and Comesomatidae. Nematode assemblages of Moinho are composed by 20 genera belonging to 13 families from which the genera *Metachromadora* (56%), *Terschellingia* (14%), *Sabatieria* (7%) and *Axonolaimus* (5%) account for 84% of the total relative density. The nematode assemblages collected at Navigator site were composed by 29 genera belonging to 14 families with genera *Terschellingia* (52%), *Metachromadora* (15%), *Sabatieria* (9%) and *Anoplostoma* (5%) accounting for 82% of the total relative density. The nematodes identified at Tróia sampling site were composed of 20 genera from 12 families with genera *Metachromadora* (49%), *Terschellingia* (16%), *Ptycholaimellus* (7%) and *Sabatieria* (7%) representing 80% of the assemblages collected (Fig. 4 and Appendix A, Fig. A.3).

**Table 3.** Mean density  $\pm$  standard error (SE), n=3, of the nematode genera (number of individuals per  $10\text{ cm}^{-2}$ ), at each sampling site (Moinho, Navigator and Tróia). Trophic group (TG) and  $c-p$  value of each genera included. Only the most abundant genera are included in this table.

Genera	TG	$c-p$ -value	Moinho	Navigator	Tróia
<i>Metachromadora</i>	2B	2	$7557.7 \pm 803$	$412.8 \pm 127$	$1872.5 \pm 249$
<i>Terschellingia</i>	1A	3	$1868.2 \pm 777$	$1413.8 \pm 844$	$613.6 \pm 111$
<i>Sabatieria</i>	1B	2	$1146.1 \pm 653$	$256.2 \pm 40$	$285.4 \pm 50$
<i>Axonolaimus</i>	1B	2	$733.8 \pm 294$	$12.5 \pm 6$	$68.4 \pm 11$
<i>Sphaerolaimus</i>	2B	3	$730.9 \pm 410$	$45.7 \pm 6$	$42.1 \pm 4$
<i>Ptycholaimellus</i>	2A	3	$371.4 \pm 113$	$19 \pm 7$	$286.2 \pm 212$
<i>Anoplostoma</i>	1B	2	$204.7 \pm 94$	$131.5 \pm 44$	$95.6 \pm 56$
<i>Daptonema</i>	1B	2	$169.7 \pm 68$	$23.8 \pm 11$	$16.3 \pm 12$
<i>Daptonema sp1</i>	1B	2	$149.1 \pm 115$	$28.5 \pm 9$	$59 \pm 34$
<i>Spilophorella</i>	2A	2	$99.4 \pm 77$	0	$7.9 \pm 6$
<i>Microlaimus</i>	2A	2	$64.1 \pm 49$	$52 \pm 40$	$29.7 \pm 23$
<i>Comesoma</i>	1B	2	$49.7 \pm 38$	$3.2 \pm 2$	0
<i>Dichromadora</i>	2A	2	$49.7 \pm 38$	$7.9 \pm 3$	$49.1 \pm 38$
<i>Oncholaimellus</i>	2B	3	$49.7 \pm 38$	$27.8 \pm 21$	0
<i>Praeacanthonchus</i>	2A	4	$49.7 \pm 38$	$3.3 \pm 2$	$24.3 \pm 10$
<i>Anticoma</i>	1A	2	$35.1 \pm 27$	0	0
<i>Cyatholaimus</i>	2A	2	$35.1 \pm 27$	$27.1 \pm 11$	0
<i>Prochromadorella</i>	2A	2	$35.1 \pm 27$	0	0
<i>Viscosa</i>	2B	3	$35.1 \pm 27$	$34.9 \pm 13$	$73.4 \pm 47$
Total			$13466.8 \pm 3745$	$2706.3 \pm 1304$	$3842.8 \pm 1036$

SIMPER analysis showed that *Metachromadora*, *Terschellingia*, *Sabatieria* and *Axonolaimus* were the genera that most contributed for the similarity within each site, while *Metachromadora*, *Terschellingia* and *Axonolaimus* were the genera that most contributed for the dissimilarity between sites (Appendix B, Fig. B.3). Although the

assemblages of Moinho and Navigator were clearly separated, the nematode community patterns showed distinct spatial distribution comparing with bacterial communities.

#### 2.4.5 Structural diversity, trophic composition and functional diversity

**Table 4.** Mean  $\pm$  standard error (SE), n=3 of diversity descriptors of nematode assemblages (S) genera, (d) Margalef, (H) Shannon (logo based); (ITD $^{-1}$ ) reciprocal Index Trophic Diversity and (MI) Maturity Index. from each sampling site: Moinho (MOI), Navigator (NAV), Tróia (TROIA).

<b>Samples</b>	<b>S</b>	<b>d</b>	<b>H'(log.)</b>	<b>ITD<math>^{-1}</math></b>	<b>MI</b>
MOI	11.3 $\pm$ 0.9	1.1 $\pm$ 0.08	1.4 $\pm$ 0.1	2 $\pm$ 0.1	2.2 $\pm$ 0.06
NAV	17.6 $\pm$ 1.5	2.2 $\pm$ 0.3	1.9 $\pm$ 0.2	2.5 $\pm$ 0.2	2.4 $\pm$ 0.09
TROIA	13 $\pm$ 1.2	1.4 $\pm$ 0.1	1.6 $\pm$ 0.09	2.5 $\pm$ 0.15	2.3 $\pm$ 0.02

According to PERMANOVA analysis based on structural diversity descriptors (d, H', ITD $^{-1}$  and MI), significant differences were obtained between "Sites" ( $p = 0.038$ ) for Margalef's richness index (d) (Appendix B, Table B.4), whose highest diversity values were obtained at Navigator (Table 4). In addition to the high abundance of omnivores/predators (2B) at all sampling sites, particularly at Moinho (52% of total density), at Navigator selective (1A) and non-selective (1B) deposit feeders accounted for 63% of the Navigator assemblages. Tróia nematode assemblages were mainly comprised of omnivores/predators (2B: 45%) and selective deposit feeders (1A: 18%) (Table 3). PERMANOVA analysis of the nematode trophic composition data revealed significant differences between "Sites" ( $p=0.0029$ ) (Appendix B, Table B.4).

The ITD $^{-1}$  values ranged from 1.7 to 3 and were very similar between assemblages for all sites. The MI varied from 2.1 to 2.7 and the highest mean value was obtained in Navigator assemblages. These results revealed the colonizer strategy (*c-p value* 2) dominated at Moinho (57%) and Tróia (42%). Navigator sampling site was PERMANOVA analysis of the functional diversity descriptors revealed no significance differences between "Sites" (ITD $^{-1}$ ,  $p = 0.246$ ; MI,  $p=0.064$ ) (Appendix B, Table B.4), highlighting the prevalence of similar trophic diversity and opportunistic strategies among nematodes inhabiting all three sites. dominated (46%) by the genera classified as *c-p value* 3.

#### 2.4.6 Environmental variables influencing the spatial patterns of bacterial and nematodes assemblages

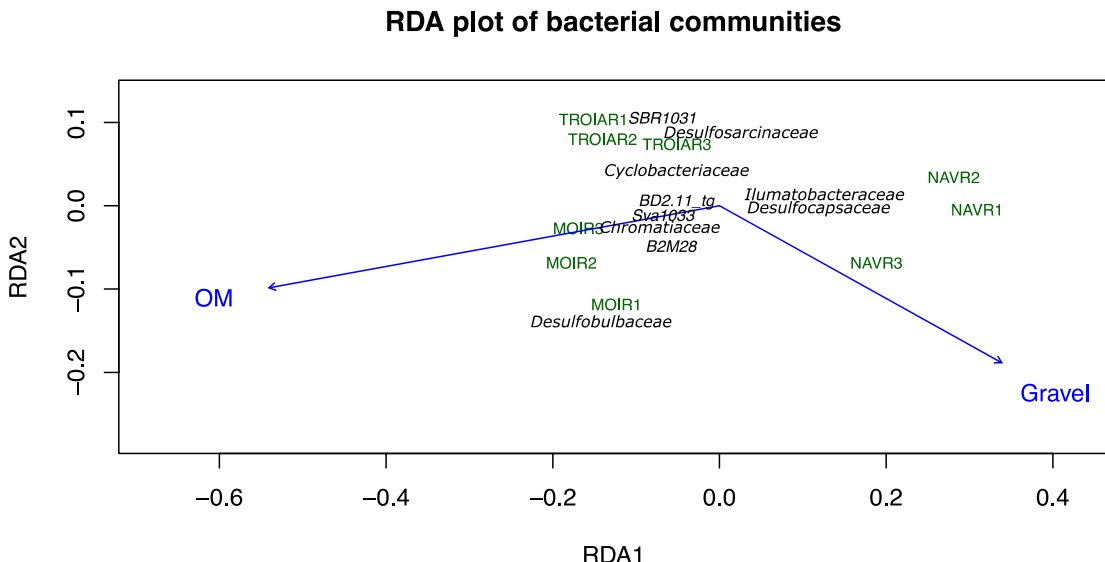


**Figure 5 (A).** Constrained redundancy analysis displaying contributions of environmental factors to bacterial composition (RDA1= 56% and RDA2 = 8%). The species that are displayed in the graph have a goodness of fit higher than 0.4.

The RDA ordination on bacterial communities constrained by the environmental variables was highly significant ( $F = 5.44$ ,  $p=0.001$ , adjusted  $R^2Ad = 0.53$ ) (Fig. 5A). The cumulative explained proportion of both axes was remarkably high reaching 64.44%. The environmental variables that emerged as significant were % Gravel ( $p=0.045$ ) and % OM ( $p=0.005$ ). According to triplot (Fig. 5A), there was a very clear separation of all sites, particularly Navigator with clear separation from Moinho and Tróia along the first axis accounting for the highest proportion explained (56.27 %) of the total variability in community data. High proportions of gravel were strongly associated with NAVR3. *Desulfocapsaceae* and *Ilumatobacteraceae* families were associated to NAVR1 and NAVR2. Moinho was characterized by high OM deposits with certain affinity of: *Desulfobulbaceae*, *B2M28*, *Chromatiaceae*, and *Sva1033* families. Tróia sampling sites (TROIAR1-R3) were tightly grouped together with strong affinity of *SBR1031*, *Desulfosarcinaceae*, *Cyclobacteriaceae* as well as *BD2.11\_terrrestrial group* (Fig. 5A).

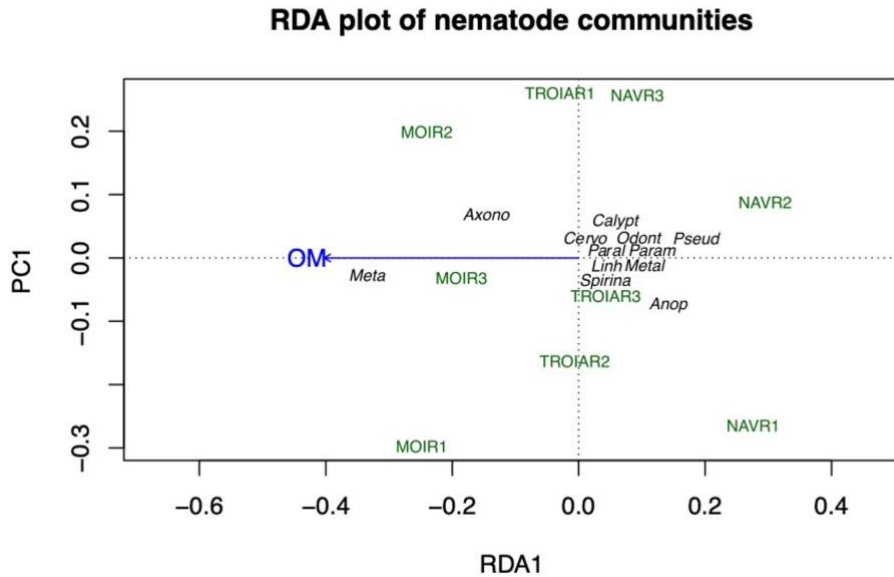


**Figure 5 (B).** Constrained redundancy analysis displaying contributions of environmental factors to nematode assemblages (RDA1= 25.5% and RDA2 = 28.5%). The species that are displayed in the graph have a goodness of fit higher than 0.2.

The RDA ordination on nematode's assemblages data constrained by the environmental variables was significant ( $F=2.40$   $p=0.023$ , adjusted  $R^2_{Adj}=0.15$ ), however after forward selection of the variables, solely OM emerged as a significant variable ( $p=0.025$ ), leaving only first RDA axis explaining 25% of the variability in the variance in nematode assemblages data (Fig. 5B). Contrary to bacterial communities, there is no obvious site separation, and it can be also observed a certain dispersal of all of the sites along both axes. Navigator sampling stations are separated from the remaining locations along the first axis. The only significant environmental variable emerged was OM that was highly associated to MOIR3 characterized the presence of *Metachromadora* genus. Genera associated to NAVR2 included *Odontophora* and *Calyptromema*. *Axonolaimus* was correlated with MOIR2 while *Metalinhomoeus* and *Spirina* were associated to TROIAR3. The presence of *Anoplostoma* was related to NAVR1. Moinho and Tróia were not separated at the RDA plot, but the separation of sites was rather exhibited at the level of sampling stations, within each site than by the level of sites. The result of Procrustean test that analysed the correlation between both ordinations was not significant (Correlation in a symmetric Procrustes rotation: 0.6743,  $p=0.142$ ) indicating significantly different patterns in the ordination for nematode and bacterial communities.

## 2.5 Discussion

The high spectrum of environmental conditions registered in estuarine sediment are well known to capture a variety of adaptive responses in benthic communities (Sroczyńska et al., 2021). In this study, the spatial distributions of bacterial and nematode assemblages were studied at three different sites of Sado Estuary to evaluate the hypothesis that spatial distribution of both communities follow close patterns, responding congruently to the sediment conditions. Concerning environmental variables, the results showed a clear spatial distribution pattern undermining significant differences between sites for both communities. Still, we could not observe these patterns between bacterial communities and nematodes assemblages: bacterial communities of Navigator were separated from the other communities, while nematode assemblages of Moinho were set apart from the Navigator and Troia sites.

The influence of the environmental conditions on the spatial distribution patterns of the bacterial communities is well known (Jessen et al., 2017). *Desulfobacterota* was one of the most abundant phyla present at all sites, known to play important roles in most of the biogeochemical processes in the anoxic layer of estuarine sediments (e.g., anaerobic processes in S and C cycles) (Baker et al., 2015; Jessen et al., 2017; Raggi et al., 2020). The presence of *Woeseiaceae* and *Halieaceae* families were also detected in all sampling sites, which is corroborated by their wide occurrence and contribution to the biogeochemical processes in marine sediments (Spring et al., 2015; Marshall et al., 2021). Symbiotic organisms from the family *Rhodobacteraceae* (De Mesel et al., 2006) and sulfur-oxidizing bacteria *Candidatus Thiobios* were also detected in abundance in all sampling sites. These organisms are recognized to be involved in symbiotic mechanisms with nematodes, providing them beneficial physiologic adaptations (such as protection against adverse conditions) (Ott et al., 2004; Bayer et al., 2009; Zimmermann et al., 2016). In the case of Moinho site, the high prevalence of *Desulfobulbaceae* family may evidence the anoxic conditions of the sediments, since the metabolic processes of these sulphate reducers are mainly involved in anaerobic degradation of OM (Raggi et al., 2020). Cyanobacteria phylum was responsible for separating bacterial communities of Navigator from the other sites, with the exclusive presence of the unicellular and pseudo-filamentous genus *Pleurocapsa* (Kolda et al., 2020). These organisms are regarded as ecological important groups in estuarine and coastal environments being primary producers and N/C fixators. Their increased growth highlights the presence of opportunistic species with the release of cyanotoxins (Kolda et al., 2020). The distribution patterns of bacterial communities at the Navigator site are strictly related with the high proportions of %Gravel and SAL, which is in accordance with

Kolda et al., (2020), that showed the preference of cyanobacteria for a sandy gravel type of sediment.

At Sado's Estuary, the density of nematode assemblages was high considering other Portuguese estuaries (SW coast of Europe) such as Mira and Mondego (Alves et al., 2013; Materatski et al., 2015). The Moinho sampling site registered the highest nematode density, which may be related with high OM content available at the bottom of the sediments (Moens et al., 2005; Adão et al., 2009). The predominance of sandy sediments in Navigator and Tróia sampling sites contributed to the low nematode density but a diversity increase, possibly related with the broader range of microhabitats available for nematodes in these sediments when compared to muddy ones (Steyaert et al., 2003). In all sampling sites, the dominant genera were *Metachromadora*, *Sabatieria*, *Axonolaimus* and *Terschellingia*, similar composition to mud-flat areas of Mondego estuary (Alves et al., 2013) and also to the previous study in Sado estuary (Sroczyńska et al., 2021). The spatial distribution patterns base on ITD<sup>-1</sup> and MI indexes were also similar to those verified in Mondego, Mira and Sado estuaries (Alves et al., 2009; Materatski et al., 2015; Sroczyńska et al., 2021a). However, the trophic composition of nematode assemblages showed different results from previous studies (i.e., usually dominated by non-selective deposit feeders (1B) and epistrate feeders (2A) (Alves et al., 2013; Branco et al., 2018). The omnivores/predators (2B) were abundant in all sampling sites, which are mainly grazers of microphytobenthos and bacteria (D'Hondt et al., 2018; Van der Heijden et al., 2019). These organisms are usually able to vary in their feeding mode in response to the food availability being difficult to draw a general trend in abundance of these feeding groups (De Mesel et al., 2006; Van der Heijden et al., 2019). Nematode assemblages sampled in Navigator showed a high percentage of non- and selective deposit feeders (1A and 1B) such as *Terschellingia* and *Sabatieria*, which are usually favoured by the depositional nature and hypoxic conditions of the sediment. These observations highlighted the possibility that the bacterial composition might be related to the feeding preferences of nematodes and to their affinity for cyanobacterial biofilms (Derycke et al., 2016; D'Hondt et al., 2018). Moreover, Vafeiadou et al., (2013) and Sahraean et al., (2017) also demonstrated by stable isotope analysis that *Terschellingia* can thrive under conditions that benefit the chemoautotrophic prokaryotic activity by using methane-derived carbon as energy source. Despite the high abundance and co-occurring of *Terschellingia* and *Cyanobacteria* at Navigator, it was not possible to draw conclusion about the type of nematode-bacteria interactions at this stage. Apart from the shared environmental preferences and other indirect relationships, further hypothesis-based studies are needed to better understand the potential interactions between co-occurring taxa.

The RDA analysis demonstrated that variables that contribute most to spatial distribution patterns for both nematode and bacterial communities, were OM and %Gravel. Besides bacterial-based RDA had only two environmental variables significantly correlated with the community ordination, its overall significance and remarkably high *AdjRsquare* indicates that only these two variables were able to predict the majority of the variability occurred in bacterial community data. These observations were not reported by other studies, so far. Nematode assemblages are considered a good ecological indicator to specific sampling locations (Branco et al., 2018). In this study, the distribution patterns of this community may suggest that their responses are driven by site specific factors, acting at the small spatial scale.

## 2.6 Concluding remarks

Using a multivariate approach on two datasets delivered from metagenomic assessment (16S rRNA amplicon sequencing) of bacteria and morphological assessment of nematodes allowed us to analyse the spatial distributional patterns under different ecological sediment conditions. We conclude the spatial pattern of nematodes is driven by small-scale factors within each site, explained by the sediment OM content. However, the spatial pattern of bacteria is driven by factors acting on larger scale between sites, explained by the %Gravel and sediment OM content. The methodology applied was not sensitive enough to ascertain estuarine sediment bacteria-nematode interactions. However, the spatial patterns presented by both communities in this study set a fundamental ground for future research on functional interactions between bacteria and nematodes.

## 2.7 References

Adão H, Alves AS, Patrício J, et al (2009) Spatial distribution of subtidal Nematoda communities along the salinity gradient in southern European estuaries. *Acta Oecologica* 35:287–300. <https://doi.org/10.1016/j.actao.2008.11.007>

Alves AS, Adão H, Patrício J, et al (2009) Spatial distribution of subtidal meiobenthos along estuarine gradients in two southern European estuaries (Portugal). *J Mar Biol Assoc United Kingdom* 89:1529–1540. <https://doi.org/10.1017/S0025315409000691>

Alves ASS, Adão H, Ferrero TJJ, et al (2013) Benthic meiofauna as indicator of ecological changes in estuarine ecosystems: The use of nematodes in ecological

quality assessment. Ecol Indic 24:462–475.  
<https://doi.org/10.1016/J.ECOLIND.2012.07.013>

Anderson MJ, Gorley RN, Clarke KR (2008) PERMANOVA+ for PRIMER: Guide to Software and Statistical Methods. In: Plymouth, UK

Baker BJ, Lazar CS, Teske AP, Dick GJ (2015) Genomic resolution of linkages in carbon, nitrogen, and sulfur cycling among widespread estuary sediment bacteria.  
<https://doi.org/10.1186/s40168-015-0077-6>

Bayer C, Heindl NR, Rinke C, Lücker S, Ott J & Bulgheresi S (2009) Molecular characterization of the symbionts associated with marine nematodes of the genus Robbea. Environ Microbiol Rep 1:136–144. <https://doi.org/10.1111/j.1758-2229.2009.00019.x>

Beninger P. G. (2018) (ed.), Mudflat Ecology, Aquatic Ecology Series 7, Springer Nature Switzerland. [https://doi.org/10.1007/978-3-319-99194-8\\_591](https://doi.org/10.1007/978-3-319-99194-8_591)

Bettencourt A M, Bricker S B, Ferreira J G, Franco A, Marques J C, Melo J J, Nobre A, Ramos L, Reis C S, Salas F, Silva M C, Simas T, & Wolff W J (2004). Typology and reference conditions for Portuguese transitional and coastal waters. Institute of Marine Research.

Bezerra TN, Eisendle U, Hodda M, et al (2021) Nemys: World Database of Nematodes. Anisakidae Railliet & Henry, 1912.

<http://nemys.ugent.be/aphia.php?p=taxdetails&id=19961>. Accessed 29 Sep 2021

Bokulich N, Robeson M, Dillon M, et al (2021) bokulich-lab/RESCRIPT: 2021.8.0.dev0. <https://doi.org/10.5281/ZENODO.4811136>

Bolyen E, Rideout JR, Dillon MR, et al (2019) QIIME 2: Reproducible, interactive, scalable, and extensible microbiome data science. <https://doi.org/10.7287/peerj.preprints.27295v2>

Bonaglia S, Nascimento FJA, Bartoli M, Klawonn I., Brüchert V. (2014) Meiofauna increases bacterial denitrification in marine sediments. Nat Commun 5, 5133.<https://doi.org/10.1038/ncomms6133>

Bongers, T., 1990. The Maturity Index, the evolution of nematode life history traits, adaptive radiation and cp-scaling. Plant Soil 212, 13–22.

Bongers, T., Alkemade, R., Yeates, G.W., 1991. Interpretation of disturbance-induced maturity decrease in marine nematode assemblages by means of the Maturity Index. *Mar. Ecol. Prog. Ser.* 76, 135–142.

Branco J, Pedro S, Alves AS, Ribeiro C, Materatski P, Pires R, Caçador I, Adão H (2018) Natural recovery of *Zostera noltii* seagrass beds and benthic nematode assemblage responses to physical disturbance caused by traditional harvesting activities. *J Exp Mar Bio Ecol* 502:191–202. <https://doi.org/10.1016/J.JEMBE.2017.03.003>

Broman E, Bonaglia S, Holovachov O, Marzocchi U, Hall P & Nascimento F (2020) Uncovering diversity and metabolic spectrum of animals in dead zone sediments. *Commun Biol* 3:1–12. <https://doi.org/10.1038/s42003-020-0822-7>

Bulseco A N, Vineis J H, Murphy A E, Spivak A, Giblin E A, Tucker J, Bowen L J(2020) Metagenomics coupled with biogeochemical rates measurements provide evidence that nitrate addition stimulates respiration in salt marsh sediments. *Limnol Oceanogr* 65:S321–S339. <https://doi.org/10.1002/lio.11326>

Caeiro S, Costa MH, Ramos TB, Fernandes F, Silveira N, Coimbra A, Medeiros G & Painho M (2005) Assessing heavy metal contamination in Sado Estuary sediment: An index analysis approach. *Ecol Indic* 5:151–169. <https://doi.org/10.1016/j.ecolind.2005.02.001>

Callahan B J, McMurdie P J, Rosen M J, Han W A, Johnson A J & Holmes P S (2016) DADA2: High-resolution sample inference from Illumina amplicon data. *Nat Methods*, 137 13:581–583. <https://doi.org/10.1038/nmeth.3869>

Caporaso J G, Lauber C L, Walters W A, Berg-Lyons D, Huntley J, Fierer N, Owens M S, Betley J, Fraser L, Bauer M, Gormley N, Gilbert J A, Smith G & Knight R (2012) Ultra-high-throughput microbial community analysis on the Illumina HiSeq and MiSeq platforms. *ISME J* 6:1621–1624. <https://doi.org/10.1038/ismej.2012.8>

Clarke, K.R., Warwick, R.M., 2001. Changes in Marine Communities: an Approach to Statistical Analysis and Interpretation, second ed.

Costa P, Caeiro S, Lobo J, Martins M, Ferreira M A, Caetano M, CarlosVale C, Del Valls A T, Costa M H (2011) Estuarine ecological risk based on hepatic histopathological indices from laboratory and in situ tested fish. *Marine Pollution Bulletin* 62 (2011) 55–65. <https://doi.org/10.1016/j.marpolbul.2010.09.009>

D'Hondt AS, Stock W, Blommaert L, Moens T, Sabbeb K (2018) Nematodes stimulate biomass accumulation in a multispecies diatom biofilm. *Mar Environ Res* 140:78–89. <https://doi.org/10.1016/j.marenvres.2018.06.005>

De Mesel I, Derycke S, Swings J, Vincx M, Moens T (2006) Role of nematodes in decomposition processes: Does within-trophic group diversity matter? *Mar Ecol Prog Ser* 321:157–166. <https://doi.org/10.3354/meps321157>

Derycke S, De Meester N, Rigaux A, Creer S., Bik H., Thomas W. K., Moens T. (2016) Coexisting cryptic species of the *Litoditis marina* complex (Nematoda) show differential resource use and have distinct microbiomes with high intraspecific variability. *Mol Ecol* 25:2093–2110. <https://doi.org/10.1111/mec.13597>

Hargrave B T, Holmer M, Newcombe C P (2008) Towards a classification of organic enrichment in marine sediments based on biogeochemical indicators. *Mar Pollut Bull* 56:810–824. <https://doi.org/10.1016/J.MARPOLBUL.2008.02.006>

Heip C, Vincx M, Vranken G (1985) The ecology of marine nematodes

Vincx M (1996) Meiofauna in marine and freshwater sediments. In: Meiofauna in marine and freshwater sediments. In Hall G.S. (ed.) *Methods for the Examination of Organismal Diversity in Soils and Sediments*, Wallinfort, UK. pp 187–195

Jessen G L, Lichtschlag A, Ramette A, Pantoja S, Rossel E P, Schubert J C, Struck U & Boetius A (2017) Hypoxia causes preservation of labile organic matter and changes seafloor microbial community composition (Black Sea). *Sci Adv* 3:e1601897. <https://doi.org/10.1126/sciadv.1601897>

Kennedy P, Kennedy H, and Papadimitriou S (2005) The effect of acidification on the determination of organic carbon, total nitrogen and their stable isotopic composition in algae and marine sediment. *Rapid Commun. Mass Spectrom.* 2005; 19: 1063–1068. doi: 10.1002/rcm.1889

Kindt R, Coe R (2005) Tree Diversity Analysis. A manual and software for common statistical methods and biodiversity studies. <https://doi.org/10.13140/RG.2.1.1993.7684>

Kolda A, Ljubešić Z, Gavrilović A, Jug-Dujaković J, Pikelj K & Kapetanović D (2020) Metabarcoding Cyanobacteria in coastal waters and sediment in central and southern Adriatic Sea. *hrcak.srce.hr* 79:157–169. <https://doi.org/10.37427/botcro->

2020-021

Legendre P, Gallagher ED (2001) Ecologically meaningful transformations for ordination of species data. *Oecologia* 129:271–280. <https://doi.org/10.1007/s004420100716>

Margalef, D.R., 1958. Information theory in ecology. *Gen. Syst.* 3, 36–71.

Marshall A, Longmore A, Phillips L, Tang C, Hayden L H, Heidelberg K B, Mele P (2021) Nitrogen cycling in coastal sediment microbial communities with seasonally variable benthic nutrient fluxes. *Aquat Microb Ecol* 86:1–19. <https://doi.org/10.3354/ame01954>

Materatski P, Vafeiadou A-MM, Ribeiro R, Moens T, Adão H (2015) A comparative analysis of benthic nematode assemblages from *Zostera noltii* beds before and after a major vegetation collapse. *Estuar Coast Shelf Sci* 167:256–268. <https://doi.org/10.1016/j.ecss.2015.07.001>

McMurdie P J & Holmes S (2013) phyloseq: An R Package for Reproducible Interactive Analysis and Graphics of Microbiome Census Data. *PLoS One* 8:e61217. <https://doi.org/10.1371/JOURNAL.PONE.0061217>

16S Metagenomic Sequencing Library Preparation Reference guide Part#15044223.Rev.B (<https://support.illumina.com>)" (accessed: 23-06-2023).

Moens T, Bouillon S, Gallucci F (2005) Dual stable isotope abundances unravel trophic position of estuarine nematodes. *J Mar Biol Assoc United Kingdom* 85:1401–1407. <https://doi.org/10.1017/S0025315405012580>

Nascimento F J A, Näslund J, Elmgren R (2012) Meiofauna enhances organic matter mineralization in soft sediment ecosystems. *Limnol Oceanogr* 57:338–346. <https://doi.org/10.4319/lo.2012.57.1.0338>

Ott J, Bright M, Bulgheresi SV (2004) Symbioses between Marine Nematodes and Sulfur-oxidizing Chemoautotrophic Bacteria

Platt H, Warwick R (1983) Freeliving marine nematodes. Part 1: British enoplids. Pictorial key to world genera and notes for the identification of British species.

Peres-Neto P R, Jackson D A (2001) How well do multivariate data sets match? The advantages of a Procrustean superimposition approach over the Mantel test. *Oecologia* 2001 1292 129:169–178. <https://doi.org/10.1007/S004420100720>

Quast C, Pruesse E, Yilmaz P, Gerken J, Schweer T, Yarza P, Peplies J, Glöckner O F (2013) The SILVA ribosomal RNA gene database project: improved data processing and web-based tools. *Nucleic Acids Res* 41:D590–D596. <https://doi.org/10.1093/NAR/GKS1219>

R Core Team (2012) R: A language and environment for statistical computing

Raggi L, García-Guevara F, Godoy-Lozano E E, Martínez-Santana A, Escobar-Zepeda A, Gutierrez-Rios M R, Loza A, Merino E, Sanchez-Flores A, Licea-Navarro A, Pardo-Lopez L, Segovia L & Juarez K (2020) Metagenomic Profiling and Microbial Metabolic Potential of Perdido Fold Belt (NW) and Campeche Knolls (SE) in the Gulf of Mexico. *Front Microbiol* 11:1825. <https://doi.org/10.3389/fmicb.2020.01825>

Ridall A, Ingels J (2021) Suitability of Free-Living Marine Nematodes as Bioindicators: Status and Future Considerations. *Front Mar Sci* 0:863. <https://doi.org/10.3389/ FMARS.2021.685327>

Sahraean N, Bezerra T C, Ejlali Khanaghah K, Mosallanejad H, Ranst V E & Moens T (2017) Effects of pollution on nematode assemblage structure and diversity on beaches of the northern Persian Gulf. *Hydrobiologia* 799:349–369. <https://doi.org/10.1007/s10750-017-3234-z>

Schratzberger M, Ingels J (2018) Meiofauna matters: The roles of meiofauna in benthic ecosystems. *J Exp Mar Bio Ecol* 502:12–25. <https://doi.org/10.1016/j.jembe.2017.01.007>

Schratzberger M, Somerfield P J (2020) Effects of widespread human disturbances in the marine environment suggest a new agenda for meiofauna research is needed. *Sci. Total Environ.* 728:138435

Schuelke T, Pereira T J., Hardy S M, Bik H M (2018) Nematode-associated microbial taxa do not correlate with host phylogeny, geographic region or feeding morphology in marine sediment habitats. *Mol Ecol* 27: 1930–1951.

Semprucci F, Balsamo M (2014) Free-Living Marine Nematodes as Bioindicators: Past, Present and Future Perspectives. *Trends Environ Sci* 17–36

Shannon C E, Weaver W (1963) The Mathematical Theory of Communication. Univ Illinois Press Illinois

Spring S, Scheuner C, Göker M, Klenk H P (2015) A taxonomic framework for emerging groups of ecologically important marine gammaproteobacteria based on the reconstruction of evolutionary relationships using genome-scale data. *Front Microbiol* 0:281. <https://doi.org/10.3389/FMICB.2015.00281>

Sroczyńska K, Chainho P, Vieira S, Adão H (2021) What makes a better indicator? Taxonomic vs functional response of nematodes to estuarine gradient. *Ecol Indic* 121:107113. <https://doi.org/10.1016/j.ecolind.2020.107113>

Sroczyńska K, Conde A, Chainho P, Adão H (2021a) How nematode morphometric attributes integrate with taxonomy-based measures along an estuarine gradient. *Ecol Indic* 124:107384. <https://doi.org/10.1016/j.ecolind.2021.107384>

Steyaert M, Vanaverbeke J, Vanreusel A, Barranguet C, Lucas C & Vincx M (2003) The importance of fine-scale, vertical profiles in characterising nematode community structure. *Estuar Coast Shelf Sci* 58:353–366. [https://doi.org/10.1016/S0272-7714\(03\)00086-6](https://doi.org/10.1016/S0272-7714(03)00086-6)

Teixeira M, Terrinha P, Roque C, Voelker A, Silva P, Salgueiro E, Abrantes F, Naughton F, Mena A, Ercilla G & Casas D (2020) The Late Pleistocene-Holocene sedimentary evolution of the Sines Contourite Drift (SW Portuguese Margin): A multiproxy approach. *Sedimentary Geology* 407 (2020) 105737.

Vafeiadou A-MM, Materatski P, Adão H, De Troch M & Moens T (2013) Food sources of macrobenthos in an estuarine seagrass habitat (*Zostera noltii*) as revealed by dual stable isotope signatures. *Mar Biol* 160:2517–2523. <https://doi.org/10.1007/s00227-013-2238-0>

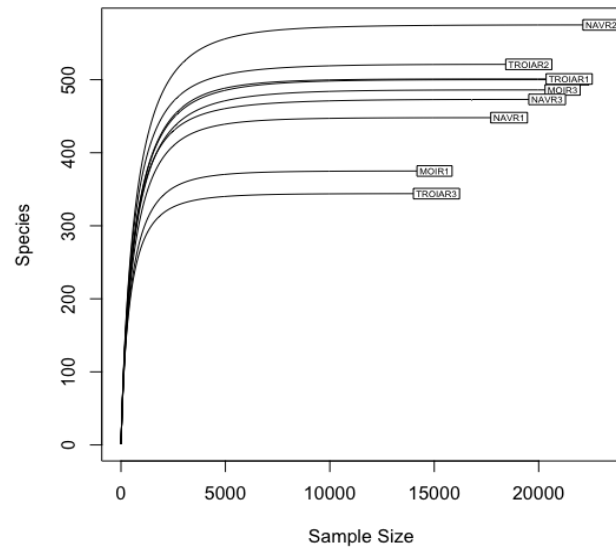
Van der Heijden L H, Graeve M, Asmus R, Rzeznik-Orignac J, Niquile N, Bernier Q, Guillou G, Asmus H & Lebreton B (2019) Trophic importance of microphytobenthos and bacteria to meiofauna in soft-bottom intertidal habitats: A combined trophic marker approach. *Mar Environ Res* 149:50–66. <https://doi.org/10.1016/j.marenvres.2019.05.014>

Wang W, Tao J, Liu H, Li P, Chen S, Wang P & Zhang C (2020) Contrasting bacterial and archaeal distributions reflecting different geochemical processes in a sediment core from the Pearl River Estuary. *AMB Express* 10:1–14. <https://doi.org/10.1186/s13568-020-0950-y>

Warwick R M, Platt H M, Sommerfield P J (1998) Free-living marine nematodes, Part 3, British Monhysterids. Field Studies Council, Shrewsbury

Wieser W (1956) Some free-living marine nematodes. Galathea Rep

Zimmermann J, Wentrup C, Sadowski M, Blazeják A, Gruber-Vodicka R H, Kleiner M, Ott A J, Cronholm B, De Wit P, Erséus C & Dubilier N (2016) Closely coupled evolutionary history of ecto- and endosymbionts from two distantly related animal phyla. Mol Ecol 25:3203–3223. <https://doi.org/10.1111/mec.13554>

**Supplementary information of Chapter 2***Appendix A - Figures*

**Figure A.1** Rarefaction curve of reads clustered in OTUs each sampling site Moinho (MOIR1-R3), Navigator (NAVR1-R3) and Tróia (TROIAR1-R3).

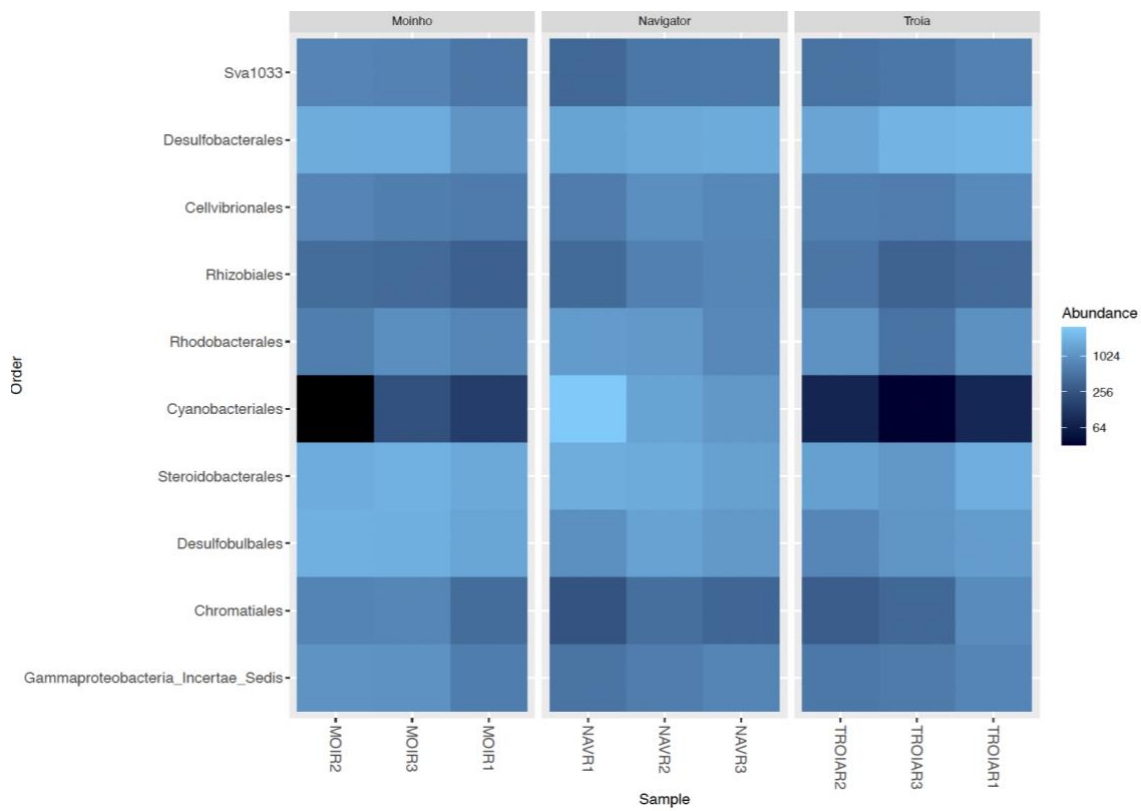


**Figure A.2** Heatmap of the top 10 of most abundant orders represented in the bacterial communities of each site Moinho (MOIR1-R3); Navigator (NAVR1-R3) and Tróia (TROIAR1-R3) and were sorted by Bray Curtis similarity.

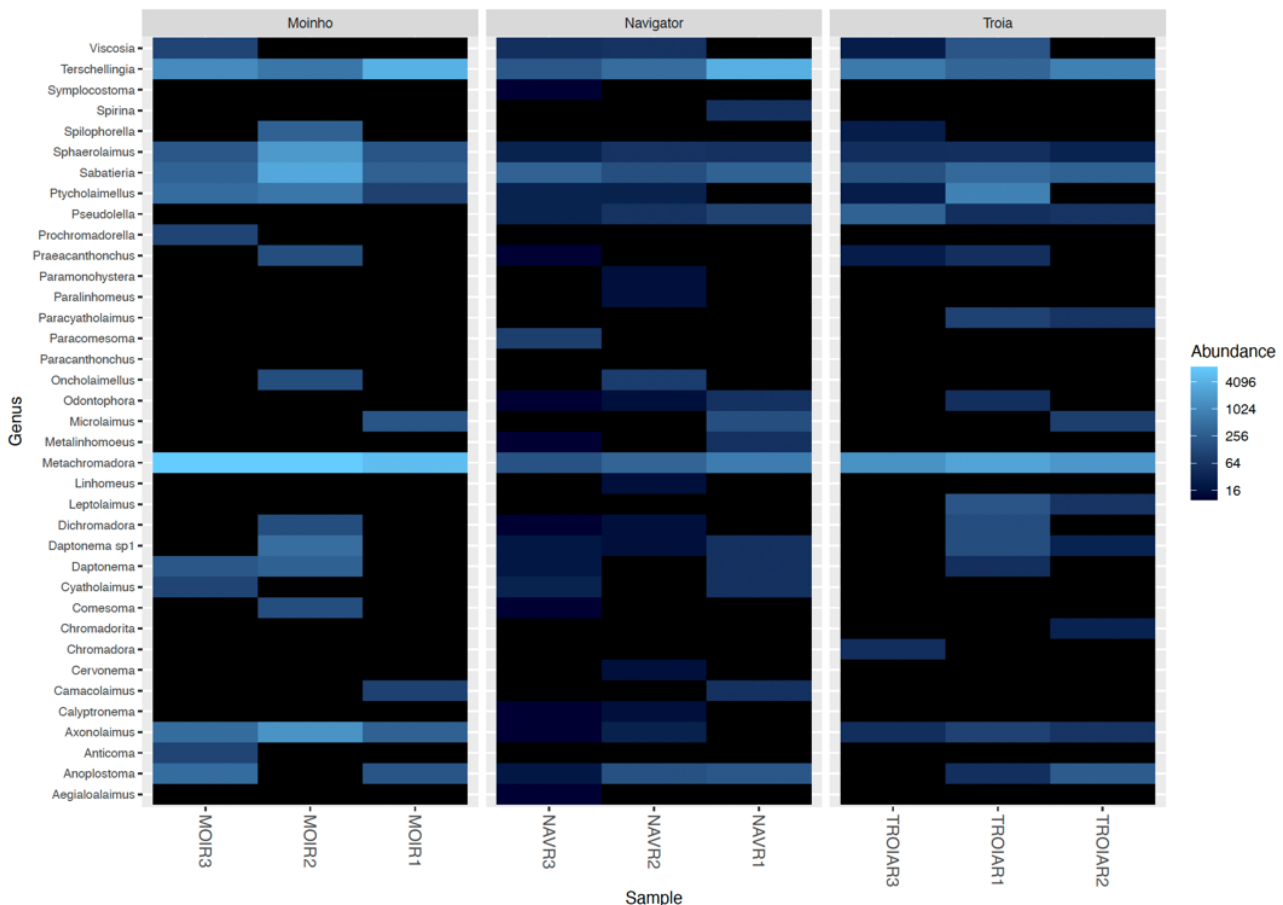


**Figure A.3** Heatmap showing the density at Genus-level of nematode communities in each site Moinho (MOIR1-R3); Navigator (NAVR1-R3) and Tróia (TROIAR1-R3) and were sorted by Bray Curtis similarity.

## Appendix B - Tables

**Table B.1** Mean $\pm$ SE, n=3, of the environment parameters measured in sediments from each sampling site - Moinho (MOI), Navigator (NAV) and Tróia (TROI). Granulometric parameters (%) are Gravel, Sand and Fine fraction (FF). The elemental analysis (w%) are organic matter (OM), Total Nitrogen and Carbon (TN and TC). Sal: salinity.

	MOI	NAV	TROI
<b>GRAVEL</b>	2.27 $\pm$ 0.61	3.7 $\pm$ 0.56	0.06 $\pm$ 0.03
<b>SAND</b>	16.8 $\pm$ 2.5	78.6 $\pm$ 2.1	79.0 $\pm$ 7.2
<b>FF</b>	80.9 $\pm$ 2.2	17.6 $\pm$ 2.6	20.8 $\pm$ 7.2
<b>OM</b>	11.1 $\pm$ 0.3	3.7 $\pm$ 0.6	6.8 $\pm$ 0.3
<b>TN</b>	0.16 $\pm$ 0.002	0.04 $\pm$ 0.002	0.08 $\pm$ 0.01
<b>TC</b>	1.46 $\pm$ 0.02	0.6 $\pm$ 0.04	0.8 $\pm$ 0.1
<b>SAL</b>	29.8 $\pm$ 0.17	34.7 $\pm$ 0.13	35.2 $\pm$ 0.5

**Table B.2** Kruskal-Wallis test: bacterial communities alpha diversity significance between groups (Moinho, Navigator, Tróia),  $p<0.05$ .

		<i>H</i>	<i>p-value</i>	<i>q-value</i>
All groups		0.8	0.670	
Group 1	Group 2			
Moinho (n=3)	Navigator (n=3)	1.190	0.275	0.825
Troia (n=3)	Moinho (n=3)	0.827	0.827	
Navigator (n=3)	Troia (n=3)	0.047	0.827	0.827

**Table B.3** SIMPER summarized table of the bacterial and nematode communities, with the genera that most contributed for (dis)similarities (%), within and between sites (Moinho, Navigator and Tróia).

		Moinho	Navigator	Tróia
Bacteria (genera)	Moinho	Average similarity = 71,75%  <i>Woeseia</i> , <i>Sva0081_sediment_group</i> , <i>Sva1033</i>		
	Navigator	Average dissimilarity = 35,9 %  <i>Pleurocapsa_PCC-7319</i> , <i>Cyanobacterium_CLg1</i> , <i>Chroococcidiopsis_PCC-6712</i>	Average similarity = 68,56 %  <i>Woeseia</i> , <i>Sva0081_sediment_group</i> , <i>Sva1033</i>	
	Tróia	Average dissimilarity = 29,94%  <i>SEEP-SRB1</i> , <i>SBR1031</i> , <i>Mariprofundus</i>	Average dissimilarity = 32 %  <i>Pleurocapsa_PCC-7319</i> , <i>Cyanobacterium_CLg1</i> , <i>Myxosarcina_GI1</i>	Average similarity = 70,68 %  <i>Woeseia</i> , <i>Sva0081_sediment_group</i> , <i>Sva1033</i>
Nematode (genera)	Moinho	Average similarity = 61,41%  <i>Metachromadora</i> , <i>Terschellingia</i> , <i>Axonolaimus</i>		
	Navigator	Average dissimilarity = 58,35 %  <i>Metachromadora</i> , <i>Terschellingia</i> , <i>Axonolaimus</i> , <i>Sphaerolaimus</i>	Average similarity = 55,24 %  <i>Terschellingia</i> , <i>Metachromadora</i> , <i>Sabatieria</i>	
	Tróia	Average dissimilarity = 48,91%  <i>Metachromadora</i> , <i>Terschellingia</i> , <i>Axonolaimus</i> , <i>Sphaerolaimus</i>	Average dissimilarity = 45,77 % <i>Metachromadora</i> , <i>Terschellingia</i> , <i>Ptycholaimellus</i> , <i>Anoplostoma</i>	Average similarity = 62,38 % <i>Metachromadora</i> , <i>Terschellingia</i> , <i>Sabatieria</i>

**Table B.4** One- way PERMANOVA test of nematodes assemblages, with "Sites" (3 level fixed) for all variables analysed. Bold values represent significant differences between sites (NAV, MOI, TROIA), ( $p \leq 0.05$ ).

Source of variation	Degree of freedom	Sum squares	Mean square	Pseudo-F	P(perm)	Unique perms	P(MC)
<b>Nematode total density</b>							
Site	2	4742.9	2371.5	2.8302	<b>0.012</b>	273	<b>0.015</b>
Residual total	6	5027.4	837.9				
Total	8	9770.3					
<b>Number of genera</b>							
Site	2	1583	791.51	4.8494	0.055	172	0.053
Residual total	6	979.31	163.22				
Total	8	2562.3					
<b>Shannon-Wiener index</b>							
Site	2	164.96	82.482	2.9409	0.115	273	0.113
Residual total	6	168.28	28.046				
Total	8	333.24					
<b>Margalef index</b>							
Site	2	1235.9	617.93	6.0071	<b>0.046</b>	275	<b>0.038</b>
Residual total	6	617.21	102.87				
Total	8	1853.1					
<b>Trophic composition</b>							
Site	2	2927.7	1463.8	7.1508	<b>0.0029</b>	280	<b>0.0064</b>
Residual total	6	1228.3	204.71				
Total	8	4156					
<b>ITD -1</b>							
Site	2	261.08	130.54	1.7498	0.246	276	0.249
Residual total	6	447.6	74.601				
Total	8	708.68					
<b>MI</b>							
Site	2	47.797	23.899	3.8445	0.064	271	0.085
Residual total	6	37.297	6.2162				
Total	8	85.094					



**CHAPTER 3 - ASSESSING SPATIAL AND TEMPORAL PATTERNS OF  
BENTHIC BACTERIAL COMMUNITIES IN RESPONSE TO DIFFERENT  
SEDIMENT CONDITIONS**

Published in Marine and Environmental Research (2025)

<https://doi.org/10.1016/j.marenvres.2025.106963>

### 3.1 Abstract

Benthic bacterial communities are sensitive to habitat condition and present a fast response to environmental stressors, which makes them powerful ecological indicators of estuarine environments. The aim of this work is to study the spatial-temporal patterns of benthic bacterial communities in response to contrasting environmental conditions and assess their potential as ecological indicators of estuarine sediments. We characterized the diversity of bacterial communities in three contrasting sites on Sado Estuary (SW Coast, Portugal) and 4 sampling occasions, using 16S metagenomic approach. Based on previous studies, we hypothesized that diversity patterns of bacterial communities will be distinct between sites and across sampling occasions. Bacterial communities were more influenced by each site conditions than by temporal variations in the sediments. The main drivers of bacterial distribution were sediments' composition, organic contents, and hydrodynamic activity. This work provided an important baseline dataset from Sado estuary to explore bacterial networks concerning benthic ecosystem functioning.

**Keywords:** 16S metagenomic; Diversity patterns; Ecological indicators; Sediment status; Benthic; Ecosystem functioning.

### 3.2 Introduction

Estuaries are complex ecological systems, where the transition from fresh water to sea water occurs (Bonaglia et al., 2014; Schratzberger et al., 2020). The water mixture results on high levels of nutrients in the water column and sediments, making estuaries one of the most productive ecosystems in the world (Elliott and Quintino, 2007). Estuaries present a great diversity of natural habitats, and many supports human activities (Elliott and Quintino, 2007; Schratzberger and Ingels, 2018; Schratzberger et al., 2020; Ridall and Ingels, 2021). However, the intensification of the anthropogenic activities has resulted on an overload of nutrients, organic matter, and contaminants (e.g. metals, pesticides, pharmaceuticals) from terrestrial sources on these habitats, modulating nutrient cycling, stability of communities and food-web structures (Elliott and Quintino, 2007; Grill et al., 2019).

Important processes, such as recycling of nutrients and the degradation of pollutants, occur in soft-sediment intertidal and subtidal habitats. Benthic microorganisms from these sediments are considered mediators of biogeochemical processes that sustain the biosphere (Ridall and Ingels, 2021), being the first to be affected by environmental disturbances (Schratzberger and Ingels, 2018). As result, the rapid response to biotic/abiotic stressors makes benthic microbial communities powerful bioindicators to evaluate the sediment quality status (Giere, 2009; Patrício et al., 2012; Branco et al., 2018; Schratzberger and Somerfield, 2020; Sagova-Mareckova et al., 2021). Despite of being recognized for their importance in environmental processes, they are rarely used as bioindicators in routine assessments. The environmental monitoring strategies rely on benthic indexes, which are mostly related with the analysis of benthic macroinvertebrates communities (Borja et al., 2015). In case of disturbances in these ecosystems, the need of representative samples and the time-consuming processes in taxonomic identification may represent obstacles to obtain a rapid and reliable evaluation (Rumohr, 2009; Goodwin et al., 2017; Pawłowski et al., 2018). However, recent advances in environmental genomics have improved our knowledge on biodiversity, providing a holistic view of the ecosystems and predicting shifts of biological communities as a response to natural and anthropogenic disturbances (Jessen et al., 2017, Nigel, 2012). The rRNA gene amplicon-based metagenomic has been used to characterize microbial communities (e.g. bacteria, archaea, and protists) and predict the ecological conditions of sediments with high precision (Nawaz et al., 2018; Mahamoud et al., 2018; Stoeck et al., 2018) and this is also due to the high adaptability of these microorganisms to natural and anthropogenic pressures (Jessen et al., 2017; Zhao et al., 2019; Vieira et al., 2023). Moreover, the composition and metabolic activities of bacterial communities

already proved to be directly influenced by the physical-chemical properties of the sediment making them highly sensitive to environmental changes (Caruso et al., 2016; Rocca et al., 2019; Buongiorno et al., 2019; Jokanovi et al., 2021; Vieira et al., 2023). Bacteria are not only recognized as mediators of energy flow, but also for establishing positive interactions with other benthic organisms such as nematodes, improving their living conditions by reducing the toxicity of hypoxic environments (Giere, 2009; Bonaglia et al., 2014; Ridall and Ingels, 2021). The functional skills of bacteria and their sensitivity to heavy metals and hydrocarbon pollutants exposure have been widely recognized, considering them bioindicators of these pollutants in estuarine sediments (Li et al., 2020; Du et al., 2022). High concentrations of pollutants trigger a fast and structural response in bacterial communities, replacing sensitive taxa with tolerant ones that thrive by degrading many of the toxic compounds present in sediments (Pinto et al., 2015; Li et al., 2020; Du et al., 2022) (e.g. *Flavobacterium* degrade polychlorinated biphenyl (PCB), in Zeng et al. (2020)). Our previous study showed that benthic bacterial communities could be useful for the assessment of ecological status of estuarine sediments on a spatial perspective, by reflecting in their composition and diversity the environmental conditions of each site in Sado estuary (Vieira et al., 2023). It remains unclear if these communities are also reliable to describe the seasonality environmental changes. Several studies have already shown that bacterial communities can reveal habitat specificity in their composition, reflecting the site-specific conditions of the sediment (Shah et al., 2022; Vieira et al., 2023). Studies that rely only on metabolite profiling can obtain redundant results being difficult to detect differences between communities in space and time (Shah et al., 2022). Thus, the main objective of this work is to analyze the spatial-temporal patterns of benthic bacterial communities in response to contrasting environmental conditions, and further assess their potential as ecological indicators to monitoring the estuarine sediments condition. The Sado Estuary was used as case study. Located on the southwest coast of Portugal, this estuary is known not only for its ecological value (i.e., rich in nature reserves) but also for being highly disturbed by local industries and shipping activities (Bettencourt et al., 2004; Caeiro et al., 2005). Under these conditions, we hypothesized that: the diversity patterns of bacterial communities will be significantly different between sites and across sampling occasions, revealing to be a good proxy of the ecological condition of the sediment.

### 3.1 Material and Methods

### **3.1.1 Study area and sampling design**

The Sado estuary is considered the second largest estuarine system in Portugal, covering an approximate area of 240 km<sup>2</sup> (Fig. 1). For this study, three sampling sites (Gambia, Navigator and Tróia) were selected based on the estimated variations in the biogeochemical and trophic conditions of the sediments (Sroczyńska et al., 2021) and considering the water hydrodynamics within the estuary (high/low water residence time), salinity gradient, and the nature of nearby anthropogenic activities previously studied in Sado estuary (Sroczyńska et al., 2021; Shah et al., 2022; Vieira et al., 2023).

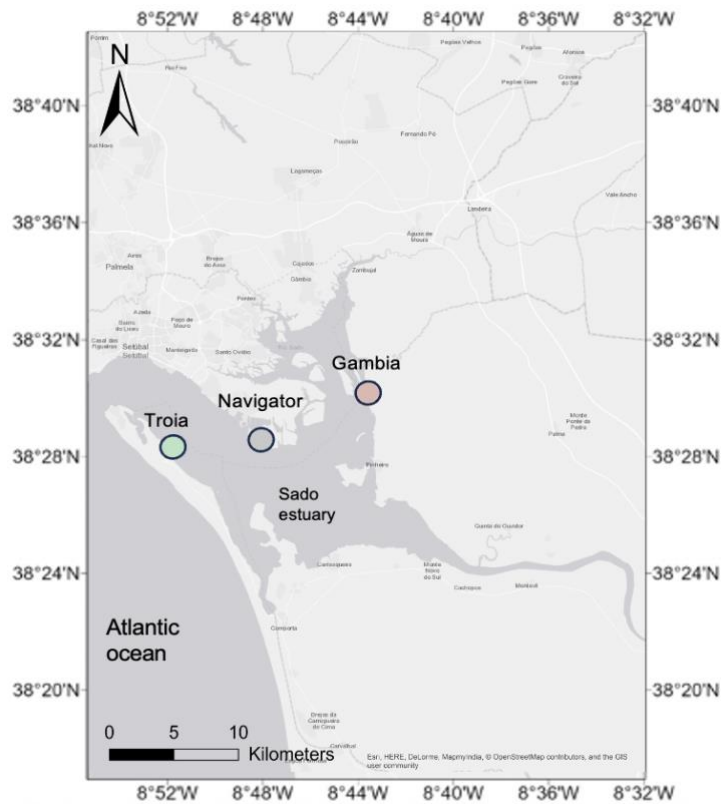


**Figure 1.** Sado estuary located at southwest of Portugal ( $38^{\circ} 31' 14''$  N,  $8^{\circ} 53' 32''$  W). The selected sampling sites: Navigator (38.486502, -8.795191) (grey circle), highly industrialized area; Gambia (38.537263, -8.742584) (orange circle) with high organic inputs from aquacultures; Tróia (38.461421, -8.857838) located at mouth of estuary (adapted from Vieira et al., 2024).

To assess spatial-temporal diversity patterns, three sampling sites were selected (Fig. 1): Navigator, located in the proximity of industrial area, dominated by fine sand, clay and high organic contents; Gambia, located within the borders of the Sado Nature Reserve, affected by the surrounding aquaculture activities with the predominance of clay-fine sediments (Caeiro et al., 2005); and Tróia, located close to the estuary mouth,

is directly exposed to the main estuary channel, with high water exchange rate and high proportion of sand (Vieira et al., 2024). In each site, three sediment replicates were randomly collected for bacterial diversity and other three were collected for sediment biogeochemistry analysis. This sampling strategy was repeated in 4 distinct sampling occasions: 1) Winter 2019 (between November and December 2019); 2) Summer 2020 (between June and July); 3) Winter 2020 (between December 2020 and February 2021); 4) Summer 2021, (between May and June 2021).

### *3.1.2 Sediment sample processing*

The sediment samples for assessing physical and chemical composition were transported on ice to the laboratory and stored at  $-20^{\circ}\text{C}$  until further analysis. The determination of all sediment components followed the methodology as described in Vieira et al. (2023) and Vieira et al., (2024). This analysis evaluated the contents of: total organic matter (OM), calcium carbonate ( $\text{CaCO}_3$ ), grain size and elemental analysis total carbon (CT) and total nitrogen (NT), expressed as weight percentage (wt.%). Chlorophyll a (chl a) and phaeopigments (phaeo) were determined as described by Lorenzen (1967). Briefly, approximately 0.5 g of sediment samples were extracted with 3 mL of ice-cold spectrophotometric grade 90 % (v/v) acetone. Furthermore, samples were placed in an ultrasound bath and extracted for 24 h at  $-20^{\circ}\text{C}$  in the dark. Samples were centrifuged at  $4.000\times g$  for 15 min at  $4^{\circ}\text{C}$  after extraction, and the supernatant was used for the analysis. Concentration values for phaeopigments were obtained after acidification of the supernatant with 0.5 M Hydrochloric acid (HCl). The concentration of metals in the sediments was also measured (expressed mg/kg). Fourteen elements were analyzed: Li, Sr, Mn, Ni, Cr, Be, U, Ba, Co, Cu, Zn, As, Pb and Hg. The element Hg was quantified by thermal pyrolysis atomic absorption analysis (LECO 254 Advanced Mercury Analyser, AMA) as described by Costley et al. (2000). The other elements were analyzed using the procedure of Catry et al. (2021). They were quantified by Inductively Coupled Plasma – Mass Spectrometry (ICP-MS) (PerkinElmer NEXION, 2000C) after a total decomposition carried out in a closed Teflon vessel microwave assisted system (CEM MARS 5). The quality control of this procedure was assured using procedural blanks, duplicate samples (coefficient of variation  $<10\%$ ), and the analysis of the MESS-4 CRM, which were prepared using the same analytical procedure and reagents.

### *3.1.3 Total DNA extraction of sediment and amplicon sequencing*

The sediment samples for Total DNA extraction were collected from the top 3 cm core (Stoeck et al., 2018) and snap-freezed in dry ice. At lab, all samples were stored at  $-80^{\circ}\text{C}$  until DNA extraction. The optimal size for a sediment sample depends on the

size and biomass of the microbial communities, being the volume of 0.2–0.5 g recommended for an accurate microbial diversity measurement (Xie and Müller, 2019). Total DNA extraction from 0.25 g of the sediment was conducted under sterile conditions, using the MOBIO PowerSoil® kit (QIAGEN, Valencia, CA, USA) following the manufacturer's instructions. For cell lysis, the samples were homogenized using a Precellys 24 Tissue Homogenizer (Bertin Instruments, Maryland USA). The homogenization was performed for a total of 6 min, completing with two cycles of 20 s each at a speed of 5000 rpm. The quality and quantity of total DNA in the samples were analyzed using the NanoDropTM2000 Spectrophotometer and the Qubit4® fluorometer (Thermo Fisher Scientific). To confirm the presence of amplifiable DNA in the samples, amplicon amplification was performed using primers that flank the V4 region of the 16S rRNA gene (515F–806R) (Gregory Caporaso et al., 2012). A total of 36 samples were selected and sent for sequencing on Illumina MiSeq 2x 250bp (Illumina, Inc. San Diego, CA, USA) using V3-V4 region at EUROFINS Genomics (Cologne, Germany). The 16S rRNA gene library pipeline is available in 16S Metagenomic Sequencing Library Preparation Reference guide Part#15044223 Rev.B (16S metagenomic sequencing library), with reference to primers used for V3-V4 region (FOR: CCTACGGGNGGCWGCAG; REV: GACTACHVGGGTATCTAATCC).

### 3.1.4 Bioinformatics analyses and data availability

Raw Illumina data was demultiplexed and quality-filtered using the defaults parameters of in Quantitative Insights into Microbial Ecology (QIIME2 version 2022.11) (Bolyen et al., 2019), following the standard pipeline analysis. Pair-ends reads were denoised using DADA2 plugin (Callahan et al., 2016), that discarded biased reads (e.g., chimeras, singlettons) and determined the amplicon sequence variants (ASVs). The ASVs were assigned taxonomy at 99% similarity using classify-sklearn plugin (Pedregosa et al., 2011) against SILVA v138 reference database (Bokulich et al., 2021). Representative sequences were assigned taxonomy using a trained Naïve Bayes classifier (SILVA 138) (Quast et al., 2013) for V3-V4 hyper variable region from 16S rRNA. The ASVs classified as chloroplast, mitochondria, eukaryote, archaea, and unassigned were also removed. Filtered ASVs table was rarefied at minimum depth 10 to a maximum depth of 17000 sequences per sample after confirmation with a rarefaction plugin (Appendix A, Figure A.1). Raw data have been deposited into the NCBI SRA repository under the Bioproject PRJNA680980 and accessions from SRR22230853 to SRR22230888.

### 3.1.5 Data analysis

Statistical analyses of 16S rRNA metagenomics was performed on QIIME2, version 2023.2) (Bolyen et al., 2019), R packages phyloseq (version 1.42.0) (McMurdie and Holmes, 2013) and microVIZ (version 0.11.0) (Barnett et al., 2021). The principal component analysis (PCA) PRIMER v6 software package (Clarke and Warwick, 2001) with permutational analysis of variance (PERMANOVA) add-on package (Anderson et al., 2008) were used to test significant differences of bacteria diversity and two way-crossed similarity percentage analysis SIMPER (cut-off percentage 100%) was used to calculate dissimilarities between sites.

#### 3.1.5.1 Environmental variables

The environmental raw data used in this study is the same as Vieira et al. (2024), the sampling strategy and campaigns were also the same. Principal Component Analysis (PCA) was performed to detect spatial and temporal distributions of physicochemical parameters. All variables were log10 transformed (except for pH) and normalized, then were tested, and removed the variables that demonstrated the lowest contribution to the PCA axes, and with high correlation with other variables (NT, Li, Sr, Mn, Ni, U, Zn, As, Co, Cu, T, Sal, O2 and pH). PCA plot was done using the function "fviz pca\_biplot" using R package "FactoMineR" (version 2.9) (Lê et al., 2008). To check for the significance of the PCA, a PCA test (R package "PCATest" (version 0.0.1) (Camargo, 2022) was applied with the following parameters: Number of random permutations: 1000 and Number of bootstrap replicates to build 95% confidence intervals of the observed statistics: 1000, level for statistical tests:  $p < 0.05$ .

#### 3.1.5.2 Composition of bacterial communities

Bacterial  $\alpha$ - and  $\beta$ -diversity indexes were calculated with the "q2-diversity" plugin. Several metrics were calculated for  $\alpha$ -diversity: Observed ASVs, Chao1, se.Chao1, Abundance-based coverage estimator (ACE), se.ACE, Shannon and Simpson. To avoid misinterpreted values from Shannon and Simpson diversity indices, the values were converted into effective numbers of species, Shannon ( $H_1$ ) effective numbers for Shannon ( $H_1 = \exp(H')$  and InvSimpson (Jost, L. 2006; Leinster and Cobbold, 2012). To detect significant differences within groups of  $\alpha$ -diversity metrics was calculated the Faith PD using "qiime diversity-lib faith-pd" plugin (Faith, 1992; Armstrong et al., 2021). The Faith's Phylogenetic Diversity (Faith PD) significance was determined with Kruskal-

Wallis test,  $p < 0.05$ . While the  $\beta$ -diversity significance was obtained performing one-way PERMANOVA,  $p < 0.05$ .

The PERMANOVA analysis were carried out with a two-factor design: factor “Site”: “Navigator”; “Gambia” and “Tróia” (3 levels, fixed) and factor “sampling\_occasion”: “Winter 19”, “Summer 20”; “Winter 20” and “Summer 21” (4 levels, random) (Clarke and Warwick, 2001),  $p < 0.05$ . Before PERMANOVA dataset was transformed squared root according to Clarke and Warwick (2001) and Anderson et al. (2008). To have a broader overview of the distribution patterns from bacterial communities (across “sites” and “sampling\_occasions”), Principal Coordinates Analysis (PCoA) was performed using resembled matrix of ASVs. The dataset was transformed in centered log ratio (CLR) and resembled in a Bray-Curtis dissimilarity matrix, then was plotted using the R package “MicrobiotaProcess” (version 1.10.3). The relative contribution of each taxon to the dissimilarities between sites was calculated using the two way-crossed similarity percentage analysis SIMPER (cut-off percentage 100%).

### 3.1.5.3 *Environmental variables influencing bacterial communities*

Spearman correlations were used to test the effect exerted by environmental variables on the ASVs relative abundances of top 10 families. With this test the environmental variables that presented the highest contribution for the composition of the communities were considered to calculate the Redundancy analysis (RDA). RDA analysis was performed with the R packages “vegan” (version 2.6–4) and “QsRutils” (version 0.1.5). Redundancy analysis (RDA) was used to test linear combinations between bacterial communities and environmental variables that best explain the variation of the bacterial communities’ patterns. Before analyses, the response dataset (ASVs relative abundance, filtered at family level) was transformed into a CLR matrix and all constrained variables were log-transformed. The variance inflation factor (VIF) was calculated for the explanatory environmental data to check for linear dependencies and to ensure that only variables with small VIFs ( $<10$ ) were included. To find the best RDA model, was used vegan R package, function `ordistep()`, then RDA plot performed by using microVIZ, R packages (Barnett et al., 2021; R Core Team, 2022).

## 3.2 Results

### 3.2.1 *Physical-chemical characterization of Sado estuary sediments*

The physical-chemical analysis revealed distinct compositions of sediment in each sampling site (Appendix A, Tables A.1 and A.2). Navigator sediments were

predominantly muddy, characterized by high levels of clay (1.7–5%), OM (18.3–52.1%), CT (0.38–1.66%) and NT (0.02–0.57%), while Gambia sediment composition was mostly defined by the highest proportion of gravel (5–31.4%). In contrast, Tróia sediments presented increased levels of sand (84.3–97.7%), CaCO<sub>3</sub> (3.1–7%) and chla and phaeo ratio (chla\_phaeo), suggesting a high quality of the OM. Navigator and Gambia sediments had the highest levels of heavy metals, such as Sr (110.3 ± 18.6 mg/kg), Cr (29.3 ± 3.8 mg/kg), and Pb (29.3 ± 3.3 mg/kg), while the Tróia sediments showed the lowest levels of these metals (Sr (74.4 ± 3.3 mg/kg) Cr (3.6 ± 0.1 mg/kg) and Pb (12.2 ± 0.4 mg/kg)) (Supplementary Table S2). These results were in line with the Principal Component Analysis (PCA) and differentiated all sites, especially Tróia that is totally separated from the others (Fig. 2).

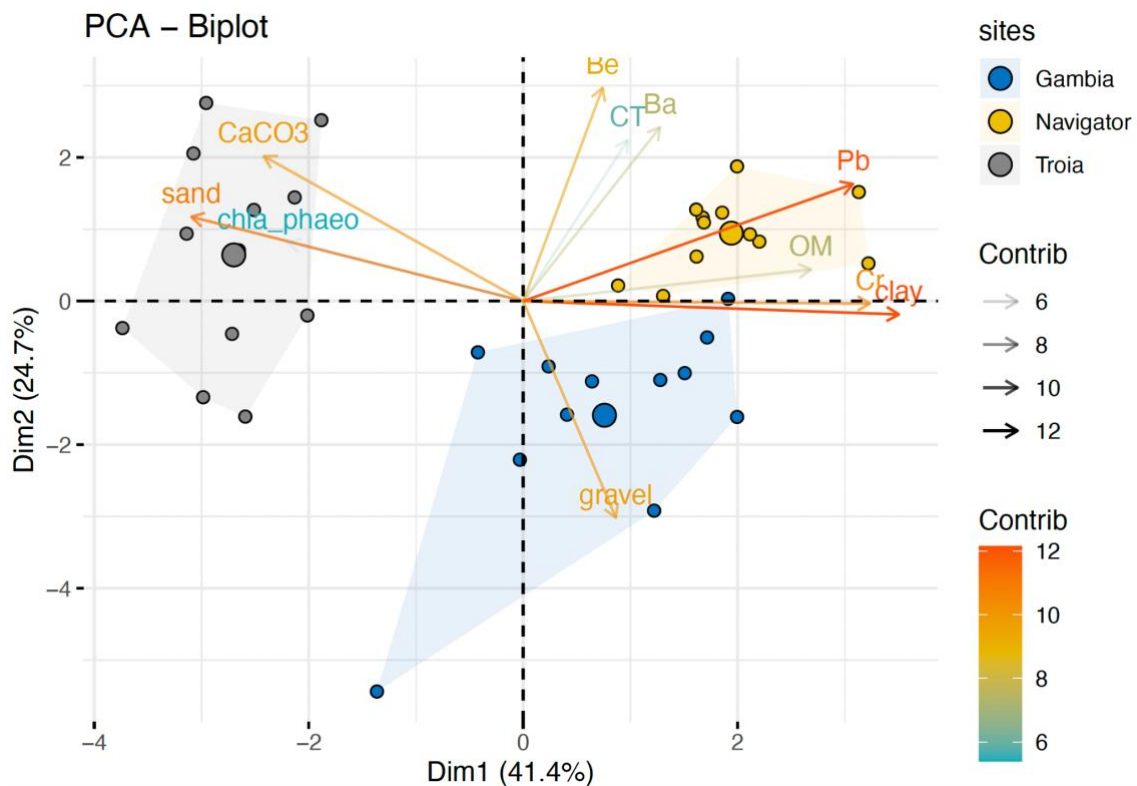


**Figure 2.** Principal component analysis (PCA) biplot based on scaled environmental and biogeochemical variables measured for the three sampling sites in Sado estuary, colored by estuary “confidence” convex type. Variable’s vectors are colored based on their contributions to the principal components (gradient colors and transparency of vectors varying between 6 and 12 is result of cos2 index that classify the variable vectors by their quality and contribution (“contrib”), with the color red representing highest contributions, yellow intermediate and blue representing lowest contributions. The dots represent the cluster centroids for group variables.

Both axes were significantly representative of the data distribution, according to PCAtest, the first accounted for 41.4% (95%-CI:36.9–50.6) and second accounted for 24.7% (95%-CI:43–56.9). Together explained 66.1% of the total variation observed (Fig. 2). These results showed that the variables sand, OM, CT, CaCO<sub>3</sub>, chla\_phaeo, Cr and Pb had significant influence in the first axis while the variables gravel, Be and Ba had in the second axis.

### 3.2.2 Bacterial community composition and diversity

Overall, a total of 46 phyla were assigned using SILVA 138 (Quast et al., 2013). The top 5 most abundant phyla were described considering the respective % of total abundance of bacterial communities. The most abundant phyla were *Pseudomonadota* (41.5%), *Desulfobacterota* (25.5%), *Bacteroidota* (15%), *Actinobacterota* (3.3%) and *Acidobacterota* (3%). The dominant classes were *Gammaproteobacteria* (35%), *Bacteroidia* (14%), *Desulfobacteria* (12.3%), *Desulfobulbia* (7.2%) and *Alphaproteobacteria* (6.4%). The most abundant orders were *Desulfobacterales* and *Steroidobacterales* (>10%), *Flavobacteriales* (>6%), *Cellvibrionales* (4%), and *Gammaproteobacteria* (3.6%) (Fig. 3).

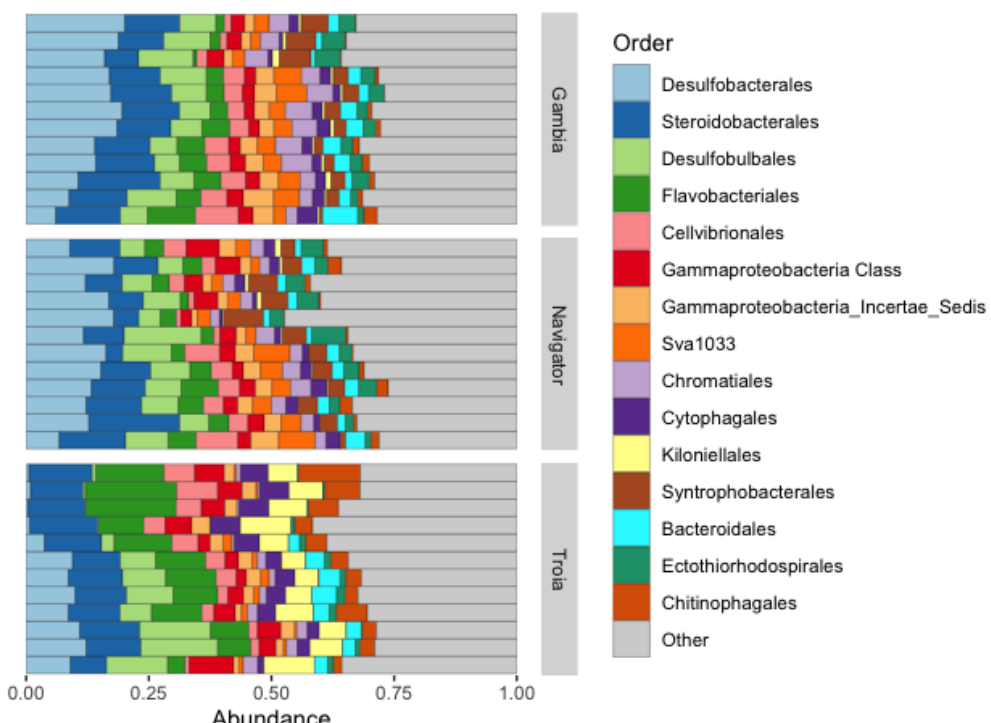


**Figure 3.** Relative abundance of the amplicon sequence variants (ASVs) of the most representative orders (n=15) in each sampling site (Gambia, Navigator and Tróia, n=12) across all sampling occasions. The X-axis is the relative abundance from 0 to 1, which corresponds to 0 -100 %. The “Other” represent the less abundant orders.

Bacterial communities of Navigator and Gambia were predominantly characterized by the phyla *Desulfobacterota* (30.9–31.4%) and *Pseudomonadota* (37.2–41.4%) with the orders *Steroidobacterales* (9.6–11.5%), *Sva1033* (3.8%), *Chromatiales* (2.7–4.3%), *Desulfobacterales* (13.5–15%) and *Desulfobulbales* (7.4–7.5%) (Fig. 3). These orders are mainly represented by the families *Woeseiaceae* (9.6–11.5%), *Sva1033* (3.6–3.8%), *Chromatiaceae* (2.1–3.2%), *Desulfobulbaceae* (3.6–4.7%) and *Desulfosarcinaceae* (13.2–14.8%) (Fig. 4), to which belongs, respectively, the genera *Woeseia* (1.4–4.2%), *Candidatus\_Thiobios* (1.3%), *Sva1033* (1.2%) and *Sva0081\_sediment\_group* (1.2%). In Tróia sediments, the most frequent phyla were *Pseudomonadota* (44.5%) and *Bacteroidota* (23.5%) with the orders *Kiloniellales* (6.8%), *Steroidobacterales* (11.1%) and *Flavobacteriales* (10.8%) which were described by the families *Kiloniellaceae* (6.8%), *Woeseiaceae* (11.4%) and *Flavobacteriaceae* (9.7%) (Fig. 4). The most abundant genera of these families were *Tistlia* (1.4%), *Woeseia* (1.2%), *Olleya* (0.6%) and *Aquibacter* (0.6%), respectively.

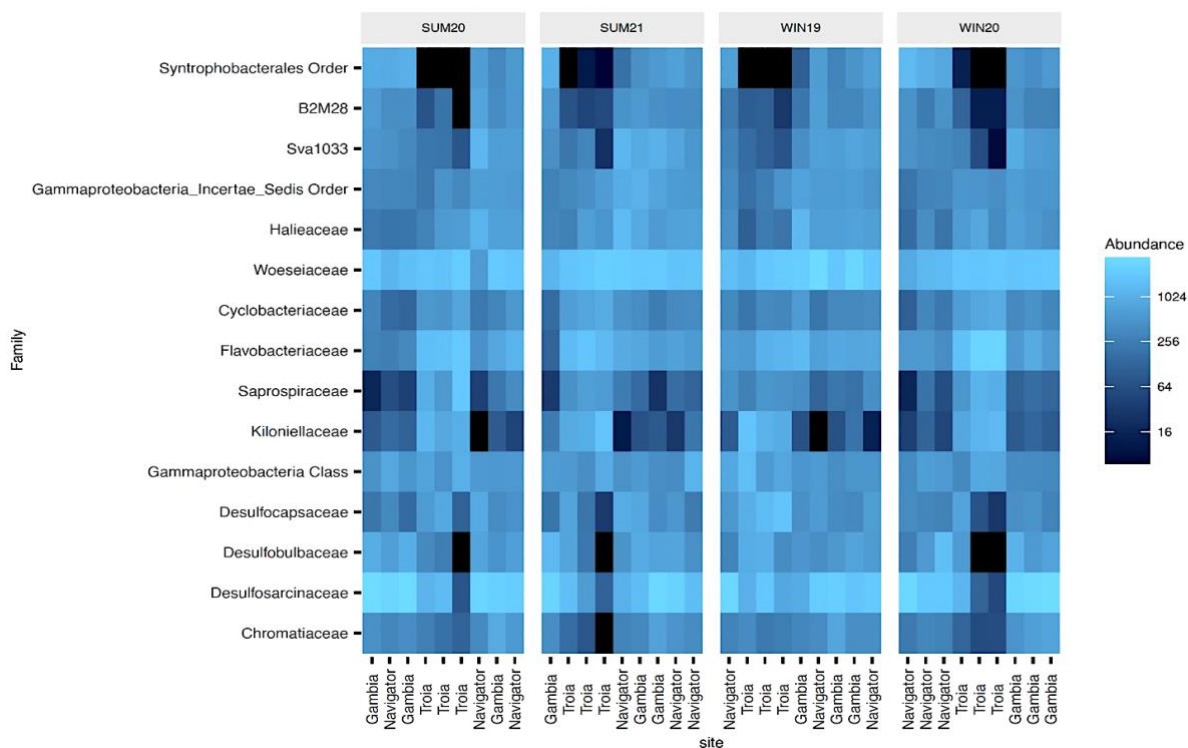


**Figure 4.** Heatmap plot of the relative abundance of the ASVs, based on Bray-Curtis dissimilarity, of the most representative families ( $n=15$ ) of each site (Navigator, Gambia and Tróia) across the sampling occasions winter 2019 (WIN19), summer 2020 (SUM20), winter 2020 (WIN20) and summer 21 (SUM21).

Alpha diversity was calculated considering a good coverage value (99.9%) to ensure the local species diversity. All calculated metrics are summarized in Appendix A, Table A.3. The species richness was estimated among sites, using the Chao1 index and

ACE. The lowest richness was obtained in the samples of Navigator communities, while the highest richness was reported in the samples of Gambia. Diversity metrics were calculated using InvSimpson and exponential of  $\exp(H')$  to be understood as effective number of species, since the data is ASV counts and not species units. The most diverse communities were obtained in Navigator and Tróia, while the less diverse was in Gambia (Appendix A, Table A.3). These results separated Gambia communities from Navigator and Tróia communities, that become more closer by the high richness and diversity patterns. Concerning to the temporal perspective the diversity of the communities was higher in winter sampling occasions (winter 19 and winter 20) than at summer sampling occasions (summer 20 and summer 21). However, the diversity of the communities was more divergent between sites than across sampling occasions. Evenness index was very similar between samples. The Faith PD significance, determined by Kruskal-Wallis test, presented significant differences within groups ( $p = 0.018$ ) (Table 1), showing an increasing variability within the communities of each site. Concerning beta diversity, significant differences were detected in bacterial communities only between sites ( $p = 0.0003$ ) (Table 2).

**Table 1.** Alpha diversity significance between groups, for each site (Gambia, Navigator and Tróia) using Kruskal-Wallis test. Bold values represent significant differences between sites. The replicates  $n=12$  assume the 3 replicates in each sampling occasion ( $n=4$ ). Significant levels considered:  $p \leq 0.05$  (\*),  $p \leq 0.01$  (\*\*) and  $p \leq 0.001$  (\*\*\*) $H$ : Kruskal-Wallis statistic;  $p$ -value: significance level;  $q$ -value false discovery rate (FDR).

	H	p-value	q-value
All groups	7.98	<b>0.018**</b>	
Group 1	Group 2		
Gambia (n=12)	Navigator (n=12)	6.45	<b>0.011**</b>
	Tróia (n=12)	1.92	0.165
Navigator (n=12)	Tróia (n=12)	3.63	0.056
			0.085

**Table 2.** Two-way PERMANOVA test, Beta-diversity of bacterial communities, between "Sites" (si) (3 level, fixed) and across "sampling occasions" (sa) (4 levels, random) for all variables analyzed. Bold values represent significant differences between sites (Navigator, Gambia and Tróia). Significant levels considered  $p \leq 0.05$  (\*),  $p \leq 0.01$  (\*\*) and  $p \leq 0.001$  (\*\*\*)<sup>1</sup>. Res: residual; df: Degrees of freedom; SS: Sum square; MS: Mean Square; Pseudo-F: Friedman test; P(perm) p-value from permutation test; Unique perms: Unique permutations; P(MC): p-value (Monte Carlo).

Source	df	SS	MS	Pseudo-F	P(perm)	Unique perms	P(MC)
si	2	43809	21905	10.826	<b>0.0003***</b>	9898	0.0001
sa	3	5838.8	1946.3	1.1448	0.2621	9891	0.2849
sixsa	6	12140	2023.4	1.1902	0.2064	9859	0.2217
Res	24	40802	1700.1				
Total	35	1.03E+05					

### 3.2.3 Spatial and temporal patterns of bacterial communities

PCoA ordination based on the relative abundance of the ASVs of all taxa was in accordance with beta diversity significance, demonstrating a clear separation between bacterial communities from Tróia and the bacterial communities of Gambia and Navigator, along the PCoA1 axis (Fig. 5). The two first PCoA axes (PCoA1 and PCoA2) account for almost 44% of the total variation. In Tróia communities, the main contributors for this separation were the high abundance of the families *Kiloniellaceae*, *Woeseiaceae*, and *Flavobacteriaceae* which includes genera *Tistlia*, *Woeseia* and *Olleya*, respectively. However, bacterial communities of Navigator and Gambia presented a high level of similarity due to the increased prevalence of the order *Syntrophobacterales* and the families *Chromatiaceae* which includes genus *Candidatus\_Thiobios*. Concerning the temporal variations, bacterial communities did not show a clear pattern between sampling occasions, neither the seasonality was evidenced in the PCA communities' distribution.

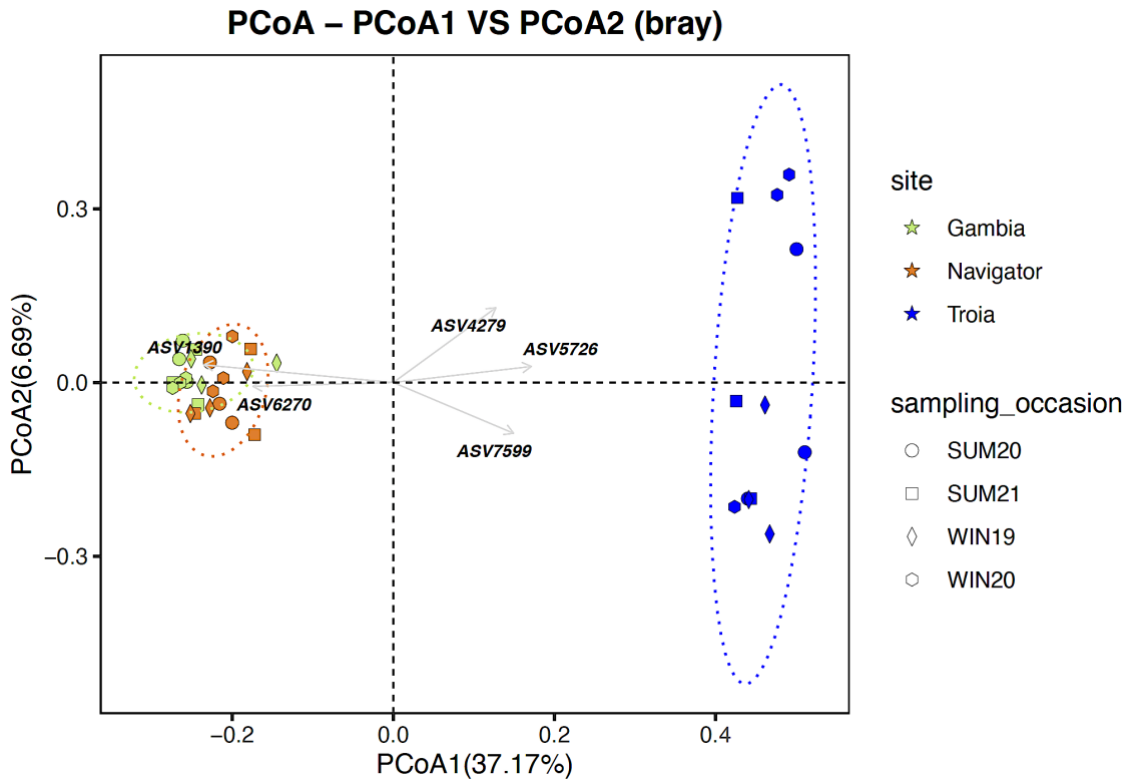


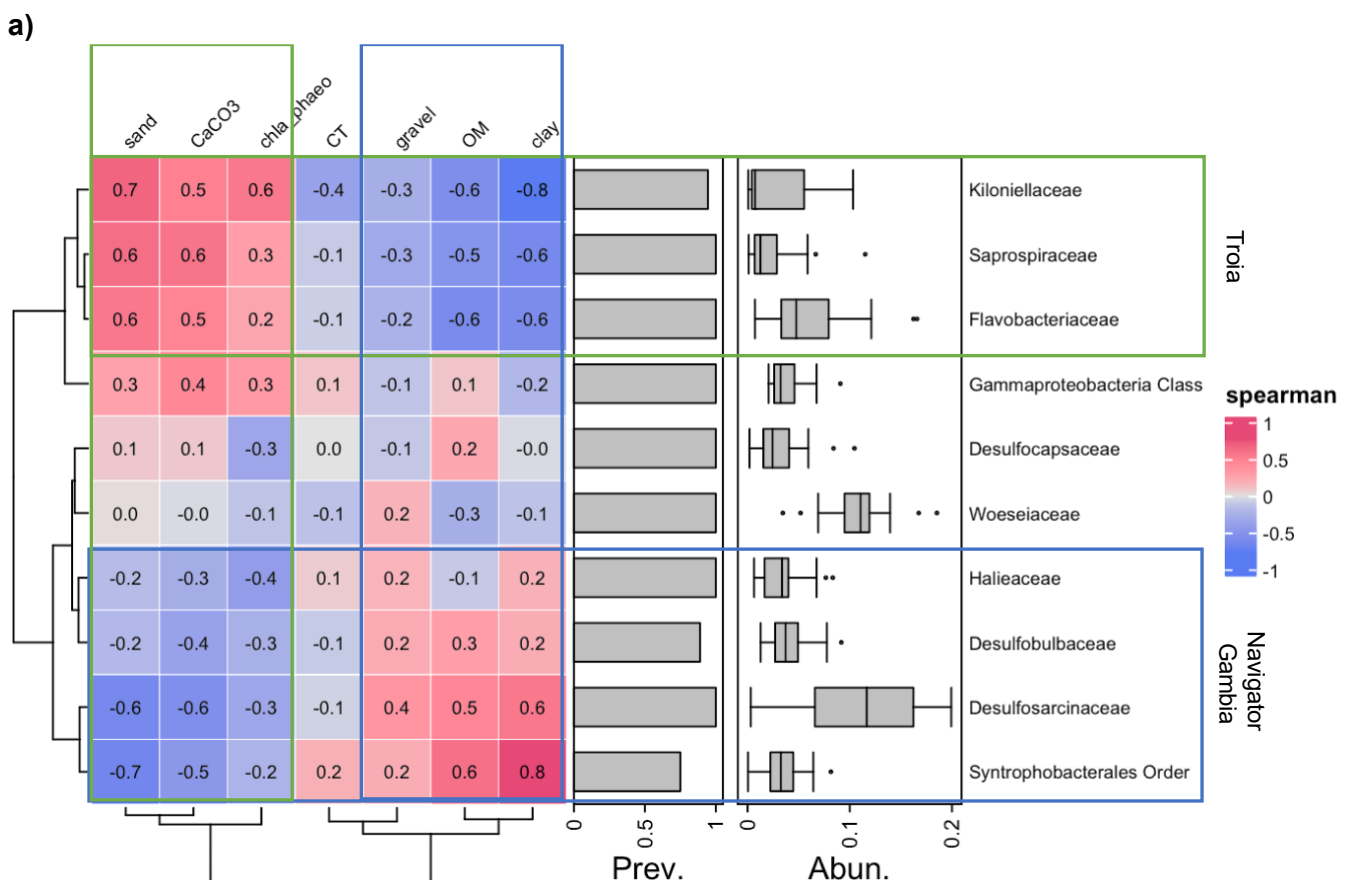
**Figure 5.** Principal component analysis (PCoA) plot based on Bray-Curtis dissimilarity, according to ASVs relative abundance of all taxa obtained in each “site”. PCoA1 = 37.17 % and PCoA2 = 6.69 %. The vectors are the most representative taxa of the variability observed in bacterial communities. The vectors are represented by the ASVs sequences that correspond to a family taxon: ASV1390 (*Syntrophobacterales*), ASV6270 (*Chromatiaceae*), ASV4279 (*Flavobacteriaceae*), ASV5726 (*Kiloniellaceae*) and ASV 7599(*Woeseiaceae*).

Supporting previous results, the SIMPER analysis revealed that the order *Syntrophobacterales* and the families *Woeseiaceae*, *Desulfosarcinaceae* and *Chromatiaceae* contributed the most for the similarity within Navigator and Gambia bacterial communities (similarity  $\geq 40\%$ ). While the families that contributed the most for the similarity within Tróia were *Kiloniellaceae*, *Woeseiaceae*, *Flavobacteriaceae* and *Geminicoccaceae* (similarity 34.6%). In terms of dissimilarity between sites, the main contributors were the genera *Woeseia*, *Candidatus\_Thiobios* and *Sulfurovum* (Gambia vs Navigator, dissimilarity 61.7%), *Woeseia*, *Candidatus\_Thiobios* and *Tistlia* (Gambia vs Tróia, dissimilarity 92.3%) and the genera *Tistlia*, *Candidatus\_Thiobios*, *Sva1033* and *Sulfurovum* (Navigator vs Tróia, dissimilarity 91.5%). Between sampling occasions, the SIMPER analysis showed that genera *Woeseia* and *Candidatus\_Thiobios*, due to their relative abundance, contributed to the differences between all sampling occasions ( $>60\%$  dissimilarity). The variability of Navigator's bacterial communities among sampling occasions (approx. 60% dissimilarity) is related with the prevalence of the genera *Sulfurovum* and *Desulfatiglans* in winter 2019 and 2020 and *SEEP-SRB1* and

*Sva1033* in summer 2020 and 2021. The temporal variability of bacterial communities in Gambia revealed that the prevalence of *SEEP-SRB1* and *Sva1033* separated the summer communities from the others, while *Draconibacterium* and *Bacteroidetes\_BD2-2* were representative winter communities. The variability of Tróia's communities in winter was represented by the families *Desulfobulbaceae* (win 19), *Flavobacteriaceae* (win 20), *Rhodospirillaceae* (win 19) (Fig. 4) and the genera *Aquibacter* and *Aquimarina* (win 20) accounting for more than 60% of dissimilarity between sampling occasions.

### 3.2.4 Environmental variables influencing the patterns of bacterial communities

To assess the influence of the environmental variables on the diversity patterns of the bacterial communities, all variables were sorted and grouped by order of magnitude, whereby metals were separated from the other variables. The variables that were least correlated with each other were selected to be used in the Spearman correlation test (Fig. 6a and b), then were crossed with relative abundance of ASV for the 10 most abundant families.



b)

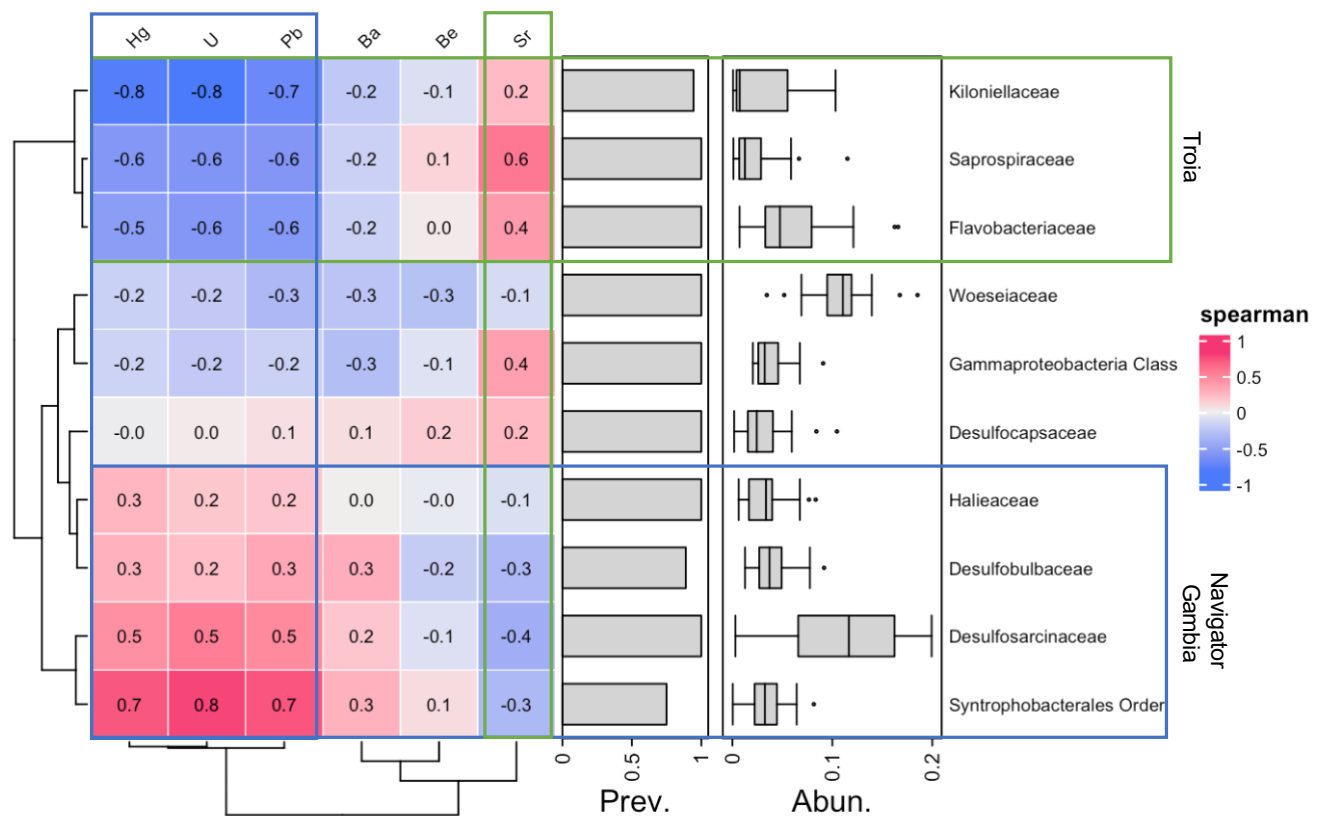


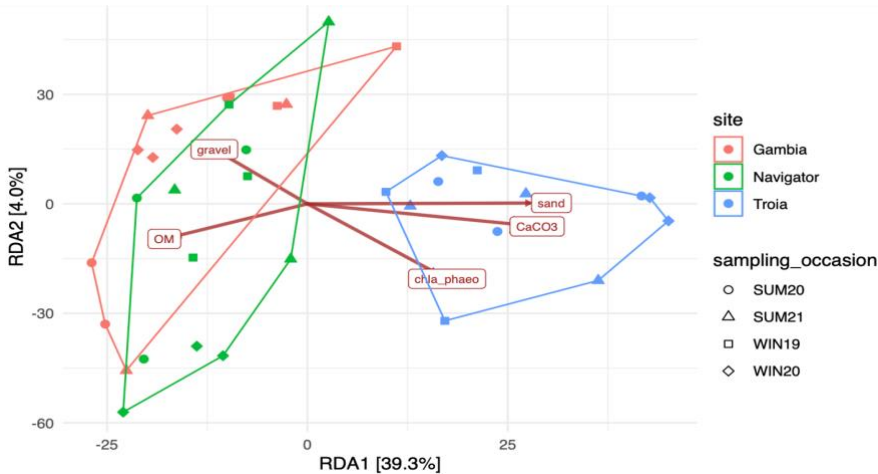
**Figure 6.** Heatmap presenting the Spearman correlation between top 10 most abundant families, (transformed by centered log ratio-transformed (CLT) and all representative environmental variables: **a)** sediment variables (organic matter (OM), gravel, clay, total carbon (CT), chlorophyll *a* and phaeopigments ratio (chl<sub>a</sub>\_phaeo), carbonate of calcium (CaCO<sub>3</sub>) and sand); and **b)** Metals (Sr, Pb, U, Ba, Be, and Hg). In both, the “Abun.” is bacterial community abundance and “Prev.” is prevalence of the Top10 families. The green square corresponds to the dominant taxa vs constrained variables of Navigator and Gambia sites and the blue square represents Tróia dominant taxa vs constrained variable.

Spearman correlation test showed a clear separation between anaerobic and aerobic bacteria, which is consistent with the high prevalence and abundance of these groups in Navigator and Gambia (anaerobic taxa involved in sulfur and carbon cycle) and Tróia (aerobic taxa involved in carbon cycle and mineralization processes). The most abundant families of Tróia bacterial communities (*Flavobacteriaceae*, *Saprospiraceae* and *Kiloniellaceae*) were positively correlated with sediment variables chla\_phaeo, CaCO<sub>3</sub> and sand, being negatively correlated with gravel, OM and clay (Fig. 6a). Regarding the metal variables correlations, they follow the same trend with Sr being positively correlated while Pb, U, Be, Ba, and Hg were negatively correlated (Fig. 6b). In opposite, the variables Hg, U, Pb, OM, clay and gravel were highly correlated with anaerobic bacteria, such as the phylum *Desulfobacterota* with the order

*Syntrophobacterales* and the families *Desulfobulbaceae*, *Desulfosarcinaceae* and *Sva1033* which describe the communities of Gambia and Navigator (Fig. 6a and b).

To evaluate the bacterial communities constrained by the environmental variables it was performed the constrained redundancy analysis (RDA). To avoid bias, all constrained variables were standardized and log10 transformed (when required). However, to better understand the influence of metals in the most abundant groups of bacterial communities, RDA for metals was performed separately from the other variables, avoiding the noise of potential dependencies within constrained variables. (Fig. 7a and b). The environmental variables were grouped by order of magnitude, whereby metals were separated from the other variables (Fig. 7a and b). The RDA of the constrained variables of the first matrix, explained 45.2% of the variation of the bacterial communities (Fig. 7a) and the second matrix the RDA of the constrained variables (metals), explained 37.5% (Fig. 7b). Permutation test for RDA under reduced model was performed for both matrices (metals and other variables), being statistically significant ( $p = 0.001$ ) (Supplementary Table A4). All explanatory variables were tested to validate their efficiency to explain the variation of the communities. Variance inflation factors (VIF) were calculated for both matrices, to determine the collinearity among the environmental variables of each matrix. The variables Clay, CT, NT, Mn, As, Cu, Li, Co, Zn, Pb, Ni and Cr presented high collinearity values  $VIF > 10$  being removed from the analysis. Fitting environmental vectors onto an ordination, in the first matrix the OM,  $\text{CaCO}_3$  and sand significantly explained the amount of variation on their own (Fig. 7a) and in the second matrix were the variables Sr and U (Fig. 7b). The constrained variables  $\text{CaCO}_3$ , sand, chla\_phaeo ratio and the metal Sr clearly describe the Tróia communities separating from the Navigator and Gambia communities. In contrast, bacterial communities from Navigator and Gambia were positively correlated with the constrained variables OM, gravel and the other metals Hg, Ba and U. Meanwhile, the temporal pattern was not evident within communities in the RDA analysis (Fig. 7a and b).

a)



b)

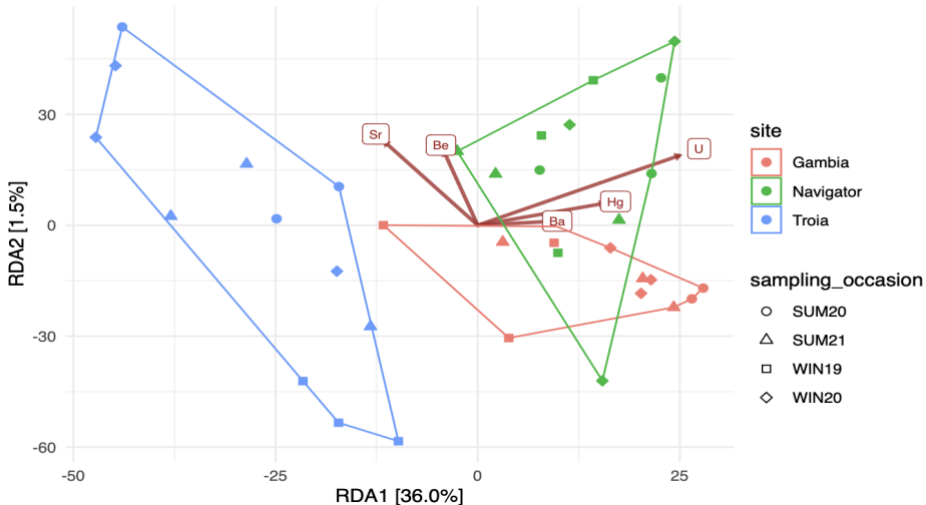


**Figure 7.** RDA Constrained redundancy analysis displaying contributions of environmental variables for the distribution of bacterial communities filtered at family level: **a)** bacterial communities constrained by sediment variables: OM, chla\_phaeo, CaCO<sub>3</sub> and sand (RDA1 = 39.3 % and RDA2 = 5.9%); and **b)** bacterial communities constrained by metals contents (Hg, Sr, U, Be and Ba) (RDA1 = 36.0 % and RDA2 = 1.5%). The vectors are the constrained variables, the main contributors for distribution of the data.

### 3.3 Discussion

Benthic bacteria are known to act as ecosystem engineers mediating several biogeochemical processes and restoring the ecosystems health (Schratzberger and Ingels, 2018). Several studies have confirmed that bacterial metabolic pathways correlate with the environmental conditions of sediments, highlighting the ability to shape the communities and adapt their functionalities (Caruso et al., 2016; Wasmund et al., 2017; Du et al., 2022; Guo et al., 2023). These communities are sensitive to

environmental changes and have already proved to influence the diversity and distribution patterns of other benthic communities such as nematodes (Bonaglia et al., 2014; Schratzberger and Ingels, 2018; Vieira et al., 2023). This study assessed the spatial-temporal diversity patterns of bacterial communities in estuarine conditions, along three contrasting sampling sites (Navigator, Gambia and Tróia) and temporal occasions (winter 2019 and 2020; Summer, 2020 and 2021). The results of this study partially supported our initial hypothesis. The diversity patterns of bacterial communities differed significantly in response to spatial variations of sediment, although temporal variations were not significantly evident in the bacterial communities.

Based on the environmental variables, a clear pattern between sites was observed, which contributed to the diversity patterns of each bacterial community. Our findings indicate that the responses of the communities are more influenced by the specific conditions of each site than by temporal variations in sediment. Bacteria can adapt and alter their functionalities in response to different environmental conditions (Wasmund et al., 2017; Du et al., 2022; Guo et al., 2023), coupled with stochastic events that usually occur in estuarine environments (Böer et al., 2009; Aguilar and Sommaruga, 2020). In estuaries, the influence of environmental variables on the structure and distribution of benthic communities is well known (Jessen et al., 2017; Vieira et al., 2023). The sediments can intercept a large amount of OM promoting a strong biogeochemical activity (Liu et al., 2015). In this study, the variables nutrients contents (e.g., OM, TN, TC), granulometry and other factors such as proxies of primary production (e.g. chla\_phaeo and CaCO<sub>3</sub>) and some metals (e.g. Sr, Be, Ba, Hg and U) represented a significant contribution for the communities' composition. The variable OM played a crucial role by shaping the diversity patterns and separating the Navigator and Gambia communities from the communities of Tróia. The sediments of Navigator and Gambia, registered high levels of OM, gravel, clay, and metals such as Pb, As, Hg and Cr. The high redox cline characterizes these hypoxic environments which favors the high prevalence of Sulfur bacteria (Du Laing, 2011; Guo et al., 2023). This was in line with our observations, being the *Desulfobacterota* phylum one of most dominant taxa and positively correlated with the OM and gravel variables. This taxon is considered one of the most important taxonomic groups in terms of abundance and activity in muddy sediments, known to metabolize pollutants and other chemical substances under anoxic conditions (Robador et al., 2016; Jessen et al., 2017; Wasmund et al., 2017). On the other hand, sediments of Tróia were sandier, with high proportions of sand and CaCO<sub>3</sub>, which was in line with the occurrence of aerobic bacteria that potentially remineralize the OM (e.g., families *Flavobacteriaceae*, *Sapspiraceae* and *Kiloniellaceae*) (Jessen et al., 2017; Imhoff and Wiese, 2014). Members of the *Flavobacteriaceae* family showed

positive correlation with chla\_phaeo, CaCO<sub>3</sub> and sand, which were the main contributors of Tróia sediment composition. Bacteria from this taxon are strictly aerobic, facilitators of primary decomposition and degradation of several pollutants (Waśkiewicz, 2014; Pinto et al., 2015; Wasmund et al., 2017; Zhang et al., 2023). The chla\_phaeo ratio in Troia sediments demonstrated high quality of OM, revealing bacterial efficiency in the mineralization processes (Ingels et al., 2009; Jessen et al., 2017).

The presence of heavy metals in Sado estuary sediments was previously reported (Caeiro et al., 2005; Vieira et al., 2022). The high concentrations of metals such as Cr, Pb and Hg in Navigator site are mostly due to specific environment conditions such as low hydrodynamics and the clay composition of the sediments. The first sediment layers are characterized by fine-grained fraction of organic contents that play an important role in metal affinity and allocation, intercepting a wide variety of heavy metals from the surrounding anthropogenic activities (Giere, 2009; Du Laing 2011; Du et al., 2022). According to the characteristics of the Navigator and Gambia sediments, it should be highlighted that the order *Syntrophobacterales* was positively correlated with most of all analyzed metals Hg, U, Pb and Ba. These results demonstrate the influence of certain metals in the composition of bacterial communities, facilitating the prevalence of bacterial taxa that thrive in metal-polluted areas (Pinto et al., 2015; Li et al., 2020).

In a broader perspective, bacterial communities were highly diverse, presenting high values of alpha diversity. Differences in the origin and quality of OM, which is common in estuarine sediments, also favor the selection of different niches, increasing the diversity within bacterial communities (Guo et al., 2023; Sun et al., 2021). According to Zhang et al. (2023) and Fortunato et al. (2012), a reduced variation in  $\alpha$ -diversity metrics was observed in all communities over the sampling occasions, this may be a result of long-term of environmental adaptation from bacteria due to the functionality redundancy. The variability of bacterial communities appears to be overwhelmed by other variables that strongly shape the communities in a spatial and temporal scale (e.g. river discharges, organic upload, salinity gradient) (Fortunato et al., 2012). Against our assumptions, the sediments of Gambia revealed the highest bacterial richness, especially during the winter 2020 and summer 2021. The results are consistent with the high concentration of pigments (chla and phaeo) indicating a high quality of OM in sediments (Ingels et al., 2009). These changes in the nutrient fluxes and metabolic activities, could be explained by the hydrodynamic activity which determine the occurrence of primary productors and the occupation of microorganisms to broader niches (Jessen et al., 2017; Guo et al., 2023). Tróia bacterial communities, were consistently highly diverse in all sampling occasions, probably due to the sediment

properties and the redox fluctuations caused by increased hydrodynamics compared with other sites (Gambia and Navigator located within the estuary) (Guo et al., 2023).

The results from RDA analysis highlighted the clear spatial diversity patterns of bacterial communities, especially Tróia communities from the other sampling sites (Navigator and Gambia). The biogeochemical composition of the sediment was the drive factor influencing the bacterial community's diversity. Oxygen depletion is also a structuring factor in the composition and diversity patterns of the metabolic groups of these communities, highlighting the importance of its contribution to the assessment of the sediments ecological condition (Jessen et al., 2017; Sagova-Mareckova et al., 2021). Metals also demonstrated to be good drivers of bacterial communities' distribution patterns. Most of all were strongly associated to the communities of Navigator and Gambia, which are the most organically disturbed areas, with a high residence time. Bacterial diversity and communities' patterns were not driven by temporal variations but from stochastic events that usually occur in estuarine environments.

### 3.4 Concluding remarks

Benthic microorganisms are considered mediators of biogeochemical processes that sustain the biosphere (Ridall and Ingels, 2021). The fast response to biotic/abiotic stressors makes them good ecological indicators to assess the sediment quality status (Schratzberger and Ingels, 2018; Grill et al., 2019; Ridall and Ingels, 2021; Sagova-Mareckova et al., 2021). Our study allowed to describe different levels of environment conditions analyzing the diversity and composition of bacterial communities, proving to be a promising indicator of sediment environmental status of the Sado estuary. The physical composition of the sediment, the hydrodynamic activity and organic contents were the main drivers of bacterial distribution patterns, clearly distinguishing the bacterial communities in Tróia from those in Gambia and Navigator sediments.

The bacterial communities in Tróia were mainly composed by aerobic groups, which is known for being more efficient in mineralization processes. This was in line with the high-quality organic matter obtained in Tróia sediments (high chlorophyll a/pheopigment). Navigator and Gambia bacterial communities were mainly composed by anaerobic groups, with specialized functions influenced by environmental factors like temperature and pollutants (e.g. methane or other non-methane hydrocarbons). The no significant variability in the temporal scale was already confirmed in other studies and could be explained by the bacterial functional redundancy, entangled with by stochastic events that usually occur in estuarine environments (Böer et al., 2009).

This study provided an important temporal bacterial baseline dataset from Sado estuary to explore the importance of bacterial networks to ecosystem functioning and benthic food web dynamics as well as their potential environmental drivers.

### 3.5 References

16S metagenomic sequencing library

16S metagenomic sequencing library 16S metagenomic sequencing library preparation reference guide. <https://support.illumina.com>. (Accessed 23 June 2023).

Aguilar, P., Sommaruga, R., 2020. The balance between deterministic and stochastic processes in structuring lake bacterioplankton community over time. *Mol. Ecol.* 29, 3117–3130. <https://doi.org/10.1111/mec.15538>, 2020.

Anderson, M.J., Gorley, R.N., Clarke, K.R., 2008. In: Plymouth, U.K. (Ed.), *PERMANOVA +for PRIMER: Guide to Software and Statistical Methods*.

Armstrong, G., Cantrell, K., Huang, S., McDonald, D., Haiminen, N., Carrieri, A.P., Zhu, Q., Gonzalez, A., McGrath, I., Beck, K.L., Hakim, D., Havulinna, A.S., M'eric, G., Niiranen, T., Lahti, L., Salomaa, V., Jain, M., Inouye, M., Swafford, A.D., Kim, H.C., Parida, L., V'azquez-Baeza, Y., Knight, R., 2021. Efficient computation of Faith's phylogenetic diversity with applications in characterizing microbiomes. *Genome Res.* 31 (11), 2131–2137. <https://doi.org/10.1101/gr.275777.121>. Epub 2021 Sep 3. PMID: 34479875; PMCID: PMC8559715.

Barnett, J.M.D., Arts, C.W.I., Penders, J., 2021. microViz: an R package for microbiome data visualization and statistics. *J. Open Source Softw.* 6 (63), 3201. <https://doi.org/10.21105/joss.03201>.

Bettencourt, A.M., Bricker, S.B., Ferreira, J.G., Franco, A., Marques, J.C., Melo, J.J., Nobre, A., Ramos, L., Reis, C.S., Salas, F., Silva, M.C., Simas, T., Wolff, W.J., 2004. Typology and reference conditions for Portuguese transitional and coastal waters. Institute of Marine Research.

Böer, Simone I., Hedtkamp, Stefanie I.C., van Beusekom, Justus E.E., Fuhrman, Jed A., Boetius, Antje, Ramette, Alban, July 2009. Time- and sediment depth-related variations in bacterial diversity and community structure in subtidal sands. *ISME J.* 3 (7), 780–791. <https://doi.org/10.1038/ismej.2009.29>.

Bokulich, N., Robeson, M., Dillon, M., et al., 2021. Bokulich-lab/RESCRIPt: 2021. <https://doi.org/10.5281/ZENODO.4811136>.

Bolyen, E., Rideout, J.R., Dillon, M.R., et al., 2019. Qiime 2: reproducible, interactive, scalable, and Extensible microbiome data science. <https://doi.org/10.7287/peerj.pr eprints.27295v2>.

Bonaglia, S., Nascimento, F.J.A., Bartoli, M., Klawonn, I., Brüchert, V., 2014. Meiofauna increases bacterial denitrification in marine sediments. *Nat. Commun.* 5, 5133. <https://doi.org/10.1038/ncomms6133>.

Borja, A., Marín, S.L., Muxika, I., Pino, L., Rodríguez, J.G., 2015. Is there a possibility of ranking benthic quality assessment indices to select the most responsive to different human pressures? *Mar. Pollut. Bull.* 97, 85–94. <https://doi.org/10.1016/j.marpolbul.2015.06.030>.

Branco, J., Pedro, S., Alves, A.S., Ribeiro, C., Materatski, P., Pires, R., Caçador, I., Adão, H., 2018. Natural recovery of *Zostera noltii* seagrass beds and benthic nematode assemblage responses to physical disturbance caused by traditional harvesting activities. *J. Exp. Mar. Biol. Ecol.* 502, 191–202. <https://doi.org/10.1016/J.JEMBE.2017.03.003>.

Buongiorno, J., Herbert, L., Wehrmann, L., Michaud, A., Laufer, K., Røy, H., et al., 2019. Complex microbial communities drive iron and sulfur cycling in Arctic fjord sediments. *Appl. Environ. Microbiol.* 85, e00949, 19. 2019.

Caeiro, S., Costa, M.H., Ramos, T.B., Fernandes, F., Silveira, N., Coimbra, A., Medeiros, G., Painho, M., 2005. Assessing heavy metal contamination in Sado Estuary sediment: an index analysis approach. *Ecol. Indicat.* 5, 151–169. <https://doi.org/10.1016/j.ecolind.2005.02.001>.

Callahan, B.J., McMurdie, P.J., Rosen, M.J., Han, W.A., Johnson, A.J., Holmes, P.S., 2016. DADA2: high-resolution sample inference from Illumina amplicon data. *Nat. Methods* 137 (13), 581–583. <https://doi.org/10.1038/nmeth.3869>.

Camargo, A., 2022. PCAtest: testing the statistical significance of Principal Component Analysis in R. *PeerJ* 10, e12967. <https://doi.org/10.7717/peerj.12967>.

Caruso, G., et al., 2016. Microbial assemblages for environmental quality assessment: knowledge, gaps and usefulness in the European marine strategy framework

directive. *Crit. Rev. Microbiol.* 42 (6), 883–904. <https://doi.org/10.3109/1040841X.2015.1087380>.

Catry, T., Vale, C., Pedro, P., Pereira, E., Mil-Homens, M., Raimundo, J., Tavares, D., Granadeiro, P.J., 2021. Elemental composition of whole body soft tissues in bivalves from the Bijagós Archipelago, Guinea-Bissau. *Environmental Pollution* 288, 117705. <https://doi.org/10.1016/j.envpol.2021.117705>. ISSN 0269-7491.

Clarke, K.R., Warwick, R.M., 2001. *Changes in Marine Communities: an Approach to Statistical Analysis and Interpretation*, second ed.

Costley, C.T., Mossop, K.F., Dean, R.J., Garden, M.L., Marshall, J., Carroll, J., 2000. Determination of mercury in environmental and biological samples using pyrolysis atomic absorption spectrometry with gold amalgamation. *Anal. Chim. Acta* 405 (1–2), 179–183. [https://doi.org/10.1016/S0003-2670\(99\)00742-4](https://doi.org/10.1016/S0003-2670(99)00742-4). ISSN 0003-2670, 2000.

Du, M., Zheng, M., Liua, A., Wang, L., Pan, X., Liu, J., Ran, X., 2022. Effects of emerging contaminants and heavy metals on variation in bacterial communities in estuarine sediments. *Sci. Total Environ.* 832, 155118. <https://doi.org/10.1016/j.scitotenv.2022.155118>, 2022.

Du Laing, G., 2011. Redox metal processes and controls in estuaries. In: Wolanski, E., McLusky, D. (Eds.), *Treatise on Estuarine and Coastal Science*. Academic Press, ISBN 9780080878850, pp. 115–141. <https://doi.org/10.1016/B978-0-12-374711-2.00406-X>.

Elliott, M., Quintino, V., 2007. The Estuarine Quality Paradox, Environmental Homeostasis and the difficulty of detecting anthropogenic stress in naturally stressed areas. *Mar. Pollut. Bull.* 54 (2007), 640–645. <https://doi.org/10.1016/j.marpolbul.2007.02.003>.

Faith, D.P., 1992. Conservation evaluation and phylogenetic diversity. *Biol. Conserv.* 61, 1–10.

Fortunato, C., Herfort, L., Zuber, P., et al., 2012. Spatial variability overwhelms seasonal patterns in bacterioplankton communities across a river to ocean gradient. *ISME J.* 6, 554–563. <https://doi.org/10.1038/ismej.2011.135>, 2012.

Giere, O., 2009. *Meiobenthology. The Microscopic Motile Fauna of Aquatic Sediments.* Springer-Verlag, Heidelberg, 2009.

Goodwin, K.D., et al., 2017. DNA sequencing as a tool to monitor marine ecological status. *Front. Mar. Sci.* <https://doi.org/10.3389/fmars.2017.00107>.

Grill, G., et al., 2019. Mapping the world's free-flowing rivers. *Nature* 569, 215–221. <https://doi.org/10.1038/s41586-019-1111-9>.

Guo, Z., Li, Y., Shao, M., Sun, T., Lin, M., Zhang, T., Hu, K., Jiang, H., Guan, X., 2023. Succession and environmental response of sediment bacterial communities in the Liao River Estuary at the centenary scale. *Mar. Environ. Res.* 188, 105980. <https://doi.org/10.1016/j.marenvres.2023.105980>, 2023.

Imhoff, J.F., Wiese, J., 2014. The Order Kiloniellales. In: Rosenberg, E., DeLong, E.F., Lory, S., Stackebrandt, E., Thompson, F. (Eds.), *The Prokaryotes*. Springer, Berlin, Heidelberg. [https://doi.org/10.1007/978-3-642-30197-1\\_301](https://doi.org/10.1007/978-3-642-30197-1_301).

Ingels, J., Kiriakoulakis, K., Wolff, A.G., Vanreusel, A., 2009. Nematode diversity and its relation to the quantity and quality of sedimentary organic matter in the deep Nazaré Canyon, Western Iberian Margin. *Deep-Sea Res. I* 56 (2009), 1521–1539. <https://doi.org/10.1016/j.dsr.2009.04.010>.

Gregory Caporaso, J., Lauber, Christian L., Walters, William A., Berg-Lyons, Donna, Huntley, James, Fierer, Noah, Owens, Sarah M., Betley, Jason, Fraser, Louise, Bauer, Markus, Gormley, Niall, Gilbert, Jack A., Smith, Geoff, Knight, Rob, August 2012. Ultra-high-throughput microbial community analysis on the Illumina HiSeq and MiSeq platforms. *ISME J.* 6 (8), 1621–1624. <https://doi.org/10.1038/ismej.2012.8>.

Jessen, L.G., Lichtschlag, A., Ramette, A., Pantoja, S., Rossel, E.P., Schubert, J.C., Struck, U., Boetius, A., 2017. Hypoxia causes preservation of labile organic matter and changes seafloor microbial community composition (Black Sea). *Sci. Adv.* 3 (2). <https://doi.org/10.1126/sciadv.1601897>.

Jokanovi, S., Kajan, K., Perovi, S., Ivani, M., Maci, V., Orlic, S., 2021. Anthropogenic influence on the environmental health along Montenegro coast based on the bacterial and chemical characterization. *Environmental Pollution* 271, 116383. <https://doi.org/10.1016/j.envpol.2020.116383>.

Jost, L., 2006. Entropy and diversity. *Oikos* 113 (2), 363–375. <https://doi.org/10.1111/j.2006.0030-1299.14714.x>.

L'ê, S., Josse, J., Husson, F., 2008. FactoMineR: an R package for multivariate analysis. *J. Stat. Software* 25, 1–18.

Leinster, T., Cobbold, C.A., 2012. Measuring diversity: the importance of species similarity. *Ecology* 93 (3), 477–489.

Li, C.C., Quan, Q., Gan, Y., Dong, J., Fang, J., Wang, L., Liu, J., 2020. Effects of heavy metals on microbial communities in sediments and establishment of bioindicators based on microbial taxa and function for environmental monitoring and management. *Sci. Total Environ.* 749, 141555. <https://doi.org/10.1016/j.scitotenv.2020.141555>.

Liu, X., Hu, H.W., Liu, Y.R., et al., 2015. Bacterial composition and spatiotemporal variation in sediments of Jiaozhou Bay, China. *J. Soils Sediments* 15, 732–744. <https://doi.org/10.1007/s11368-014-1045-7>.

Lorenzen, C.J., 1967. Determination of chlorophyll and Pheo-pigments: spectrophotometric Equations. *Limnol. Oceanogr.* 12 (2), 343–346. <https://doi.org/10.4319/lo.1967.12.2.0343>.

Mahamound, A., Lyautey, E., Bonnneau, C., Dabrin, A., Pesce, S., 2018. Environmental concentrations of Copper, alone or in mixture with Arsenic, can impact river sediment microbial community structure and functions. *Sec. Microbiotechnology* 9, 2018. <https://doi.org/10.3389/fmicb.2018.01852>.

McMurdie, P.J., Holmes, S., 2013. phyloseq: An R package for reproducible interactive analysis and graphics of microbiome census data. *PLoS ONE* 8 (4), e61217. <https://doi.org/10.1371/journal.pone.0061217>.

Nawaz, A., Purahong, W., Lehmann, R., Herrmann, M., Totsche, K.U., Küsel, K., Wubet, T., Buscot, F., 2018. First insights into the living groundwater mycobiome of the terrestrial biogeosphere. *Water Res.* 145, 50–61. <https://doi.org/10.1016/j.watres.2018.07.067>.

Nigel, G. Yoccoz., 2012. The future of environmental DNA in ecology. *Mol. Ecol.* 21, 2031–2038. <https://doi.org/10.1111/j.1365-294X.2012.05505.x>.

Panieri, G., Argentino, C., Ramalho P. S., Vulcano F., Savini A., Fallati L., Brekke T., Galimberti G., Riva F., Balsa J., Eilertsen H. M., Stokke R., Steen H. I., Sahy D., Kalenitchenko D., Büenz S., Mattingsdal R., 2023. An Arctic natural oil seep investigated from space to the seafloor, *Science of The Total Environment*, V.907, 2024, <https://doi.org/10.1016/j.scitotenv.2023.167788>.

Patrício, J., Adão, H., Neto, J.M., Alves, A.S., Traunspurger, W., Marques, J.C., 2012. Do nematode and macrofauna assemblages provide similar ecological assessment information? *Ecol. Indic.* 14, 124–137. <https://doi.org/10.1016/j.ecolind.2011.06.027>.

Pawlowski, et al., 2018. The future of biotic indices in the ecogenomic era: Integrating (e) DNA metabarcoding in biological assessment of aquatic ecosystems. *Sci. Total Environ.* 637, 1295–1310. <https://doi.org/10.1016/j.scitotenv.2018.05.002>, 638, 2018.

Pedregosa, F., Varoquaux, G., Michel, V., Thirion, B., 2011. Scikit-learn: machine learning in python. *Journal of machine learning research* 12 (Oct), 2825–2830.

Pinto, A.B., Pagnocca, F.C., Pinheiro, M.A., Fontes, R.F., de Oliveira, A.J., 2015. Heavy metals and TPH effects on microbial abundance and diversity in two estuarine areas of the southern-central coast of São Paulo State, Brazil. *Mar. Pollut. Bull.* 96, 410–417. <https://doi.org/10.1016/j.marpolbul.2015.04.014>.

Quast, C., Pruesse, E., Yilmaz, P., Gerken, J., Schweer, T., Yarza, P., Peplies, J., Glockner, O.F., 2013. The SILVA ribosomal RNA gene database project: improved data processing and web-based tools. *Nucleic Acids Res.* 41, D590–D596. <https://doi.org/10.1093/NAR/GKS1219>.

R Core Team, 2022. A Language and Environment for Statistical Computing. Version 2022.07.2 Build 576. R Foundation for Statistical Computing, Vienna. <https://www.r-project.org>.

Ridall, A., Ingels, J., 2021. Suitability of free-living marine nematodes as bioindicators: status and future considerations. *Front. Mar. Sci.* 863. <https://doi.org/10.3389/FMARS.2021.685327>, 0.

Robador, A., Müller, A., Sawicka, J., 2016. Activity and community structures of sulfate-reducing microorganisms in polar, temperate and tropical marine sediments. *ISME J.* 10, 796–809. <https://doi.org/10.1038/ismej.2015.157>.

Rocca, D.J., Simonin, M., Blaszczak, R.J., Ernakovich, J., Gibbons, M.S., Midani, S.F., Washburne, D.A., 2019. The microbiome stress project: toward a Global Meta-analysis of environmental stressors and their effects on microbial communities. *Sec. Microbiotechnology* 9, 2018. <https://doi.org/10.3389/fmicb.2018.03272>.

Rumohr, H., 2009. Soft-bottom macrofauna: collection, treatment, and quality assurance of samples. *ICES Tech. Mar. Environ. Sci.* 20. <https://doi.org/10.25607/OPB-238>.

Sagova-Mareckova, M., Boenigk, J., Bouchez, A., Cermakova, K., Chonova, T., Cordier, T., Eisendle, U., Elersek, T., Fazi, S., Fleituch, T., Frühe, L., Gajdosova, M., Graupner, N., Haegerbaeumer, A., Kelly, A.-M., Kopecky, J., Leese, F., N̄oges, P., Orlic, S., Panksep, K., Pawlowski, J., Petrusek, A., Piggott, J.J., Rusch, J.C., Salis, R., Schenk, J., Simek, K., Stoicek, A., Strand, D.A., Vasquez, M.I., Vrålstad, T., Zlatkovic, S., Zupancic, M., Stoeck, T., 2021. Expanding ecological assessment by integrating microorganisms into routine freshwater biomonitoring. *Water Res.* 191 (2021), 116767. <https://doi.org/10.1016/j.watres.2020.116767>. ISSN 0043-1354.

Schratzberger, M., Ingels, J., 2018. Meiofauna matters: the roles of meiofauna in benthic ecosystems. *J. Exp. Mar. Biol. Ecol.* 502, 12–25. <https://doi.org/10.1016/j.jembe.2017.01.007>.

Schratzberger, M., Somerfield, P.J., 2020. Effects of widespread human disturbances in the marine environment suggest a new agenda for meiofauna research is needed. *Sci. Total Environ.* 728, 138435. <https://doi.org/10.1016/j.scitotenv.2020.138435>.

Shah, R.M., Stephenson, S., Crosswell, J., Gorman, D., Hillyer, E.K., Palombo, A.E., Jones, A.H.O., Cook, S., Bodrossy, L., Van de Kamp, J., Walsh, K.T., Bissett, A., Steven, D.L.A., David, J., Beale, J.D., 2022. Omics-based ecosurveillance uncovers the influence of estuarine macrophytes on sediment microbial function and metabolic redundancy in a tropical ecosystem. *Sci. Total Environ.* 809, 151175. <https://doi.org/10.1016/j.scitotenv.2021.151175>. ISSN 0048-9697, 2022.

Sroczyńska, K., Chainho, P., Vieira, S., Adão, H., 2021. What makes a better indicator? Taxonomic vs functional response of nematodes to estuarine gradient. *Ecol. Indicators.* 121, 107113. <https://doi.org/10.1016/j.ecolind.2020.107113>.

Stoeck, T., Frühe, L., Forster, D., Cordier, T., Martins, C.I., Pawlowski, J., 2018. Environmental DNA metabarcoding of benthic bacterial communities indicates the benthic footprint of salmon aquaculture *Mar. Pollut. Bull.* 127, 139–149.

Sun, X., Cao, X., Zhao, D., Zeng, J., Huang, R., Duan, M., Yu, Z., 2021. The pattern of sedimentary bacterial communities varies with latitude within a large eutrophic lake. *Limnologica* 87, 125860. <https://doi.org/10.1016/j.limno.2021.125860>.

Vieira, S., Barrulas, P., Chainho, P., et al., 2022. Spatial and temporal distribution of the Multi-element Signatures of the estuarine non-indigenous Bivalve *Ruditapes philippinarum*. *Biol. Trace Elem. Res.* 200, 385–401. <https://doi.org/10.1007/s12011-021-02629-x>.

Vieira, S., Sroczyńska, K., Neves, J., Martins, M., Costa, M.H., Adão, H., Vicente, S.L.C., 2023. Distribution patterns of benthic bacteria and nematode communities in estuarine sediments. *Estuar. Coast Shelf Sci.* 291, 108448. <https://doi.org/10.1016/j.ecss.2023.108448>.

Vieira, S., Maurer, A.-F., Dias, C.B., Neves, J., Martins, M., Lobo-Arteaga, J., Adão, H., Sroczyńska, K., 2024. Food web attributes to assess spatial–temporal dynamics in estuarine benthic ecosystem. *Ecol. Indicat.* 166, 112243. <https://doi.org/10.1016/j.ecolind.2024.112243>, 2024.

Waśkiewicz, L., 2014. Irzykowska in *Encyclopedia of Food Microbiology*, second ed.

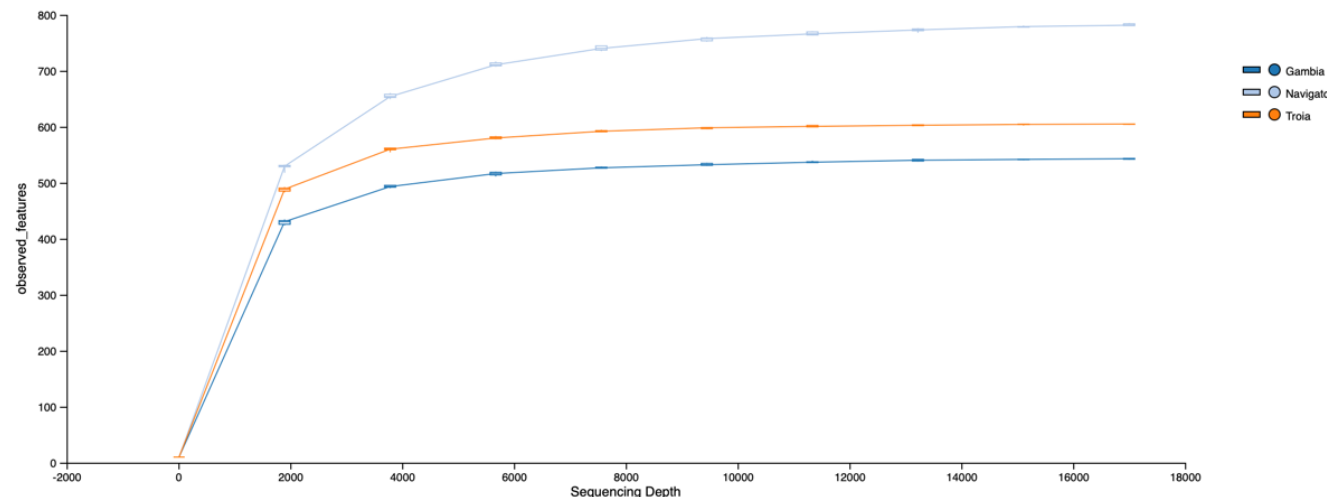
Wasmund, K., Mußmann, M., Loy, A., 2017. The life sulfuric: microbial ecology of sulfur cycling in marine sediments. *Environmental Microbiology Reports* 9 (4), 323–344. <https://doi.org/10.1111/1758-2229.12538>.

Xie, X., Müller, 2019. Enhanced aniline degradation by *Desulfatiglans anilini* in a synthetic microbial community with the phototrophic purple sulfur bacterium *Thiocapsa roseopersicina*. *Syst. Appl. Microbiol.* 42, 125998. <https://doi.org/10.1016/j.syapm.2019.06.003>.

Zeng, X.Y., Li, S.W., Leng, Y., Kang, X.H., 2020. Structural and functional responses of bacterial and fungal communities to multiple heavy metal exposure in arid loess. *Sci. Total Environ.* 723, 138081. <https://doi.org/10.1016/j.scitotenv.2020.138081>.

Zhang, Z., Han, P., Zheng, Y., et al., 2023. Spatiotemporal dynamics of bacterial taxonomic and functional Profiles in estuarine intertidal Soils of China coastal Zone. *Microb. Ecol.* 85, 383–399. <https://doi.org/10.1007/s00248-022-01996-9>.

Zhao, Y., Bai, Y., Guo, Q., Li, Z., Qi, M., Ma, X., Wang, H., Kong, D., Wang, A., Liang, B., 2019. Bioremediation of contaminated urban river sediment with methanol stimulation: metabolic processes accompanied with microbial community changes. *Sci. Total Environ.* 653, 649–657. <https://doi.org/10.1016/j.scitotenv.2018.10.396>, 2019.

**Supplementary information of Chapter 3***Appendix A – Figures and Tables*

**Figure. A.1** Rarefaction curve of ASVs reads from each sampling site Navigator, Gambia and Tróia.

**Table A.1** Mean $\pm$ SE, n=3 of the raw data of the environmental and biogeochemical parameters measured in each site (Navigator, Gambia and Tróia), across the 4 sampling occasions (winter 2019 and 2020, summer 2020 and 2021). Granulometric parameters (expressed in %) are clay, sand and gravel. The elemental composition (expressed in weight %) are organic matter (OM), Total Nitrogen and Carbon (NT and CT), pigments measured (expressed in mg/g) are chlorophyl a (chl a) and phaeopigment (Phaeo) the quality of organic matter “freshness” was calculated the ratio of both pigments, chlorophyl a/phaeopigment (chl a\_phaeo). The instant variables measured *in situ* were Temperature (°C), Salinity, Oxygen (mg/L) and pH. (adapted from Vieira et al., 2024).

Sampling occasions		Winter 2019			Summer 2020			Winter 2020			Summer 2021		
Sites		Navigator	Gambia	Tróia	Navigator	Gambia	Tróia	Navigator	Gambia	Tróia	Navigator	Gambia	Tróia
Granulometry	Clay	30.1 $\pm$ 3.1	13.5 $\pm$ 0.2	1.8 $\pm$ 0.2	20.9 $\pm$ 1	17.4 $\pm$ 5.1	1.7 $\pm$ 0.1	35.2 $\pm$ 6.6	15.8 $\pm$ 1.7	1.5 $\pm$ 0.5	25.8 $\pm$ 2.3	16.3 $\pm$ 2.2	2.9 $\pm$ 0.4
	Sand	66.2 $\pm$ 2.6	71.5 $\pm$ 5.5	93.8 $\pm$ 1.9	73.1 $\pm$ 1.7	67.5 $\pm$ 4.1	97.3 $\pm$ 0.1	61.8 $\pm$ 6.1	68.7 $\pm$ 1	95.2 $\pm$ 1.1	72.2 $\pm$ 2.6	66.6 $\pm$ 0.6	91.6 $\pm$ 2.8
	Gravel	3.8 $\pm$ 0.7	14.9 $\pm$ 5.6	4.4 $\pm$ 1.8	5.9 $\pm$ 1.5	15.1 $\pm$ 6.4	1 $\pm$ 0.1	3 $\pm$ 0.7	15.5 $\pm$ 1	3.3 $\pm$ 1	2 $\pm$ 0.3	16.9 $\pm$ 2.1	5.4 $\pm$ 2.8
Elemental composition	Organic Matter	3.9 $\pm$ 0.6	0.6 $\pm$ 0.04	1.9 $\pm$ 0.3	2.3 $\pm$ 0.3	1.7 $\pm$ 0.3	0.4 $\pm$ 0.02	2.4 $\pm$ 0.3	0.8 $\pm$ 0.05	0.4 $\pm$ 0.02	2.1 $\pm$ 0.1	1.2 $\pm$ 0.1	0.5 $\pm$ 0.04
	Total Carbon	0.9 $\pm$ 0.3	0.7 $\pm$ 0.4	0.6 $\pm$ 0.06	1.1 $\pm$ 0.1	0.4 $\pm$ 0.1	0.7 $\pm$ 0.1	1.1 $\pm$ 0.1	0.5 $\pm$ 0.03	0.5 $\pm$ 0.04	0.9 $\pm$ 0.1	0.4 $\pm$ 0.05	0.6 $\pm$ 0.03
	Total Nitrogen	0.06 $\pm$ 0.2	0.05 $\pm$ 0.02	0.02 $\pm$ 0.008	0.07 $\pm$ 0.006	0.03 $\pm$ 0.01	0.01 $\pm$ 0.003	0.3 $\pm$ 0.09	0.05 $\pm$ 0.005	0.08 $\pm$ 0.002	0.07 $\pm$ 0.007	0.04 $\pm$ 0.006	0.01 $\pm$ 0.003
	CaCO <sub>3</sub>	2.4 $\pm$ 0.5	1 $\pm$ 0.06	4.3 $\pm$ 0.3	2.6 $\pm$ 0.5	1.6 $\pm$ 0.3	4.6 $\pm$ 0.9	2.1 $\pm$ 0.05	1.2 $\pm$ 0.04	3.5 $\pm$ 0.3	1.7 $\pm$ 0.1	1.3 $\pm$ 0.05	3.7 $\pm$ 0.3
	Chlorophyl a	15.6 $\pm$ 3.9	10.3 $\pm$ 0.9	26.7 $\pm$ 2.1	9.8 $\pm$ 0.1	55.5 $\pm$ 2.4	11.1 $\pm$ 1.4	31.1 $\pm$ 6.6	10.8 $\pm$ 1.9	6.7 $\pm$ 0.5	4.8 $\pm$ 0.8	7.7 $\pm$ 0.7	4.9 $\pm$ 0.6
	Phaeopigments	14.7 $\pm$ 3.7	7.8 $\pm$ 0.5	14.5 $\pm$ 1	10.6 $\pm$ 1.2	115.1 $\pm$ 32.7	5.2 $\pm$ 0.9	40.1 $\pm$ 9.4	5.1 $\pm$ 1.5	4.5 $\pm$ 0.8	1.6 $\pm$ 0.2	3.6 $\pm$ 0.4	1.3 $\pm$ 0.2
	Chla_phaeo	1.1 $\pm$ 0.02	1.3 $\pm$ 0.1	1.8 $\pm$ 0.06	0.9 $\pm$ 0.1	0.7 $\pm$ 0.3	2.2 $\pm$ 0.1	0.8 $\pm$ 0.02	2.5 $\pm$ 0.6	1.7 $\pm$ 0.3	2.9 $\pm$ 0.1	2.1 $\pm$ 0.05	4 $\pm$ 0.4
Instant variables	Temperature	15.3 $\pm$ 0.1	11.1 $\pm$ 0.2	15.3 $\pm$ 0.1	28.5 $\pm$ 0.5	24.4 $\pm$ 0.2	23.9 $\pm$ 0.1	13.5 $\pm$ 0.2	16.8 $\pm$ 0.2	16.8 $\pm$ 0.2	23.8 $\pm$ 0.9	23.6 $\pm$ 0.1	20.7 $\pm$ 0.2
	Salinity	31.9 $\pm$ 0.9	30.6 $\pm$ 0.7	31.8 $\pm$ 0.9	36.5 $\pm$ 0.3	17.7 $\pm$ 0.1	16.4 $\pm$ 0.04	15.9 $\pm$ 0.05	14.7 $\pm$ 0.05	14.7 $\pm$ 0.5	15 $\pm$ 0.5	14 $\pm$ 1.5	15.3 $\pm$ 0.3
	Oxygen	9.2 $\pm$ 0.1	14.5 $\pm$ 2.5	9.2 $\pm$ 0.1	8.3 $\pm$ 1.3	9.5 $\pm$ 0.4	12.1 $\pm$ 0.3	9.6 $\pm$ 0.4	17.9 $\pm$ 0.4	13.9 $\pm$ 0.3	5.3 $\pm$ 0.6	8.8 $\pm$ 0.4	8.6 $\pm$ 0.2
	pH	7.9 $\pm$ 0.01	7.9 $\pm$ 0.05	7.9 $\pm$ 0.01	8.1 $\pm$ 0.1	7.8 $\pm$ 0.02	7.9 $\pm$ 0.04	8.3 $\pm$ 0.3	8.6 $\pm$ 0.3	8.9 $\pm$ 0.04	7.8 $\pm$ 0.1	8.1 $\pm$ 0.1	8.3 $\pm$ 0.02

**Table A.2** Mean  $\pm$  SE (n=3), metal concentrations measured in sediment samples from each site (Navigator, Gambia and Tróia) across 4 sampling occasions (Winter 2019 and 2020, Summer 2020 and 2021). The analyzed metals were Li, Sr, Mn, Ni, Cr, Be, U, Ba, Co, Cu, Zn, As, Pb and Hg (expressed in mg/kg), (adapted from Vieira et al., 2024).

Sampling occasions		Winter 2019			Summer 2020			Winter 2020			Summer 2021		
Sites		Navigator	Gambia	Tróia	Navigator	Gambia	Tróia	Navigator	Gambia	Tróia	Navigator	Gambia	Tróia
Metals	Li	28.7 $\pm$ 2.8	20.4 $\pm$ 0.7	11.5 $\pm$ 0.3	30.8 $\pm$ 2.7	25.6 $\pm$ 0.9	12.1 $\pm$ 0.3	28 $\pm$ 1.3	20.9 $\pm$ 3.5	11.5 $\pm$ 0.05	29 $\pm$ 0.7	16.9 $\pm$ 2.3	13.5 $\pm$ 0.2
	Sr	110.3 $\pm$ 18.6	45.6 $\pm$ 0.9	74.4 $\pm$ 3.3	61.3 $\pm$ 0.9	50.4 $\pm$ 0.6	69.8 $\pm$ 1.2	96.1 $\pm$ 20.6	48.8 $\pm$ 4.1	97.9 $\pm$ 20.4	61.2 $\pm$ 3.6	62.5 $\pm$ 1.3	73.5 $\pm$ 1.7
	Mn	100.6 $\pm$ 6.9	61.7 $\pm$ 4.3	45.6 $\pm$ 2.9	111.4 $\pm$ 9.2	83.9 $\pm$ 5.8	49.6 $\pm$ 2.7	115.1 $\pm$ 3.7	71.1 $\pm$ 12.9	39.9 $\pm$ 0.2	103.9 $\pm$ 3.6	62.2 $\pm$ 10	52.7 $\pm$ 3.3
	Ni	15.1 $\pm$ 2.1	7.8 $\pm$ 0.9	3.8 $\pm$ 0.08	18.7 $\pm$ 1.3	93.4 $\pm$ 61.8	8.3 $\pm$ 0.9	15.7 $\pm$ 0.8	9.6 $\pm$ 2.2	4.3 $\pm$ 0.06	15.8 $\pm$ 0.7	10.4 $\pm$ 1.6	9.5 $\pm$ 1.1
	Cr	29.3 $\pm$ 3.8	15 $\pm$ 3.3	3.6 $\pm$ 0.1	29.9 $\pm$ 3.2	157.9 $\pm$ 105	4.8 $\pm$ 0.3	26.5 $\pm$ 1.9	16.5 $\pm$ 7	3.5 $\pm$ 0.03	29.7 $\pm$ 0.2	11.7 $\pm$ 3.5	6.1 $\pm$ 0.4
	Be	1 $\pm$ 0.1	0.6 $\pm$ 0.04	0.6 $\pm$ 0.2	1.2 $\pm$ 0.07	0.8 $\pm$ 0.03	0.7 $\pm$ 0.1	0.9 $\pm$ 0.06	0.6 $\pm$ 0.2	1.4 $\pm$ 0.06	1.2 $\pm$ 0.08	0.8 $\pm$ 0.09	1.4 $\pm$ 0.4
	U	3.3 $\pm$ 0.6	1.2 $\pm$ 0.07	0.4 $\pm$ 0.02	2.2 $\pm$ 0.2	1.4 $\pm$ 0.1	0.4 $\pm$ 0.01	1.9 $\pm$ 0.1	1.4 $\pm$ 0.2	0.4 $\pm$ 0.01	1.8 $\pm$ 0.1	0.8 $\pm$ 0.09	0.5 $\pm$ 0.03
	Ba	246 $\pm$ 7	236.7 $\pm$ 5	234.7 $\pm$ 7	255.7 $\pm$ 2	252.2 $\pm$ 6.3	226.7 $\pm$ 12.5	230.4 $\pm$ 8.8	223.5 $\pm$ 24.6	245.3 $\pm$ 7.8	251.1 $\pm$ 4.7	244.7 $\pm$ 6.8	238.8 $\pm$ 13
	Co	4.6 $\pm$ 0.7	2.7 $\pm$ 0.4	0.6 $\pm$ 0.02	4.9 $\pm$ 0.4	4.9 $\pm$ 0.9	0.8 $\pm$ 0.05	4.3 $\pm$ 0.3	3 $\pm$ 1.1	0.6 $\pm$ 0.03	4.6 $\pm$ 0.1	2 $\pm$ 0.6	0.9 $\pm$ 0.05
	Cu	28.6 $\pm$ 6.7	8 $\pm$ 1.9	1.6 $\pm$ 0.2	32.9 $\pm$ 0.5	20.5 $\pm$ 4.3	2.4 $\pm$ 0.4	19.6 $\pm$ 1.4	11.2 $\pm$ 5.4	1.8 $\pm$ 0.3	37.8 $\pm$ 5.3	10.2 $\pm$ 3.1	3.7 $\pm$ 0.3
	Zn	82.3 $\pm$ 21.9	26.5 $\pm$ 7.5	3.1 $\pm$ 0.8	95.6 $\pm$ 5	41.7 $\pm$ 3.8	7.9 $\pm$ 1.9	63.9 $\pm$ 8.5	25.4 $\pm$ 9.6	4.6 $\pm$ 0.3	109.3 $\pm$ 19.5	20.6 $\pm$ 6.4	9.5 $\pm$ 0.8
	As	13.8 $\pm$ 2.9	4.7 $\pm$ 0.9	1.7 $\pm$ 0.1	12.9 $\pm$ 0.6	7.9 $\pm$ 0.8	1.6 $\pm$ 0.2	12.2 $\pm$ 1.9	7.3 $\pm$ 1.3	2.3 $\pm$ 0.2	11.3 $\pm$ 1.3	4.5 $\pm$ 1.3	0.9 $\pm$ 0.2
	Pb	25.4 $\pm$ 3.9	14.7 $\pm$ 1	12.2 $\pm$ 0.4	27.3 $\pm$ 0.9	17.9 $\pm$ 0.6	12.4 $\pm$ 0.6	22.1 $\pm$ 1.8	14.1 $\pm$ 2.4	12.9 $\pm$ 0.4	29.3 $\pm$ 3.3	14.9 $\pm$ 0.9	13.1 $\pm$ 0.6
	Hg	0.3 $\pm$ 0.07	0.3 $\pm$ 0.2	0.03 $\pm$ 0.0007	0.3 $\pm$ 0.05	0.1 $\pm$ 0.003	0.02 $\pm$ 0.004	0.3 $\pm$ 0.05	0.06 $\pm$ 0.01	0.03 $\pm$ 0.006	0.3 $\pm$ 0.06	0.04 $\pm$ 0.01	0.05 $\pm$ 0.002

**Table A.3** Mean  $\pm$  SE, (n=3) of alpha diversity descriptors (Observed ASVs, Chao1, se.Chao1 (standard error of Chao1), Abundance-based coverage estimator (ACE), se.ACE (standard error of ACE), Shannon (H), Effective numbers for Shannon ( $H1=exp(H')$ ), Simpson (D) and Inverse Simpson index (InvSimpson)) calculated for each sampling site (Navigator, Gambia and Tróia) across 4 sampling occasions (Winter 2019 and 2020, Summer 2020 and 2021).

Sampling occasions	Winter 2019			Summer 2020			Winter 2020			Summer 2021		
	Sites	Navigator	Gambia	Tróia	Navigator	Gambia	Tróia	Navigator	Gambia	Tróia	Navigator	Gambia
Observed	448.3 $\pm$ 28.9	648.3 $\pm$ 91.5	604.3 $\pm$ 24.5	626 $\pm$ 111	674 $\pm$ 93.8	573.7 $\pm$ 24.5	538.3 $\pm$ 24	783 $\pm$ 24	654 $\pm$ 42	628 $\pm$ 15	834 $\pm$ 108.7	560 $\pm$ 33.4
Chao1	450.3 $\pm$ 29.9	654 $\pm$ 94.2	608.8 $\pm$ 25.2	635.6 $\pm$ 116.5	682.6 $\pm$ 99	577.2 $\pm$ 25.2	543.8 $\pm$ 24.7	789.3 $\pm$ 25	659.4 $\pm$ 44.2	633.7 $\pm$ 15.5	855.9 $\pm$ 115.8	563.7 $\pm$ 33.6
se.chao1	7.1 $\pm$ 1.2	4.1 $\pm$ 0.8	3.7 $\pm$ 1.2	3.2 $\pm$ 1.1	1.8 $\pm$ 0.8	3.7 $\pm$ 0.8	8.1 $\pm$ 1.4	3.8 $\pm$ 1	3.1 $\pm$ 0.6	4 $\pm$ 1.5	4.6 $\pm$ 1.8	3.1 $\pm$ 1.5
ACE	450.1 $\pm$ 29.7	653.3 $\pm$ 94	606.6 $\pm$ 24.7	632.7 $\pm$ 114.6	681.9 $\pm$ 98.2	574.9 $\pm$ 24.7	541.4 $\pm$ 24.3	787.5 $\pm$ 24.4	656.7 $\pm$ 42.8	631.5 $\pm$ 15.5	850.5 $\pm$ 114.9	562.5 $\pm$ 33.5
se.ACE	13.8 $\pm$ 0.1	10.6 $\pm$ 0.4	11.7 $\pm$ 0.7	11.6 $\pm$ 1.2	8.8 $\pm$ 0.6	10.7 $\pm$ 0.5	13.6 $\pm$ 1.3	11.8 $\pm$ 0.2	10 $\pm$ 0.4	12 $\pm$ 1.2	11.5 $\pm$ 1.4	10.1 $\pm$ 0.4
Shannon	5.5 $\pm$ 0.05	5.8 $\pm$ 0.1	6 $\pm$ 0.02	5.7 $\pm$ 0.1	5.9 $\pm$ 0.08	6 $\pm$ 0.02	5.7 $\pm$ 0.04	6 $\pm$ 0.08	6 $\pm$ 0.05	5.9 $\pm$ 0.03	6 $\pm$ 0.06	5.9 $\pm$ 0.07
Shannon(H1)	389.3 $\pm$ 26.7	304.1 $\pm$ 12.7	406.5 $\pm$ 22.3	349.4 $\pm$ 35.1	251.3 $\pm$ 16	398.8 $\pm$ 8.3	410.4 $\pm$ 27.2	348.3 $\pm$ 10.4	364.1 $\pm$ 24.8	365.6 $\pm$ 37.3	321.3 $\pm$ 42	394.9 $\pm$ 11.5
Simpson	1.6 $\pm$ 0.0005	2.5 $\pm$ 0.00000.5	1.4 $\pm$ 0.0006	1.6 $\pm$ 0.0004	7.9 $\pm$ 0.0004	1.4 $\pm$ 0.00000.5	5 $\pm$ 0.0003	000000.34 $\pm$ 0.0008	1.6 $\pm$ 0.0002	1.6 $\pm$ 0.0002	6.5 $\pm$ 0.0004	5.9 $\pm$ 0.0003
InvSimpson	195.6 $\pm$ 16.5	183.3 $\pm$ 10.1	264.1 $\pm$ 14.9	186.8 $\pm$ 8.2	145.9 $\pm$ 13.8	273.3 $\pm$ 2.6	180.4 $\pm$ 11	198.9 $\pm$ 7.3	245.3 $\pm$ 21	199.4 $\pm$ 16.6	169.3 $\pm$ 15.1	285.2 $\pm$ 9.5

**Table A.4:** Permutation test for RDA under reduced model. Number of permutations: 999. Model: rda(formula = bio\_family ~ Sr + Be + U + Ba + Hg, data = env\_metal). Biologic data is the abundance ASVs filtered in family level. Level significance p<0.05 for the selected variables. Df: Degrees of freedom, F: F-test, Pr(>F): p-value (\*\*\*): <0.0001.

	<b>Df</b>	<b>Variance</b>	<b>F</b>	<b>Pr(&gt;F)</b>
Model	5	168.36	2.2561	0.001***
Residual	30	447.73		



**CHAPTER 4 - FOOD WEB ATTRIBUTES TO ASSESS SPATIAL-TEMPORAL  
DYNAMICS IN ESTUARINE BENTHIC ECOSYSTEM**

Published in Ecological Indicators (2024)

<https://doi.org/10.1016/j.ecolind.2024.112243>

## 4.1 Abstract

Threatened benthic ecosystems need urgent tools for effective bioassessment and relevant management. EU Marine Strategy Framework Directive (MSFD) obligates member states to achieve GES (Good Environmental Status) for 11 descriptors of environmental state (MSFD; 2008/56/EC). From all of the descriptors, D4 that focuses on Food Webs is the most functional-oriented indicator, but also the most challenging to implement due to our limited knowledge on benthic interactions. Particularly, it is still unclear how spatially and temporally regulated abiotic variables determine the entire benthic food webs, and which benthic food web attributes best respond to these spatially and temporally derived environmental variations. To fill this gap, we measured the natural isotopic ratios ( $\delta^{13}\text{C}$  and  $\delta^{15}\text{N}$ ) of macrobenthic organisms and their food sources and build twelve food web topologies across three distinct sites (Navigator, Gambia, Tróia) in summer and winter during two consecutive years. To assess these food web topologies, we applied isotopic metrics, further integrated with univariate and multivariate analysis to find food web-based indicators that best respond to these spatial and temporal variability.

We found clear spatial patterns associated to an increase in primary production and quantity and quality of organic matter (OM). Sites with higher organic load and less quality OM (Navigator and Gambia) had simpler food webs, likely associated to high abundance of opportunistic meiobenthic species. Site located inside protected area (Tróia) with high quality OM had the most complex food web characterized by high diversity of specialist consumers that used more efficiently available resources. Similarity metrics were valuable complementary tool that helped to further disentangle the causes of spatial variability, in this case distinguishing between two food webs (Navigator and Gambia) that had similar structures but different resource utilization.

The temporal patterns were not so evident than the spatial patterns, although significant differences were reported between sampling occasions for the same metrics (maximum trophic position and the percentage of carnivores and omnivores,  $p<0.05$ ). The most complex Tróia's food web demonstrated greater responsiveness in capturing temporal differences in resource use, suggesting that more complex food webs are better equipped to reflect temporal variability. The integration of isotopic metrics complemented with multivariate and univariate analyses proved to be an important tool for the analysis of different aspects of the benthic food web complexity in a spatial-temporal context

providing a promising approach to assess the functional integrity of the estuarine ecosystems, especially in the context of the descriptor 4 within MSFD.

**Keywords:** Benthic food web, functional diversity, isotopic metrics, spatial and temporal scale, descriptor 4, MSFD.

## 4.2 Introduction

EU Marine Strategy Framework Directive (MSFD) obligates member states to achieve GES (Good Environmental Status) for 11 descriptors of environmental state (MSFD; 2008/56/EC). From all of the descriptors, descriptor 4 (D4) that focuses on Food Webs is the most functional-oriented indicator of the ecosystem status, but also the most challenging to implement due to our limited capacity to quantify functional interactions in marine environment, especially at the base of the food web (Rombouts et al., 2013). Consequently, present indicators under D4 are highly imbalanced, limited to well-studied pelagic habitats or economically important guilds (fish, birds) rarely accounting for the benthic habitats and ecosystem-based processes, hence are not efficient to detect environmental disturbance (Rogers et al., 2010). According to Environmental Report 2020, achievement of GES in marine waters has very little progressed, while 60 % of EU surface waters are still not meeting Water Directive standards, underscoring the urgent need for the development of new tools that would facilitate our understanding of the complex interactions among organisms and their environment to support their wider implementation in the bioassessment strategies.

Estuarine and coastal benthic ecosystems represent one of the major sources of essential services for human well-being (Bonaglia et al., 2014; Schratzberger and Somerfield, 2020). The functional integrity of these ecosystems is maintained by multiple intra and interspecific interactions between organisms that mediate the energy transfer to higher trophic levels (Schratzberger & Somerfield, 2020; Ridall & Ingels., 2021). The proxy to evaluate the efficacy of which this energy is transferred to higher trophic compartments can be assessed by analyzing the food web structure. Food webs reflect structural organization of biota and their interactions, whereas food webs delivered metrics allow to visualize this complex information in a manageable way (Jackson et al., 2012; Gray et al., 2014; Bergamino et al. 2015; Szczepanek et al., 2021). Therefore, they are attractive to managers allowing to account for both direct and indirect effects of environmental disturbance in a single network (Tam et al., 2017).

In estuaries spatially and temporally regulated set of environmental variables determines distribution of biotic communities and their functional traits (Sroczyńska et al., 2021; Tsikopoulou et al., 2021). However, to date only few studies determined how spatially and temporally regulated abiotic variables determine the entire benthic food webs (Liu et al., 2020, Szczepanek et al., 2021; Ziolkowska & Sokolowski, 2022), and more importantly it is still unknown what are the benthic food web attributes that best respond to these spatially and temporally derived environmental variations. So far, we know that seasonally and spatially regulated inputs of organic matter (OM), primary

productivity, as well as physical and environmental variables have a profound impact on the food web structure (Nelson et al., 2015). In most cases, nutrient availability increases primary productivity and the abundance and diversity of primary and secondary consumers, which further reflects in higher complexity of the food web structure (Donázar- Aramendía et al., 2019, Ziolkowska & Sokolowski 2022). However, when nutrient input exceeds the oxygen availability, the diversity of primary producers is reduced, promoting a higher abundance of opportunistic species at the lower trophic levels (Guen et al., 2019; Xu et al., 2022). The consequence of this shift is a reduction of the prey diversity, ultimately resulting in the diminishment of trophic connections and shrinking of the trophic niche (Thompson et al., 2012; Burdon et al., 2021; Xu et al., 2022).

It becomes evident that more hypothesis-driven studies are needed to understand how benthic food webs respond to environmental drivers over spatial and temporal scales, and which food web attributes best reflect these changes. To fill this gap, we measured the natural isotopic ratios ( $\delta^{13}\text{C}$  and  $\delta^{15}\text{N}$ ) of macrobenthic organisms and their food sources and constructed twelve food web topologies across three distinct sites and over 4 different sampling occasions. To assess these food web topologies, we applied isotopic metrics (Layman et al., 2007, Jackson et al., 2012, Cucherouette et al., 2015) that were demonstrated to be successful in quantifying multiple anthropogenic impacts on food webs (Donázar-Aramendía et al., 2019; Sroczynska et al., 2021) as well as inferring important information on trophic diversity, food web stability or trophic resilience (Layman et al., 2012; Jackson et al., 2012). These metrics were further integrated with univariate and multivariate analysis to find benthic food web-based indicators that best respond to these spatial and temporal variability. Finally, this study aims to contribute to a new paradigm of analyzing ecological data based on empirically derived integrated functional (food web) attributes for better assessment of the benthic ecosystem status (Baiser et al., 2019).

#### 4.2.1 Study conceptualization and hypothesis

The Sado estuary, situated in SW Portugal, offers an ideal study location due to its unique blend of anthropogenically disturbed regions and areas of high ecological significance. Previous studies on this estuary demonstrated strong spatial and temporal differences in the distribution of meio- (Sroczynska et al., 2021a, Vieira et al., 2023) and macrobenthic (Caeiro et al., 2005; Brito et al., 2023) species composition as well as functional traits (Sroczynska et al., 2021a). The main variables responsible for the spatial-temporal differences in community distribution patterns were related to sediment grain size and OM inputs, whereas differences in oxygen concentration were

demonstrated to be decisive for the functional traits composition patterns. Sites with clay predominance and an increased organic input demonstrated to have less diverse communities with the predominance of small opportunistic taxa.

Spatial and temporal changes in food web structure are usually associated with seasonal variations of primary production and fluvial discharge of terrestrial OM (Szczepanek et al., 2021) that together determine the trophic conditions of the sediments. Therefore, the sampling sites selected for this study (Navigator, Gambia and Tróia) present divergent conditions described by differences in biogeochemical properties of the sediment, mainly related to sediment grain size and quality and quantity of OM. The temporal scale of the study included winter and summer months along two consecutive years.

Given that the structuring of benthic food webs in spatial and temporal contexts depends on organic matter inputs and environmental conditions, we anticipate that communities inhabiting sites with substantial organic matter input (e.g., Gambia and Navigator), but limited oxygen availability, are likely to exhibit a less diverse range of available food sources. This, as observed in our earlier studies, has led to a decrease in benthic community diversity and has promoted a greater abundance of opportunistic species at the lower trophic levels. Drawing from above, our first hypothesis (H1, Table 1) presumes that sites with larger OM input (Gambia and Navigator) will present a narrower trophic niche size and reduced trophic diversity, reflected in lower isotopic and diversity metrics (Table 1). At the same time, we hypothesize that communities at these sites will have a lower species richness, but with more scattered isotopic values, which will be reflected in an increase in the isotopic divergence and uniqueness metrics.

We further hypothesize that we find greater similarity, reflected in the overlap metrics (H2, Table 1), between sites with similar trophic conditions (Gambia and Navigator). Regarding temporal scale, in colder seasons, the reduced primary productivity and the increased terrestrial and freshwater OM inputs produces less diverse benthic communities with few top predators, which, overall, should reduce trophic interactions. Therefore, we hypothesize that winter food webs will present reduced isotopic diversity including maximum trophic position (H3, Table 1) in comparison to summer seasons. Instead, summer seasons that present an increase in primary productivity and peak in species reproduction will have a higher resource diversity and will host a more diverse community of benthic species, which will translate into an increase of maximum trophic position, diversity and redundancy. We also hypothesize (H4, Table 1) that we will observe more similar food webs during the same season (e.g., win19/win20 or sum20/sum21) than when comparing food webs across different seasons.

**Table 1** Summary of the selected metrics in relation to the hypothesis tested in this study (H1–H4). Along with each metric name and hypothesis, the spatial and temporal scale, how the metric is measured, and the ecological meaning of the metrics are presented.

Scale	Metric	How the metric is measured	Ecological meaning of the metrics
<b>H1:</b> Communities at sites with higher organic matter input (Gambia and Navigator), but little oxygen availability will have less diverse availability of food source what will impact benthic community diversity, promoting higher abundance of opportunistic species at the lower trophic level decreasing trophic diversity metrics (CR, NR, TA and Max TP, Irac, Ieve and % of omnivores and carnivores) but will increase Idiv and <i>IUni</i> .			
Spatial	CR	<b>Carbon range</b> -difference between the most $^{13}\text{C}$ depleted and enriched species (Jackson et al. 2012)	Diversity of the basal resources
	NR	<b>Nitrogen range</b> - difference between the most $^{15}\text{N}$ depleted and enriched species (Jackson et al. 2012)	Extent of vertical food web structure
	TA	<b>Total Area</b> encompassed by the consumers food web using mean $^{13}\text{C}$ and $^{15}\text{N}$ consumers isotopic values that includes all species in the isotopic space (Layman et al. 2007)	Diversity of the resource use by the consumers (trophic diversity)
	Irac	<b>Isotopic richness</b> - corresponds to TA (Volume of the minimum convex hull that includes all species), but considers scaled ( $\delta^{15}\text{N}$ - $\delta^{13}\text{C}$ ) isotopic values (Cucherousset & Villéger, 2015)	Diversity of the resource use by the consumers (trophic diversity)
	Max TP	<b>Maximum trophic position</b> of the species at a given site using the site mean $\delta^{15}\text{N}$ of basal resources as a baseline (Winemiller et al. 2007)	Realized food chain length
	Ieve	<b>Isotopic evenness</b> - Regularity in the distribution of taxa in the isotopic scaled space (Cucherousset & Villéger, 2015)	Equitability in the resource use
	IUni	<b>Isotopic uniqueness</b> - Average closeness of organisms in the isotopic scaled space (Cucherousset & Villéger, 2015)	inverse of the trophic redundancy, proxy for the ecosystem resilience
	Idiv	<b>Isotopic divergence</b> - accounts for the distribution of consumers, within the convex hull area, Idiv is close to 1 when most of the organisms have extreme isotopic values and	Balance in the distribution between different trophic groups in the community (primary producers and top predators), i.e., high Idiv can be sign of

		<p>is close to 0 when most of the organisms are close to the centre of gravity of the convex hull (Cucherousset &amp; Villéger, 2015).</p>	<p>the presence of large invasive predators.</p>
	lDis	<p><b>Isotopic dispersion</b> - weighted-deviation to the average position of points in the stable isotope space divided by the maximal distance to the centre of gravity (Cucherousset &amp; Villéger, 2015).</p>	<p>Is a scaled multidimensional variance accounting for both the convex hull area and the isotopic divergence.</p>
	omniv_car	<p><b>Omnivore and Carnivore percentage</b> - % of omnivores and carnivores relative to all of the trophic guilds</p>	<p>Proxy for ecosystem stability</p>

**H2:** Greater overlap reflected in lnes and lsim will be found between similar sites (Gambia and Navigator).

Spatial (isotopic overlap)	Isotopic nestedness (lnes)	Ratio between shared area of two food webs (communities) and the smallest convex hull area (Cucherousset & Villéger, 2015)	Complementarity or redundancy in resource use by two communities
	Isotopic similarity (lsim)	Ratio between the volume shared and the volume of the union between two convex hull areas between two communities (Cucherousset & Villéger, 2015)	Similarity in filling the isotopic space by the consumers between two communities

**H3:** Colder seasons (winter) have a reduced primary productivity, but increased terrestrial and freshwater OM input which will produce less diverse benthic communities, being responsible for reduced isotopic diversity metrics especially reflected in Max TP. Summer seasons with an increase in primary productivity and peak in species reproduction will have a higher resource diversity and will host more benthic species, which will translate into an increase of Max TP and higher % of carnivores and omnivores as well as their trophic diversity metrics (CR, NR, TA, Iric, IEve) and reduced IUni.

Temporal	Metrics as above
<b>H4:</b> Greater similarity in food webs during the same season (e.g., win19/win20 or sum20/sum21) than when comparing food webs across different seasons.	
Temporal (isotopic overlap)	Metrics as above

## 4.3 Material and Methods

### 4.3.1 Study area

Sado estuary is the second largest estuarine system in Portugal, with an area of approximately 240 km<sup>2</sup>, and is one of the most important wetlands in Europe (Bettencourt et al., 2004) (Fig. 1). The intertidal areas comprise approximately 78 km<sup>2</sup>, of which 30% are salt marshes and intertidal flats (Caeiro et al., 2005), with semi-diurnal mesotidal regime and tidal amplitude varying between 0.6 m and 1.6 m during spring and neap tides, respectively. Salinity is influenced by the Sado river flow (annual mean of 40 m<sup>3</sup>s<sup>-1</sup>) changing with seasonal and inter-annual conditions and temperature can range from 10 to 26°C (Bettencourt et al., 2004). The Sado Estuary (SW coast, Portugal) comprises large adjacent urban and heavy industrial areas with many polluting activities, although parts of the Estuary are environmentally protected, reflecting the importance of ecological conservation and biomonitoring (Vieira et al., 2022).

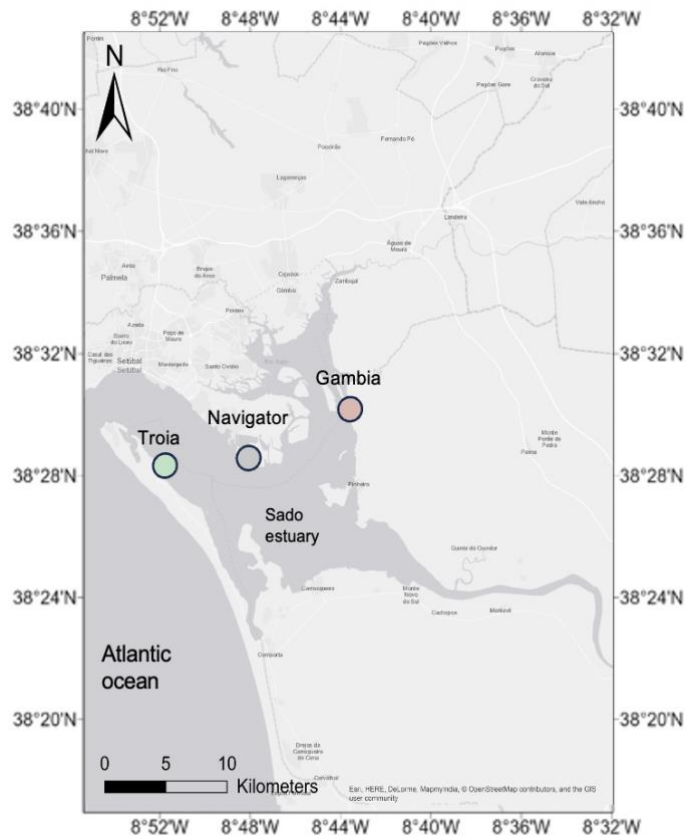


**Figure 1.** Sado estuary located at southwest of Portugal (38° 31' 14" N, 8° 53' 32" W). The selected sampling sites: Navigator (38.486502, -8.795191), highly industrialized area; Gambia (38.537263, -8.742584) with high organic inputs from aquacultures; Tróia (38.461421, -8.857838) located at mouth of estuary.

#### 4.3.2 Sampling design

The sampling sites were selected based on the expected differences in biogeochemical and trophic conditions of the sediments according to water hydrodynamics within an estuary (high/low water residence time), salinity gradient and the type of neighboring anthropogenic activities (Caeiro et al., 2005; Sroczyńska et al., 2021). Based on these criteria three sampling sites were proposed: (1) Navigator is located in the proximity of an industrial area, dominated by fine sand, clay and high organic contents (Vieira et al., 2023); (2) Gambia is located within the borders of the Sado Nature Reserve, affected by the surrounding aquaculture activities with the predominance of clay-fine sediments (Brito et al., 2023); (3) Tróia is located close to the estuary mouth, directly exposed to hydrodynamic forces, that bring well oxygenated water, and with predominance of sandy sediments (Sroczyńska et al., 2021a). All three sites were sampled during four campaigns: winter 2019 (win19), summer 2020 (sum20), winter 2020 (win20) and summer 2021 (sum21).

#### 4.3.3 Sediment biogeochemistry and environmental parameters

Sediment samples were collected by core (141cm<sup>2</sup>) to the depth of 10 cm and were stored at - 20°C until further analysis. Total organic matter (OM\_per) (%), grain size (%), elemental Carbon (C\_total\_per) and elemental Nitrogen (N\_total\_per) was determined as described in Vieira et al., (2023) according to Costa et al., (2011) and Teixeira et al., (2020). Chlorophyll a (Chla\_mg\_g) and phaeopigments (Phaeo\_mg\_g) were determined as described by Lorenzen (1967). Approximately 0.5 g of sediment samples were extracted with 3 mL of ice-cold spectrophotometric grade of 90 % (v/v) acetone. Samples for extraction were placed in an ultrasound bath for 24 hours at -20 °C in the dark. After that period, samples were centrifuged for 15 minutes, at 4.000 rpm and at 4°C, and the supernatant was used for the analysis. Concentration values for Phaeo\_mg\_g was obtained after acidification of the supernatant with 0.5 M Hydrochloric acid (HCl).

The concentration of 14 elements (Li, Sr, Mn, Ni, Cr, Be, U, Ba, Co, Cu, Zn, As, Pb and Hg) were quantified from the sediment samples collected at each site (mg/kg). Mercury was quantified by thermal pyrolysis atomic absorption analysis (LECO 254 Advanced Mercury Analyser, AMA), described by Costley et al., (2000). Whereas the elements Li, Sr, Mn, Ni, Cr, Be, U, Ba, Co, Cu, Zn, Pb and metalloid As were analyzed applying the procedure described in Catry et al., (2021). The metals were quantified by Inductively Coupled Plasma – Mass Spectrometry (ICP-MS) (Perkin Elmer NEXION 2000C) after the total acid decomposition of organic debris, carried out in a closed Teflon vessel microwave assisted system (CEM MARS 5). The quality control of this procedure

was assured using procedural blanks, duplicate samples (coefficient of variation < 10%), and the analysis of the MESS-4 CRM, which were prepared using the same analytical procedure and reagents.

At each sampling site, sediment interstitial water parameters were measured such as salinity (Sal), Oxygen (O<sub>2</sub>) (mg/L), pH and Temperature (T) (°C) using a VWR pHenomenal ® MU 600 H.

#### 4.3.4 Sample collection for stable isotope analysis

At each sampling site, basal food sources and macrobenthic organisms were sampled during a period of low tide. The sampling was performed in win19 (November), sum20 (June); win20 (December) and sum21 (May).

Basal food sources such as macroalgae, seagrass and marine plants were randomly hand-picked including entire sampling area. Samples for microphytobenthos (MPB) were collected at three randomly chosen locations (within each site). It was collected approximately 2000 mL of sediment from the first sediment layer (~1-2 cm), to ensure enough concentration of microphytobenthic cells for isotopic analysis. Samples for Particulate Organic Matter (POM) were collected from small pools, when the pools were not available the water was sampled directly from the adjacent channel.

Macrofauna was collected: 1) quantitatively with a core (141cm<sup>2</sup>) to 30 cm depth and sieved over a 1 mm mesh at three random locations within each site, and 2) qualitatively by hand picking the organisms from the sampling area. For quantitative sampling, to collect representative number of individuals, two replicates were used at each location, with a total of 6 cores per site. Macrofaunal taxa that were hand-picked were chosen to account for a wide spectrum of functional groups and trophic positions. Both types of samples (quantitative and qualitative) were further transported to the lab in the cold containers for further analysis.

#### 4.3.5 Sample processing in the lab

Samples of hand-picked fresh macroalgae, seagrass and plants were gently washed, separated, identified and dried in the oven for 48 hours at 60°C. The epipelagic fraction of MPB was collected via migration through the lens tissue method (Eaton & Moss, 1966). For the POM analysis, 1.5 L of seawater was filtered over pre-combusted Whatman GF/F filters and oven dried for 48h at 60 °C.

The sediment samples, collected for the quantitative approach, were washed with sea water and sieved. Each organism that was picked, rinsed with sea water and identified to the lowest possible taxonomic level according to specialized monographs and literature (e.g., Fauvel, 1927; Hayward & Ryland, 2017). The online database World

Register of Marine Species (<http://www.marine-species.org>) was used to further check the validity of species names. After identification, all macrofauna organisms were incubated for 4–5 h in filtered habitat water to allow gut clearance, further were frozen in liquid nitrogen and placed in the oven to dry for 48 h at 60 °C. For larger individuals, the muscle tissue was used for isotopic analysis, while for the smaller individuals, the entire body was used. Before weighing samples into pre-combusted tin cups (8 x 5 mm. Elemental Micro- analysis Ltd.), all samples (food sources, MPB and macrobenthos) were grounded to a homogeneous powder, while the filters containing POM were gently scraped directly into the cups.

#### 4.3.6 Stable isotope analysis

Around 1-2 mg of the pre-weighed samples were combusted into CO<sub>2</sub> and N<sub>2</sub> in an elemental analyzer (EA, Flash 2000HT, Thermo Fisher Scientific), which provided carbon and nitrogen contents (%C and %N). Isotopic ratios of carbon and nitrogen ( $\delta^{13}\text{C}$  and  $\delta^{15}\text{N}$ ) were obtained on an isotope ratio mass spectrometer (IRMS, Delta V Advantage, Thermo Fisher Scientific) coupled to the EA via Conflo IV interface. The raw data was normalized by three-point calibrations for C isotopes, using international reference materials IAEA-CH6 (sucrose,  $d^{13}\text{C}$ : -10.45‰), IAEA-600 (caffeine,  $d^{13}\text{C}$ : -27.77‰), as well as EEZ-20 ( $d^{13}\text{C}$  = -12.3‰), and a three-point calibration for N isotopes using IAEA-N-1 (ammonium sulfate,  $d^{15}\text{N}$ : +0.43‰), IAEA-600 (caffeine,  $d^{15}\text{N}$ : +1‰), and IAEA-N-2 (ammonium sulfate,  $d^{15}\text{N}$ : +20.3‰) composition. Calibrated in-house standards L-alanine ( $d^{13}\text{C}$ : -18.39 ± 0.16‰;  $d^{15}\text{N}$ : +0.91 ± 0.18‰) was used as check standard. Two-point calibration was used for C isotopes, involving either Rice flour IRF01 ( $d^{13}\text{C}$ : -27.44‰) or casein ( $d^{13}\text{C}$ : -20.81‰) with glucose ( $d^{13}\text{C}$ : -10.96‰), and Rice flour IRF01 ( $d^{15}\text{N}$ : 4.32‰) or casein ( $d^{15}\text{N}$ : 5.6‰) with IAEA-600 (caffeine,  $d^{15}\text{N}$ : +1‰). The standard uncertainty calculator provided in Szpak et al., (2017) was used to calculate precision (( $u$  ( $Rw = 0.24\%_{\text{AAFM2}}$  for  $\delta^{13}\text{C}$  and 0.27‰ for  $\delta^{15}\text{N}$ ) and accuracy (( $u(\text{bias}) = 0.22\%_{\text{for } \delta^{13}\text{C}}$  and  $0.33\%_{\text{for } \delta^{15}\text{N}}$ )) combining all data. Total analytical uncertainty ( $uc$ ) was estimated to be 0.32‰ for  $\delta^{13}\text{C}$  and 0.43‰ for  $\delta^{15}\text{N}$  (see Table A.1. C and N isotopic signatures of consumers).

#### 4.3.7 Data analysis

##### 4.3.7.1 Isotopic metrics

All isotopic metrics are presented in Table 1. The community-wide metrics:  $\delta^{15}\text{N}$  range (NR),  $\delta^{13}\text{C}$  range (CR) were calculated as the difference between the maximum and minimum value of  $\delta^{15}\text{N}$  and  $\delta^{13}\text{C}$  respectively. Total area encompassed by the

consumers (*TA*) was calculated for each site using mean consumer species  $\delta^{15}\text{N}$  and  $\delta^{13}\text{C}$  values. *Max.TP* for an individual from each site was calculated according to Winemiller et al., (2007) where:

$$TP_{SI} = \lambda + (\delta^{15}\text{N}_{sc} - \delta^{15}\text{N}_{baseline})/\Delta n$$

gamma represents the trophic level of the baseline (1 for basal resources),  $\delta^{15}\text{N}_{sc}$  is the nitrogen isotope signature of the consumer being evaluated and  $\delta^{15}\text{N}$  baseline is the mean nitrogen isotope signature of basal resources (POM, MPB, algae and aquatic plants). For  $\Delta n$ , which is the trophic level enrichment of  $\delta^{15}\text{N}$  value, the value 2.3‰ was used (Zandee & Rasmussen, 2001). The isotopic metrics (*Iric*, *Ieve*, *IUni*, *Idiv*) and overlap metrics (*Ines* and *Isim*) were calculated according to Cucherousset & Villéger, (2015). Prior to metric calculations, mean raw isotopic values for each  $\delta^{15}\text{N}$  and  $\delta^{13}\text{C}$  were corrected by a community centroid approach to have the same range (0–1) in order to correct for the natural variability in the isotopic values among sites with different isotopic baselines (Villéger et al., 2008). This was achieved by estimating the spatial values for isotope data by taking the mean distance of macrobenthic taxa from the community mean at each site, following Schmidt et al., (2011). Isotopic richness (*Iric*), isotopic divergence (*Idiv*), isotopic evenness (*IEve*), isotopic dispersion (*Idis*) and isotopic uniqueness (*IUni*) were measured as described in Table 1. For further description of these metrics, see Cucherousset & Villéger (2015). Overlap metrics (*Isim* and *Ines*) were derived from functional ecology that are based on the volume of the intersection between two convex hulls (Villéger et al., 2011, 2013). Isotopic similarity (*Isim*) is the ratio between the volume of the intersection and the volume of the union of the two groups of organisms in the stable isotope space (Villéger et al., 2011). *Ines* is the complementary metric to *Isim*, which is the ratio between the volume of the intersection and the minimal volume filled by a group. The index of *omniv\_car* was calculated for each site separately as the % of all of the consumers classified as carnivores and omnivores (according to Fauvel, (1927); Hayward & Ryland, (2017)) relative to all of the trophic groups present.

#### 4.3.7.2 Multivariate and univariate analysis

Principal component analysis (PCA) was applied to a dataset with all variables from Table A.2, appendix A and isotopic diversity metrics (*CR*, *NR*, *TA*, *Iric*, *Max.TP*, *Idiv*, *IDis*, *IUni*, *IEve*, *car\_perc* and *omniv\_car\_perc*) (Table 2). Some environmental and biogeochemical variables (except for pH) were log10 transformed (all metals, Chla\_mg\_g, Phaeo\_mg\_g, Chla\_Phaeo, Temp, Sal, O<sub>2</sub>); variables that were expressed

as % (% of clay, % of sand, % of gravel, % of OM, % of total carbon, % of total nitrogen, % of  $\text{CaCO}_3$ ), were transformed using arcsine square root transformation. PCA was first done including all the transformed variables; afterwards, the variables that had the lowest contribution to the PCA axes, as well as those that had high ( $>0.9$ ) correlation with other variables were removed. The variables removed were: (N\_total\_per, Phaeo\_mg\_g, Chla\_phaeo\_ratio, Li, Sr, Mn, Ni, U, Zn, As, Co, Cu, T, Sal, O2 and pH). To check for the significance of the PCA, a PCA test (R package “PCATest”, Camargo, (2022)) was applied with the following parameters: number of random permutations: 1000; number of bootstrap replicates to build 95%-confidence intervals of the observed statistics: 1000; alpha level for statistical tests: 0.5. PCA plot was done using the function “fviz pca.biplot” using R package “FactoMineR” (Lê et al., 2008). After applying a PCATest, only variables that were correlated more than 0.5 to PCs were considered. The variables considered were: CR, NR, TA, Max.TP, Iric, omniv\_car. PCATest was applied in the same way and with the same input parameters as done for the biogeochemical and environmental variables.

All the isotopic and trophic diversity metrics were tested between sites and sampling occasions using two-way analysis of variance (ANOVA, fixed factors were “site” with three levels and “sampling occasion” with four levels). Prior to analyses all the metrics were normalized and checked for the normality and homogeneity of the variance using Shapiro-Wilk normality test and Levene's Test for Homogeneity of Variance (center = median,  $p<0.05$ ). The Tukey's test was performed to the metrics that obtained significant differences, considering 5 % significance. Analysis was performed in R studio using the “Vegan” package, function “aov” (Chambers et al., 1992).

## 4.4 Results

### 4.4.1 Biogeochemical and environmental characteristics of the study sites

The sediment biogeochemistry and the environmental variables measured *in situ* are summarized in Table A.2. The sediment biogeochemical analysis revealed differences between all three sites. Sediment at Navigator was predominantly muddy, characterized by the highest mean values of Clay\_per ( $20.9 \pm 1$  to  $35.2 \pm 6.6$  %), enriched in OM\_per ( $2.1 \pm 0.1$  to  $3.9 \pm 0.6$  %) and C\_total\_per ( $0.9 \pm 0.03$  to  $1.1 \pm 0.1$  %). Navigator had also the highest content of metals. Sediment in Gambia was mostly characterized by the highest proportion of Gravel\_per ( $14.9 \pm 5.6$  to  $16.9 \pm 2.1$ %) and intermediate values of OM\_per % ( $0.6 \pm 0.04$  to  $1.7 \pm 0.3$ ). In contrast, predominance of Sand\_per and  $\text{CaCO}_3$ \_per ( $91.6 \pm 2.8$  to  $97.3 \pm 0.1$  and  $3.5 \pm 0.3$  to  $4.6 \pm 0.9$  %, respectively) as well as reduced contents of Clay\_per and OM\_per ( $1.5 \pm 0.5$  to  $2.9 \pm 0.4$  and  $0.4 \pm 0.02$  to

$1.9 \pm 0.3\%$ , respectively) were found in Tróia sediments. Navigator and Gambia had high content of Chla, whereas Tróia sediments had the highest values of Chla\_phaeo representing the proxy for the freshness and quality of the phytodetrital organic matter. Oxygen ( $O_2$ ) that was measured at each site showed the lowest values in Navigator and Gambia varying between  $5.3 \pm 0.6$  to  $9.6 \pm 0.4$  and  $8.8 \pm 0.4$  to  $17.9 \pm 0.4$  mg/L, respectively, while Tróia registered the highest values varying between  $8.6 \pm 0.2$  and  $13.9 \pm 0.3$  mg/L.

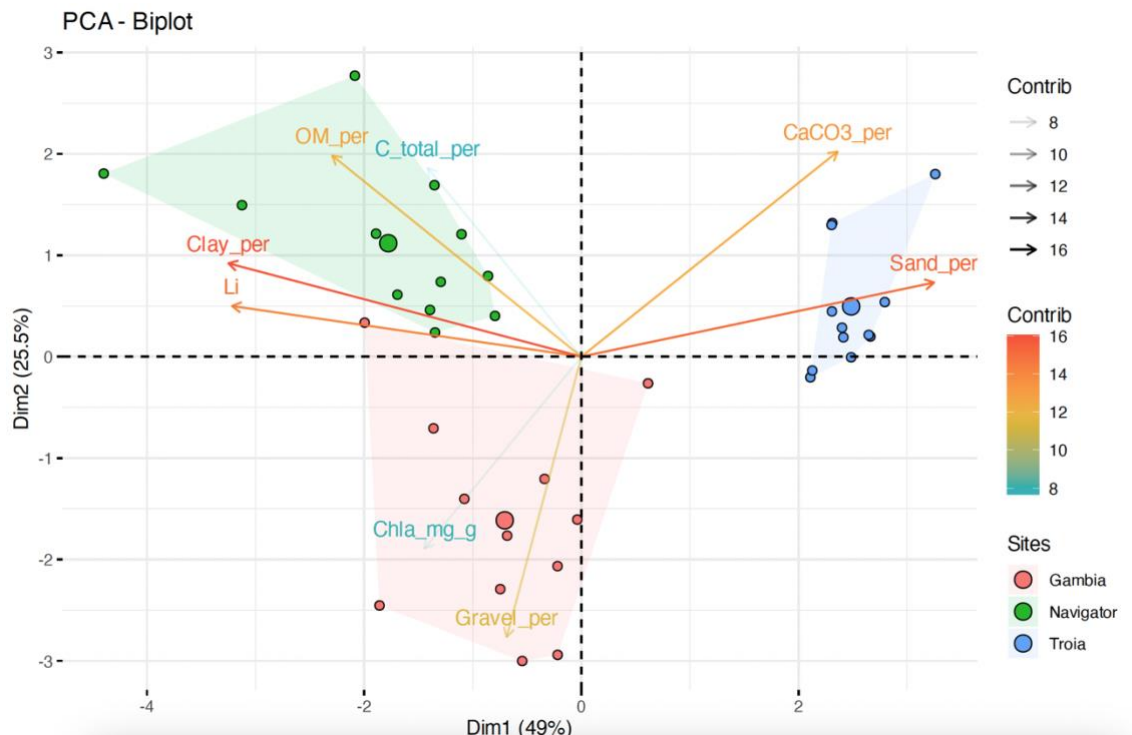


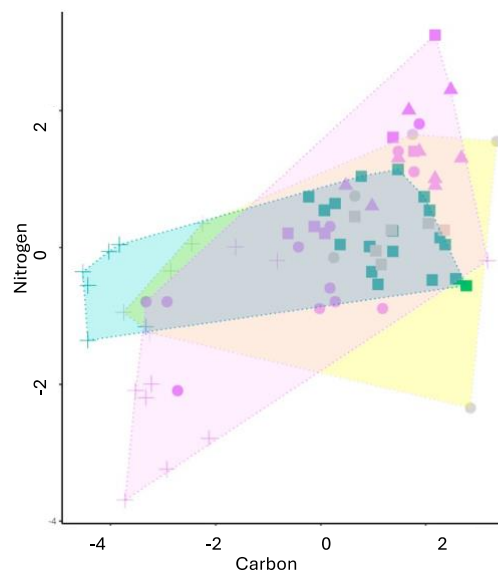
**Figure 2.** Principal component analysis (PCA) biplot based on scaled environmental and biogeochemical variables measured at three study sites in Sado estuary, coloured by estuary “confidence” convex type. Variable’s vectors are presented based on their contributions to the principal components (gradient colours and transparency of vectors) with red representing high contributions, yellow intermediate and blue representing very low contributions. The dots represent the cluster centroids for group variables.

PCA analysis clearly differentiated all three sites demonstrating clear differences in biogeochemical sediment condition between sites. Both axes were significant according to PCAtest (1000 bootstrap replicates, 1000 random permutations). The first PC accounted for 49.0% (95%-CI:43.9-55.7) of the total variation. The second PC axis accounted for 25.5% (95%-CI:20.7-32.8) of the total variation and all together both PC axes explained 74.5% of the variation observed (Fig. 2). All of the 8 variables had significant loadings on either first (Clay\_per, Sand\_per, OM\_per, CaCO3\_per, Li,

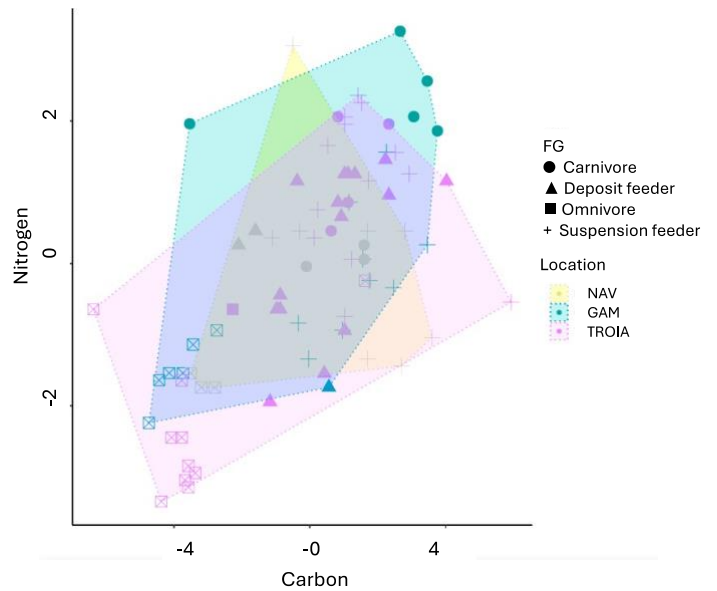
Chla\_mg\_g) or second (Gravel\_per, C\_total\_per) PC axes. The contribution of these variables for each site was: Clay\_per (-0.94 with PC1) and OM\_per (-0.66 with PC1) in Navigator, Gravel\_per (-0.80 with PC2) and Chla\_mg\_g (-0.54 with PC2) in Gambia and Sand\_per (0.94 with PC1) and CaCO3 (0.68 with PC1) in Tróia (numbers in parentheses represent correlations of empirical PC's with variables).

#### 4.4.2 Spatial variation of the benthic food web structure

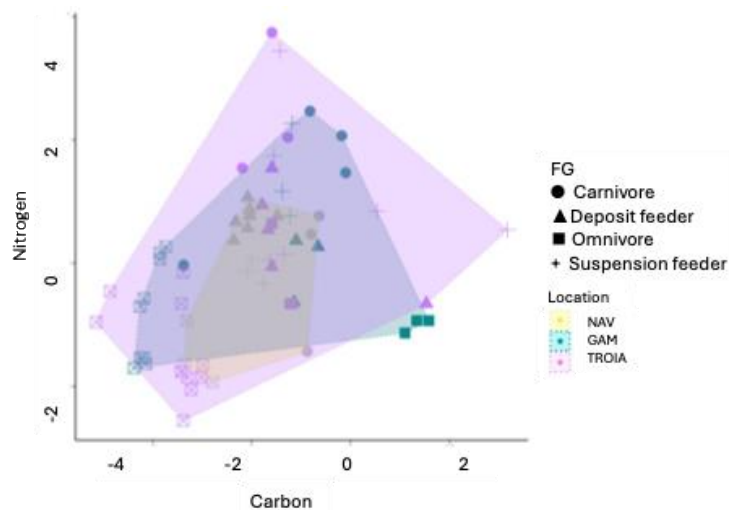
Winter 19



Summer 20



Winter 20



Summer 21

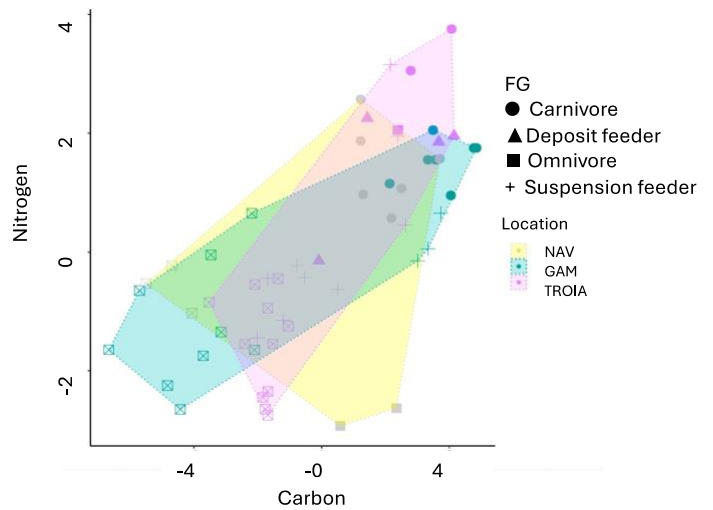


**Figure 3.** Plots with all sites pooled per sampling occasions (winter 2019 and 2020 and summer 2020 and 2021). In the x-axis and y-axis are the isotopic signatures of carbon ( $\delta^{13}\text{C}$ ) and nitrogen ( $\delta^{15}\text{N}$ ), respectively. The convex hull volume represented by the yellow, green, and purple areas,

correspond to Navigator, Gambia and Tróia, respectively. The Feeding guilds (FG) are represented by geometric shapes.

The convex hull biplots clearly reveal distinct isotopic niches between Navigator, Gambia, and Tróia. Navigator and Gambia presented smaller trophic niches and chain lengths compared to Tróia (Fig. 3 and Fig. A.1, appendix A). This pattern was supported by the metrics *CR*, *NR*, *TA*, *Max TP* and *Iric* that reached the highest values for Tróia in three sampling occasions (win19, win 20 and sum 20) (Table 2). Besides Navigator and Gambia had fewer consumers (mostly suspension feeders and omnivores) (Fig. 3, winter 19 and summer 20), they occupied distinct edges of the isotopic space, which was reflected in an increased isotopic divergence (*Idiv*) and isotopic dispersion (*IDis*). High proportion of omnivores also contributed to high observed *omniv\_car* ratio (Table 2).

**Table 2.** Food web isotopic and diversity metrics calculated for each community sampled in three sampling sites (Navigator, Gambia and Tróia) of Sado Estuary across 4 sampling occasions (win19, sum20, win20 and sum21). Isotopic and diversity metrics: Carbon Range (*CR*); Nitrogen Range (*NR*); Total Area (*TA*); Maximum Trophic Position (*Max TP*); Isotopic Richness (*Iric*); Isotopic divergence (*Idiv*), Isotopic dispersion (*IDis*), Isotopic evenness (*IEve*), Isotopic uniqueness (*IUni*), Carnivorous percentage (*car\_perc*) and omnivores and carnivorous ratio (*omniv\_car*).

Sampling occasion	Site	Isotopic and diversity metrics										
		<i>CR</i>	<i>NR</i>	<i>TA</i>	<i>Max TP</i>	<i>Iric</i>	<i>Idiv</i>	<i>IDis</i>	<i>IEve</i>	<i>IUni</i>	<i>car_perc</i>	<i>omniv_car</i>
win19	Navigator	7.10	4.00	17.84	1.08	0.29	0.73	0.57	0.63	0.24	0	65.00
	Gambia	5.90	2.50	10.68	1.98	0.17	0.80	0.47	0.69	0.32	0	75.00
	Tróia	6.90	6.80	20.45	2.82	0.33	0.69	0.42	0.71	0.28	33.00	50.00
sum20	Navigator	7.10	4.80	18.90	3.13	0.22	0.73	0.52	0.61	0.24	18.00	71.00
	Gambia	7.40	5.50	31.38	2.99	0.37	0.73	0.58	0.75	0.21	24.00	67.00
	Tróia	10.30	5.70	35.94	3.17	0.42	0.71	0.46	0.68	0.18	9.00	39.00
win20	Navigator	6.80	3.00	14.15	2.30	0.10	0.80	0.47	0.69	0.29	19.00	38.00
	Gambia	5.50	4.20	36.46	2.56	0.26	0.74	0.63	0.63	0.30	18.00	32.00
	Tróia	14.20	6.30	66.21	3.39	0.47	0.68	0.43	0.62	0.23	9.00	27.00
sum21	Navigator	11.50	5.50	35.15	3.30	0.30	0.71	0.62	0.75	0.62	38.00	57.00

	Gambia	8.80	4.60	28.78	3.04	0.24	0.81	0.63	0.73	0.45	33.3	47.60
	Tróia	9.60	3.50	24.80	4.08	0.21	0.76	0.49	0.65	0.24	8.30	33.30

In contrast, Tróia had a larger number of consumers occupying a broader isotopic space, mainly deposit feeders and omnivores (Fig.3 and Fig. A.1, appendix A), that contributed to higher *Max.TP* and *Iric* values (except at sum21) (Table 2). Large number of consumers occupying similar trophic levels in Tróia increased redundancy in Tróia's food web structure (decreased values of *IUni*, Table 2). Additionally, biplots highlighted that Tróia food web was characterized by the presence of secondary consumers and the high number of top predators (Fig. 3, Fig. A.1, appendix A), represented by the highest values of *Max.TP* in comparison to remaining sites (Table 2). Nevertheless, the only significant differences in *Max.TP* were detected between Navigator and Tróia ( $p=0.037$ ), but not Tróia and Gambia as shown in appendix A, Table A.3. The abundance of top predators in Tróia exceeded that observed in Navigator and Gambia in win19, revealing high complexity of Tróia's food web structures as indicated by high observed isotopic evenness and isotopic richness (Table 2).

PCA based on food web metrics demonstrated a clear separation, along the first PC axis, of Tróia food web from those of Gambia and Navigator (Fig. 4). According to PCAtest only the first PC axis was significant accounting for 60.3% (95%-CI:40.9-79.6) of the total variation. Besides the second PC axis did not appear to be significant it accounted for another 18.9 % of the variation. The main variables that significantly contributed to this separation were *CR*, *NR*, *TA*, *Iric* and *Idiv* that had significant loadings on the first PC axis. Tróia's food web was distinct from the remaining two sites by having higher correlation values for *NR* (0.83), *Iric* (0.88), *TA* (0.89), *CR* (0.82) and *Max.TP* (0.59). Whereas *Idiv* (-0.81) and *omniv\_car* (-0.51) were associated to Navigator and Gambia's food webs as indicated by the respective correlations with the first PC axes (in brackets). It is worth to note that only *NR*, *TA* and *Iric* had significant correlations with the first PC axis, according to PCAtest.

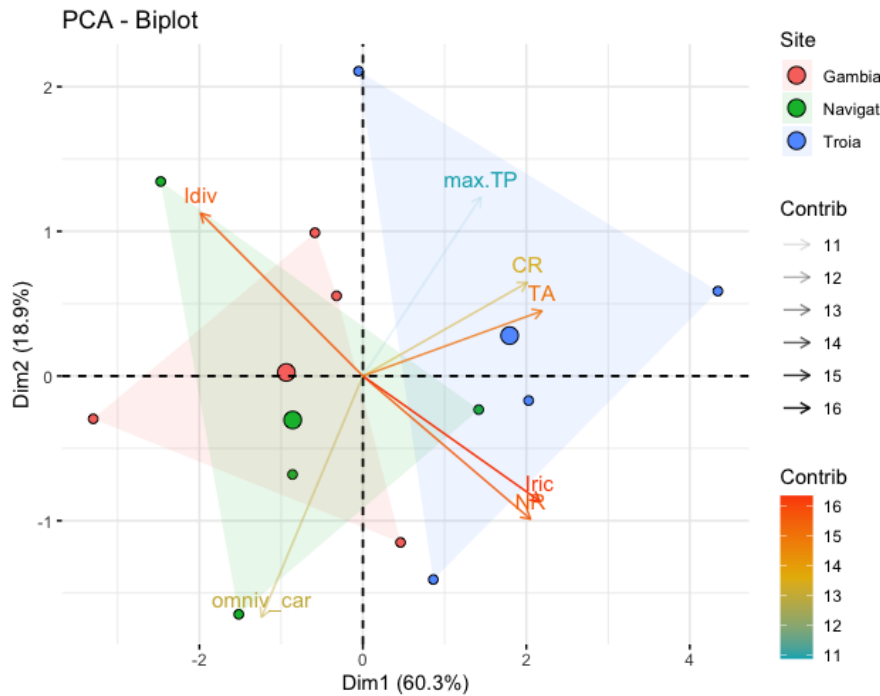


**Figure 4.** Principal component analysis (PCA) biplot based on scaled metrics (*CR*, *NR*, *TA*, *Iric*, *Idiv* and *Omniv\_car*) used to characterize the food web structure analyzed at three study sites (Navigator, Gambia and Tróia in Sado estuary, coloured by estuary “confidence” convex type. Variable’s vectors are presented based on their contributions to the principal components (gradient colors and transparency of vectors) with gray representing high contributions, yellow intermediate and blue representing very low contributions. The dots represent the cluster centroids for group variables.

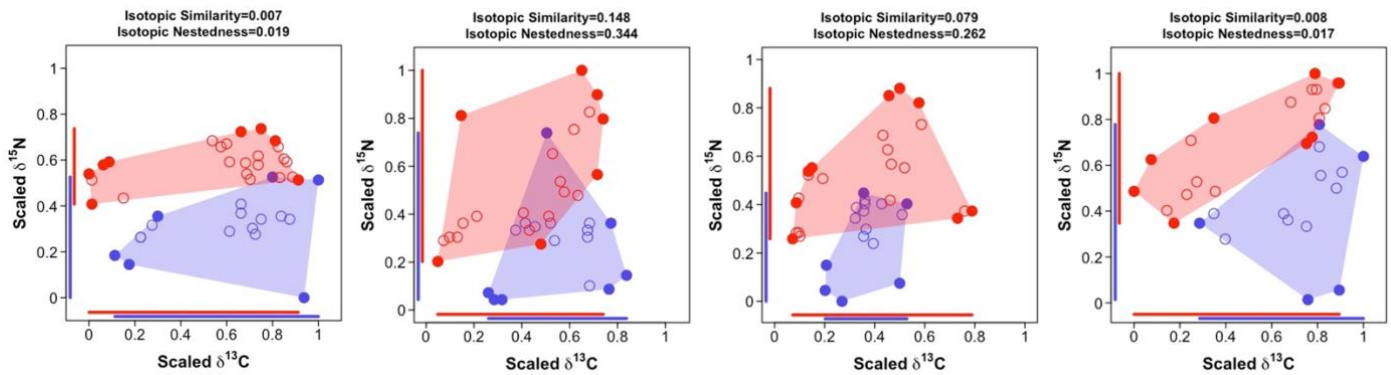
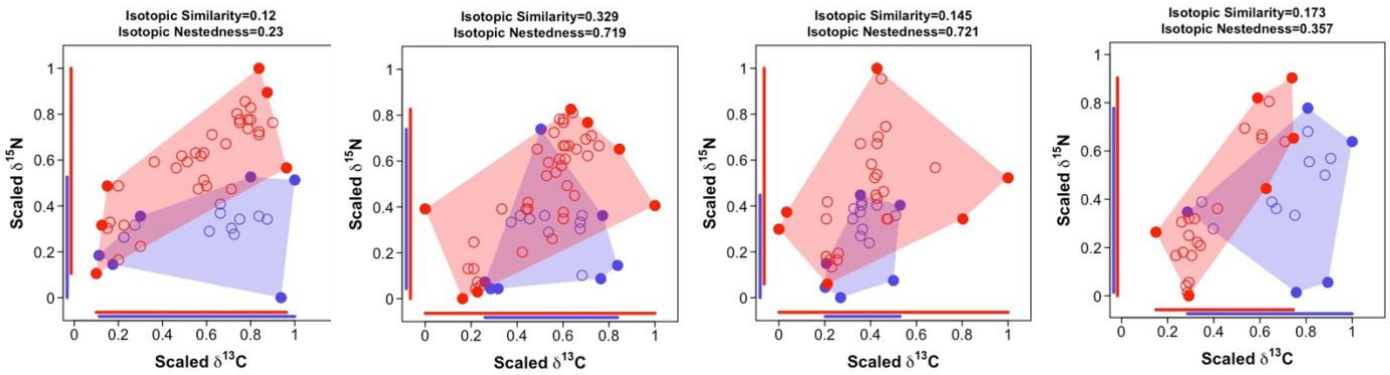
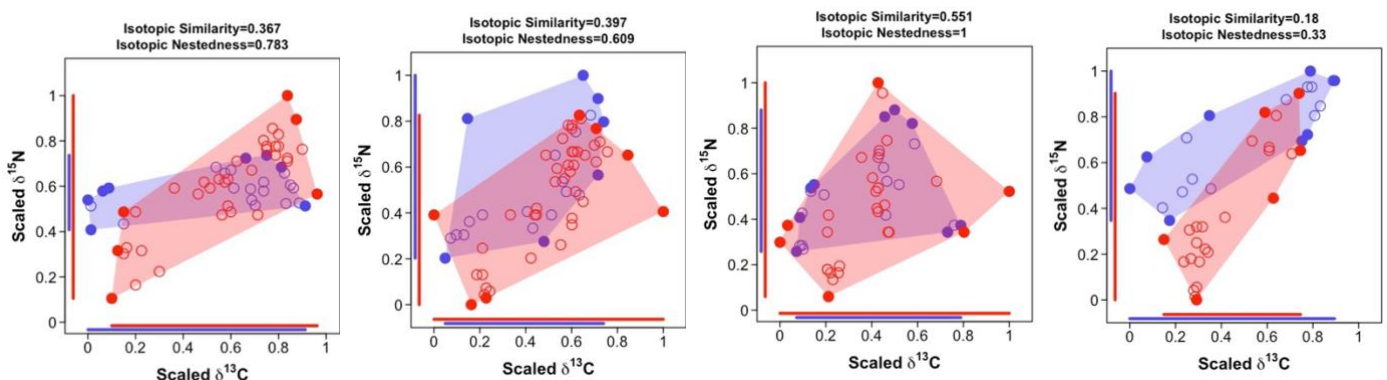
Regarding isotopic overlap, Navigator exhibited the most distinct food web structure, compared to Gambia and Tróia, registering the lowest similarity (*Isim*) values (varying between 0.007 and 0.329) when compared with other two sites (Fig.5). However, Gambia and Tróia presented the highest *Isim* (varying between 0.18 and 0.551), between each other, consistently for all of the sampling occasions (Fig. 5). The highest similarity between Gambia and Tróia was observed in win20, as reflected in both *Ines* and *Isim* metrics indicating that a large part of the Gambia’s food web overlaps with that of Tróia (Fig.5 *iii*).

Winter 19

Summer20

Winter 20

Summer21

*i) Navigator (blue) vs Gambia (red)**ii) Navigator (blue) vs Tróia (red)**iii) Gambia (blue) vs Tróia (red)*

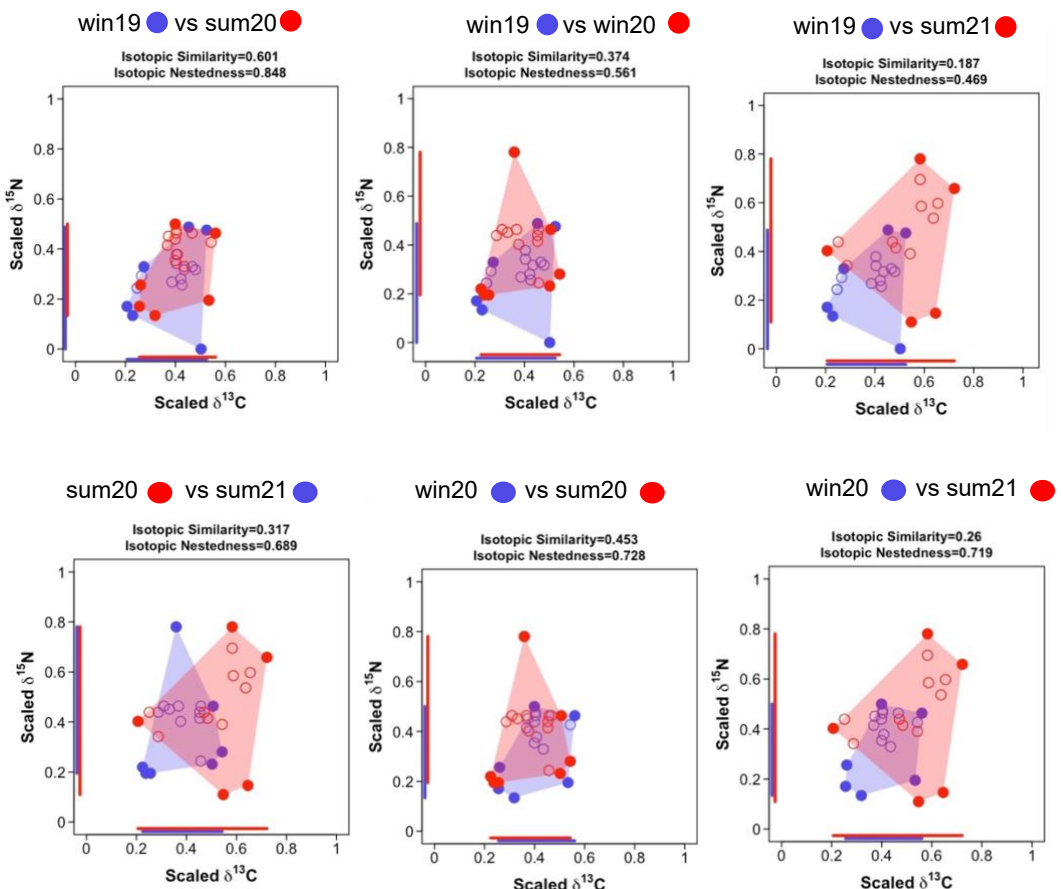
**Figure 5.** Isotopic overlap metrics in a two-dimensional isotopic space (d<sup>13</sup>C and d<sup>15</sup>N), between two sites across the 4 sampling occasions (win19, sum20, win20 and sum21). *i)* Navigator vs Gambia (blue and red, respectively); *ii)* Navigator vs Tróia (blue and red, respectively); *iii)* Gambia vs Tróia (blue and red, respectively). Isotopic overlap metrics were measured using the isotopic richness of the two sites (i.e., convex hull volume represented by the red and blue areas, respectively) and the volume of isotopic space they shared. Isotopic similarity is the ratio between the volume shared (purple area). Isotopic nestedness is the ratio between the volume shared and

the volume of the smallest convex hull (in blue). Isotopic overlap on each stable isotope axis is showed by the overlap of the colored segments representing range of scaled values for each site.

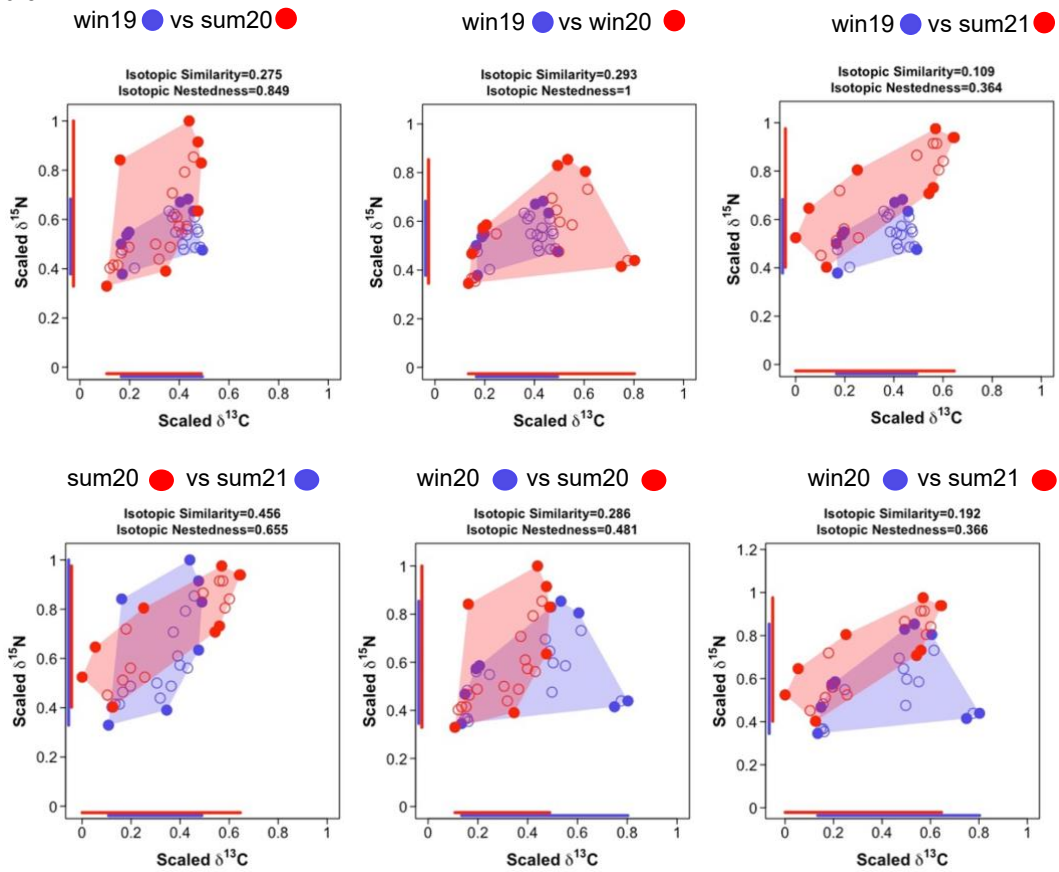
#### 4.4.3 Temporal variation of the benthic food web structure

Throughout the seasons, the convex hulls of Tróia and Gambia were consistently more similar than that of Navigator (Fig.6). Navigator vs Gambia presented the smallest overlap between each other in all of the sampling occasions with the lowest observed values of *Isim* and *Ines*. These divergences become even more evident in win19 and sum21, suggesting a distinct resource use composition in each of these food webs (Fig.6). Tróia's trophic niche was the least variable along the seasons, consistently registering the highest values of *Max TP*, isotopic redundancy and trophic diversity.

#### a) Navigator



## b) Gambia



## c) Tróia

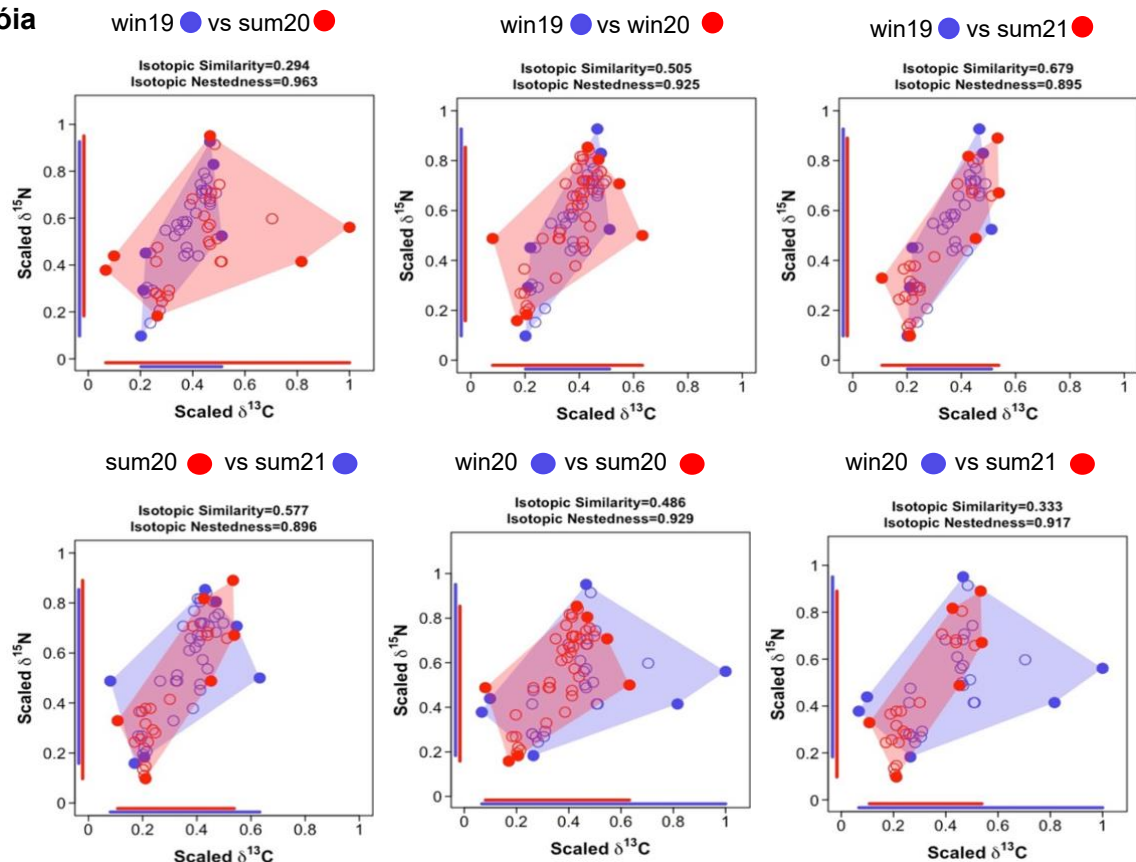


**Figure 6.** Isotopic overlap metrics in a two-dimensional isotopic space (13C and 15N), between seasons: win19 vs sum20 / win20/ sum21; win20 vs sum20/ sum21 and sum20 vs sum21 in each site. **a)** Navigator; **b)** Gambia and **c)** Tróia. Isotopic overlap metrics were measured using the isotopic richness of the two sites (i.e., convex hull volume represented by the red and blue areas, respectively) and the volume of isotopic space they shared (i.e., volume of their intersection, delimited by the purple line). Isotopic similarity is the ratio between the volume shared (purple area) and the volume of the union of the two convex hulls. Isotopic nestedness is the ratio between the volume shared and the volume of the smallest convex hull (in blue). Isotopic overlap on each stable isotope axis is shown by the overlap of the colored segments representing a range of values for each site.

In winter of 2019, Gambia and Navigator food webs exhibited similar trophic guild compositions, predominantly consisting of omnivorous and suspension feeders. In subsequent seasons, its diversity increased with the presence of more predators and other type of consumers, such as deposit feeders, herbivores and carnivores (Fig.3). Despite these variations, the presence of omnivores and suspension feeders in the food web was consistently maintained throughout the seasons. The flattening structure of the food web is a result of high isotopic dispersion combined with low values of *Max.TP*, *lric* and high values of *ldiv* throughout the seasons.

Concerning the convex hulls overlap, Navigator and Gambia's food webs revealed a similar pattern by presenting the highest similarity between win19 vs win20 and win20 vs sum20, while the lowest similarity was registered in win19 vs sum21 (Fig.6a and Fig.6b). Along the analyzed sampling occasions, an increase in the isotopic space and complexity at both sites was observed, with the appearance of other consumers belonging to distinct trophic groups (e.g., herbivores and deposit feeders). This increase was also reflected in the increase in Omnivore and Carnivore ratio (*omniv\_car*)  $p=0.00492$ , whose Tukey's test reported significant differences ( $p<0.05$ ) between the win19 vs win20 and win20 vs sum20 levels (Table A.3).

Tróia's food webs throughout the sampling occasions were the least variable, registering consistently the highest values of *Max TP*, high isotopic redundancy and trophic diversity. This was also evident in very high nestedness values for Tróia food webs between sampling occasions (89.5-96.3 %, Fig. 6c). Nevertheless, a seasonal pattern was observed in Tróia food web, indicating differences in food web structure between summer and winter seasons (Fig. 6c).

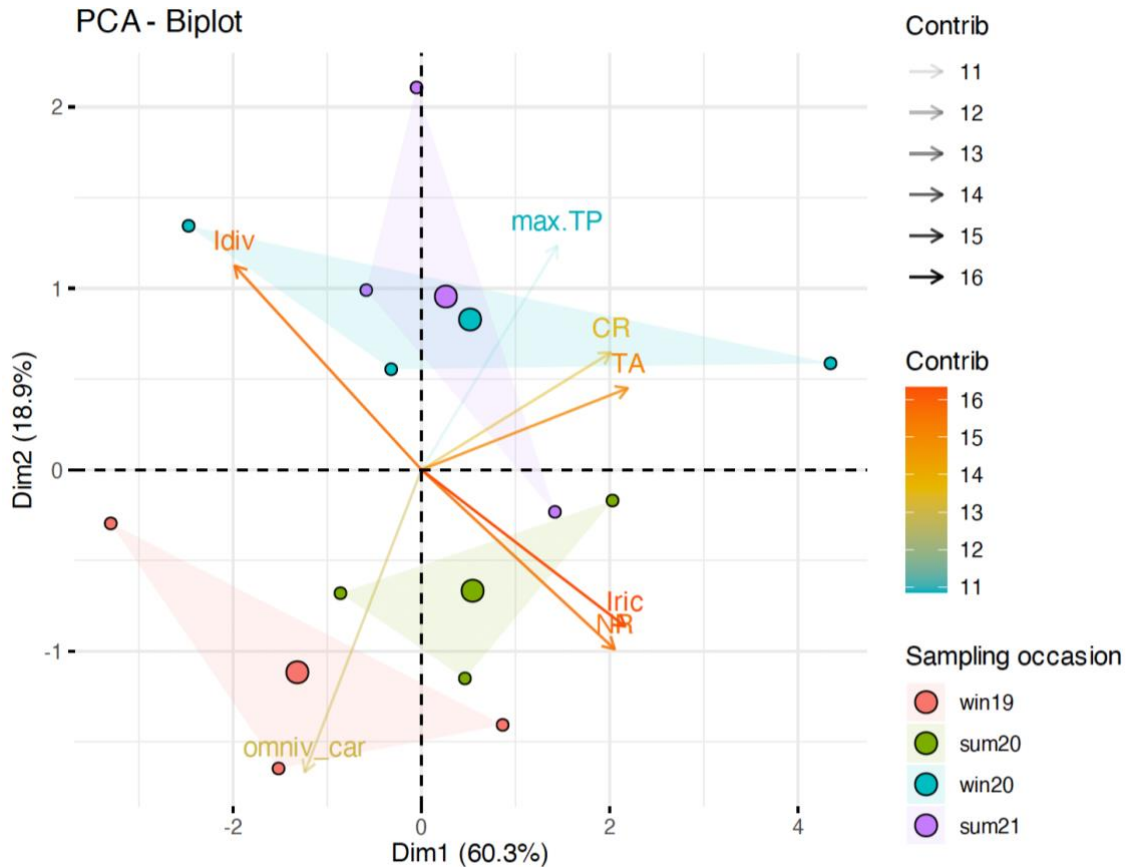


**Figure 7.** Principal component analysis (PCA) biplot based on scaled metrics (*CR*, *NR*, *TA*, *Iric*, *Idiv*, *Max TP* and *Omniv\_car*) used to characterize the food web structures analyzed across 4 seasons (win19, sum20, win20 and sum21) in Sado estuary, coloured by estuary “confidence” convex type. Variable’s vectors are presented based on their contributions to the principal components (gradient colours and transparency of vectors) with grey representing high contributions, yellow intermediate and blue representing very low contributions. The dots represent the cluster centroids for group variables.

PCA based on isotopic and diversity metrics demonstrated a partial seasonal separation of win19 and sum20 in the first axis (Fig.7). Metrics that contributed to this separation were *NR* and *Iric*, associated with sum20, and *omniv\_car* that was positively associated with win19. There was a clear annual pattern along the second axes that separated win19 and sum20 from win20 and sum21. The metrics responsible for this differentiation were *TA*, *Max TP*, *CR* and *Idiv* that were associated with win20 and sum21, while *NR*, *Iric* and *omniv\_car* were associated with win19 and sum20. This separation could be associated with the general increase of the isotopic niches and isotopic diversity metrics in Navigator and Gambia (by hosting more predatory consumers) in win20 and sum21. Nevertheless, according to PCAtest, the second PC axis was not significant indicating that temporal effect, especially the one associated to interannual variation is less strong than spatial pattern that was observed between Tróia and remaining two sites.

## 4.5 Discussion

### 4.5.1 Spatial variation of the benthic food web structure

Isotopic and diversity metrics, coupled with multivariate analysis, were useful in discriminating spatial patterns in benthic food webs. In accordance with our first hypothesis (Table 1), we found smaller trophic niches and chain lengths at Navigator and Gambia, as indicated by the respective metrics, compared to Tróia. Navigator and Gambia are both located in the inner estuary, where limited oxygen exchange and site-specific anthropogenic activities (e.g., aquaculture activities, paper factory respectively) are directly responsible for the observed organic enrichment. The simpler food webs in Navigator and Gambia are corroborated by the very low diversity of predatory and omnivory macrofauna consumers found at these two sites compared to Tróia. As demonstrated elsewhere (Dorgham, 2014; Hale et al., 2016) organic enrichment affects food web structure directly through siltation (increase in turbidity), habitat modification and oxygen reduction, leading to the disappearance of sensitive species. Similarly, a direct consequence of the organic load in Navigator and Gambia might have negatively affected the communities of more sensitive taxonomic groups, such as echinoderms, sponges and other vulnerable species. This has resulted in lower taxonomic and trophic diversity found at these two sites compared to the remarkably high benthic diversity in Tróia.

Indirectly an excessive organic enrichment may promote hypoxic conditions, triggering shifts in primary production and benefitting opportunistic species at the base of the trophic level (Zheng et al., 2020). For example, lower quality OM (estimated by *Chla:pheo ratio* values) at Navigator and Gambia was previously demonstrated to be highly influential for meiofauna distributional patterns in Sado estuary (Vieira et al., 2023). This contributed to a high biomass of small opportunistic species and fewer predators at sites with high OM loads (Sroczynska et al., 2021). Since many macrofauna species directly feeds on meiofauna, a less diverse meiofauna community previously found at Navigator and Gambia can be directly responsible for the lower observed diversity of intermediate consumers, such as deposit feeding polychaetes (Vafeiadou et al., 2013). This resulted in less benthic omnivores and predators in Navigator and Gambia compared to Tróia. Similar findings were reported for the Baltic Sea, where the authors demonstrated that the available biomass of primary consumers (meiofauna and small macrobenthic consumers) determines the abundance of large omnivores and carnivores (Szczepanek et al., 2021).

In contrast Tróia benefits from the tidal dynamics and higher oxygen exchange between the inner estuary and the marine environment, characterized by predominantly

sandy sediments with low organic matter, reflecting an environment with high-quality food sources, as evidenced by *Chla:pheo ratio* values. Tróia's food web reported high number of pathways and interactions, composed of secondary consumers, and a high number of top predators. This higher taxonomic and trophic diversity of benthic consumers in Tróia has led to a broader used of resources by primary consumers, as evidenced by a wider species distribution along the carbon axis.

Despite Navigator and Gambia sharing more similar sediment biogeochemical conditions, we did not observe a higher overlap between them, contrary to our second hypothesis (H2, Fig. 1). In fact, Navigator and Gambia exhibited very low isotopic niche overlap, with the lowest similarity values (*l<sub>sim</sub>* and *l<sub>nes</sub>*). Instead, Gambia's food web showed greater similarity to Tróia's food web. The low similarity and nestedness between Gambia and Navigator were attributed to a better efficiency in the use of resources by the consumers in Gambia (estimated by the high values of chlorophyl a, pheopigments and ratio of both, Table S.1; and the high values of *l<sub>disp</sub>* and *l<sub>ric</sub>*, Table 2). This can be attributed to the emergence of new macrobenthic consumers in Gambia, particularly more carnivores and deposit-feeders (since summer 2020), which have used more efficiently the available food resources and, thereby, increased the isotopic space occupied by the consumers.

However, we observed that consumers within the same trophic guilds in Gambia occupied higher positions on the trophic level compared to the same consumer species in Navigator (Fig.3 and Fig. A.1). This could be explained by the abrupt increase in Chla (5 orders of magnitude), phaeopigments (10 orders of magnitude) and carbon range values from summer 2020 in Gambia (Table S.1), which stimulated primary production and likely triggered shifts in resources, leading to increased energy transfer to higher trophic levels (Zheng et al., 2020). Similar findings were reported for the Polish coastal area, where the authors found that in sites with increased organic input from riverine discharge, the omnivores occupied higher trophic levels, likely due to an increased availability of meiobenthic prey (Szczepanek et al., 2021).

In summary, the quantity and quality of OM proved to be an important variable in shaping spatial patterns in benthic food web structure. Moreover, similarity metrics were a valuable complementary tool that helped to further disentangle the causes of spatial variability, in this case distinguishing between two food webs (Navigator and Gambia) that had similar structures but different resource utilization.

#### 4.5.2 Temporal variation of the benthic food web structure

Summer increase in temperature and photoperiod stimulates primary productivity, increasing secondary and tertiary production, increasing the complexity of the food webs

(Humphries et al., 2017). Contrary to our hypothesis (H3, Table 1), no seasonal pattern was observed in food webs concerning primary productivity. The highest Chla and phaeopigments were detected in win20 and sum20, indicating that primary productivity is not directly influenced by the seasonal effects. Instead, various factors potentially contribute to the abundance and diversity of food sources in Sado estuary. As previously demonstrated, increases in organic inputs to the system are not always congruent with the seasonal variations, they can also occur on a microscale (Moens & Beninger, 2018; Young et al., 2019), or may be linked to the spatially heterogeneous nature of the estuary itself (Elliott & Quintino, 2007).

Previously studies demonstrated that spatial differences in sediment conditions, often associated with anthropogenically mediated variations in local OM exert primary control on community distribution in this estuary (Vieira et al., 2023). These spatial differences are more influential for community structure than temporally derived variations in basal resources. Similarly, any seasonal patterns in food web structure are likely masked by more pronounced spatial differences, which are characteristic of each site within the estuary.

We also hypothesized (H4, Table 1) to find more similar food webs at the same season (win19/win20 vs sum20/sum21) than among different seasons. Contrary to our hypothesis, we observed a gradual increase in trophic diversity, particularly with the emergence of herbivores and other carnivores, along with a concomitant increase in food web complexity (as indicated by isotopic metrics) in Navigator and Gambia throughout the seasons. Significant differences were found for maximum trophic position and the percentage of carnivores and omnivores between winter 19 and other seasons, regardless of the site. Seasonal variations were more evident in Tróia's food web, as evidenced by the lowest observed similarities between seasons (win19 vs sum 20 and win20 vs sum21), reflecting temporal differences in the availability and diversity of food sources. We propose that the more complex food webs in Tróia exhibit better responses to seasonal shifts. These food webs are composed of more specialist consumers, that more efficiently use the available resources, hence, any temporally derived variability in food sources leads to a corresponding shift in isotopic position of these consumers (Ziółkowska & Sokołowski, 2022). In contrast, the food webs in Navigator and Gambia, are composed of consumers with more generalistic behavior and high plasticity, enabling them to quickly adapt to local variations in OM availability (Szczepanek et al., 2021), which is reflected in more flexible positioning of these consumers in the isotopic space. As a result, temporal shifts associated with resource utilization are more difficult to capture in such webs.

## 4.6 Concluding remarks

The integration of isotopic metrics complemented with multivariate and univariate analyses proved to be an important tool for the analysis of different aspects of the benthic food web complexity in a spatial-temporal context. Isotopic diversity metrics were useful to examine the structure of the food web, while similarity metrics provided insight into the differences in resource utilization. Tróia's food web demonstrated greater responsiveness in capturing temporal differences in resource use, suggesting that more complex food webs are better equipped to reflect temporal variability.

Multivariate analyses were useful in identifying spatial and temporal patterns demonstrating the strong influence of OM on spatial benthic food web discrimination. Meanwhile, univariate analyses revealed significant differences between maximum trophic position and the percentage of carnivores and omnivores between sites, indicating the potential for these metrics to serve as indicators of the ecosystem change in the future.

In summary, we concluded that the combination of different isotopic and diversity metrics coupled with univariate and multivariate analyses is a very promising approach to assess the functional integrity of the estuarine ecosystems, especially in the context of the descriptor 4 within MSFD. The suggested analysis of benthic food web attributes can be easily applied to any ecosystem or particular type of disturbance, potentially improving the accuracy of assessing GES under D4. Knowing that current indicators under D4 of MSFD are mostly focused on economically important guilds (fish, birds), often overlooking benthic habitats and ecosystem-based processes, this study offers valuable insights for developing new strategies to assess benthic ecosystems.

## 4.7 References

Baiser, B., Gravel, D, Cirtwill, AR, et al. (2019) Ecogeographical rules and the macroecology of food webs. *Global Ecol Biogeogr.* 28: 1204–1218. <https://doi.org/10.1111/geb.12925>

Bergamino, L. & Richoux N. B., (2015). Spatial and Temporal Changes in Estuarine FoodWeb Structure: Differential Contributions of Marsh Grass Detritus. *Estuaries and Coasts* (2015) 38:367–382, DOI 10.1007/s12237-014-9814-5.

Bettencourt, A.M., Bricker, S.B., Ferreira, J.G., Franco, A., Marques, J.C., Melo, J.J., Nobre, A., Ramos, L., Reis, C.S., Salas, F., Silva, M.C., Simas, T., Wolff, W.J., (2004).

Typology and Reference Conditions for Portuguese Transitional and Coastal Waters. Institute of Marine Research.

Bonaglia, S., Nascimento, F.J.A., Bartoli, M., Klawonn, I., Brüchert, V., (2014). Meiofauna increases bacterial denitrification in marine sediments. *Nat. Commun.* 5, 5133. <https://doi.org/10.1038/ncomms6133>.

Brito A. C., Pereira H., Picado A., Cruz J., Cereja R., Biguino B, Chainho P, Nascimento A, Carvalho F, Cabral S, Santos C, Palma C, Borges C, Dias J M. (2023) Increased oyster aquaculture in the Sado Estuary (Portugal): How to ensure ecosystem sustainability? *Science of the Total Environment* 855. <http://dx.doi.org/10.1016/j.scitotenv.2022.158898>

Burdon, F. J. (2021). Understanding the connectivity of ecosystems in the Anthropocene. *Journal of Animal Ecology*, 90, 1600–1604 <https://doi.org/10.1111/1365-2656.13550>

Caeiro, S., Costa, M.H., Ramos, T.B., Fernandes, F., Silveira, N., Coimbra, A., Medeiros, G., Painho, M., (2005). Assessing heavy metal contamination in Sado Estuary sediment: an index analysis approach. *Ecol. Indicat.* 5, 151–169. <https://doi.org/10.1016/j.ecolind.2005.02.001>.

Camargo, A., (2022). PCAtest: testing the statistical significance of principal component analysis in R. *PeerJ*, 10, e12967.

Catry T. et al. (2021). Elemental composition of whole body soft tissues in bivalves from the Bijagós Archipelago, Guinea-Bissau, *Environmental Pollution*, Volume 288, 117705, ISSN 0269-7491, <https://doi.org/10.1016/j.envpol.2021.117705>

Chambers, J. M., Freeny, A and Heiberger, R. M. (1992). Analysis of variance; designed experiments. Chapter 5 of *Statistical Models in S* eds J. M. Chambers and T. J. Hastie, Wadsworth & Brooks/Cole.

Costa, P., Caeiro, S., Lobo, J., Martins, M., Ferreira, M.A., Caetano, M., CarlosVale, C., Del Valls, A.T., Costa, M.H., (2011). Estuarine ecological risk based on hepatic histopathological indices from laboratory and in situ tested fish. *Mar. Pollut. Bull.* 62, 55–65. <https://doi.org/10.1016/j.marpolbul.2010.09.009>, 2011.

Costley T. K., Mossop F K, Dean R J., Garden M L., Marshall J., Carroll J. (2000). Determination of mercury in environmental and biological samples using pyrolysis

atomic absorption spectrometry with gold amalgamation, *Analytica Chimica Acta*, Volume 405, Issues 1–2, Pages 179-183, ISSN 0003-2670, [https://doi.org/10.1016/S0003-2670\(99\)00742-4](https://doi.org/10.1016/S0003-2670(99)00742-4).

Cucherouette, J. & Villéger, S., (2015). Quantifying the multiple facets of isotopic diversity: New metrics for stable isotope ecology" *Ecological Indicators* 56, 152–160. <http://dx.doi.org/10.1016/j.ecolind.2015.03.032>

Donázar-Aramendía, Sánchez-Moyano, J.E., García-Asencio, I., Miró, J. M., Megina, C., García-Gómez, J.C., (2019). Human pressures on two estuaries of the iberian peninsula are reflected in food web structure. *Scientific Reports* (2019) 9:11495. <https://doi.org/10.1038/s41598-019-47793-2>

Dorgham, M. M. (2014). "Effects of Eutrophication," in *Eutrophication: Causes, Consequences and Control*, vol. Vol. 2 . Eds. A. A. Ansari and S. S. Gill (Dordrecht: Springer), 29–44. doi: 10.1007/978-94-007-7814-6\_3

Eaton, J. W., & Moss, B., (1966). The estimation of numbers and pigment content in epipelagic algal populations. *Limnology and Oceanography*, 11(4), 584-595.

Fauvel, P. (1927). Polychètes sédentaires: addenda aux errantes, archiannélides, myzostomaires. *Faune de France*, 16, 1-494.

Gray, C., et al. (2014). Ecological networks: the missing links in biomonitoring science. *Journal of Applied Ecology*, 51(5), 1444-1449

Guen I. C., Tecchio, S., Dauvin J-C., Roton G.D., Lobry J., Lepagef M., Morin J., Lassalle G., Raoux A., Niquil N. (2019). Assessing the ecological status of an estuarine ecosystem: linking biodiversity and food-web indicators. *Estuarine, Coastal and Shelf Science* 228 (2019) 106339. <https://doi.org/10.1016/j.ecss.2019.106339>

Hale, S. S., Cicchetti, G., and Deacutis, C. F. (2016). Eutrophication and Hypoxia Diminish Ecosystem Functions of Benthic Communities in a New England Estuary. *Front. Mar. Sci.* 3. doi: 10.3389/fmars.2016.00249

Hayward, P. J., & Ryland, J. S. (Eds.). (2017). *Handbook of the marine fauna of North-West Europe*, Great Britain. Oxford university press.

Humphries, M. M., Studd, E. K., Menzies, A. K., & Boutin, S. (2017). To everything there is a season: summer-to-winter food webs and the functional traits of keystone species. *Integrative and Comparative Biology*, 57(5), 961-976.

Jackson, M. C., I. Donohue, A. L. Jackson, J. R. Britton, D. M. Harper & J. Grey, (2012). Population-level metrics of trophic structure based on stable isotopes and their application to invasion ecology. *PLoS ONE*. <https://doi.org/10.1371/journal.pone.0031757>.

Layman, C. A., B. D. Araujo, R. Boucek, C. M. Hammerschlag-Peyer, E. Harrison, Z. R. Jud, P. Matich, A. E. Rosenblatt, J. J. Vaudo, L. A. Yeager & D. M. Post, (2012). Applying stable isotopes to examine food web structure: an overview of analytical tools. *Biological Reviews* 87: 545–562.

Layman, C.A., Arrington, D.A., Montana, C.G., Post, D.M., (2007). Can stable isotope ratios provide for community-wide measures of trophic structure? *Ecology* 88,42–48, <http://dx.doi.org/10.1890/0012-9658>

Lê, S., Josse, J., & Husson, F., (2008). FactoMineR: an R package for multivariate analysis. *Journal of statistical software*, 25, 1-18.

Lepage, M., Harrison, T., Breine, J., et al., (2016). An approach to intercalibrate ecological classification tools using fish in transitional water of the Northeast Atlantic. *Ecol.Indicat.* 67, 318–327

Liu Q., Yia Y, Hou C., Wua X., Song J., 2020. Response of trophic structure and isotopic niches of the food web to flow regime in the Yellow River estuary. *Marine Geology* 430 (2020) 106329. <https://doi.org/10.1016/j.margeo.2020.106329>

Lorenzen, C. J. (1967). Determination of Chlorophyll and Pheo-Pigments: Spectrophotometric Equations. *Limnology and Oceanography*, 12(2), 343–346.<https://doi.org/10.4319/lo.1967.12.2.0343>

Elliott M., Quintino V. (2007). The Estuarine Quality Paradox, Environmental Homeostasis and the difficulty of detecting anthropogenic stress in naturally stressed areas. *Marine Pollution Bulletin* 54 (2007) 640–645. doi:10.1016/j.marpolbul.2007.02.003

Moens, T., Beninger, P.G. (2018). Meiofauna: An Inconspicuous but Important Player in Mudflat Ecology. In: Beninger, P. (eds) *Mudflat Ecology*. Aquatic Ecology Series, vol 7. Springer, Cham. [https://doi.org/10.1007/978-3-319-99194-8\\_5](https://doi.org/10.1007/978-3-319-99194-8_5)

Nelson, J. A., Deegan, L., & Garrett, R. (2015). Drivers of spatial and temporal variability in estuarine food webs. *Marine Ecology Progress Series*, 533, 67-77.

Ridall, A., Ingels, J., (2021). Suitability of free-living marine nematodes as bioindicators: status and future considerations. *Front. Mar. Sci.* 0, 863. <https://doi.org/10.3389/FMARS.2021.685327>.

Rogers, S., et al. (2010). Marine Strategy Framework Directive—Task Group 4 Report Food Webs. European Commission Joint Research Centre, ICES

Rombouts, I., et al. (2013). Food web indicators under the Marine Strategy Framework Directive: from complexity to simplicity? *Ecol. Ind.* 29, 246- 25

Rooney, N., McCann, K., Gellner, G., & Moore, J. C. (2006). Structural asymmetry and the stability of diverse food webs. *Nature*, 442(7100), 265-269.

Schmidt, S. N., C. J. Harvey & M. J. Vander Zanden, (2011). Historical and contemporary trophic niche partitioning among Laurentian Great Lakes coregonines. *Ecological Applications* 3: 888–896.

Schratzberger, M., Somerfield, P.J., (2020). Effects of widespread human disturbances in the marine environment suggest a new agenda for meiofauna research is needed. *Sci. Total Environ.* 728, 138435.

Sroczynska, K., Chainho, P., Vieira, S., Adão, H., (2021). What makes a better indicator? Taxonomic vs functional response of nematodes to estuarine gradient. *Ecol. Indicat.* 121, 107113 <https://doi.org/10.1016/j.ecolind.2020.107113>.

Sroczynska, K., Conde, A., Chainho, P., Adão, H., (2021a). How nematode morphometric attributes integrate with taxonomy-based measures along an estuarine gradient. *Ecol. Indicat.* 124, 107384. <https://doi.org/10.1016/j.ecolind.2021.107384>

Sturbois, A., Riera P., Desroy N., Brébant, T., Carpentier A., Ponsero A., Schaal G. Spatio-temporal patterns in stable isotope composition of a benthic intertidal food web reveal limited influence from salt marsh vegetation and green tide. *Marine Environmental Research* 175 (2022) 105572, <https://doi.org/10.1016/j.marenvres.2022.105572>

Szczepanek, M., Silberberger M., J., Koziorowska-Makuch, K., Nobili, E., Kedra, M. (2021). The response of coastal macrobenthic food-web structure to seasonal and regional

variability in organic matter properties. *Ecological Indicators* 132 (2021) 108326. <https://doi.org/10.1016/j.ecolind.2021.108326>

Szpak, P., Metcalfe, Z. J., Macdonald, A. R., (2017). Best practices for calibrating and reporting stable isotope measurements in archaeology, *Journal of Archaeological Science: Reports*, Volume 13, 2017, Pages 609-616, ISSN 2352-409X, <https://doi.org/10.1016/j.jasrep.2017.05.007>.

Tam, J. C., et al. (2017). Towards ecosystem-based management: identifying operational food-web indicators for marine ecosystems. *ICES Journal of Marine Science*, 74(7), 2040-2052

Teixeira, M., Terrinha, P., Roque, C., Voelker, A., Silva, P., Salgueiro, E., Abrantes, F., Naughton, F., Mena, A., Ercilla, G., Casas, D., 2020. The late pleistocene-holocene sedimentary evolution of the sines Contourite drift (SW Portuguese Margin): a multiproxy approach. *Sediment. Geol.* 407, 105737, 2020.

Thompson R. M, Brose U., Dunne J.A., Hall Jr. R. O, Hladz S., Kitching L. R., Martinez D. N., Rantala H., Romanuk N. T., Stouffer B. D., Jason M. Tylianakis M. J. (2012). Food webs: reconciling the structure and function of biodiversity. *Trends in Ecology and Evolution*, Vol. 27, No. 12 689. DOI: <https://doi.org/10.1016/j.tree.2012.08.005>

Tsikopoulou I, Dimitriou PD, Karakassis I, Lampadariou N, Papadopoulou N and Smith CJ. (2021). Temporal Variation in the Ecological Functioning of Benthic Communities After 20 Years in the Eastern Mediterranean. *Front. Mar. Sci.* 8:768051. doi: 10.3389/fmars.2021.768051

Vafeiadou A. M., Materatski P., Adão H., Troch M., Moens T. (2013). Food sources of macrobenthos in an estuarine seagrass habitat (*Zostera noltii*) as revealed by dual stable isotope signatures. *Mar Biol* (2013) 160:2517–2523.

Vesal, S. E., Auriemma, R., Libralato, S., Nasi, F., & Del Negro, P. (2022). Impacts of organic enrichment on macrobenthic production, productivity, and transfer efficiency: What can we learn from a gradient of sewage effluents? *Marine Pollution Bulletin*, 182, 113972.

Vieira, S., Barrulas, P., Chainho, P. et al. Spatial and Temporal Distribution of the Multi-element Signatures of the Estuarine Non-indigenous Bivalve *Ruditapes philippinarum*. *Biol Trace Elem Res* 200, 385–401 (2022). <https://doi.org/10.1007/s12011-021-02629-x>

Vieira S., Sroczynska K., Neves J., Martins M., Costa M.H., Adão H., Vicente S.L.C., (2023). Distribution patterns of benthic bacteria and nematode communities in estuarine sediments. *Estuarine, Coastal and Shelf Science* 291, 108448. <https://doi.org/10.1016/j.ecss.2023.108448>

Villéger, S., Grenouillet, G., Brosse, S., 2013. Decomposing functional -diversity reveals that low functional -diversity is driven by low functional turnover in European fish assemblages. *Glob. Ecol. Biogeogr.* 22, 671–681, <http://dx.doi.org/10.1111/geb.12021>

Villéger, S., N. W. H. Mason & D. Mouillot, (2008). New multidimensional functional diversity indices for a multifaceted framework in functional ecology. *Ecology* 89: 2290–2301.

Villéger, S., Novack-Gottshall, P.M., Mouillot, D., 2011. The multidimensionality of the niche reveals functional diversity changes in benthic marine biotas across geological time. *Ecol. Lett.* 14, 561–568, <http://dx.doi.org/10.1111/j.1461-0248.2011.01618.x>

Winemiller K.O., Akin S., Zeug S. C., (2007). Production sources and food web structure of a temperate tidal estuary: integration of dietary and stable isotope data. *Mar Ecol-Prog Ser.* 2007; 343: 63–76. doi: 10.3354/meps06884

Xu, W., Shin, K.S.P., Sun J., (2022). Organic Enrichment Induces Shifts in the Trophic Position of Infauna in a Subtropical Benthic Food Web, Hong Kong. *Frontiers in Marine Science*, Volume 9 | Article 937477. doi: 10.3389/fmars.2022.937477

Young, M., Howe, E., O'Rear, T., Berridge, K., Moyle, P. (2021). Food Web Fuel Differs Across Habitats and Seasons of a Tidal Freshwater Estuary. *Estuaries and Coasts* 44:286–301. <https://doi.org/10.1007/s12237-020-00762-9>

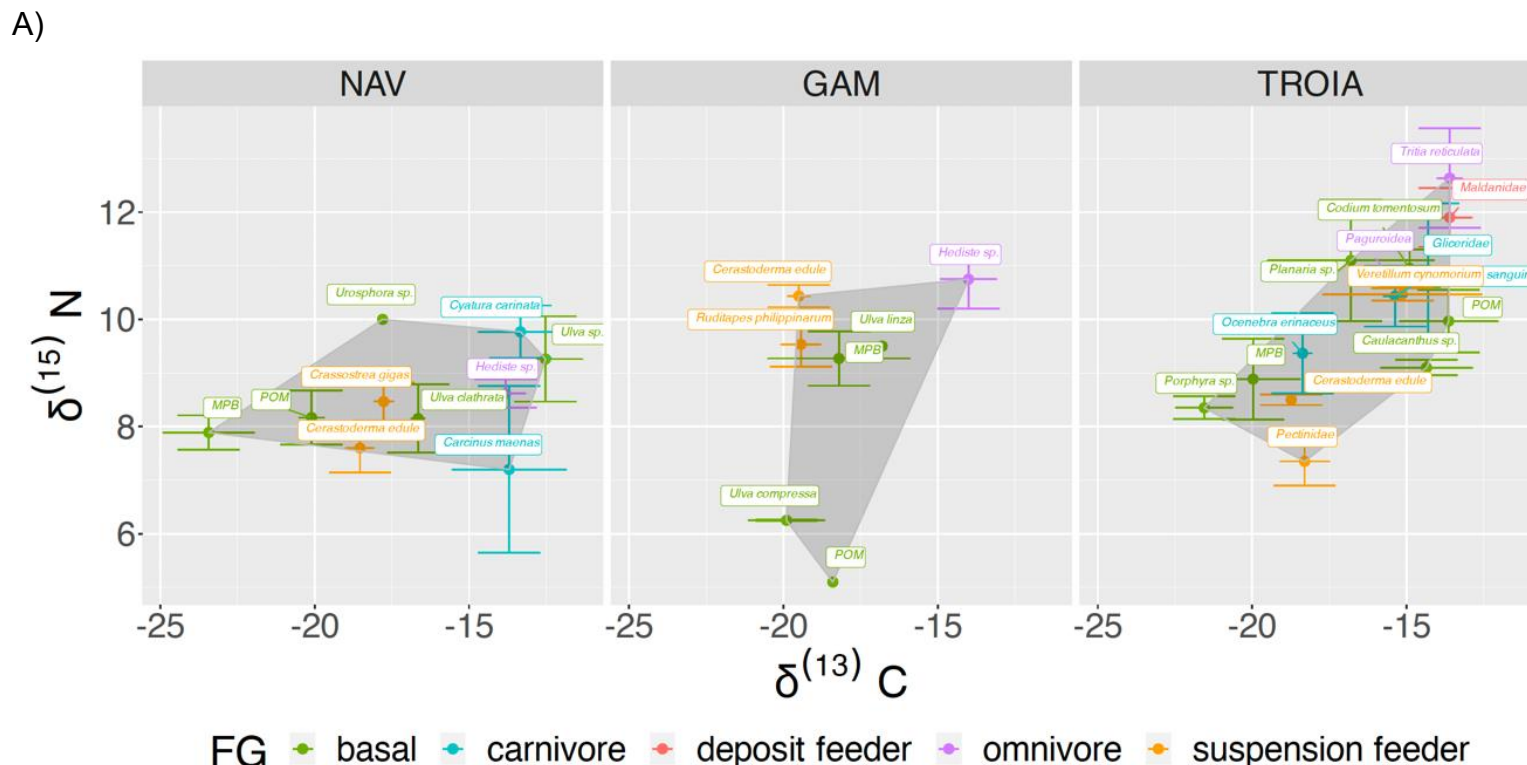
Zandee M. Jake Vander, Rasmussen Joseph B. , (2001), Variation in  $\delta^{15}\text{N}$  and  $\delta^{13}\text{C}$  trophic fractionation: Implications for aquatic food web studies, *Limnology and Oceanography*, 8, doi: 10.4319/lo.2001.46.8.2061.

Ziółkowska M., and Sokołowski A. (2022). Variation of food web structure in macrobenthic communities in low diversity system as determined by stable isotope-based community-wide metrics. *Estuarine, Coastal and Shelf Science*, Volume 274, ISSN 0272-7714, <https://doi.org/10.1016/j.ecss.2022.107931>.

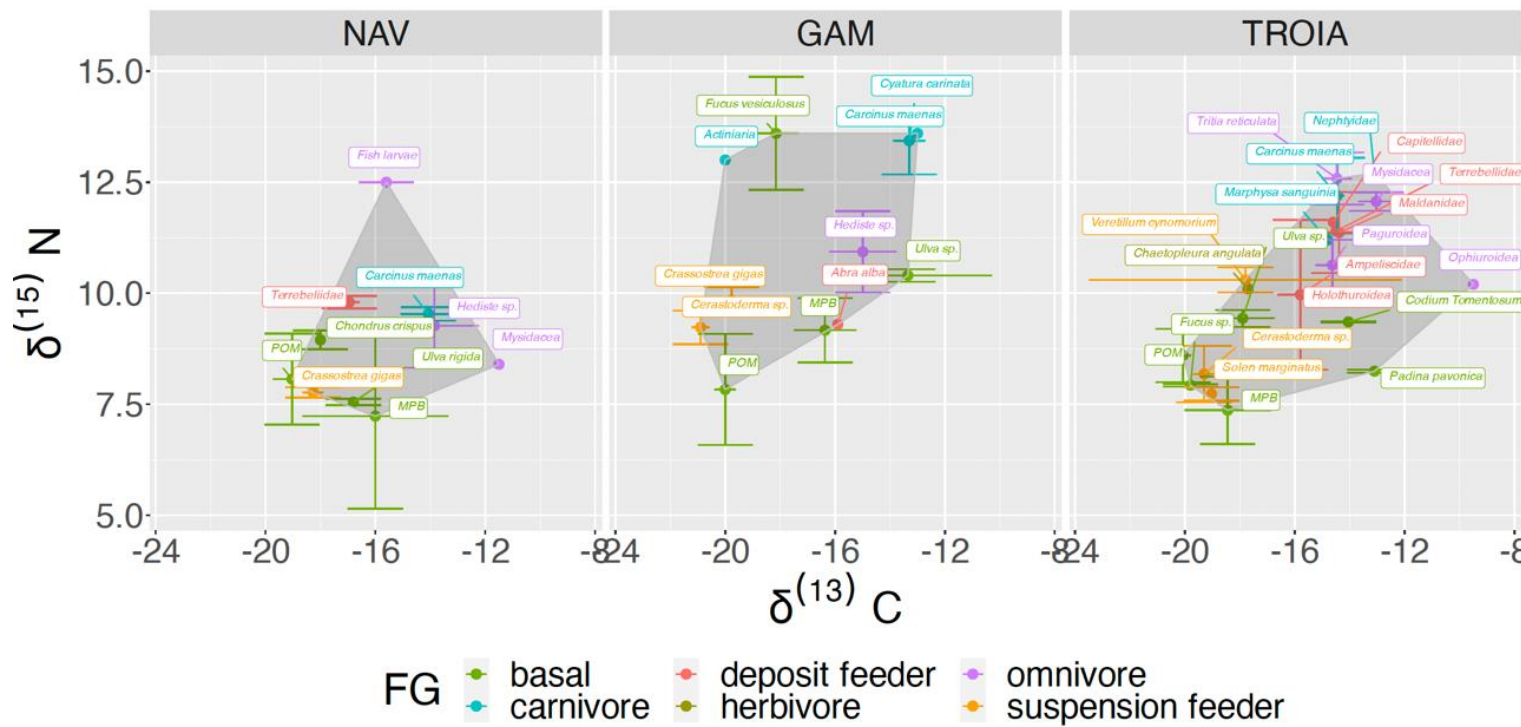
Zheng, X., Como, S., Huang, L., and Magni, P. (2020). Temporal Changes of a Food Web Structure Driven by Different Primary Producers in a Subtropical Eutrophic Lagoon. *Mar. Environ. Res.* 161, 105128. doi: 10.1016/j.marenvres.2020.105128

## Supplementary information of chapter 4

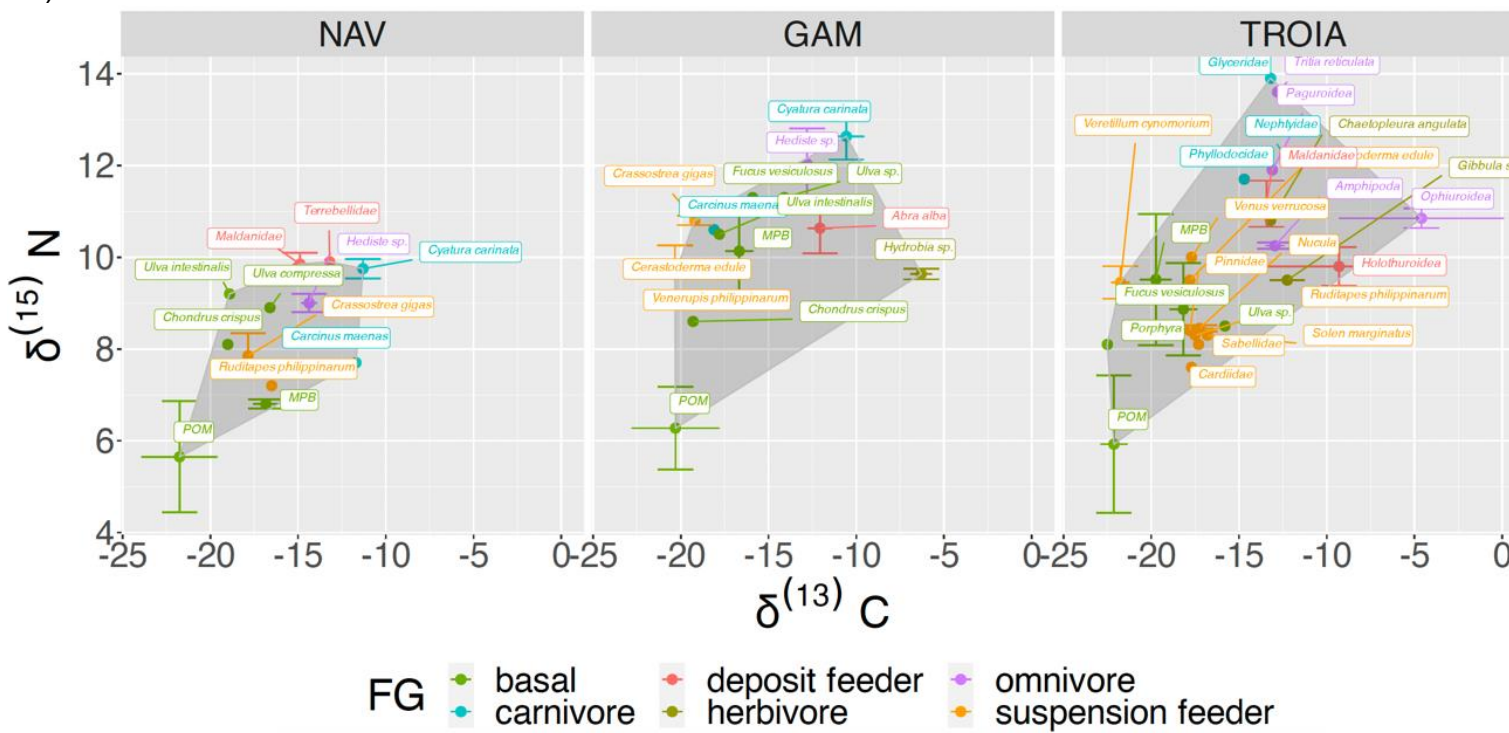
## Appendix A – Figures and tables



B)



C)



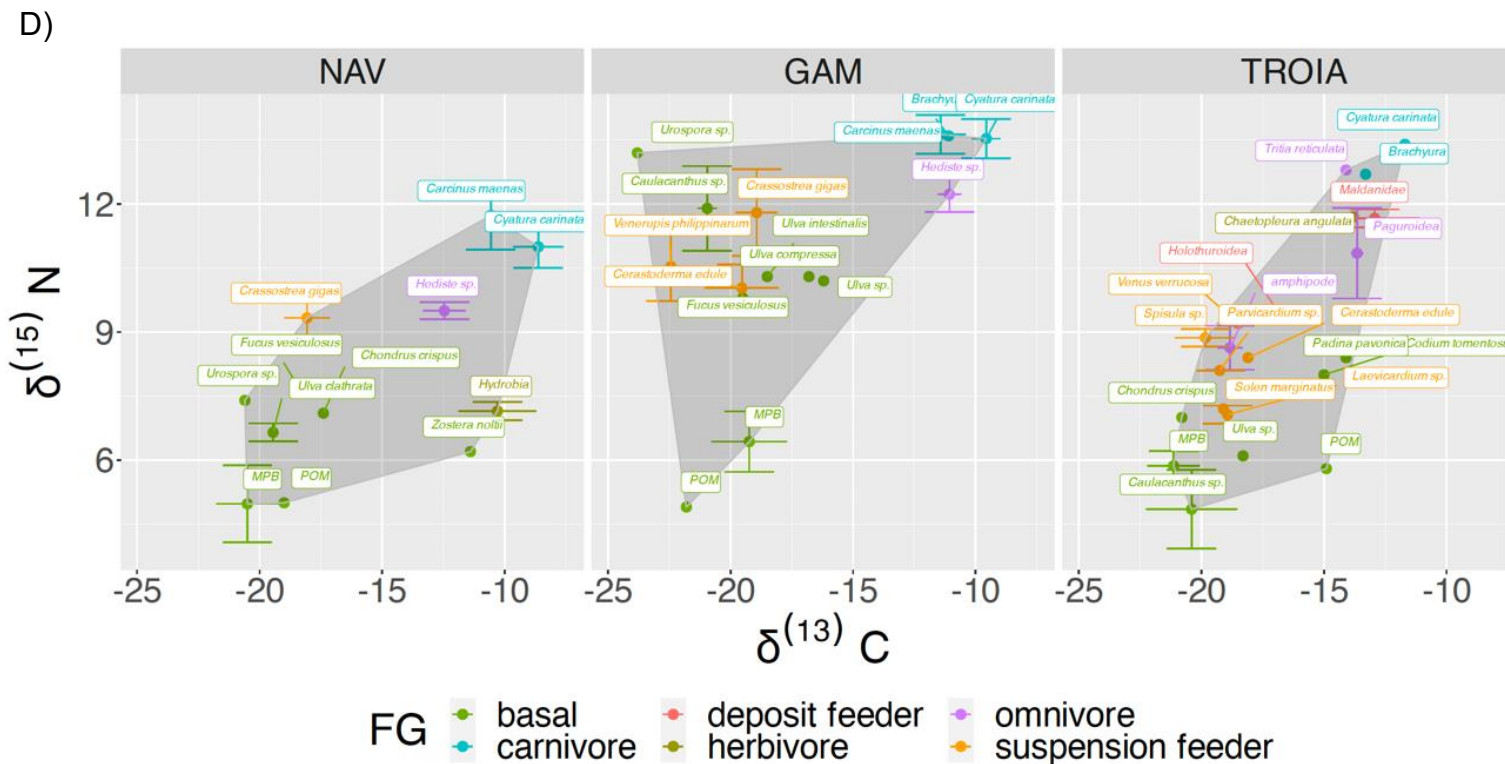


**Figure A.1.** Biplots of carbon ( $\delta^{13}\text{C}$ ) and nitrogen ( $\delta^{15}\text{N}$ ) isotopic signatures (representing mean and standard deviation) for each taxon with colors depicting different FG (Feeding Guild) assignment (according to Fauvel 1927; Hayward & Ryland, 1995), at three study sites for (A) win19, (B) sum20, (C) win20 and (D) sum21. Convex hull areas are drawn only for consumers (shaded area) and represent total area in the biplot occupied by all the consumers.

**Table A.1.** Mean  $\pm$  SE of C and N isotopes measured from the consumers, Feeding Guild (FG), consumer level. From each site Navigator (NAV), Tróia (TROI) and Gambia (GAM) and across all seasons (winter 19, summer 20, winter 20 and summer 21).

Sample ID	Species	FG	Consumer	d15N	d13C
NAVw19	<i>Hediste</i> sp.	omnivore	secondary	8.62 $\pm$ 0.11	-13.81 $\pm$ 0,28
NAVw19	<i>Carcinus maenas</i>	carnivore	secondary	7.20 $\pm$ 0.69	-13.70 $\pm$ 0.82
NAVw19	<i>Cyatura carinata</i>	carnivore	secondary	9.76 $\pm$ 0.22	-13.33 $\pm$ 0.60
NAVw19	<i>Cerastoderma edule</i>	suspension feeder	primary	7.60 $\pm$ 0.20	-18.53 $\pm$ 0.20
NAVw19	<i>Crassostrea gigas</i>	suspension feeder	primary	8.46 $\pm$ 0.15	-17.76 $\pm$ 0.13
GAMw19	<i>Hediste</i> sp.	omnivore	secondary	10.74 $\pm$ 0.24	-14.00 $\pm$ 0.40
GAMw19	<i>Cerastoderma edule</i>	suspension feeder	primary	10.43 $\pm$ 0.09	-19.50 $\pm$ 0.16
GAMw19	<i>Ruditapes philippinarum</i>	suspension feeder	primary	9.53 $\pm$ 0.18	-19.43 $\pm$ 0.28
TROIw19	Gliceridae	carnivore	secondary	10.91 $\pm$ 0.55	-14.30 $\pm$ 0.36
TROIw19	<i>Marpphysa sanguinia</i>	carnivore	secondary	10.43 $\pm$ 0.25	-15.36 $\pm$ 0.16
TROIw19	<i>Ocenebra erinaceus</i>	carnivore	secondary	9.36 $\pm$ 0.33	-18.36 $\pm$ 0.13
TROIw19	Maldanidae	deposit feeder	secondary	11.95 $\pm$ 0.27	-13.37 $\pm$ 0.25

GAMS20	<i>Cyatura carinata</i>	carnivore	secondary	13.43±0.40	-15.55±0.53
GAMS20	Actiniaria	carnivore	secondary	12.97	-19.99
GAMS20	<i>Abra alba</i>	deposit feeder	primary	9.32	-15.91
GAMS20	<i>Hediste</i> sp.	omnivore	secondary	10.93±0.40	-14.98±0.53
GAMS20	<i>Cerastoderma</i> sp.	suspension feeder	primary	9.23±0.16	-20.90±0.13
GAMS20	<i>Crassostrea gigas</i>	suspension feeder	primary	9.83±0.13	-19.76±0.22
NAVS20	<i>Carcinus maenas</i>	carnivore	secondary	9.53±0.07	-14.06±0.43
NAVS20	Terrebeliidae	deposit feeder	secondary	9.81±0.07	-16.94±0.18
NAVS20	<i>Hediste</i> sp.	omnivore	secondary	9.28±0.42	-13.85±0.71
NAVS20	Fish larvae	omnivore	secondary	12.49±0.01	-15.63±0.002
NAVS20	Mysidacea	omnivore	secondary	8.39	-11.53
NAVS20	<i>Crassostrea gigas</i>	suspension feeder	primary	7.80±0.05	-18.30±0.05
TROIS20	Nephtyidae	carnivore	secondary	12.74	-13.14
TROIS20	<i>Carcinus maenas</i>	carnivore	secondary	12.21±0.35	-14.39±0.08
TROIS20	<i>Morphysa sanguinia</i>	carnivore	secondary	11.15	-14.77

TROIS20	Maldanidae	deposit feeder	secondary	11.37±0.4	-14.39±0.7
TROIS20	Ampeliscidae	deposit feeder	secondary	9.97±0.75	-15.80±0.35
TROIS20	Capitellidae	deposit feeder	secondary	11.58	-14.59
TROIS20	Terrebellidae	deposit feeder	secondary	11.38	-14.51
TROIS20	Holothuroidea	deposit feeder	secondary	9.83	-14.35
TROIS20	<i>Chaetopleura angulata</i>	herbivore	secondary	10.09	-17.75
TROIS20	Paguroidea	omnivore	secondary	10.63±0.25	-14.63±0.26
TROIS20	<i>Tritia reticulata</i>	omnivore	secondary	12.58±0.26	-14.47±0.22
TROIS20	Mysidacea	omnivore	secondary	12.07±0.09	-13.03±0.27
TROIS20	Ophiuroidea	omnivore	secondary	10.21	-9.51
TROIS20	<i>Cerastoderma sp.</i>	suspension feeder	primary	8.18±0.28	-19.30±0.16
TROIS20	<i>Solen marginatus</i>	suspension feeder	primary	7.73±0.06	-19.03±0.02
TROIS20	<i>Veretillum cynomorium</i>	suspension feeder	secondary	10.27±0.11	-17.79±2.51
GAMw20	<i>Cyatura carinata</i>	carnivore	secondary	12.64±0.22	-10.55±0.43
GAMw20	<i>Carcinus maenas</i>	carnivore	secondary	10.57	-18.11

GAMw20	<i>Abra alba</i>	deposit feeder	primary	10.65±0.26	-1.052±0.29
GAMw20	<i>Hydrobia</i> sp.	herbivore	primary	9.61±0.05	-6.33±0.27
GAMw20	<i>Hediste</i> sp.	omnivore	secondary	12.04±0.35	-12.81±0.11
GAMw20	<i>Venerupis philippinarum</i>	suspension feeder	primary	9.07±0.03	-20.15±0.06
GAMw20	<i>Cerastoderma edule</i>	suspension feeder	primary	9.64±0.04	-20.33±0.09
GAMw20	<i>Crassostrea gigas</i>	suspension feeder	primary	10.79±0.03	-19.20±0.07
NAVw20	<i>Cyatura carinata</i>	carnivore	secondary	9.76±0.09	-11.27±0.14
NAVw20	Maldanidae	deposit feeder	secondary	9.88±0.11	-14.90±0.16
NAVw20	<i>Carcinus maenas</i>	carnivore	secondary	7.73	-11.68
NAVw20	Terrebellidae	deposit feeder	secondary	9.93	-13.22
NAVw20	<i>Hediste</i> sp.	omnivore	secondary	9.01±0.07	-14.36±0.18
NAVw20	<i>Ruditapes philippinarum</i>	suspension feeder	primary	7.25	-16.52
NAVw20	<i>Crassostrea gigas</i>	suspension feeder	primary	7.88±0.20	-17.9±0.02
TROlw20	Nephtyidae	carnivore	secondary	12.22	-12.42
TROlw20	Glyceridae	carnivore	secondary	13.91	-13.17

TROlw20	Phyllodocidae	carnivore	secondary	11.68	-14.69
TROlw20	Maldanidae	deposit feeder	secondary	11.19±0.22	-13.44±0.11
TROlw20	Holothuroidea	deposit feeder	primary	9.79±0.19	-9.29±2.45
TROlw20	<i>Chaetopleura angulata</i>	herbivore	secondary	10.80	-13.22
TROlw20	<i>Gibbula</i> sp.	herbivore	primary	9.48±0.004	-12.22±0.03
TROlw20	Paguroidea	omnivore	secondary	11.90	-13.12
TROlw20	<i>Tritia reticulata</i>	omnivore	secondary	13.64	-12.82
TROlw20	Ophiuroidea	omnivore	secondary	10.88±0.09	-4.59±2.08
TROlw20	Amphipoda	omnivore	secondary	10.26±0.02	-12.96±0.22
TROlw20	<i>Veretillum cynomorium</i>	suspension feeder	secondary	9.47±0.15	-21.74±0.23
TROlw20	<i>Venus verrucosa</i>	suspension feeder	primary	10.02	-17.67
TROlw20	<i>Ruditapes philippinarum</i>	suspension feeder	primary	8.29	-17.54
TROlw20	<i>Cerastoderma edule</i>	suspension feeder	primary	9.54	-17.81
TROlw20	Sabellidae	suspension feeder	primary	8.15	-17.31
TROlw20	<i>Solen marginatus</i>	suspension feeder	primary	8.29	-16.82

TROlw20	Pinnidae	suspension feeder	primary	8.44	-17.78
TROlw20	Cardiidae	suspension feeder	primary	7.61	-17.67
TROlw20	Nucula	suspension feeder	primary	8.46±0.01	-17.26±0.32
GAMS21	<i>Carcinus maenas</i>	carnivore	secondary	13.59±1.64	-11.42±0.57
GAMS21	<i>Cyatura carinata</i>	carnivore	secondary	13.53±0.20	-9.54±0.25
GAMS21	<i>Brachyura</i>	carnivore	secondary	13.63	-11.06
GAMS21	<i>Hediste</i> sp.	omnivore	secondary	12.23±0.17	-11.06±0.19
GAMS21	<i>Cerastoderma edule</i>	suspension feeder	primary	10.04±0.23	-19.53±0.64
GAMS21	<i>Venerupis philippinarum</i>	suspension feeder	primary	10.55±0.36	-22.40±0.52
GAMS21	<i>Crassostrea gigas</i>	suspension feeder	primary	11.79±0.46	-18.96±0.37
NAVS21	<i>Cyatura carinata</i>	carnivore	secondary	11.03±0.22	-8.64±0.44
NAVS21	<i>Carcinus maenas</i>	carnivore	secondary	11.71±0.37	-10.59±0.02
NAVS21	<i>Hydrobia</i>	herbivore	primary	7.11±0.09	-10.26±0.69
NAVS21	<i>Hediste</i> sp.	omnivore	secondary	9.52±0.09	-12.49±0.39
NAVS21	<i>Crassostrea gigas</i>	suspension feeder	primary	9.36±0.16	-18.04±0.40

TROIS21	<i>Cyatura carinata</i>	carnivore	secondary	13.37	-11.72
TROIS21	Brachyura	carnivore	secondary	12.74	-13.30
TROIS21	Maldanidae	deposit-feeder	secondary	11.64±0.08	-12.91±0.80
TROIS21	Holothuroidea	deposit-feeder	primary	9.47	-16.94
TROIS21	<i>Chaetopleura angulata</i>	herbivore	secondary	11.73	-13.81
TROIS21	amphipode	omnivore	secondary	8.62±0.22	-18.82±0.20
TROIS21	<i>Tritia reticulata</i>	omnivore	secondary	12.80	-14.14
TROIS21	Paguroidea	omnivore	secondary	10.87±0.46	-13.63±0.09
TROIS21	<i>Solen marginatus</i>	suspension feeder	primary	7.16	-19.08
TROIS21	<i>Cerastoderma edule</i>	suspension feeder	primary	8.35	-18.09
TROIS21	<i>Venus verrucosa</i>	suspension feeder	primary	9.21	-18.47
TROIS21	<i>Parvicardium</i> sp.	suspension feeder	secondary	8.09±0.01	-19.26±0.22
TROIS21	<i>Spisula</i> sp.	suspension feeder	primary	8.87±0.10	-19.83±0.54
TROIS21	<i>Laevicardium</i> sp.	suspension feeder	primary	7.04±0.09	-18.96±0.02

**Table A.2.** Mean $\pm$ SE, n=3 of the environment and biogeochemical parameters measured in each site (Navigator, Gambia and Tróia), across the 4 seasons (win19, sum20, win20 and sum21). Granulometric parameters (%) are Clay\_per, Sand\_per, Gravel\_per. The elemental analysis (w%) are organic matter (OM\_per), Total Nitrogen and Carbon (N\_total\_per and C\_total\_per), pigments measured (mg.g $^{-1}$ ) are Chlorophyl a (Chla\_mg.g $^{-1}$ ) and Phaeopigment (Phaeo\_mg.g $^{-1}$ ) the freshness calculated by the ratio between Chla and Phaeo pigments (Chla\_phaeo). Metals concentration (mg/kg) Li, Sr, Mn, Ni, Cr, Be, U, Ba, Co, Cu, Zn, As, Pb and Hg. Instant variables, measured in each site Temperature (Temp) °C, Salinity (Sal), Oxygen (O2) mg/L and pH.

Seasons		win19			sum20			win20			sum21		
Sites		Navigator	Gambia	Tróia	Navigator	Gambia	Tróia	Navigator	Gambia	Tróia	Navigator	Gambia	Tróia
Granulometry	Clay_per	30.1 $\pm$ 3.1	13.5 $\pm$ 0.2	1.8 $\pm$ 0.2	20.9 $\pm$ 1	17.4 $\pm$ 5.1	1.7 $\pm$ 0.1	35.2 $\pm$ 6.6	15.8 $\pm$ 1.7	1.5 $\pm$ 0.5	25.8 $\pm$ 2.3	16.3 $\pm$ 2.2	2.9 $\pm$ 0.4
	Sand_per	66.2 $\pm$ 2.6	71.5 $\pm$ 5.5	93.8 $\pm$ 1.9	73.1 $\pm$ 1.7	67.5 $\pm$ 4.1	97.3 $\pm$ 0.1	61.8 $\pm$ 6.1	68.7 $\pm$ 1	95.2 $\pm$ 1.1	72.2 $\pm$ 2.6	66.6 $\pm$ 0.6	91.6 $\pm$ 2.8
	Gravel_per	3.8 $\pm$ 0.7	14.9 $\pm$ 5.6	4.4 $\pm$ 1.8	5.9 $\pm$ 1.5	15.1 $\pm$ 6.4	1 $\pm$ 0.1	3 $\pm$ 0.7	15.5 $\pm$ 1	3.3 $\pm$ 1	2 $\pm$ 0.3	16.9 $\pm$ 2.1	5.4 $\pm$ 2.8
Elemental composition	OM_per	3.9 $\pm$ 0.6	0.6 $\pm$ 0.04	1.9 $\pm$ 0.3	2.3 $\pm$ 0.3	1.7 $\pm$ 0.3	0.4 $\pm$ 0.02	2.4 $\pm$ 0.3	0.8 $\pm$ 0.05	0.4 $\pm$ 0.02	2.1 $\pm$ 0.1	1.2 $\pm$ 0.1	0.5 $\pm$ 0.04
	C_total_per	0.9 $\pm$ 0.3	0.7 $\pm$ 0.4	0.6 $\pm$ 0.06	1.1 $\pm$ 0.1	0.4 $\pm$ 0.1	0.7 $\pm$ 0.1	1.1 $\pm$ 0.1	0.5 $\pm$ 0.03	0.5 $\pm$ 0.04	0.9 $\pm$ 0.1	0.4 $\pm$ 0.05	0.6 $\pm$ 0.03
	N_total_per	0.06 $\pm$ 0.2	0.05 $\pm$ 0.02	0.02 $\pm$ 0.008	0.07 $\pm$ 0.006	0.03 $\pm$ 0.01	0.01 $\pm$ 0.003	0.3 $\pm$ 0.09	0.05 $\pm$ 0.005	0.08 $\pm$ 0.002	0.07 $\pm$ 0.007	0.04 $\pm$ 0.006	0.01 $\pm$ 0.003
	CaCO <sub>3</sub> _per	2.4 $\pm$ 0.5	1 $\pm$ 0.06	4.3 $\pm$ 0.3	2.6 $\pm$ 0.5	1.6 $\pm$ 0.3	4.6 $\pm$ 0.9	2.1 $\pm$ 0.05	1.2 $\pm$ 0.04	3.5 $\pm$ 0.3	1.7 $\pm$ 0.1	1.3 $\pm$ 0.05	3.7 $\pm$ 0.3
	Chla_mg_g	15.6 $\pm$ 3.9	10.3 $\pm$ 0.9	26.7 $\pm$ 2.1	9.8 $\pm$ 0.1	55.5 $\pm$ 2.4	11.1 $\pm$ 1.4	31.1 $\pm$ 6.6	10.8 $\pm$ 1.9	6.7 $\pm$ 0.5	4.8 $\pm$ 0.8	7.7 $\pm$ 0.7	4.9 $\pm$ 0.6
	Phaeo_mg_g	14.7 $\pm$ 3.7	7.8 $\pm$ 0.5	14.5 $\pm$ 1	10.6 $\pm$ 1.2	115.1 $\pm$ 32.7	5.2 $\pm$ 0.9	40.1 $\pm$ 9.4	5.1 $\pm$ 1.5	4.5 $\pm$ 0.8	1.6 $\pm$ 0.2	3.6 $\pm$ 0.4	1.3 $\pm$ 0.2
	Chla_phaeo	1.1 $\pm$ 0.02	1.3 $\pm$ 0.1	1.8 $\pm$ 0.06	0.9 $\pm$ 0.1	0.7 $\pm$ 0.3	2.2 $\pm$ 0.1	0.8 $\pm$ 0.02	2.5 $\pm$ 0.6	1.7 $\pm$ 0.3	2.9 $\pm$ 0.1	2.1 $\pm$ 0.05	4 $\pm$ 0.4
Metals (mg/kg)	Li	28,7 $\pm$ 2,8	20,4 $\pm$ 0,7	11,5 $\pm$ 0,3	28 $\pm$ 1,3	20,9 $\pm$ 3,5	11,5 $\pm$ 0,05	30,8 $\pm$ 2,7	25,6 $\pm$ 0,9	12,1 $\pm$ 0,3	29 $\pm$ 0,7	16,9 $\pm$ 2,3	13,5 $\pm$ 0,2
	Sr	110,3 $\pm$ 18,6	45,6 $\pm$ 0,9	74,4 $\pm$ 3,3	96,1 $\pm$ 20,6	48,8 $\pm$ 4,1	97,9 $\pm$ 20,4	61,3 $\pm$ 0,9	50,4 $\pm$ 0,6	69,8 $\pm$ 1,2	61,2 $\pm$ 3,6	62,5 $\pm$ 1,3	73,5 $\pm$ 1,7
	Mn	100,6 $\pm$ 6,9	61,7 $\pm$ 4,3	45,6 $\pm$ 2,9	115,1 $\pm$ 3,7	71,1 $\pm$ 12,9	39,9 $\pm$ 0,2	111,4 $\pm$ 9,2	83,9 $\pm$ 5,8	49,6 $\pm$ 2,7	103,9 $\pm$ 3,6	62,2 $\pm$ 10	52,7 $\pm$ 3,3

	Ni	15,1±2,1	7,8±0,9	3,8±0,08	15,7±0,8	9,6±2,2	4,3±0,06	18,7±1,3	93,4±61,8	8,3±0,9	15,8±0,7	10,4±1,6	9,5±1,1
	Cr	29,3±3,8	15±3,3	3,6±0,1	26,5±1,9	16,5±7	3,5±0,03	29,9±3,2	157,9±105	4,8±0,3	29,7±0,2	11,7±3,5	6,1±0,4
	Be	1±0,1	0,6±0,04	0,6±0,2	0,9±0,06	0,6±0,2	1,4±0,06	1,2±0,07	0,8±0,03	0,7±0,1	1,2±0,08	0,8±0,09	1,4±0,4
	U	3,3±0,6	1,2±0,07	0,4±0,02	1,9±0,1	1,4±0,2	0,4±0,01	2,2±0,2	1,4±0,1	0,4±0,01	1,8±0,1	0,8±0,09	0,5±0,03
	Ba	246±7	236,7±5	234,7±7	230,4±8,8	223,5±24,6	245,3±7,8	255,7±2	252,2±6,3	226,7±12,5	251,1±4,7	244,7±6,8	238,8±13
	Co	4,6±0,7	2,7±0,4	0,6±0,02	4,3±0,3	3±1,1	0,6±0,03	4,9±0,4	4,9±0,9	0,8±0,05	4,6±0,1	2±0,6	0,9±0,05
	Cu	28,6±6,7	8±1,9	1,6±0,2	19,6±1,4	11,2±5,4	1,8±0,3	32,9±0,5	20,5±4,3	2,4±0,4	37,8±5,3	10,2±3,1	3,7±0,3
	Zn	82,3±21,9	26,5±7,5	3,1±0,8	63,9±8,5	25,4±9,6	4,6±0,3	95,6±5	41,7±3,8	7,9±1,9	109,3±19,5	20,6±6,4	9,5±0,8
	As	13,8±2,9	4,7±0,9	1,7±0,1	12,2±1,9	7,3±1,3	2,3±0,2	12,9±0,6	7,9±0,8	1,6±0,2	11,3±1,3	4,5±1,3	0,9±0,2
	Pb	25,4±3,9	14,7±1	12,2±0,4	22,1±1,8	14,1±2,4	12,9±0,4	27,3±0,9	17,9±0,6	12,4±0,6	29,3±3,3	14,9±0,9	13,1±0,6
	Hg	0,3±0,07	0,3±0,2	0,03±0,0007	0,3±0,05	0,06±0,01	0,03±0,006	0,3±0,05	0,1±0,003	0,02±0,004	0,3±0,06	0,04±0,01	0,05±0,002
Instant variables	Temp	15.3 ± 0.1	11.1 ± 0.2	15.3 ± 0.1	28.5 ± 0.5	24.4 ± 0.2	23.9 ± 0.1	13.5 ± 0.2	16.8 ± 0.2	16.8 ± 0.2	23.8 ± 0.9	23.6 ± 0.1	20.7 ± 0.2
	Sal	31.9 ± 0.9	30.6 ± 0.7	31.8 ± 0.9	36.5 ± 0.3	17.7 ± 0.1	16.4 ± 0.04	15.9 ± 0.05	14.7 ± 0.05	14.7 ± 0.5	15 ± 0.5	14 ± 1.5	15.3 ± 0.3
	O2	9.2 ± 0.1	14.5 ± 2.5	9.2 ± 0.1	8.3 ± 1.3	9.5 ± 0.4	12.1 ± 0.3	9.6 ± 0.4	17.9 ± 0.4	13.9 ± 0.3	5.3 ± 0.6	8.8 ± 0.4	8.6 ± 0.2
	pH	7.9 ± 0.01	7.9 ± 0.05	7.9 ± 0.01	8.1 ± 0.1	7.8 ± 0.02	7.9 ± 0.04	8.3 ± 0.3	8.6 ± 0.3	8.9 ± 0.04	7.8 ± 0.1	8.1 ± 0.1	8.3 ± 0.02

**Table A.3.** Results for a two-way factorial ANOVA of isotopic and diversity metrics, calculated for each community sampled at three sites (Navigator, Gambia and Tróia) of Sado Estuary, along 4 seasons (win19, sum20, win20 and sum21). ANOVA test and Tukey's post-hoc multiple comparisons were performed considering the significance levels of  $p<0.05$  (\*) and  $p<0.001$  (\*\*).

Metrics	Source of variation	Df	Sum Sq	Mean Sq	F value	Pr(>F)	Tukey's post-hoc
<b>CR</b>							
	sites	2	22.98	11.492	2.156	0.197	
	seasons	3	17.34	5.779	1.084	0.425	
	residual	6	31.98	5.330			
<b>NR</b>							
	sites	2	4.625	2.312	1.073	0.400	
	seasons	3	1.620	0.540	0.250	0.858	
	residual	6	12.935	2.156			
<b>TA</b>							
	sites	2	485.4	242.7	1.277	0.345	
	seasons	3	775.4	258.5	1.360	0.341	
	residual	6	1140.0	190.0			
<b>Max.TP</b>							
	sites	2	1.857	0.9284	6.110	0.0357*	Troia > Navigator*

	seasons	3	3.750	1.2500	8.226	0.0151*	win19> sum 20*
	residual	6	0.912	0.1520			win19> sum21*
Iric							
	sites	2	0.03762	0.018811	1.572	0.283	
	seasons	3	0.01236	0.004121	0.344	0.795	
	residual	6	0.07180	0.011967			
Idiv							
	sites	2	0.007525	0.003763	1.910	0.228	
	seasons	3	0.001897	0.000632	0.321	0.810	
	residual	6	0.011819	0.001970			
IDis							
	sites	2	0.03484	0.017420	5.617	0.0422*	Troia > Gambia*
	seasons	3	0.01298	0.004327	1.395	0.3324	
	residual	6	0.01861	0.003101			
IEve							
	sites	2	0.003309	0.001655	0.549	0.604	
	seasons	3	0.006348	0.002116	0.701	0.585	
	residual	6	0.018100	0.003017			

IUnic						
	sites	2	0.03031	0.01515	1.736	0.254
	seasons	3	0.08387	0.02796	3.202	0.105
	residual	6	0.05238	0.00873		
car_perc						
	sites	2	41.9	20.94	0.092	0.914
	seasons	3	386.4	128.79	0.565	0.658
	residual	6	1368.5	228.09		
omniv_car						
	sites	2	999.2	499.6	11.06	0.00971 ** Tróia > Gambia* Tróia > Navigato*
	seasons	3	1761.2	587.1	13.00	0.00492 ** win20 > sum20* win 19 > win20**
	residual	6	271.0	45.2		



**CHAPTER 5 - SPATIAL AND TEMPORAL DISTRIBUTION PATTERNS OF THE  
ESTUARINE NEMATODE ASSEMBLAGES AND THEIR RELATIONSHIP WITH  
BENTHIC BACTERIA COMMUNITIES**

*In revision* Estuaries and Coasts 2025

## 5.1 Abstract

Benthic nematodes and bacteria are highly sensitive to habitat conditions being valuable ecological indicators. Previous studies have shown that nematode assemblages are more sensitive to site-specific conditions than benthic bacterial communities, highlighting the spatial diversity of the distribution patterns for both communities. Still, the effect of the temporal changes on the communities' composition distribution patterns in the sediment habitat conditions remains unknown, which raised the following scientific question: How do temporal changes in sediment habitat conditions influence the composition and distribution patterns of both communities? This study compares the spatial and temporal distribution patterns of nematode and bacteria communities, based on communities' diversity and abundance at three different sites in Sado estuary, through four sampling occasions. We hypothesize that: (1) the nematode assemblages present different distribution patterns between sites and across sampling occasions; and (2) both communities are affected differently to site-specific conditions. Two-factor PERMANOVA test ("site" and "sampling occasion") revealed significant variability ( $p<0.05$ ) on nematode assemblages composition caused by specific sediment conditions. The responses of both communities were partially similar, strongly influenced by the spatial variability conditions, although nematode assemblages were more sensitive to the temporal variability of each site than bacterial communities. Temporal distribution patterns observed in nematode assemblages suggests they are more susceptible to short-term environmental changes, making them potential ecological indicators of fast shifts. The complementary responses of nematode and bacterial communities could be exploited on the framework of environmental monitoring.

**Keywords:** Spatial and temporal patterns, nematode assemblages, bacterial community, benthic responses.

## 5.2 Introduction

Estuarine sediments sustain life for a myriad of organisms, where the environmental heterogeneity occurs at several scales influencing their diversity and distribution patterns (Moens & Benniger, 2018). In these environments, the magnitude and direction of the ecological responses are difficult to predict since a multitude of factors interact simultaneously shaping the benthic communities (Steyaert et al., 2003; Schratzberger & Ingels, 2018).

Benthic communities are highly sensitive to habitat conditions (Ruaró et al., 2016; Branco et al., 2018, Ridall & Ingels, 2021) highlighting their ability as valuable ecological indicators (Giere, 2009; Ridall & Ingels, 2021). As example, several meiofauna organisms, such as nematodes, have been used to evaluate the integrity of the aquatic ecosystems (Semprucci & Balsamo, 2014; Zeppilli et al., 2015; Branco et al., 2018; Haegerbaeumer et al. 2019). Nematodes are considered the most abundant group, widely distributed, and respond rapidly to environmental changes (Giere 2009). In parallel, with the advances in environmental genomics, benthic microorganisms are also becoming valuable bioindicators in routine monitoring (Sagová-Marecková et al., 2021), highlighting the importance of their functional and metabolic pathways in the regulation of the trophic state of the sediment and their sensitivity to metal pollution (Pawlowski et al., 2018; Vieira et al., 2023; Vieira et al., 2025). Both nematodes and bacteria have been proven to play important roles in efficiency ecosystem processes that occur in sediments (Nascimento et al., 2012; Bonaglia et al., 2014),, with direct implications for ecosystem health (Schratzberger & Ingels, 2018). Nevertheless, the exact contribution of these organisms remains unclear due to their multiple and complex interactions in response to different environment conditions (Schratzberger & Ingels, 2018). The effect of spatial changes of the sediment habitat conditions on the composition and diversity of bacteria and nematode communities, has been studied in Sado estuary on the SW coast of Portugal (Vieira et al., 2023). Vieira and colleagues (2023) showed the spatial distribution of both communities were mainly driven by the sediment organic matter (OM) in different magnitudes. Nematode assemblages revealed to be more sensitive to site-specific conditions than benthic bacterial communities.

Another study focused solely on the effect of spatial and temporal changes in sediment conditions on the composition of benthic bacterial communities and showed that the communities respond strictly to the spatial variability of the sediment (Vieira et al., 2025). The lack of significant temporal changes in the communities' distribution patterns was consistent with the strong influence of stochastic events, coupled with the

functional redundancy that characterizes microbial communities on muddy sediments (Moens & Benniger, 2018).

Given the lack of temporal variability in the bacterial communities and the high sensitivity of the nematodes to site-specific conditions, it remains uncertain whether these effects maintain over time in the distribution patterns of nematode assemblages, raising the following scientific question: How do temporal changes in sediment habitat conditions influence the composition and distribution patterns of both communities? The present study aims mainly the comparison of the spatial-temporal distribution patterns of both nematode and bacteria communities based on their diversity and abundance in three different sites of Sado estuary during four sampling occasions. We hypothesize that: (H1) the nematode and bacterial communities present different distribution patterns between sites and across sampling occasions; and (H2) both communities are affected differently to site-specific conditions.

### 5.3 Material and Methods

#### 5.3.1 Study area and sampling design

The Sado estuary, which covers a vast area of 240 km<sup>2</sup>, is the second largest estuarine system in Portugal, is regarded as one of Europe's most important wetlands (Bettencourt et al., 2004) (Fig. 1). Around 30% of this area is composed of salt marshes and intertidal flats with an important ecological value by accommodating "Estuário do Sado Nature Reserve" (Caeiro et al., 2005). Sado estuary is a semi-diurnal mesotidal system and during spring and neap tides have a tidal amplitude varying between 0.6 m and 1.6 m. This estuary is influenced by Sado river flow (annual mean of 40m<sup>3</sup>s<sup>-1</sup>) (Bettencourt et al., 2004) and by different weather conditions (seasonal and inter-annual events). Temperature can vary between 10 and 26°C and salinity ranges between 0.75 at upstream to 35.34 at downstream (Sroczyńska et al., 2021). On the basis of the heterogeneity and typology of this estuarine ecosystem, the sampling sites were selected based on different biogeochemical and trophic conditions of the sediments, the hydrodynamic activity of the estuary (high/low water residence time), salinity gradient (mesohaline area), all influenced of nearby anthropogenic activities (Caeiro et al., 2005; Kennedy et al., 2005; Sroczyńska et al., 2021). Take into account these criteria the selected sampling sites were: 1) Navigator, surrounded by industrial activities, where sediment is mainly muddy with silty-fine sediments with high organic contents (Caeiro et al., 2005); 2) Gambia located inside the "Estuário do Sado Natural Reserve" surrounded by oysters farming and other aquaculture activities with the grain size were dominated by high proportion of clay-fine sediments (Vieira et al., 2022); and 3) Tróia located at the

mouth is characterized by high water exchange rate and sediments with high proportion of sand (Sroczyńska et al., 2021b), (Fig.1).

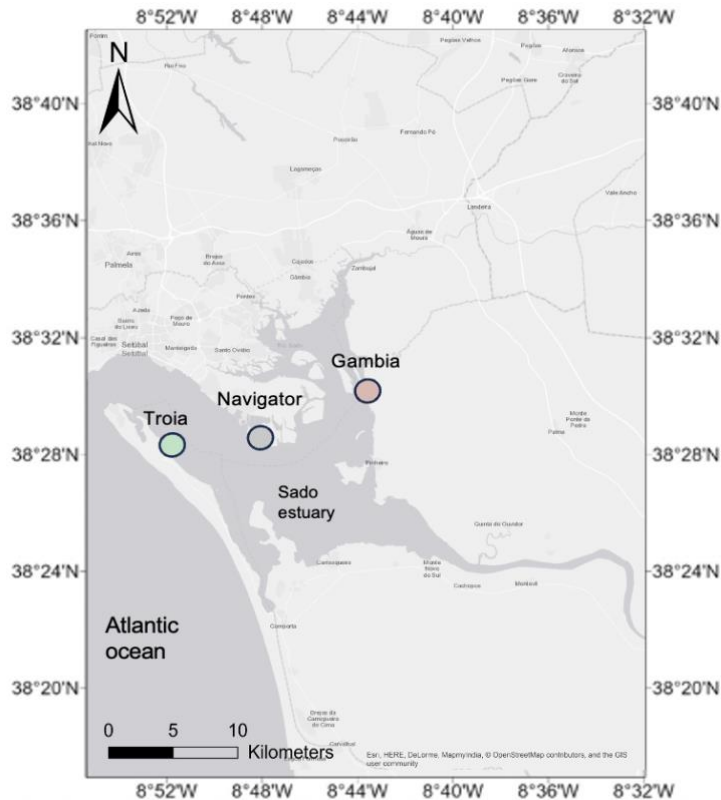


**Figure 1.** Sado estuary located at southwest of Portugal ( $38^{\circ} 31' 14''$  N,  $8^{\circ} 53' 32''$  W). The selected sampling sites: Navigator ( $38.486502$ ,  $-8.795191$ ) (grey circle), highly industrialized area; Gambia ( $38.537263$ ,  $-8.742584$ ) (orange circle) with high organic inputs from aquacultures; Tróia ( $38.461421$ ,  $-8.857838$ ) located at mouth of estuary (adapted from Vieira et al., 2024a).

To assess the density and diversity of the spatial and temporal distribution patterns of the nematode assemblages, the sampling strategy applied was: at each sampling “site” three sampling stations were selected, and at each station three sediment replicates were randomly collected, during four “sampling occasions” ( $n=27$ ), namely, winter 2019 (November and December), summer 2020 (June and July), winter 2020 (December 2020 and February 2021) and summer 2021, (May and June 2021). For the sediment biogeochemistry analysis, the sediment was collected at each station ( $n=9$ ). Simultaneously, the instantaneous parameters of the water were measured (salinity, temperature, pH and dissolved oxygen) using a VWR pHenomenal ® MU 600 H.

### 5.3.2 Sampling and sample treatment

#### 5.3.2.1 Sediment physical-chemical processing

The environmental data was retrieved from two studies (Vieira et al., 2024 and 2025). The variables considered were: Total Organic Matter (OM), sediment grain size, Calcium Carbonate ( $\text{CaCO}_3$ ), elemental analysis of the Total Carbon (CT) and Total Nitrogen (NT). The sediment chlorophyll a (chl<sub>a</sub>) and phaeopigments (phaeo) were used to calculate the chl<sub>a</sub> and phaeo ratio (chl<sub>a</sub>\_phaeo), which represents an indicator of the freshness and quality of phytodetrital organic (Ingels et al., 2009). Thirteen elements (Li, Sr, Mn, Ni, Cr, Be, U, Ba, Co, Cu, Zn, As and Pb) were quantified following Neves et al., (2025).

#### 5.3.2.2 Nematode assemblages

Nematode samples were collected by forcing a hand core (3.8 cm inner diameter) to a depth of 3 cm into sediment, and each sample was fixed using 4% buffered formalin (itwreagents, Spain). The samples were initially rinsed using a sieve with a mesh size of 1000  $\mu\text{m}$  and then a sieve with a mesh size of 38  $\mu\text{m}$ . The remaining fraction was washed and centrifuged three times, using colloidal silica polymer LUDOX HS-40 at (specific gravity 1.18  $\text{g cm}^{-3}$ ), which allowed separate nematodes from sediment (Heip et al., 1985). To calculate the relative density of each sample, nematodes were counted under a stereomicroscope (stereomicroscope Leica M205 (100x magnification). Then a set of 120 nematodes were randomly picked from each replicate and fixed in slides according to Vincx (1996). Taxonomic identification was made until genera (Olympus BX50 light microscope and cell software D Olympus, Japan), which is considered an accurate resolution to assess the density and diversity patterns of nematode communities (Warwick et al. 1990; Moreno et al. 2008). To support the identification, a Pictorial Keys was used (Warwick et al., 1998; Platt and Warwick, 1988), and online identification keys/literature available in the Nemys eds (2024).

### 5.3.3 Data analysis

#### 5.3.3.1 Environmental variables

Spatial-temporal and distribution patterns of the environmental variables were obtained from previous work (Vieira et al., 2024 and 2025). Principal Component Analysis (PCA) was performed to explore the multidimensional patterns of the environmental data. The variables were chlorophyll a (chl<sub>a</sub>), phaeopigments (phaeo), chl<sub>a</sub> and phaeo ratio (chl<sub>a</sub>\_phaeo), temperature (Temp), salinity (Sal), oxygen dissolved

(O<sub>2</sub>) and all metals, in exception of the pH, were log10 transformed. The other variables, such as clay, sand, gravel, OM, CT, NT, and CaCO<sub>3</sub>, were expressed as % and transformed using arcsine square root transformation. PCA analysis was performed using the function "fviz pca\_biplot" from R package "FactoMineR" (Lê et al., 2008). The variables that presented low variability contribution to the PCA axes and high correlation within each other, were removed from the analysis. The significance of the PCA was tested with PCA test R package "PCATest" (Camargo et al., 2022) applying the following conditions: the number of random permutations was 1000; the number of bootstrap replicates to build 95% confidence intervals of the observed statistics was 1000; and 0.05 as alpha level for statistical significance.

#### 5.3.3.2 *Nematode communities: density and diversity*

Principal Coordinates Analysis (PCoA) was performed to explore the spatial and temporal distribution patterns of the nematode assemblages using R packages phyloseq (version 1.42.0) (McMurdie and Holmes, 2013) and microVIZ (0.11.0) (Barnett et al., 2021). To analyze the relative contribution of each taxon for the (dis)similarities between "site" and across "sampling occasion", the SIMPER two-way crossover similarity percentage analysis (90% cut-off percentage) was calculated based on Bray Curtis method.

Nematode communities' diversity and richness were calculated using PRIMER v6 software package (Clarke & Warwick, 2001). The following metrics were determined: Margalef's richness Index (d) (Margalef, 1958), Pielou's evenness (J'), Shannon Wiener diversity (H0) (Shannon & Weaver, 1963) and Simpson (1-λ). The index of trophic diversity (ITD) (Heip et al., 1985) was calculated based on the trophic composition of the communities and expressed by the reciprocal index (ITD-1). To assess the trophic composition of the communities, nematode genus was assigned to a feeding type classification based on mouth morphology as developed by Wieser (1956), namely selective (1A) and non-selective (1B) deposit feeders, epigrowth feeders (2A) and omnivores/predators (2B). The Maturity index (MI) is based on the life strategy that classifies each nematode genus to a colonizer/persister scale (c-p scale), varying from 2 (colonizers) to 5 (persisters) (Bongers et al., 1991; Bongers et al., 1999). Permutational analysis of variance (PERMANOVA) based on a two-factor design was carried out to assess spatial and temporal patterns in nematode assemblages using the PRIMER v6 software package (Clarke & Warwick, 2001) and the PERMANOVA add-on package (Anderson et al., 2008). The two-factor design was comprised by the factor "site" ("Navigator"; "Gambia" and "Tróia", 3 levels, fixed) and the "sampling occasion" factor

("winter 2019", "summer 2020"; "winter 2020" and "summer 2021", 4 levels, random). This multivariate approach was performed for all data density, diversity and functional descriptors to detect significant differences ( $p < 0.05$ ) in the composition of the assemblages between "site" and across "sampling occasion". Data dispersions were checked with PERMDISP and nematode density data were square-root transformed. Redundancy analysis (RDA) was performed, using R packages "vegan" (version 2.6-4) and "QsRutils" (version 0.1.5), in order to detect the main environmental factors responsible for the distribution patterns of the biological data. This statistical analysis allowed to modulate the effect of explanatory matrices (environmental variables) on a response matrix (nematode communities) and select the variables that better explained the variations and their patterns. Before analyses, the response dataset (relative density of each genus) was Hellinger-transformed, and all constrained variables were standardized. Then it was checked for correlations between variables using the Spearman correlation test and selected the variables less correlated to each other (such as Cu, Zn, As and Pb) and further fit in the initial RDA model. To simplify and improve the model, variables were selected using the "ordiR2step()" function, then RDA plot was performed with microVIZ (0.11.0) R packages (Barnett et al., 2021; R Core Team. 2022).

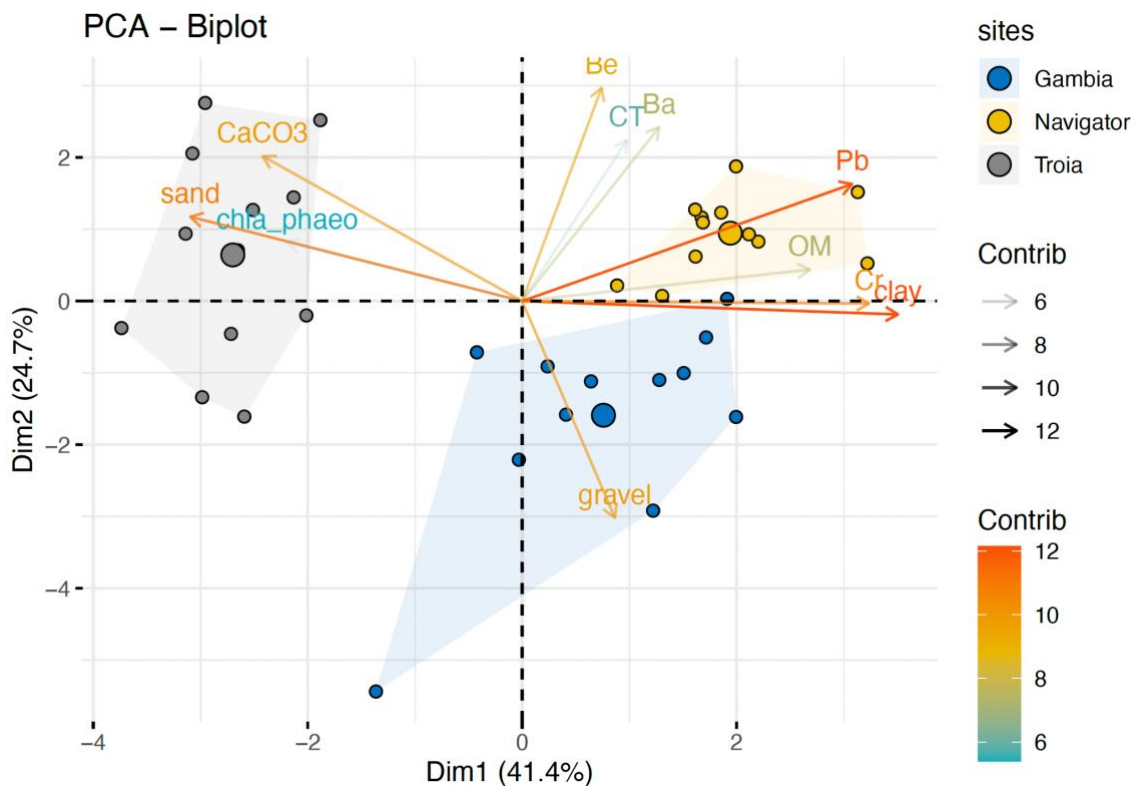
## 5.4 Results

### 5.4.1 Environmental variables

The raw data of the measured environmental variables are summarized in Table 1 (supplementary data) and the spatial-temporal distribution patterns analysis was performed Vieira et al., (2025). Sediment characteristics are clearly different at sampling sites. At Navigator, sediment was predominantly muddy, with clay content and higher contents of OM and heavy metals. While in Gambia, sediments showed highest proportion of gravel and OM contents. At Tróia site sediment characteristics exhibited clear differences, with the sediment predominantly composed of sand and  $\text{CaCO}_3$  and the lowest proportions of clay and OM. The sediment pigment concentrations of chla and phaeo were highest in the Gambia sediments during the summer of 2020, although Tróia sediments consistently show the higher chla\_phaeo ratio across all sampling occasions, indicating higher primary production and organic matter quality. The lowest concentrations of  $\text{O}_2$  water dissolved were also obtained in Navigator and Gambia sites, the highest concentrations were obtained in Tróia sampling site. PCA analysis revealed clear differences in sediment composition between sites (Figure 2, adapted from Vieira et al., 2025).

The PCA first two axes explained 65.8% of the total variation observed (Fig. 2). According to PCAtest, the first accounted for 41.4% (95%-CI:36.9–50.6) and second accounted for 24.7% (95%-CI:43–56.9). The variables clay, sand, OM, CaCO<sub>3</sub>, and chla\_phaeo presented highest contribution for the variation in the first axis, while the gravel and CT contributed to the high variability of the second axis. Navigator sampling site sediments were mostly characterized by clay, OM and Pb, though gravel was associated with Gambia sampling site sediments. Tróia sampling site sediments the high contribution for variability were explained by sand and CaCO<sub>3</sub>.

**Figure 2.** Principal component analysis (PCA) biplot based on scaled environmental and biogeochemical variables measured in sediment samples from 3 sampling sites in Sado estuary during 4 distinct sampling occasions, colored by estuary “confidence” convex type. Variable’s vectors are presented based on their contributions to the principal components (gradient colors and transparency of vectors varying between 6 and 12 is result of cos2 index that classify the



variable vectors by their quality and contribution (“contrib”), with grey representing high contributions, yellow intermediate and blue representing very low contributions. The dots represent the cluster centroids for group variables, adapted from Vieira et al., (2025).

#### 5.4.2 Nematode assemblages: density, structural and functional diversity

The mean relative densities of each taxon in the 3 sampling sites and across the 4 occasions are summarized in Table 2, supplementary data. The overall density of nematode communities varied between 345 and 8960 individuals per 10 cm<sup>-2</sup>. The highest mean values were obtained at Gambia in the sampling occasion winter 2019 (4951 ± 1233, ind. 10 cm<sup>-2</sup>), although the lowest mean values were registered at Tróia

sampling site in summer 2020 ( $735 \pm 70$ , ind.  $10 \text{ cm}^{-2}$ ). The results of two-factor PERMANOVA test for the nematode density showed significant interaction effects between the factors “site” and “sampling occasion” ( $p\text{-value} < 0.05$ ) (Table 1). Moreover, Pairwise comparisons presented significant differences ( $p\text{-value} < 0.05$ ) between most pairs of levels. This can be explained by factor “site” effect on nematode assemblages densities suggesting temporal variability at each sampling site.

**Table 1:** Two-way PERMANOVA test, between "Sites" (3 level fixed) and across "sampling occasion" (4 level, random) for all analyzed variables, (nematode Density, Diversity and Richness metrics (N) number of individuals, (S)number of Taxa, (d) Margalef, (J') Pielou's evenness, (H') Shannon, Simpson and ecological strategies metrics: Trophic composition, (ITD-1) Trophic diversity index and (MI) Maturity index. Bold values highlight significant effects and interactions ( $p < 0.05$ ). Monte Carlo test P(MC) set for 9000 permutations, ( $p < 0.05$ (\*),  $p < 0.001$ (\*\*)) and  $p < 0.001$ (\*\*\*)).

Density		df	SS	MS	Pseudo-F	P(perm)	Uniq perms	P(MC)
	site	2	1.12E+05	56198	18.976	<b>0.0002</b>	9897	<b>0.0001</b>
	sampling occasion	3	13955	4651.7	4.1785	<b>0.0001</b>	9921	<b>0.0001</b>
	site x sampling occasion	6	17769	2961.5	2.6602	<b>0.0003</b>	9886	<b>0.0003</b>
	Residuals	96	1.07E+05	1113.2				
	Total	107	2.51E+05					
N (number of individuals)								
	site	2	14101	7050.5	6.0149	<b>0.0321</b>	9942	<b>0.0233</b>
	sampling occasion	3	897.89	299.3	2.2624	0.0757	9943	0.0749
	site x sampling occasion	6	7033.1	1172.2	8.8607	<b>0.0001</b>	9945	<b>0.0001</b>
	Residuals	96	12700	132.29				
	Total	107	34732					
S (Number of taxa)								
	site	2	1899.6	949.82	2.9703	0.0894	9928	0.1001
	sampling occasion	3	905.45	301.82	1.9551	0.1076	9950	0.1121

	site x sampling occasion	6	1918.6	319.77	2.0714	<b>0.0474</b>	9943	<b>0.0508</b>
	Residuals	96	14820	154.38				
	Total	107	19544					
<b>d (Margalef)</b>								
	site	2	4894.2	2447.1	13.247	<b>0.0036</b>	9934	<b>0.0023</b>
	sampling occasion	3	771.91	257.3	1.7337	0.1533	9946	0.1498
	site x sampling occasion	6	1108.3	184.72	1.2446	0.2735	9924	0.2761
	Residuals	96	14248	148.41				
	Total	107	21022					
<b>J' (Pielou's evenness)</b>								
	site	2	2.05E-03	1.03E-03	2.0129	0.2073	9948	0.2144
	sampling occasion	3	1.79E-03	5.96E-04	1.3941	0.2374	9954	0.2458
	site x sampling occasion	6	3.06E-03	5.10E-04	1.194	0.3082	9929	0.3077
	Residuals	96	4.10E-02	4.27E-04				
	Total	107	4.79E-02					
<b>H' (Shannon )</b>								

	site	2	8.45E-02	4.23E-02	2.9177	0.1325	9937	0.1327
	sampling occasion	3	5.45E-02	1.82E-02	2.1544	0.096	9951	0.0965
	Site x sampling occasion	6	8.69E-02	1.45E-02	1.7169	0.1208	9947	0.1265
	Residuals	96	0.81011	8.44E-03				
	Total	107	1.0361					
<b>1-λ (Simpson)</b>								
	site	2	5.45E-03	2.73E-03	3.3286	0.1032	9950	0.1038
	sampling occasion	3	4.59E-03	1.53E-03	1.8637	0.1072	9947	0.143
	site x sampling occasion	6	4.91E-03	8.19E-04	0.99736	0.4481	9939	0.4236
	Residuals	96	7.88E-02	8.21E-04				
	Total	107	9.38E-02					
<b>Trophic composition</b>								
	site	2	31700	15850	16.788	<b>0.004</b>	9927	<b>0.0001</b>
	sampling occasion	3	2087.2	695.72	2.8725	<b>0.008</b>	9926	<b>0.0091</b>

ITD-1	site x sampling occasion	6	5664.8	944.14	3.8981	<b>0.0001</b>	9930	<b>0.0001</b>
	Residuals	96	23252	242.2				
	Total	107	62703					
MI	site	2	0.21625	0.1081 2	3.5238	0.1063	9943	0.0989
	sampling occasion	3	0.16959	5.65E- 02	2.08E+00	0.109	9949	0.1078
	site x sampling occasion	6	0.1841	3.07E- 02	1.13E+00	0.349	9942	0.3511
	Residuals	96	2.6048	2.71E- 02				
	Total	107	3.1747					
MI	site	2	3.18E-03	1.59E- 03	0.86961	0.429	9692	0.4621
	sampling occasion	3	3.76E-02	1.25E- 02	10.118	<b>0.0001</b>	9943	<b>0.0001</b>
	site x sampling occasion	6	1.10E-02	1.83E- 03	1.4747	0.1959	9939	0.1994
	Residuals	96	0.11892	1.24E- 03				

	Total	107	0.17066					
--	-------	-----	---------	--	--	--	--	--

Overall, 114 nematodes genera belonging to 30 families were identified across all sampling occasions. Most genera belonged to the orders Chromadorida (22 – 64%), Monhysterida (6 - 37%) and Enoplida (6 - 24%), the dominant families were Desmodoridae (12 – 60 %), Linhomoeidae (1 - 35%) and Anoplostomatidae (3 - 14%), respectively. The top 10 most abundant genera together comprised nearly 80% of the total relative density of the assemblages and they are represented in the Figure 3 and in Table 2, supplementary data.

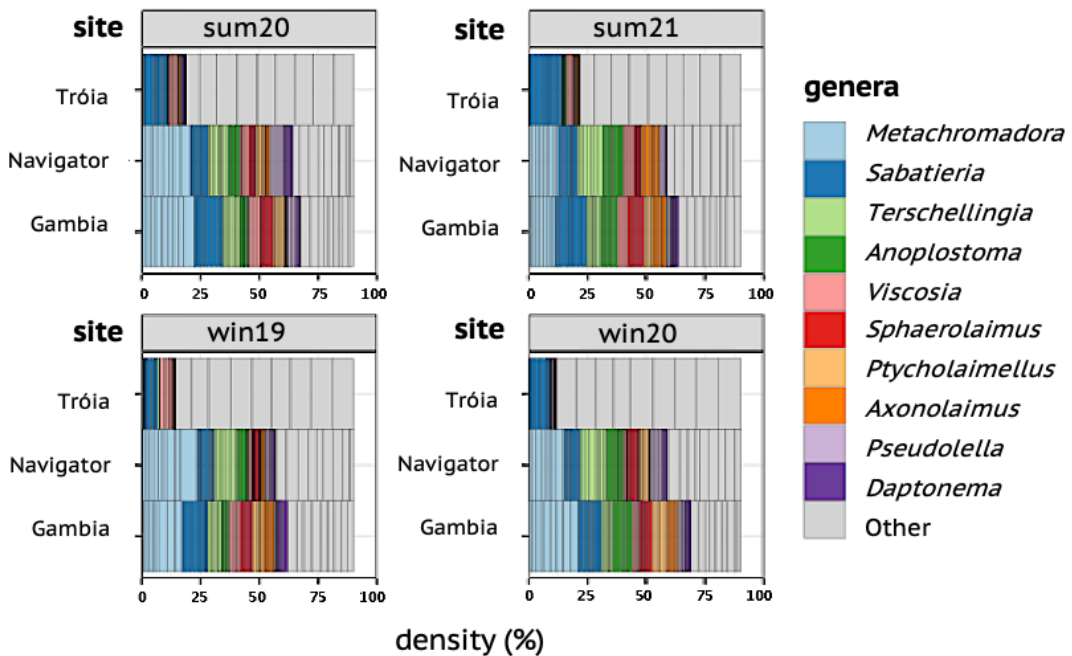


**Figure 3.** Bar plot displays the relative density (%) of the top 10 most abundant nematodes genera in each sampling site Gambia, Navigator and Tróia, across all sampling occasions (win19, sum20, win20 and sum21). The other relative frequencies are collapsed into the “Others” category.

Across all sampling occasions, Navigator communities were composed by approximately 39 genera belonging to 17 families, with *Metachromadora* (38%), *Terschellingia* (17%), *Sabatieria* (8%), and *Anoplostoma* (8%) being the most abundant taxa. In Gambia communities, there were approximately 33 genera belonging to 13 families, with *Metachromadora* (39%), *Sabatieria* (19%), *Anoplostoma* (6%), and *Terschellingia* (5%) being the most representative taxa. The nematode communities sampled in Tróia were composed by approximately, 77 genera belonging to 25 families, in which the most abundant were *Sabatieria* (20%), *Monoposthia* (16%), *Desmodora* (12%) and *Trefusia* (11%), (Figure 3).

**Table 2:** Mean $\pm$ SE n=9, of the diversity descriptors in 3 sites (Navigator, Gâmbia and Tróia), during 4 sampling occasions (winter 19, summer 20, winter 20 and summer 21): Diversity and Richness metrics (N) number of individuals, (S)number of Taxa, (d) Margalef, (J') Pielou's evenness, (H') Shannon, Simpson and ecological strategies metrics: Trophic composition, (ITD-1) Trophic diversity index and (MI) Maturity index.

Site	Sampling occasion	S (number of taxa)	N (number of individuals)	d (Margalef)	J' (Pielou's evenness)	H' (Shannon)	1- $\lambda$ (Simpson)	ITD-1	MI
Navigator	winter 2019	14 $\pm$ 1.8	176 $\pm$ 27.8	2.6 $\pm$ 0.4	0.9 $\pm$ 0.04	2.3 $\pm$ 0.2	0.9 $\pm$ 0.06	2.5 $\pm$ 0.3	2.3 $\pm$ 0.05
	summer 2020	15.5 $\pm$ 1.6	195 $\pm$ 18.4	2.7 $\pm$ 0.3	0.9 $\pm$ 0.01	2.5 $\pm$ 0.1	0.9 $\pm$ 0.02	2.4 $\pm$ 0.2	2.2 $\pm$ 0.04
	winter 2020	15.3 $\pm$ 1.5	172 $\pm$ 17.3	2.8 $\pm$ 0.3	0.9 $\pm$ 0.01	2.5 $\pm$ 0.1	0.9 $\pm$ 0.02	2.9 $\pm$ 0.3	2.4 $\pm$ 0.06
	Summer 2021	16.4 $\pm$ 1.2	233 $\pm$ 13.6	2.8 $\pm$ 0.2	0.9 $\pm$ 0.005	2.6 $\pm$ 0.06	0.9 $\pm$ 0.005	2.8 $\pm$ 0.1	2.4 $\pm$ 0.06
Gambia	winter 2019	15.4 $\pm$ 1.2	207 $\pm$ 24.2	2.7 $\pm$ 0.2	0.9 $\pm$ 0.01	2.5 $\pm$ 0.09	0.9 $\pm$ 0.01	2.5 $\pm$ 0.3	2.3 $\pm$ 0.06
	summer 2020	13.1 $\pm$ 1.3	142 $\pm$ 13.5	2.4 $\pm$ 0.3	0.9 $\pm$ 0.01	2.3 $\pm$ 0.1	0.8 $\pm$ 0.02	2.3 $\pm$ 0.2	2.2 $\pm$ 0.05
	winter 2020	14.6 $\pm$ 1	199 $\pm$ 11.6	2.6 $\pm$ 0.2	0.9 $\pm$ 0.01	2.5 $\pm$ 0.1	0.9 $\pm$ 0.01	2.4 $\pm$ 0.2	2.2 $\pm$ 0.04
	Summer 2021	16.5 $\pm$ 1	185 $\pm$ 13.6	2.9 $\pm$ 0.2	0.9 $\pm$ 0.007	2.6 $\pm$ 0.07	0.9 $\pm$ 0.007	2.8 $\pm$ 0.2	2.4 $\pm$ 0.06
Tróia	winter 2019	15.7 $\pm$ 2.8	90 $\pm$ 11.5	3.2 $\pm$ 0.5	0.9 $\pm$ 0.009	2.5 $\pm$ 0.2	0.9 $\pm$ 0.02	2 $\pm$ 0.2	2.7 $\pm$ 0.1
	summer 2020	22.8 $\pm$ 2.3	165 $\pm$ 13.6	4.3 $\pm$ 0.4	0.9 $\pm$ 0.01	2.9 $\pm$ 0.1	0.9 $\pm$ 0.01	2.5 $\pm$ 0.2	2.7 $\pm$ 0.1
	winter 2020	17.1 $\pm$ 1.9	101 $\pm$ 9.2	3.5 $\pm$ 0.4	0.9 $\pm$ 0.01	2.6 $\pm$ 0.1	0.9 $\pm$ 0.02	2.1 $\pm$ 0.2	2.6 $\pm$ 0.1
	Summer 2021	19 $\pm$ 2	97.6 $\pm$ 10.4	4 $\pm$ 0.4	0.9 $\pm$ 0.01	2.7 $\pm$ 0.1	0.9 $\pm$ 0.01	2.4 $\pm$ 0.2	2.6 $\pm$ 0.1

Diversity and richness of nematode assemblages, based on the S, d, J', H' and 1- $\lambda$  indices, were highest at the Tróia site in summer 2020, while the lower diversity and richness were obtained in the Navigator and Gambia assemblages in winter 2019 and summer 2020, respectively (Table 2). The Margalef's richness index (d), along with the number of individuals (N) and the number of taxa (S), revealed significant differences between the factors ("site" and "sampling occasion",  $p < 0.05$ ) (Table 1). In contrast, the structural diversity of nematode assemblages based on Shannon-Wiener (H') and Simpson (1- $\lambda$ ) indices, showed no significant differences across all factors and their interactions ( $p < 0.05$ ) (Table 1).

The significant differences of Margalef's Richness Index (d) were detected between "site" ( $p=0.003$ ) (Table 1). Pairwise comparisons revealed that the richness of Tróia assemblages differed significantly from that of Gambia and Navigator assemblages, being significantly higher between Navigator and Tróia assemblages ( $P$  Navigator vs Tróia = 0.004) and lower between Gambia and Tróia assemblages of ( $P$

Gambia vs Tróia = 0.05). Significant interaction effects between the factors “site” and “sampling occasion” were detected for the number of individuals (N) and number of Taxa (S) ((p= 0.0001 and 0.04, respectively, Table 1). Pairwise comparisons of the number of individuals (N) revealed significant variation across all interaction pairs, being significantly higher in summer 2021 for the Navigator assemblages and in summer 2020 for the Gambia and Tróia assemblages. While the pairwise comparisons for the number of taxa (S) showed the highest variability in Gambia and Troia assemblages in summer 2020.

The trophic composition of Troia's nematode assemblages was clearly distinct from those of Navigator and Gambia (Table 2, supplementary data). Navigator and Gambia assemblages were mainly composed by Predators/ omnivores (2B), while the predominance of non-selective deposit feeders (1B) was mostly detected in Gambia assemblages. On all occasions, selective deposit feeders (1A) were mostly present in Navigator assemblages, whereas epistratic feeders (2A) were predominant in Tróia assemblages. Supporting high variability in trophic composition, significant interaction effects were detected between “site” and “sampling occasion” (p=0.0001, Table 1). Pairwise comparisons presented significant variability (p-value < 0.05) in most pairs of levels of the factor “sampling occasion” within each “site”, being significantly higher in summer 2021 for the Navigator assemblages and in summer 2020 for the Gambia and Tróia assemblages. This was consistent with richness metrics S and N suggesting that the temporal variability affects the assemblages of each sampling site differently.

The functional diversity of nematode assemblages based on trophic diversity index (ITD<sup>-1</sup>) and Maturity Index (MI) ranged from 2.4±0.2 to 3.4±0.3 and from 2.2±0.04 to 2.7±0.1, respectively (Table 2). The trophic diversity index (ITD<sup>-1</sup>) was highest in winter 2020 and summer 2021 for the Navigator assemblages, while it was lowest in summer 2020 and winter 2020 for the Gambia assemblages. However, no significant differences were detected across all factors and their interactions (p>0.05, Table 1). These findings suggest that nematode communities might select specific feeding sources (e.g. bacteria and detritus) without significantly change overall trophic structure of the assemblages. The Maturity Index in summer 2020 was lowest in Navigator assemblages and highest in Tróia assemblages. Significant differences of MI between sampling occasions were detected (p=0.0001, Table 1). The individual pairwise comparisons of the factor “sampling occasion” highlighted the significant variability in summer 2021, revealing a distinct ecological condition for nematode assemblages to thrive in density and diversity.

#### 5.4.2 Spatial and temporal distribution patterns of nematode assemblages

The PCoA analysis based on the nematode relative densities revealed high variability in the first two PCoA axes (PCoA1 and PCoA2) accounting 51.2% of the total variation. The density spatial distribution pattern is evident, nematode assemblages of Tróia were clearly separated from the assemblages of Navigator and Gambia, along the first axis (PCoA1 45.2%) (Figure 4a). At sampling site Tróia the genus *Monoposphia* explain the dissimilarity obtained, though the genus *Metachromadora* contributed high degree of similarity of Navigator and Gambia assemblages, explained in the second axis (PCoA2, 6.03%). In contrast, density temporal distribution patterns of nematode assemblages registered low variability, without an evident interannual trend.

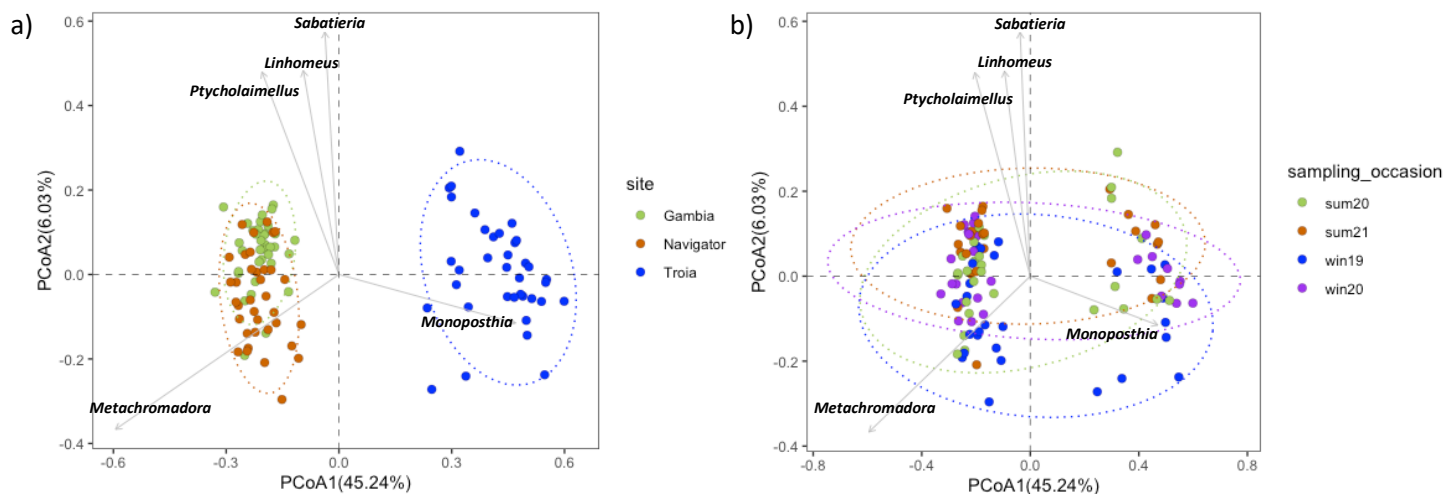


**Figure 4.** Principal component analysis (PCoA) plot based on Bray-Curtis dissimilarity, according to nematode relative density of all genera obtained for: **a)** “site” (Gambia, Navigator and Tróia) and **b)** “sampling occasions” (win19, sum20, win 20 and sum 21). The two first axes represent 51.2 % of the total variation (PCoA1 = 45.24 % and PCoA2 = 6.03 %). The vectors are the most representative genera of the variability observed in nematode communities.

The SIMPER analysis provided detailed information about the contribution of each genus for spatial and temporal patterns of the nematode assemblages (Table 4a and 4b, Supplementary data). The major contributor to similarity within all sites was the genus *Sabatieria*. *Monoposthia* and *Desmodora* genera were the highest contributors at Tróia site assemblages and *Metachromadora* and *Terschellingia* genera at Navigator and Gambia sampling sites (similarity > 60%). In opposition, the major contribution for the dissimilarities between Navigator and Gambia sites (dissimilarity 39%) were the genera *Metachromadora*, *Terschellingia* and *Sabatieria*. The highest levels of dissimilarity were detected between Tróia and Navigator assemblages (dissimilarity 73%) and Tróia and Gambia assemblages (dissimilarity 70%), which *Metachromadora*, *Terschellingia*,

*Anoplostoma* and *Sabatieria* genera explain the pattern obtained (Table 4a, Supplementary data).

The temporal distribution patterns are explained by highest values of similarity between assemblages of the winter 2020 and summer 2021 (Table 4, Supplementary data), resulting from the contribution of the genera *Metachromadora*, *Sabatieria* and *Anoplostoma*. Although, the highest levels of dissimilarities were obtained among sampling occasions winter 2019 and summer 2020 (dissimilarity 45%), which *Sabatieria*, *Metachromadora* and *Terschellingia* determine this pattern.

#### 5.4.3 Environmental variables vs nematode communities

In the RDA, nematode assemblage patterns were significantly constrained by the selected environmental variables ( $F=7.11$ ,  $p=0.001$ , adjusted  $R^2_{\text{Ad}} = 0.344$ ). After forward selection the most significant variables considered in the adjusted model were sand,  $\text{CaCO}_3$ , Li, OM, NT and *chl<sub>a</sub>\_phaeo* ( $p<0.01$ ). The total variation explained by the predictors in the fitted model was approximately 39.5%. According to RDA plot the first constrained axis explains the largest amount of variation among the constrained axes (RDA1=29.5%) (Figure 5).

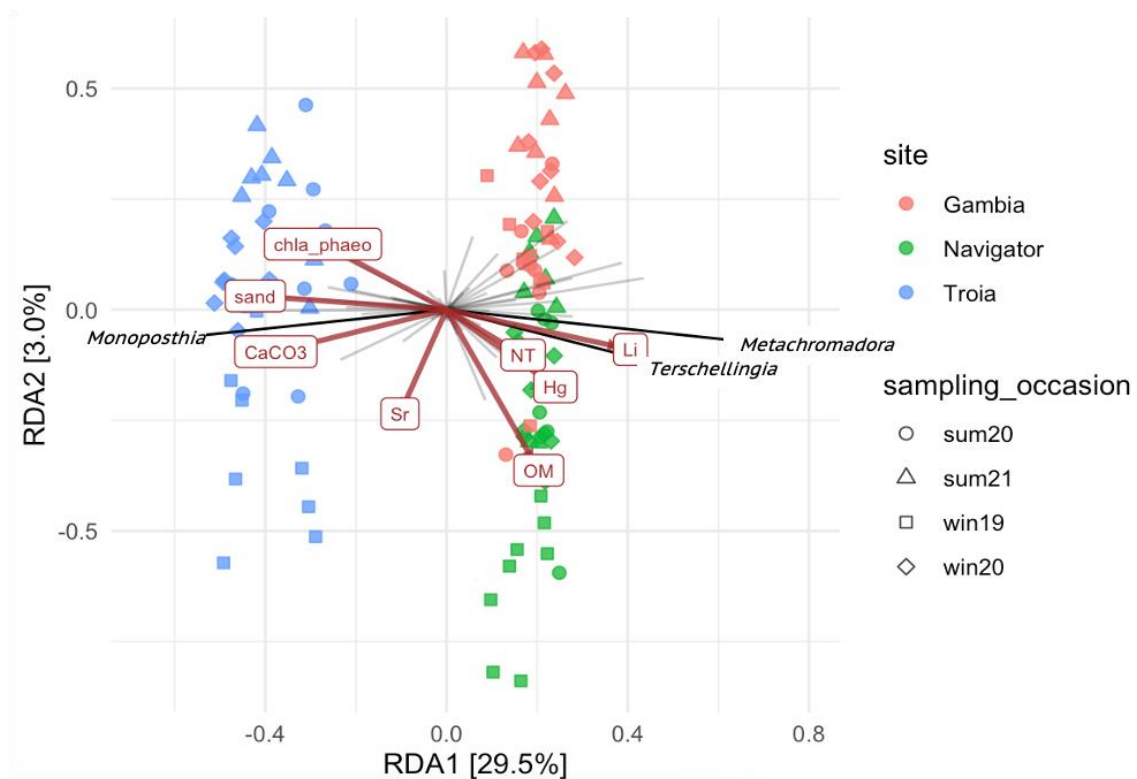


**Figure 5.** RDA Constrained redundancy analysis displaying contributions of environmental variables for the distribution of nematode communities filtered at genera level: Sand,  $\text{CaCO}_3$ , Li, OM, NT, *chl<sub>a</sub>\_phaeo*, Hg and Sr (RDA1 = 29.5% and RDA2 = 3%). The vectors are the

constrained variables and the taxa that are the main contributors for distribution of the communities.

The sand and chla\_phaeo variables were highly correlated with Tróia site assemblages. Although, the NT, Hg, Li and OM variables showed high correlation with Navigator and Gambia assemblages. *Monoposthia* genus pattern was explain mainly by CaCO<sub>3</sub> and sand, *Terschellingia* and *Metachromadora* genera patterns were highly correlated Li, NT, Hg, and OM. All variables measured could not explain the temporal distribution patterns of the nematode assemblage.

## 5.5 Discussion

Benthic nematodes are valuable ecological indicators to assess the integrity of the aquatic ecosystems (Semprucci & Balsamo, 2014; Zeppilli et al., 2015; Branco et al., 2018; Haegerbaeumer et al., 2019). They are highly sensitive to different habitat conditions (Giere, 2009; Ruaro et al., 2016; Branco et al., 2018, Ridall & Ingels, 2021) and the magnitude of their responses (micro and mesoscale) is highly related to the micro-habitat diversity, driven by small food patches, physico-chemical conditions and biotic interactions (Gallucci et al., 2008; Giere, 2009; Moens and Benninger et al., 2018).

According with the spatial distribution patterns of bacterial and nematode communities in Sado Estuary (Vieira et al., 2023), nematodes revealed to be highly sensitive to sediment site-specific conditions being more susceptible to temporal variations. However, the lack of temporal variation in bacterial community composition obtained in Vieira et al., (2025), showed that the spatial differences are more important for the community structure than temporally derived variations. This highlighted the importance of studying the effect of temporal variability on the composition and diversity of nematode assemblages and assess the responses of both communities (nematode vs. bacteria).

### 5.5.1 Does nematode assemblages and benthic bacterial communities provide similar ecological responses to the sediment condition?

The current study investigated the spatial and temporal distribution patterns of nematode assemblages in the same sites and sampling occasions as Vieira et al. (2025). Our findings revealed that the distribution patterns of both communities were strongly correlated with the spatial variation of the sediment habitat condition. However, only the nematode assemblages exhibited distinct responses driven by the interactions of the two factors “site” and “sampling occasion”.

### 5.5.1.1 Spatial distribution patterns of nematodes assemblages and benthic bacterial communities

The influence of sediment habitat condition on the spatial distribution patterns of benthic communities in estuaries is well known (Jessen et al., 2017; Branco et al., 2018; Vieira et al., 2023 and 2025). Environmental variables such as OM proved to be a structuring factor by shaping the diversity and abundance of bacterial and nematode communities (Vieira et al., 2023 and 2025). However, is also known that organic inputs are not always congruent with seasonal occurrences, stochastic events are common and they are known to spatially regulate organic matter inputs and alter the nutrient availability (Zheng et al., 2020; Xu et al., 2022; Vieira et al., 2024).

Several environmental variables contributed to similar spatial distribution patterns between nematode assemblages and bacterial communities (e.g. OM, CT, gravel, sand chla\_phaeo and CaCO<sub>3</sub>), clearly distinguishing the communities of Navigator and Gambia sites from those of Tróia site. The sampling sites Navigator and Gambia are located within the estuary, they are influenced by low hydrodynamic activity and high anthropogenic activities that directly favors the organic enrichment. The sediments were mainly composed by high proportions of OM, gravel, clay, and high concentrations of Pb, As, Hg, Li and Cr, together with low levels of oxygen which favors the sulfur reduction pathways in sediments with the high prevalence *Desulfobacterota* phylum (Guo et al., 2023; Vieira et al., 2025). Additionally, the lowest quality of OM (estimated by chla\_phaeo ratio values) reported at Navigator and Gambia sediments in the winter 2019 was consistent with the previous sediment habitat conditions (Vieira et al., 2023) resulting in less diverse benthic communities and simplification of the benthic food webs (Vieira et al., 2024). In contrast, Tróia sampling site situated in the mouth of the estuary, benefits from tidal activity, increased oxygen flow and aerobic metabolic pathways associated to OM degradation (Vieira et al., 2025). The sediments are predominantly sandy, with low OM content with high quality (estimated by chla\_phaeo ratio values). These conditions stimulate the prevalence of aerobic bacteria, such as *Flavobacteriaceae*, which potentially contribute to the OM remineralization (Jessen et al., 2017; Vieira et al., 2025). These results were consistent with the previous studies (Vieira et al., 2024), by showing that the quality of organic matter is highly correlated with the efficient use of available resources increasing the food webs complexity.

### 5.5.1.2 Spatial and temporal diversity patterns of nematode assemblages

The temporal variability in the composition distribution pattern of nematode assemblages was strongly driven by the site-specific conditions of sediment. Overall, nematode assemblages exhibit high richness following the same trend as density, with significant interaction between factors (“site” x “sampling occasion”,  $p<0.05$ ). In summer 2021, nematode assemblages of Navigator site registered the higher number of individuals (N) and significantly high variability in the trophic composition. This variability was potentially driven by the occurrence of organic enrichment and trophic shifts that improve the use of available sources, without significantly modify the assemblages’ structure (Moens and Benninger, 2018; Vieira et al., 2024). In line with our results, were Vieira et al. (2024) findings, that investigated the spatial and temporal variability of benthic food webs on same sites and sampling occasions, analyzing the isotopic signatures of carbon ( $\delta^{13}\text{C}$ ) and nitrogen ( $\delta^{15}\text{N}$ ) of macrofauna communities. Temporal patterns in the benthic food web were not as clear as spatial patterns, although high variability in the trophic interactions was observed among the sampling occasions. This was consistent with the temporal variability detected in the diversity patterns of nematode assemblages and with the predominant metabolic pathways of bacterial communities as proxies for sediment ecological condition (Vieira et al., 2025). Significant temporal variability was detected for Maturity Index (MI) of nematode assemblages being highest in summer 2021. While in the same occasion, increasing complexity and diversity was observed in the food webs of Navigator and Gambia sites (Vieira et al., 2024). This suggests a potential improvement in the quality of habitat, which was reflected in the diversity patterns of nematode assemblages and in the trophic shifts observed in the macrobenthic food web structure. The direct link between nematode assemblage composition and benthic food web complexity can be supported by fact of many macrofauna species directly feed on meiofauna (Vafeiadou et al., 2013). Besides, the diversity of meiofauna communities already proved to influence the abundance and diversity of intermediate consumers (e.g. omnivores and carnivores) (Szczepanek et al., 2021).

Temporal changes in the diversity patterns of nematode assemblages demonstrated to be dependent to specific condition of each site, making them excellent ecological indicators of local short-term environmental shifts. Whereas, the spatial variability of bacterial communities revealed to be good proxies of the sediment conditions due to the prevalence of specific metabolic pathways and the high sensitivity to metal pollution (Du et al., 2022; Li et al., 2020; Pinto et al., 2015). Their ability to

effectively detect anthropogenic disturbances, with a quick and cost-effective application, makes them a valuable tool monitoring marine ecosystems as part to assess the benthic habitat condition under the “Blue Economy” activities.

## 5.6 Concluding remarks

Nematode assemblages proved to be very sensitive to spatial and temporal variations, different responses were detected in the interaction of the factors “site” and “sampling occasion”. Temporal variability in the diversity patterns of nematode assemblages was consistent with diversity and complexity patterns of benthic food webs. Additionally, spatial variations were well described by the bacterial communities exhibiting different metabolic pathways that clearly explain the sediment habitat condition of each site. These findings also highlight the role of nematodes and bacteria in carbon fluxes within benthic food webs, by showing that diversity patterns of nematode assemblages and metabolic pathways of bacterial communities were aligned with complexity patterns of the benthic food webs.

In summary, we concluded that investigating the spatial and temporal effects of sediment habitat condition on composition distribution patterns of the nematode assemblages and bacterial communities offers valuable insights at different scales. Nematode communities respond to small shifts of the sediment habitat conditions while bacteria communities respond in a larger scale being sensitive to metal and organic pollution. The combination of both indicators can enhance environmental evaluation frameworks promoting sustainable marine resource management and conservation. This is also in line with the blue economy's emphasis on enhancing ecosystem resilience against climate change.

## 5.7 References

Anderson, M.J., Gorley, R.N., Clarke, K.R., 2008. In: Plymouth, U.K. (Ed.), PERMANOVA + for PRIMER: Guide to Software and Statistical Methods.

anthropogenic impacts? Mar Biodivers 45:505–535. <https://doi.org/10.1007/s12526-015-0359-z>

Barnett et al. 2021. microViz: an R package for microbiome data visualization and statistics. Journal of Open Source Software, 6(63), 3201, <https://doi.org/10.21105/joss.03201>

Bettencourt, A.M., Bricker, S.B., Ferreira, J.G., Franco, A., Marques, J.C., Melo, J.J., Nobre, A., Ramos, L., Reis, C.S., Salas, F., Silva, M.C., Simas, T., Wolff, W.J., 2004. Typology and Reference Conditions for Portuguese Transitional and Coastal Waters. Institute of Marine Research.

Bonaglia, S., Nascimento, F.J.A., Bartoli, M., Klawonn, I., Brüchert, V., 2014. Meiofauna increases bacterial denitrification in marine sediments. *Nat. Commun.* 5, 5133. <https://doi.org/10.1038/ncomms6133>.

Bongers, T., Alkemade, R., Yeates, G.W., 1991. Interpretation of disturbance-induced maturity decrease in marine nematode assemblages by means of the Maturity Index. *Mar. Ecol. Prog. Ser.* 76, 135–142.

Bongers, T. The Maturity Index, the evolution of nematode life history traits, adaptive radiation and cp-scaling. *Plant and Soil* 212, 13–22 (1999). <https://doi.org/10.1023/A:1004571900425>

Branco, J., Pedro, S., Alves, A.S., Ribeiro, C., Materatski, P., Pires, R., Caçador, I., Adão, H., 2018. Natural recovery of *Zostera noltii* seagrass beds and benthic nematode assemblage responses to physical disturbance caused by traditional harvesting activities. *J. Exp. Mar. Biol. Ecol.* 502, 191–202. <https://doi.org/10.1016/J.JEMBE.2017.03.003>.

Caeiro, S. et al., 2005. Assessing heavy metal contamination in Sado Estuary sediment: an index analysis approach. *Ecol. Indicat.* 5, 151–169. <https://doi.org/10.1016/j.ecolind.2005.02.001>

Camargo, A. PCATest: testing the statistical significance of principal component analysis in R. *PeerJ*, 10, e12967 (2022).

Clarke, K.R., Warwick, R.M., 2001. Changes in Marine Communities: an Approach to Statistical Analysis and Interpretation, second ed.

Du M, Zheng M, Liua A, Wang L, Pan X, Liu J, Ran X. 2022. Effects of emerging contaminants and heavy metals on variation in bacterial communities in estuarine sediments. *Science of the Total Environment* 832 (2022) 155118, <http://dx.doi.org/10.1016/j.scitotenv.2022.155118>

Gallucci F, Moens T, Vanreusel A, Fonseca G (2008) Active colonisation of disturbed sediments by deep-sea nematodes: evidence for the patch mosaic model. *Mar Ecol Prog Ser* 367:173-183. <https://doi.org/10.3354/meps07537>

Giere, O. 2009. *Meiobenthology. The Microscopic Motile Fauna of Aquatic sediments.* (Springer-Verlag, Heidelberg 2009).

Guo Z et al. 2023. Succession and environmental response of sediment bacterial communities in the Liao River Estuary at the centenary scale. *Marine Environmental Research* 188, 105980, <https://doi.org/10.1016/j.marenvres.2023.105980>

Haegerbaeumer, A., Höss, S., Traunspurger, W. (2019). Nematode-Based Effect Assessment in Freshwater Sediments. In: Seiler, TB., Brinkmann, M. (eds) *In Situ Bioavailability and Toxicity of Organic Chemicals in Aquatic Systems. Methods in Pharmacology and Toxicology.* Humana, New York, NY. [https://doi.org/10.1007/7653\\_2019\\_38](https://doi.org/10.1007/7653_2019_38)

Heip, C., Vincx, M., Vranken, G., 1985. *The Ecology of Marine Nematodes.*

Ingels J, Kiriakoulakis K, Wolff A.G, Vanreusel A., 2009. Nematode diversity and its relation to the quantity and quality of sedimentary organic matter in the deep Nazaré Canyon, Western Iberian Margin. *Deep-Sea Research I* 56 (2009) 1521–1539. doi:10.1016/j.dsr.2009.04.010

Jessen L.G., Lichtschlag A., Ramette A., Pantoja S., Rossel E. P., Schubert J. C., Struck U., Boetius A., 2017. Hypoxia causes preservation of labile organic matter and changes seafloor microbial community composition (Black Sea). *Science Advances*, Vol 3, Issue 2, doi: 10.1126/sciadv.1601897

Kennedy, P., Kennedy, H., Papadimitriou, S., 2005. The effect of acidification on the determination of organic carbon, total nitrogen and their stable isotopic composition in algae and marine sediment. *Rapid Commun. Mass Spectrom.* 19, 1063–1068. <https://doi.org/10.1002/rcm.1889>, 2005.

Lê, S., Josse, J., & Husson, F. FactoMineR: an R package for multivariate analysis. *Journal of statistical software*, 25, 1-18 (2008).

Li C.C., Quan Q., Gan Y., Dong J., Fang J., Wang L., Liu J., 2020. Effects of heavy metals on microbial communities in sediments and establishment of bioindicators

based on microbial taxa and function for environmental monitoring and management. Sci. Total Environ. 749, 141555  
<https://doi.org/10.1016/j.scitotenv.2020.141555>

Margalef, D.R., 1958. Information theory in ecology. *Gen. Syst.* 3, 36–71.

McMurdie, P.J., Holmes, S., 2013. Phyloseq: an R package for reproducible interactive analysis and graphics of Microbiome census data. *PLoS One* 8, e61217.<https://doi.org/10.1371/JOURNAL.PONE.0061217>

Moens, T., Beninger, P.G. (2018). Meiofauna: An Inconspicuous but Important Player in Mudflat Ecology. In: Beninger, P. (eds) *Mudflat Ecology*. Aquatic Ecology Series, vol 7. Springer, Cham. [https://doi.org/10.1007/978-3-319-99194-8\\_5](https://doi.org/10.1007/978-3-319-99194-8_5)

Moreno, M., Ferrero, T., Gallizia, I., Vezzulli, L., Albertelli, G., Fabiano, M., 2008. An assessment of the spatial heterogeneity of environmental disturbance within an enclosed harbour through the analysis of meiofauna and nematode assemblages. *Estuar. Coast. Shelf Sci.* 77, 565e576.

Nascimento, F.J.A., N̄aslund, J., Elmgren, R., 2012. Meiofauna enhances organic matter mineralization in soft sediment ecosystems. *Limnol. Oceanogr.* 57, 338–346. <https://doi.org/10.4319/lo.2012.57.1.0338>.

Nemys eds. (2024). Nemys: World Database of Nematodes. Accessed at <https://nemys.ugent.be> on 2024-09-10. doi:10.14284/366

Neves M.J., Martins M., Adão H., Mil-Homens M., Costa M. H., Lobo-Arteaga J., 2025. Ecological quality assessment of estuarine macrobenthic communities using an integrative approach. *Marine Pollution Bulletin*, 210, 2025,117316, <https://doi.org/10.1016/j.marpolbul.2024.117316>.

Pawlowski et al., 2018. The future of biotic indices in the ecogenomic era: Integrating (e)DNA metabarcoding in biological assessment of aquatic ecosystems *Science of The Total Environment* Volumes 637–638, 2018, Pages 1295-1310, <https://doi.org/10.1016/j.scitotenv.2018.05.002>

Pinto A.B., Pagnocca F.C., Pinheiro M.A., Fontes R.F., de Oliveira A.J., 2015. Heavy metals and TPH effects on microbial abundance and diversity in two estuarine areas of the southern-central coast of Sao Paulo State, Brazil. *Mar. Pollut. Bull.* 96, 410–417. <https://doi.org/10.1016/j.marpolbul.2015.04.014>

Platt, H., Warwick, R., 1988. Free Living Marine Nematodes. Part II: British Chromadorids. Pictorial Key to World Genera and Notes for the Identification of British Species, Leiden.

R Core Team. 2022. A language and environment for statistical computing. Version 2022.07.2 Build 576. Vienna: R Foundation for Statistical Computing. Available at <https://www.r-project.org>.

Ridall, A., Ingels, J., 2021. Suitability of free-living marine nematodes as bioindicators: status and future considerations. *Front. Mar. Sci.* 0, 863. <https://doi.org/10.3389/FMARS.2021.685327>.

Ruaro, R., Gubiani, É.A., Cunico, A.M. et al. Comparison of fish and macroinvertebrates as bioindicators of Neotropical streams. *Environ Monit Assess* 188, 45 (2016). <https://doi.org/10.1007/s10661-015-5046-9>

Sagova-Mareckova M., Boenigk J., Bouchez A., Cermakova K., Chonova T., Cordier T., Eisendle U., Elersek T., Fazi S., Fleituch T., Frühe L., Gajdosova M., Graupner N., Haegerbaeumer A., Kelly A.-M., Kopecky J., Leese F., Nõges P., Orlic S., Panksep K., Pawlowski J., Petrussek A., Piggott J.J., Rusch J.C., Salis R., Schenk J., Simek K., Stovicek A., Strand D.A., Vasquez M.I., Vrålstad T., Zlatkovic S., Zupancic M., Stoeck T., 2021. Expanding ecological assessment by integrating microorganisms into routine freshwater biomonitoring, *Water Research*, Volume 191, 2021, 116767, ISSN 0043-1354, <https://doi.org/10.1016/j.watres.2020.116767>.

Schratzberger, M., Ingels, J., 2018. Meiofauna matters: the roles of meiofauna in benthic ecosystems. *J. Exp. Mar. Biol. Ecol.* 502, 12–25. <https://doi.org/10.1016/j.jembe.2017.01.007>

Semprucci, F., Balsamo, M., 2014. Free-Living marine nematodes as bioindicators: past, present and future perspectives. *Trends Environ. Sci.* 17–36

Shannon, C.E., Weaver, W., 1963. The Mathematical Theory of Communication. Univ Illinois Press Illinois.

Sroczyńska, K., Chainho, P., Vieira, S., Adão, H., 2021. What makes a better indicator? Taxonomic vs functional response of nematodes to estuarine gradient. *Ecol. Indicat.* 121, 107113. <https://doi.org/10.1016/j.ecolind.2020.107113>

Sroczynska, K., Conde, A., Chainho, P., Adão, H., 2021b. How nematode morphometric attributes integrate with taxonomy-based measures along an estuarine gradient. *Ecol. Indicat.* 124, 107384 <https://doi.org/10.1016/j.ecolind.2021.107384>.

Steyaert, M., Vanaverbeke, J., Vanreusel, A., Barranguet, C., Lucas, C., Vincx, M., 2003. The importance of fine-scale, vertical profiles in characterising nematode community structure. *Estuar. Coast Shelf Sci.* 58, 353–366. [https://doi.org/10.1016/S0272-7714\(03\)00086-6](https://doi.org/10.1016/S0272-7714(03)00086-6).

Szczepanek, M., Silberberger, M.J., Koziorowska-Makuch, K., Nobili, E., Kedra, M., 2021. The response of coastal macrobenthic food-web structure to seasonal and regional variability in organic matter properties. *Ecol. Ind.* 132 (2021), 108326 <https://doi.org/10.1016/j.ecolind.2021.108326>.

Vafeiadou A. M., Materatski P., Adão H., Troch M., Moens T. (2013). Food sources of macrobenthos in an estuarine seagrass habitat (*Zostera noltii*) as revealed by dual stable isotope signatures. *Mar Biol* (2013) 160:2517–2523.

Vieira, S., Barrulas, P., Chainho, P., et al., 2022. Spatial and Temporal Distribution of the Multi-element Signatures of the Estuarine Non-indigenous Bivalve *Ruditapes philippinarum*. *Biol Trace Elem Res* 200, 385–401. <https://doi.org/10.1007/s12011-021-02629-x>.

Vieira, S., Sroczynska, K., Neves, J., Martins, M., Costa, M.H., Adão, H., Vicente, S.L.C., 2023. Distribution patterns of benthic bacteria and nematode communities in estuarine sediments. *Estuar. Coast. Shelf Sci.* 291, 108448 <https://doi.org/10.1016/j.ecss.2023.108448>.

Vieira, S., Maurer A-F., Dias C.B., Neves J., Martins M., Lobo-Arteaga J., Adão H., Sroczynska K., (2024) “Food web attributes to assess spatial–temporal dynamics in estuarine benthic ecosystem”, *Ecological Indicators*, Volume 166, 2024, 112243, ISSN 1470-160X, <https://doi.org/10.1016/j.ecolind.2024.112243>

Vieira, S, Helena Adão H., Vicente C.S.L., (2025) Spatial and temporal distribution pattern of sediment bacterial communities in Sado estuary (Portugal). *Marine environmental research*, Volume 204, February 2025, 106963. <https://doi.org/10.1016/j.marenvres.2025.106963>

Vincx, M., 1996. Meiofauna in marine and freshwater sediments. In: meiofauna in marine and freshwater sediments. In: Hall, G.S. (Ed.), *Methods for the Examination of Organismal Diversity in Soils and Sediments*, pp. 187–195. Wallinfort, UK.

Warwick, R., Clarke, K., Suharsono, 1990. A statistical analysis of coral community responses to the 1982-3 El Nino in the Thousand Islands, Indonesia. *Coral Reefs* 8, 171e179.

Warwick, R.M., Platt, H.M., Sommerfield, P.J., 1998. Free-living marine nematodes, Part 3, British Monhysterids. *Field StudiesCouncil*, Shrewsbury. Wieser, W., 1956. Some free-living marine nematodes. *Galathea Rep.*

Wieser, W., 1956. Some free-living marine nematodes. *Galathea Rep.*

Xu, W., Shin, K.S.P., Sun, J., 2022. Organic Enrichment Induces Shifts in the Trophic Position of Infauna in a Subtropical Benthic Food Web, Hong Kong. *Front. Mar. Sci.* 9, | 937477. <https://doi.org/10.3389/fmars.2022.937477>

Zeppilli, D., Sarrazin, J., Leduc, D. et al. Is the meiofauna a good indicator for climate change and anthropogenic impacts?. *Mar Biodiv* 45, 505–535 (2015). <https://doi.org/10.1007/s12526-015-0359-z>

Zheng, X., Como, S., Huang, L., Magni, P., 2020. Temporal Changes of a Food Web Structure Driven by Different Primary Producers in a Subtropical Eutrophic Lagoon. *Mar. Environ. Res.* 161, 105128 <https://doi.org/10.1016/j.marenvres.2020.105128>.



## Supplementary information of chapter 5

**Table S1:** Mean $\pm$ SE. n=3 of the environment and biogeochemical parameters measured in each site (Navigator. Gambia and Tróia). across the 4 seasons (win19. sum20. win20 and sum21). Granulometric parameters (%) are Clay\_per. Sand\_per. Gravel\_per. The elemental analysis (w%) are organic matter (OM\_per). Total Nitrogen and Carbon (N\_total\_per and C\_total\_per). pigments measured (mg.g $^{-1}$ ) are Chlorophyl a (Chla\_mg.g $^{-1}$ ) and Phaeopigment (Phaeo\_mg.g $^{-1}$ ) the freshness calculated by the ratio between Chla and Phaeo pigments (Chla\_phaeo). Metals concentration (mg/kg) Li. Sr. Mn. Ni. Cr. Be. U. Ba. Co. Cu. Zn. As. Pb and Hg. Instant variables. measured in each site Temperature (Temp) °C. Salinity (Sal). Oxygen (O<sub>2</sub>) mg/L and pH.

Seasons		win19				sum20				win20				sum21		
Sites		Navigator	Gambia	Tróia	Navigator	Gambia	Tróia	Navigator	Gambia	Tróia	Navigator	Gambia	Tróia	Navigator	Gambia	Tróia
Granulometry	Clay_per	30.1 $\pm$ 3.1	13.5 $\pm$ 0.2	1.8 $\pm$ 0.2	20.9 $\pm$ 1	17.4 $\pm$ 5.1	1.7 $\pm$ 0.1	35.2 $\pm$ 6.6	15.8 $\pm$ 1.7	1.5 $\pm$ 0.5	25.8 $\pm$ 2.3	16.3 $\pm$ 2.2	2.9 $\pm$ 0.4			
	Sand_per	66.2 $\pm$ 2.6	71.5 $\pm$ 5.5	93.8 $\pm$ 1.9	73.1 $\pm$ 1.7	67.5 $\pm$ 4.1	97.3 $\pm$ 0.1	61.8 $\pm$ 6.1	68.7 $\pm$ 1	95.2 $\pm$ 1.1	72.2 $\pm$ 2.6	66.6 $\pm$ 0.6	91.6 $\pm$ 2.8			
	Gravel_per	3.8 $\pm$ 0.7	14.9 $\pm$ 5.6	4.4 $\pm$ 1.8	5.9 $\pm$ 1.5	15.1 $\pm$ 6.4	1 $\pm$ 0.1	3 $\pm$ 0.7	15.5 $\pm$ 1	3.3 $\pm$ 1	2 $\pm$ 0.3	16.9 $\pm$ 2.1	5.4 $\pm$ 2.8			
Elemental composition	OM_per	3.9 $\pm$ 0.6	0.6 $\pm$ 0.04	1.9 $\pm$ 0.3	2.3 $\pm$ 0.3	1.7 $\pm$ 0.3	0.4 $\pm$ 0.02	2.4 $\pm$ 0.3	0.8 $\pm$ 0.05	0.4 $\pm$ 0.02	2.1 $\pm$ 0.1	1.2 $\pm$ 0.1	0.5 $\pm$ 0.04			
	C_total_per	0.9 $\pm$ 0.3	0.7 $\pm$ 0.4	0.6 $\pm$ 0.06	1.1 $\pm$ 0.1	0.4 $\pm$ 0.1	0.7 $\pm$ 0.1	1.1 $\pm$ 0.1	0.5 $\pm$ 0.03	0.5 $\pm$ 0.04	0.9 $\pm$ 0.1	0.4 $\pm$ 0.05	0.6 $\pm$ 0.03			
	N_total_per	0.06 $\pm$ 0.2	0.05 $\pm$ 0.02	0.02 $\pm$ 0.008	0.07 $\pm$ 0.006	0.03 $\pm$ 0.01	0.01 $\pm$ 0.003	0.3 $\pm$ 0.09	0.05 $\pm$ 0.005	0.08 $\pm$ 0.002	0.07 $\pm$ 0.007	0.04 $\pm$ 0.006	0.01 $\pm$ 0.003			
	CaCO <sub>3</sub> _per	2.4 $\pm$ 0.5	1 $\pm$ 0.06	4.3 $\pm$ 0.3	2.6 $\pm$ 0.5	1.6 $\pm$ 0.3	4.6 $\pm$ 0.9	2.1 $\pm$ 0.05	1.2 $\pm$ 0.04	3.5 $\pm$ 0.3	1.7 $\pm$ 0.1	1.3 $\pm$ 0.05	3.7 $\pm$ 0.3			
	Chla_mg_g	15.6 $\pm$ 3.9	10.3 $\pm$ 0.9	26.7 $\pm$ 2.1	9.8 $\pm$ 0.1	55.5 $\pm$ 2.4	11.1 $\pm$ 1.4	31.1 $\pm$ 6.6	10.8 $\pm$ 1.9	6.7 $\pm$ 0.5	4.8 $\pm$ 0.8	7.7 $\pm$ 0.7	4.9 $\pm$ 0.6			
	Phaeo_mg_g	14.7 $\pm$ 3.7	7.8 $\pm$ 0.5	14.5 $\pm$ 1	10.6 $\pm$ 1.2	115.1 $\pm$ 32.7	5.2 $\pm$ 0.9	40.1 $\pm$ 9.4	5.1 $\pm$ 1.5	4.5 $\pm$ 0.8	1.6 $\pm$ 0.2	3.6 $\pm$ 0.4	1.3 $\pm$ 0.2			
	Chla_phaeo	1.1 $\pm$ 0.02	1.3 $\pm$ 0.1	1.8 $\pm$ 0.06	0.9 $\pm$ 0.1	0.7 $\pm$ 0.3	2.2 $\pm$ 0.1	0.8 $\pm$ 0.02	2.5 $\pm$ 0.6	1.7 $\pm$ 0.3	2.9 $\pm$ 0.1	2.1 $\pm$ 0.05	4 $\pm$ 0.4			
Metals (mg/kg)	Li	28.7 $\pm$ 2.8	20.4 $\pm$ 0.7	11.5 $\pm$ 0.3	28 $\pm$ 1.3	20.9 $\pm$ 3.5	11.5 $\pm$ 0.05	30.8 $\pm$ 2.7	25.6 $\pm$ 0.9	12.1 $\pm$ 0.3	29 $\pm$ 0.7	16.9 $\pm$ 2.3	13.5 $\pm$ 0.2			

	Sr	110.3±18.6	45.6±0.9	74.4±3.3	96.1±20.6	48.8±4.1	97.9±20.4	61.3±0.9	50.4±0.6	69.8±1.2	61.2±3.6	62.5±1.3	73.5±1.7
	Mn	100.6±6.9	61.7±4.3	45.6±2.9	115.1±3.7	71.1±12.9	39.9±0.2	111.4±9.2	83.9±5.8	49.6±2.7	103.9±3.6	62.2±10	52.7±3.3
	Ni	15.1±2.1	7.8±0.9	3.8±0.08	15.7±0.8	9.6±2.2	4.3±0.06	18.7±1.3	93.4±61.8	8.3±0.9	15.8±0.7	10.4±1.6	9.5±1.1
	Cr	29.3±3.8	15±3.3	3.6±0.1	26.5±1.9	16.5±7	3.5±0.03	29.9±3.2	157.9±105	4.8±0.3	29.7±0.2	11.7±3.5	6.1±0.4
	Be	1±0.1	0.6±0.04	0.6±0.2	0.9±0.06	0.6±0.2	1.4±0.06	1.2±0.07	0.8±0.03	0.7±0.1	1.2±0.08	0.8±0.09	1.4±0.4
	U	3.3±0.6	1.2±0.07	0.4±0.02	1.9±0.1	1.4±0.2	0.4±0.01	2.2±0.2	1.4±0.1	0.4±0.01	1.8±0.1	0.8±0.09	0.5±0.03
	Ba	246±7	236.7±5	234.7±7	230.4±8.8	223.5±24.6	245.3±7.8	255.7±2	252.2±6.3	226.7±12.5	251.1±4.7	244.7±6.8	238.8±13
	Co	4.6±0.7	2.7±0.4	0.6±0.02	4.3±0.3	3±1.1	0.6±0.03	4.9±0.4	4.9±0.9	0.8±0.05	4.6±0.1	2±0.6	0.9±0.05
	Cu	28.6±6.7	8±1.9	1.6±0.2	19.6±1.4	11.2±5.4	1.8±0.3	32.9±0.5	20.5±4.3	2.4±0.4	37.8±5.3	10.2±3.1	3.7±0.3
	Zn	82.3±21.9	26.5±7.5	3.1±0.8	63.9±8.5	25.4±9.6	4.6±0.3	95.6±5	41.7±3.8	7.9±1.9	109.3±19.5	20.6±6.4	9.5±0.8
	As	13.8±2.9	4.7±0.9	1.7±0.1	12.2±1.9	7.3±1.3	2.3±0.2	12.9±0.6	7.9±0.8	1.6±0.2	11.3±1.3	4.5±1.3	0.9±0.2
	Pb	25.4±3.9	14.7±1	12.2±0.4	22.1±1.8	14.1±2.4	12.9±0.4	27.3±0.9	17.9±0.6	12.4±0.6	29.3±3.3	14.9±0.9	13.1±0.6
	Hg	0.3±0.07	0.3±0.2	0.03±0.0007	0.3±0.05	0.06±0.01	0.03±0.006	0.3±0.05	0.1±0.003	0.02±0.004	0.3±0.06	0.04±0.01	0.05±0.002
Instant variables	Temp	15.3 ± 0.1	11.1 ± 0.2	15.3 ± 0.1	28.5 ± 0.5	24.4 ± 0.2	23.9 ± 0.1	13.5 ± 0.2	16.8 ± 0.2	16.8 ± 0.2	23.8 ± 0.9	23.6 ± 0.1	20.7 ± 0.2
	Sal	31.9 ± 0.9	30.6 ± 0.7	31.8 ± 0.9	36.5 ± 0.3	17.7 ± 0.1	16.4 ± 0.04	15.9 ± 0.05	14.7 ± 0.05	14.7 ± 0.5	15 ± 0.5	14 ± 1.5	15.3 ± 0.3
	O2	9.2 ± 0.1	14.5 ± 2.5	9.2 ± 0.1	8.3 ± 1.3	9.5 ± 0.4	12.1 ± 0.3	9.6 ± 0.4	17.9 ± 0.4	13.9 ± 0.3	5.3 ± 0.6	8.8 ± 0.4	8.6 ± 0.2
	pH	7.9 ± 0.01	7.9 ± 0.05	7.9 ± 0.01	8.1 ± 0.1	7.8 ± 0.02	7.9 ± 0.04	8.3 ± 0.3	8.6 ± 0.3	8.9 ± 0.04	7.8 ± 0.1	8.1 ± 0.1	8.3 ± 0.02

**Table 3:** Mean density  $\pm$  standard error (SE) of all nematode genera (number of individuals per  $10\text{ cm}^2$ ) each site (Navigator, Gambia and Tróia) and sampling occasion (winter 19, summer 20, winter 20 and summer 21).

Genera	Navigatorw 19	Navigator s20	Navigatorw 20	Navigator r s21	Gambia_w 19	Gambia s20	Gambiarw 20	Gambias 21	Troia w19	Troia s20	Troia w20	Troia s21
<i>Acantholaimus</i>	0	0	0	0	0	0	$3.3 \pm 4.5$	0	$0.7 \pm 0.9$	$1.9 \pm 2.6$	0	0
<i>Actinonema</i>	0	0	0	0	0	0	0	0	$5.4 \pm 4$	$41 \pm 19.5$	$15 \pm 7$	$16 \pm 6$
<i>Aegialoalaimus</i>	$10.5 \pm 9$	$15 \pm 10$	$7.4 \pm 5.3$	0	$19 \pm 11$	$9 \pm 7$	$28 \pm 22$	$11 \pm 11$	0	0	0	$0.7 \pm 0.9$
<i>Ammotheristus</i>	0	0	0	0	0	0	0	0	$3 \pm 3.3$	$1.5 \pm 2$	0	0
<i>Amphimonhystra</i>	$3 \pm 4$	0	0	0	0	0	0	0	0	0	0	0
<i>Anoplostoma</i>	$251 \pm 215$	$120 \pm 34$	$297 \pm 149$	$515 \pm 912$	$108 \pm 61$	$61 \pm 32$	$407 \pm 142$	$266 \pm 84$	0	$1.8 \pm 2.5$	0	$3 \pm 2$
<i>Anticoma</i>	0	0	0	0	$7 \pm 9$	0	0	0	$3.7 \pm 2.5$	$6 \pm 4$	0	$2.4 \pm 2.2$
<i>Antomicron</i>	$1.7 \pm 2$	$7.3 \pm 7.4$	$3.6 \pm 3.3$	0	0	$6 \pm 5.4$	$5 \pm 7$	$9 \pm 8.5$	0	0	0	0
<i>Aponema</i>	$58 \pm 78$	$4.4 \pm 6$	0	$9 \pm 7.8$	0	0	0	$4 \pm 5.4$	0	$1.6 \pm 2$	$0.8 \pm 1$	$5 \pm 5.3$
<i>Araeolaimus</i>	0	0	0	0	0	0	0	$3 \pm 4$	0	0	$0.8 \pm 1$	0
<i>Axonolaimus</i>	$45 \pm 24$	$43.7 \pm 22.4$	$9.1 \pm 9.4$	$336 \pm 119$	$165 \pm 66$	$4 \pm 3.8$	$110 \pm 43$	$138 \pm 34$	$3.7 \pm 5$	0	$1.6 \pm 1$	$2.5 \pm 3.3$
<i>Bathyeurystomina</i>	$14 \pm 19$	0	0	0	0	0	0	0	$1 \pm 1.3$	0	$4 \pm 5$	$6 \pm 2.3$
<i>Bathylaimus</i>	0	0	0	0	0	0	0	0	$1.4 \pm 1.8$	0	0	0
<i>Bolbolaimus</i>	$7 \pm 10$	0	$5.3 \pm 7.2$	0	0	0	0	0	0	$2 \pm 2.6$	0	0
<i>Calyptronema</i>	$36.7 \pm 42$	$22.6 \pm 17$	$48 \pm 33$	$79 \pm 37$	$45 \pm 35$	$16 \pm 9$	$23 \pm 17$	$12.5 \pm 6.9$	0	$2 \pm 2.7$	0	$2 \pm 1.8$
<i>Camacolaimus</i>	0	$1.9 \pm 2.6$	0	0	$7 \pm 10$	0	0	0	0	$5.7 \pm 5$	$1.7 \pm 1.5$	$2.4 \pm 1.7$
<i>Campylolaimus</i>	0	$6.9 \pm 6.4$	0	0	0	0	0	0	0	0	0	0
<i>Ceramonema</i>	0	0	0	0	0	0	0	0	0	$14.4 \pm 9$	0	0
<i>Cervonema</i>	$94 \pm 51$	$54.4 \pm 34$	$14 \pm 13.8$	$4.5 \pm 6$	$61 \pm 31$	$15 \pm 13$	$12 \pm 8$	$8.5 \pm 8.5$	$2.5 \pm 2.2$	$4 \pm 5.5$	0	0
<i>Cheironchus</i>	0	0	0	0	0	0	0	0	0	0	$1.6 \pm 2.2$	0

<i>Choanolaimus</i>	0	0	0	0	0	0	0	0	0	4.5±4	0
<i>Choniolaimus</i>	0	0	0	0	0	0	0	0	0	0.6±0.8	0
<i>Chromadora</i>	70±42	12.3±9	64.3±22	44.6±21.5	91±30	0	42±19	12±6.6	0.7±0.9	1.8±2.5	0
<i>Chromadorina</i>	0	0	4±5	6±8	49±34	0	18±13	0	0	1.5±2	0.8±1
<i>Chromadorita</i>	16±12	0	0	0	43±30	0	0	0	13±11.5	42±16.7	33±14
<i>Chromaspirina</i>	0	0	0	0	0	0	0	0	0.7±0.9	0	0
<i>Cobia</i>	0	0	0	0	0	0	0	0	7.7±5.5	0	0
<i>Comesa</i>	0	0	0	0	0	0	0	0	2±3	0	0
<i>Comesoma</i>	9.5±6.5	0	0	0	28±26	0	0	0	0	0	0
<i>Cyatholaimus</i>	15±15.6	0	2.2±2.9	12.8±17	71±50	5.1±5	37±29	24±21	1±1.3	0	0
<i>Dagda</i>	0	16.8±22.6	36.2±31.5	16±14.3	0	0	0	0	0	6±4	0
<i>Daptonema</i>	42±27	60.1±44	12±12.5	22±19	31±25	45±32	0	21±17	67±24	25.5±11.7	31±13
<i>Daptonema sp1</i>	56±22	120±45	36.4±18.3	17.5±15.6	212±123	19±12	74±38	45±12	0	38.4±49	0
<i>Dasyhemooides</i>	0	0	0	0	0	0	0	0	1.6±2.2	3.3±3.1	0
<i>Desmodora</i>	0	0	25.6±28.7	12.9±12.6	0	0	0	0	116±54	108±55	158±46
<i>Desmoscolex</i>	0	9	0	0	0	0	0	0	2.8±2.5	29±36	1.9±2.5
<i>Dichromadora</i>	3.6±5	0	0	6±8	23.9±23.8	8.7±7	45±15	24±19	17±12	81±21	83±25
<i>Eleutherolaimus</i>	0	3.8±5	0	0	0	0	0	0	0	0	0
<i>Endeolophos</i>	0	0	0	0	0	0	0	0	0	6.5±6	0
<i>Enoploides</i>	0	0	0	0	0	0	0	0	12.8±8.5	9.7±9	12.8±10
<i>Eumorpholaimus</i>	0	0	0	0	0	0	0	0	0	6±5	0
<i>Gerlachius</i>	0	0	0	0	0	0	0	0	0	0	0
<i>Halalaimus</i>	2.6±3.5	18.5±11	5.4±7.2	10±9	0	0	11±8	15±16	1±1.4	3.8±3	2.2±1.9
										1.7±2.3	

<i>Halichoanolaimus</i>	3.6±4.9	0	0	0	0	0	0	0	2.7±3.7	5.6±3.7	1±1.4	1.5±1.3
<i>Hypodontolaimus</i>	0	0	0	0	0	0	0	0	0	5.7±5	0	0
<i>Innomonema</i>	0	0	0	0	0	0	0	0	1.4±1.9	9.5±5.5	2.4±2	0
<i>Kraspedonema</i>	0	0	0	0	0	0	0	0	0	1.8±2.5	0	18±16
<i>Latronema</i>	0	0	0	0	0	0	0	0	0	0	0	4±3.3
<i>Leptolaimus</i>	2.6±3.5	9.9±9	0	5.9±8	0	0	0	0	0	0	2.4±2.2	0.8±1.1
<i>Linhomaeus</i>	2.6±3.5	44±44	5.7±5.2	41±15	0	57±32	28±15	70±16	0.9±1.2	15±10	0	2.1±1.9
<i>Marylynia</i>	0	0	0	0	0	0	0	0	1.2±1.6	1.5±2	0	1.1±1.5
<i>Mesacanthion</i>	0	0	0	0	0	0	0	0	0	0	2.3±3	0.7±0.9
<i>Mesacanthoides</i>	0	0	0	0	0	0	0	0	0	0	0	0
<i>Metachromadora</i>	1776±453	2033±530	864±251	1077±185	2082±948	1241±248	2083±380	544±117	3.7±3.3	12±6	0	2±1.8
<i>Metadesmolaimus</i>	0	0	0	0	0	0	0	0	0.9±1.2	0	0	0
<i>Metacyatholaimus</i>	0	0	0	0	0	0	0	0	1.9±1.8	0	8±6	0
<i>Metalinhomoeus</i>	54±42	36±24	183±83	63.5±34.4	10±12	44±19	36±25	50±23	2.3±2.1	63±36	2±1.7	7.5±6.4
<i>Microlaimus</i>	11±7	0	12±9	5.9±8	0	9±8	5±6	3±4	0	0	2±2.8	1.6±2.1
<i>Molgolaimus</i>	0	2±2.6	0	0	0	0	0	0	0	21±29	0	1.3±1.7
<i>Monoposthia</i>	4.7±6	0	0	0	0	0	0	0	206±75	226±113	125±40	91±35
<i>Nannolaimoides</i>	0	0	0	0	0	0	0	0	7±10	0	0	0
<i>Nemanema</i>	10±8	10.2±9	1.8±2.5	12.9±11.8	17±12	0	0	7±6	0	0	0	0
<i>Neochromadora</i>	0	0	0	7±9.3	0	0	0	0	1.7±2	0	1±14	0
<i>Odontophora</i>	134±49	104±58	34.4±15.8	35±29	16±14	8±6	21±22	24±12	5.5±3	7.5±6	5.6±4.4	4±5
<i>Oncholaimellus</i>	7±7.7	18.6±10	0	41±21	1.4±1.9	0	0	0	0.7±0.9	19±22	0	0

<i>Onyx</i>	0	0	3.7±5	0	0	0	0	16±12	32±23	15±7	0.8±1. 1
<i>Oxystomina</i>	0	16.8±19	8.6±6	19.9±11	0	2.5±4	11±7	23±12	0	6±5	3±4 0.8±1. 1
<i>Paracanthonchus</i>	1.7±2.2	0	0	0	5±6.6	0	0	0	0.9±1.2	2±2.6	1±1.5 0
<i>Paracomesoma</i>	47.8±31.6	61±38	50±40	244±112	12±8	13±8	4±5	0	0.9±1.2	2±2	0 1.1±1. 5
<i>Paracyatholaimus</i>	0	0	6.6±6	0	9±8	2.5±4	0	0	2.5±2	0	0 3.4±4. 5
<i>Paradesmodora</i>	0	0	0	0	0	0	0	0	2.6±2	6±5.3	0 0
<i>Paralinhomeus</i>	0	0	2.1±2.9	0	4±5	0	0	0	0	11±10	0 1.1±1. 5
<i>Paramicrolaimus</i>	0	0	0	0	2±3	0	0	0	0.7±1	0	0 0
<i>Paramonohystera</i>	0	0	0	6±8	0	0	0	0	5.5±4	6±5	0.7±0.9 2.5±2. 2
<i>Paraticoma</i>	0	0	0	0	0	0	0	0	3±3.1	0	0
<i>Pareurystomina</i>	0	0	0	0	0	0	0	0	4±3	8±6.4	2.4±2.3 0
<i>Pomponema</i>	0	5.7±7.7	0	0	0	0	0	0	8±5	22±9.9	3.4±2.4 30±15
<i>Praeacanthonchus</i>	8.3±8	21±16	3.1±4.2	203±72	47±30	14±10	71±54	199±86	0	0	0 1.5±1. 3
<i>Prochromadora</i>	0	0	0	0	22±20	0	0	0	0	0	0 0
<i>Prochromadorella</i>	0	0	0	0	0	0	0	0	0.7±1	0	6±3.6 0
<i>Promonhystera</i>	0	0	0	0	0	0	0	0	0	1.6±2	0 0
<i>Prooncholaimus</i>	0	0	0	0	0	0	0	0	0	1.8±2.5	0 0
<i>Pselionema</i>	0	0	0	0	0	0	0	0	3±3.8	5.4±4.8	15±8 2.6±1. 9
<i>Pseudolella</i>	34.5±22	141±22	114.5±40.5	89.6±30. 6	29±22	55±26	71±34	34±16	0	1.9±2.6	0 1.2±1. 7
<i>Pseudonchus</i>	0	0	11.3±15.2	0	0	0	0	0	0	0	0 1.2±1. 7
<i>Pterygonema</i>	0	0	0	0	0	0	0	0	0	3.9±3.6	3.7±3.3 0
<i>Ptycholaimellus</i>	11±14.6	98±46	70.8±31.5	20±11	230±190	72±25	247±81	79±28	0	17.4±15	0 4.2±3

<i>Rhabdocoma</i>	0	0	0	0	0	0	0	1.4±1.8	15±10	0	0
<i>Rhabdodemania</i>	0	0	0	0	0	0	0	0	0	0.6±0.8	0
<i>Rhinema</i>	0	0	0	0	0	0	0	0	7.2±5.3	0	0
<i>Rhips</i>	0	0	0	0	0	0	0	6.9±5	28.5±26.5	1±1.4	3.6±2
<i>Rhynchonema</i>	0	0	0	0	0	0	4±5	0	1.4±1.8	11.5±7.5	13.8±6.6
<i>Sabatieria</i>	268±115	334.7±148.7	223.3±96.4	501±189	935±556	529±272	532±138	748±222	80±65.5	340±202.1	165.5±1.01
<i>Scaptrella</i>	0	0	0	0	0	0	0	3.7±3.7	1.6±2	0	4.7±3.1
<i>Sigmophoranea</i>	0	0	0	0	0	0	0	0	0	0.7±0.9	0
<i>Southerniella</i>	0	0	0	0	0	0	0	3±4	0	0	0
<i>Sphaerolaimus</i>	42±23	60.5±21.8	114±48.6	64±25	180±68	76±35	155±54	213±57	0	0	0.8±1
<i>Spiliphera</i>	0	0	0	0	0	0	0	0	0	0.8±0.9	0
<i>Spilophorella</i>	0	0	0	0	0	0	0	0	2±2.7	10±5	2.2±2.2
<i>Spirinia</i>	2.6±3.5	0	6.5±8.7	9±12	0	0	0	0	11.3±6	5.7±5.3	0
<i>Symplocostoma</i>	0	0	0	0	0	0	0	0	0	0	0
<i>Synonchiella</i>	0	0	0	4±5.3	0	0	0	0.8±1.8	0	0	0.7±0.9
<i>Synonchium</i>	0	0	0	0	0	0	0	0	0	1.1±1.5	0
<i>Terschellingia</i>	434±141	350.7±121.6	743±451.6	1058±42.5	273±127	142±31	144±44	207±91	3.2±4	3.4±3	0
<i>Thalassoalaimus</i>	0	5.8±7.8	3.7±5	11.3±10.4	0	0	0	0	6±8	0	0
<i>Theristus</i>	0	0	0	0	0	0	0	2.6±3.5	0	0	0
<i>Trefusia</i>	0	0	7.5±10	0	0	48±64	0	0	76.3±79	180±106	139±100
<i>Tricoma</i>	0	0	0	0	0	0	0	0	0	3.6±3.7	0
<i>Trileptum</i>	0	0	0	0	0	0	0	0	30.6±14.6	83±87	3.4±4.5
											11±4.6

<i>Triplyloides</i>	10±14	7±9.6	0	19±13.2	0	0	5±6	0	1±1.4	10±7	0	0.6±0.8
<i>Trochamus</i>	0	0	0	0	0	0	0	0	0	1.8±2.5	0	0
<i>Viscosa</i>	65±41	110±56	23.3±14.4	147.7±26	118±40	118±60	80±28	101±26	32.4±12	64±22	6±3.7	19±8
<i>Wieseria</i>	0	0	7.5±10	4±5	0	0	0	0	0	0	0	1.1±1.5
<i>Xyala</i>	0	0	0	0	0	0	0	0	0	1.6±2.2	0	1.2±1.7
Total density	3671±800	3978±591	3054±720	4779±419	4951±1233	2620±499	4310±342	2895±194	786±147	1732±143	907±151	735±70

**Table S4:** SIMPER summarized table of nematode communities, with the genera that most contributed for (dis)similarities (%), **a**) between sites (Navigator, Gambia and Tróia).and **b**) across 4 sampling occasions (winter 19, summer 20, winter 20, summer 21).

**a)**

Sites	Navigator	Gambia	Tróia
Navigator	Average similarity: 64% <i>Metachromadora. Terschellingia. Sabatieria</i>		
Gambia	Average dissimilarity 39% <i>Metachromadora. Terschellingia. Anoplostoma</i>	Average similarity: 67.8% <i>Metachromadora. Sabatieria. Sphaerolaimus</i>	
Tróia	Average similarity: 73% <i>Metachromadora. Sabatieria. Anoplostoma</i>	Average dissimilarity 71% <i>Metachromadora. Sabatieria. Terschellingia</i>	Average similarity: 56.2% <i>Monoposthia. Sabatieria. Desmodora</i>

b)

Sampling occasions	Winter 19	Summer 20	Winter 20	Summer 21
Winter 19	Average similarity: 56.7% <i>Metachromadora</i> . <i>Sabatieria</i> . <i>Monoposthia</i>			
Summer 20	Average dissimilarity 45% <i>Sabatieria</i> . <i>Metachromadora</i> . <i>Terschellingia</i>	Average similarity: 61.6% <i>Metachromadora</i> . <i>Sabatieria</i> . <i>Terschellingia</i>		
Winter 20	Average similarity: 43% <i>Metachromadora</i> . <i>Sabatieria</i> . <i>Anoplostoma</i>	Average dissimilarity 42% <i>Metachromadora</i> . <i>Sabatieria</i> . <i>Anoplostoma</i>	Average similarity: 64.5 % <i>Metachromadora</i> . <i>Sabatieria</i> . <i>Anoplostoma</i>	
Summer 21	Average dissimilarity 43% <i>Sabatieria</i> . <i>Metachromadora</i> . <i>Anoplostoma</i>	Average dissimilarity 42% <i>Sabatieria</i> . <i>Metachromadora</i> . <i>Anoplostoma</i>	Average dissimilarity 39% <i>Sabatieria</i> . <i>Metachromadora</i> . <i>Terschellingia</i>	Average similarity: 67% <i>Sabatieria</i> . <i>Metachromadora</i> . <i>Anoplostoma</i>



**CHAPTER 6 - GENERAL DISCUSSION**

## 6.1 General Discussion

In **chapter 2**, the spatial diversity patterns of bacterial and nematode communities were investigated in response to different sediment conditions in Sado estuary. Both communities showed a strong potential as ecological indicators describing the habitat condition. At each sampling site, nematode assemblages and bacterial communities had distinct compositions and ecological roles according to the physical and chemical composition of the sediments. The OM content of the muddy sediments at “Tróia” and “Moinho” sites was correlated with the predominance of anaerobic bacterial groups, while the sandy and low-organic sediments of “Navigator” site were correlated with aerobic bacterial groups, associated with mineralization processes (Jessen et al., 2017). The high density of the nematode genera *Metachromadora*, *Sabatieria*, and *Terschellingia* demonstrated a strong affinity for the hypoxic, organic-rich sediments of “Tróia” and “Moinho”. The co-occurrence of *Terschellingia* and *Cyanobacteria* in the Navigator sediments suggests a potential link between bacterial composition and the feeding preferences of nematodes (selective deposit feeders) and affinity for cyanobacteria biofilms (Derycke et al., 2016; D’Hondt et al., 2018). *Cyanobacteria* is recognized as an indicator group of stressed coastal environments (Kolda et al., 2020), while *Terschellingia* is predominantly associated with disturbed habitats (Alves et al., 2013; Vafeiadou et al., 2013; Sahraean et al., 2017). Therefore, the co-occurrence of these taxa could be explained by the influence of the surrounding anthropogenic activities at the “Navigator” site.

The diversity patterns of both communities were **strongly driven** by **OM**, proving to be a structuring factor shaping the communities’ composition. Despite the high degree of congruence in the responses of nematode and bacterial communities, both exhibited different distribution patterns. Nematodes were more sensitive to the variation of small-scale factors (**within sites**), while bacteria were more consistent, revealing a broader-scale variation (**between sites**). The high responsiveness of nematode communities at both **micro-** and **mesoscales** is a key factor influencing their distribution (Adão et al. 2009, Materatski et al. 2015, Branco et al., 2018). Various micro-habitats are created in response to small patches of food, physical-chemical disturbances, and biotic interactions (Galluci et al., 2008; Giere, 2009; Moens and Benninger et al., 2018), which in turn shape the distribution patterns of bacteria. However, our understanding of these communities’ dynamics in estuarine environments remains limited, largely due to functional redundancy. The strong correlation between community composition and environmental variables suggested that monitoring these communities provides valuable

insights into the ecological status of intertidal sediments, particularly in areas subjected to human impact. Moreover, the occurrence of these communities raises questions about their roles in trophic pathways within the benthic food webs. The similar responses of bacterial and nematode communities to sediment conditions suggest potential interactions between them. Therefore, changes at the community level may influence the base of the benthic food web, impacting higher trophic levels and the overall functioning of the ecosystem (**bottom-up effect**).

To fully understand the implications of these findings, it was important to study the spatial and temporal variability of bacterial communities and nematode assemblages separately under different environmental conditions (**Chapters 3 and 5**). The hypotheses proposed that both bacterial and nematode communities would exhibit significant spatial and temporal variation, with nematodes showing stronger variations due to their high sensitivity to small-scale environmental fluctuations. The results obtained partially supported this hypothesis: nematode assemblages exhibited more complex interactions between spatial and temporal factors than bacterial communities.

The **spatial variability** of both communities followed **similar distribution patterns**, that strongly correlated with the environmental variables OM, CT, gravel, sand, chla\_phaeo, and CaCO<sub>3</sub>. Nematode and bacterial communities from “Tróia” were clearly distinct in abundance and diversity compared to those at “Gambia” and “Navigator”, reflecting distinct site-specific responses to sediment composition, metabolic pathways, and trophic diversity. As in **Chapter 2**, muddy sediments (Navigator and Gambia) had lower nematode diversity and bacterial communities dominated by anaerobic, hypoxia-tolerant groups (e.g. *Desulfobacterota* phylum). Whereas in the “Tróia” sandy sediments, nematode communities were less abundant but highly diverse, and the bacterial communities were dominated by aerobic OM remineralizing taxa (e.g. *Flavobacteriaceae*, *Saprospiraceae* and *Kiloniellaceae*) (**Chapters 3 and 5**). Unlike nematode assemblages, bacterial communities showed no significant **temporal variations** (**Chapter 3**), highlighting their adaptability and resilience to short-term environmental changes (Böer et al., 2009; Wasmund et al., 2017; Aguilar et al., 2020). In estuaries, stochastic events are common and influence the spatial OM inputs and nutrient availability, which explains the spatial-temporal small-scale variability of the nematode assemblages (Materaski et al., 2015; Branco et al., 2018; Zheng et al., 2020; Xu et al., 2022) (**Chapter 5**).

These findings strengthen the potential of benthic bacterial and nematode communities as **indicators of ecological status** in estuarine environments. Their different **response scales** across spatial and temporal gradients not only reflected their

role as mediators of energy flow and nutrient cycling but also showed the high sensitivity of nematode assemblages to sediment characteristics and environmental conditions. Moreover, the high correlation with specific bacterial taxa and environmental variables, particularly in the context of metal pollution and organic enrichment, suggested that bacterial communities can provide valuable insights into the **ecological status** of sediments and the **metabolic pathways** of active communities involved in the biogeochemical processes.

**Benthic food webs** in the Sado estuary were studied by applying **isotopic metrics** to analyze different aspects of benthic food web complexity in a spatial-temporal context (**Chapter 4**). This novel approach made it possible to visualize complex information associated with trophic compositions and evaluate the influence of spatially and temporally regulated abiotic factors on the overall benthic food webs. By combining isotopic metrics with univariate and multivariate analyses, it was possible to identify key attributes that respond most to the environmental changes, offering a more comprehensive understanding of food web dynamics. To investigate the benthic food web dynamics, natural isotopic ratios ( $\delta^{13}\text{C}$  and  $\delta^{15}\text{N}$ ) of macrobenthic organisms and their food sources were measured to construct food web topologies at the same sites and sampling occasions studied in **Chapters 3 and 5**.

Communities in sites with high OM input and hypoxic conditions (e.g. Gambia and Navigator) were expected to have limited food source diversity, resulting in narrower trophic niches and reduced trophic diversity, exhibiting a narrower trophic niche size (*Hypothesis 1, Chapter 4*). A clear spatial pattern was observed for the food webs of these three sampling sites, due to the increased **primary production** (chl<sub>a</sub>) and **quantity/quality of OM** (observed in chl<sub>a</sub>\_phaeo ratios), confirming *Hypothesis 1*. Navigator and Gambia sampling sites, characterized by **higher organic inputs** and **lower-quality OM**, exhibited **simpler food webs**. While Troia which is located inside protected area, with **high quality OM** had the most **complex food web** characterized by high diversity of specialist consumers that used the available resources more efficiently.

The pigments quantification, **chlorophyll a** (chl<sub>a</sub>) and **phaeopigments** (phaeo), were relevant proxies of primary production that directly influenced communities' diversity, functional pathways, and trophic interactions (**Chapter 3, 4 and 5**). During these studies, an interesting event was observed in the Gambia sampling site, with an abrupt increase of chl<sub>a</sub> (5 orders of magnitude), phaeo (10 orders of magnitude) during the **winter 2019 and 2020** (**Chapter 4**). These events were consistent with the occurrence of the *Halieaceae* family, which was abundant in the Gambia bacterial

communities (**Chapter 3**). This gammaproteobacterial group, known to play an important role in response to phytoplankton blooms, improves organic matter degradation (Francis et al., 2021). Simultaneously, nematode assemblages in Gambia became more similar to those in Tróia, both in **trophic diversity** and **richness**, and increased significantly during these events, suggesting efficient use of available resources (**Chapter 5**). These findings revealed important trophic shifts, resulting in increased energy transfer to higher trophic levels and **increased trophic interactions** in the Gambia food web (observed in **Chapter 4**).

Based on the similarity between diversity patterns of benthic communities and trophic compositions, it was expected that the food webs in Navigator and Gambia would show a greater similarity, reflected in the overlap metrics (*Hypothesis 2, Chapter 4*). However, contrary to expectations, probably due to the previous events in Gambia communities, greater overlap was observed between Gambia and Tróia food webs, revealing an unexpected pattern of higher similarity. **Similarity metrics** were able to distinguish **different resource use** between similar trophic structures (Navigator and Gambia), highlighting structuring trophic shifts in Gambia food webs (new carnivores and deposit-feeders), which increased their complexity.

In a **temporal perspective**, differences were expected as seasonal and interannual variations are known to influence diversity patterns and trophic interactions, strongly influenced by the availability and diversity of food sources (Campanyà-Llovet et al., 2017; Donázar-Aramendía et al., 2019; Szczepanek et al., 2021). Therefore, it was predicted that **colder periods**, characterized by **reduced primary productivity** and increased **terrestrial and freshwater OM inputs**, would result in **less diverse** benthic communities with fewer top predators and reduced trophic interactions. The sampling design of these studies could not capture temporal patterns as clearly as spatial patterns. Although significant differences were reported between sampling occasions in the diversity patterns of nematode assemblages and macrobenthic food web structure, reflected in the metrics maximum trophic position and percentage of carnivores and omnivores. Increases in OM inputs to the system are not always congruent with the seasonal variations, as they can also occur on a microscale (Moens & Beninger, 2018; Young et al., 2021), or they can be linked to the spatially heterogeneous nature of the estuary itself. This suggests that factors beyond seasonal changes, such as anthropogenic influences on local OM inputs, may have a stronger influence on community distribution patterns, directly affecting communities' composition and benthic food web structure (Campanyà-Llovet et al., 2017).

Initially, it was also expected that **warmer periods** would **promote higher primary productivity**, while colder periods would lead to a decrease. It was expected that similar seasons would reflect similar food sources availability, leading to a higher similarity of the food webs during the same seasons (winter 19/winter 20 and summer 20/ summer 21), than among different seasons (*Hypothesis 4*). However, contrary to the hypothesis, significant differences were found for maximum trophic position and the percentage of carnivores and omnivores between **winter 19** and other sampling occasions, regardless of the site. Over time, trophic diversity increases in the “Navigator” and “Gambia” food webs, particularly due to the emergence of new herbivores and carnivores. Similar trends were seen in the diversity patterns of nematode assemblages. The diversity and functional metrics showed significant differences between **winter 2019** and **summer 2021**, mostly in “Navigator” and “Gambia” assemblages, indicating increased diversity over time. More complex food webs exhibit better responses to seasonal shifts, “Tróia’s” food web, the least disturbed site, had the lowest similarity between seasons (summers vs winters), reflecting clear **temporal shifts in availability** and **diversity of food sources**. When compared to other sites, “Tróia” provides favorable conditions for specialist genera to thrive,

Overall, the isotopic and diversity metrics combined with univariate and multivariate analyses allowed for the assessment of how the bottom-up processes can modulate the marine benthic food webs.

## 6.2 Conclusions

This study introduces a multidisciplinary and innovative approach to assess benthic ecosystem functioning by integrating benthic community diversity patterns to better understand sediment trophic conditions and their impact on energy pathways. The combination of morphological and metagenomic approaches, together with stable isotope analysis, strongly supports bacterial and nematode communities as **powerful ecological indicators** capable of **capturing the dynamics of macrobenthic food webs** of the Sado estuary. These indicators provide valuable insight into the structure of benthic food webs, particularly correlated with **OM** and **granulometry**, which are the main drivers of functional roles and carbon fluxes within benthic ecosystems.

The integrated assessment of **bottom-up trophic interactions** and **food web complexity** enabled the identification of **trophic** and **ecological indicators** that reflect ecosystem functioning and metabolic pathways (biogeochemical processes). By linking **communities' diversity** and **food web dynamics**, this work contributes significantly to the development of monitoring strategies supporting the **Descriptors 1 (biodiversity)**,

**4 (food webs), and 6 (seafloor integrity) of the Marine Strategy Framework Directive (MSFD),** while providing practical tools for guiding **habitat recovery** and sustainable **Blue Economy** activities.

Despite advances in environmental genomics, traditional morphological identification of nematodes is still widely used, despite it being time-consuming and only relying on expert taxonomic knowledge (Moens & Beninger, 2018). The integration of molecular methods such as **16S** and **18S rRNA gene** amplicon-based metagenomics can significantly improve the compatibility between datasets and support cross-domain assessments of species co-occurrence and functional traits (Nawaz et al 2018; Mahamoud et al., 2018; Stoeck et al 2018).

Further research should combine **metagenomics** with **metatranscriptomics**, enabling both taxonomic resolution and functional roles of these communities, while uncovering how their complex interactions (microbiome and host-microbe) regulate their activity (Ruppert et al., 2019). These approaches can provide not only the assessment of biodiversity patterns and functional responses to stressors, but also a complex network of microbial activity related to biogeochemical cycles, **tracking real-time** microbial processes such as nitrogen fixation, carbon sequestration, and sulphur metabolism, crucial for estuarine ecosystem functioning. This would also improve our ability to detect and predict ecological responses to anthropogenic pressures (e.g. blue economy activities) and climate related stressors such as ocean warming, acidification, and deoxygenation (Laiolo et al., 2024).

Furthermore, to enhance the capture of **temporal variability**, other sampling strategies could reveal currently undetected seasonal or short-term shifts in bacterial communities' distribution patterns. Based on the **isotopic models developed** for macrobenthic organisms, the integration of meiofauna (nematodes) into food web models is a crucial next step. Their inclusion will enhance the understanding of **omnivory levels and trophic connectivity**, bridging the gap between microfauna and macrofauna, and leading to a more complete representation of ecosystem functioning.

Overall, this approach represents a promising way to develop predictive and integrative **monitoring frameworks** based on **ecological indicators** for assessing **GES** within the **MSFD**. These indicators provide a solid base for ecosystem **restoration strategies** and sustainable **blue economy** activities, and support **stakeholder engagement** for the restoration and long-term management of coastal habitats.

### 6.3 References

Adão, H., Alves, A.S., Patrício, J., et al., (2009). Spatial distribution of subtidal Nematoda communities along the salinity gradient in southern European estuaries. *Acta Oecol.* 35, 287–300. <https://doi.org/10.1016/j.actao.2008.11.007>.

Aguilar P. & Sommaruga R., 2020. The balance between deterministic and stochastic processes in structuring lake bacterioplankton community over time. *Molecular Ecology*.2020;29:3117–3130. <https://doi.org/10.1111/mec.15538>

Alves, A.S.S., Adão, H., Ferrero, T.J.J., et al., 2013. Benthic meiofauna as indicator of ecological changes in estuarine ecosystems: the use of nematodes in ecological quality assessment. *Ecol. Indicat.* 24, 462–475. <https://doi.org/10.1016/J.ECOLIND.2012.07.013>

Böer I. S, Hedtkamp S. I. C, Beusekom J. E. E., Fuhrman J. A, Boetius A., Ramette A., Time- and sediment depth-related variations in bacterial diversity and community structure in subtidal sands, *The ISME Journal*, Volume 3, Issue 7, July 2009, Pages 780–791, <https://doi.org/10.1038/ismej.2009.29>

Branco, J., Pedro, S., Alves, A.S., Ribeiro, C., Materatski, P., Pires, R., Caçador, I., Adão, H., 2018. Natural recovery of *Zostera noltii* seagrass beds and benthic nematode assemblage responses to physical disturbance caused by traditional harvesting activities. *J. Exp. Mar. Biol. Ecol.* 502, 191–202. <https://doi.org/10.1016/J.JEMBE.2017.03.003>

Campanyà-Llovet N., Snelgrove V.R. P., Parrish C. C., 2017. Rethinking the importance of food quality in marine benthic food webs. *Progress in Oceanography*, 156,240-251. <https://doi.org/10.1016/j.pocean.2017.07.006>

D'Hondt, A.S., Stock, W., Blommaert, L., Moens, T., Sabbe, K., 2018. Nematodes stimulate biomass accumulation in a multispecies diatom biofilm. *Mar. Environ. Res.* 140, 78–89. <https://doi.org/10.1016/j.marenvres.2018.06.005>

Derycke, S., De Meester, N., Rigaux, A., Creer, S., Bik, H., Thomas, W.K., Moens, T., 2016. Coexisting cryptic species of the *Litoditis marina* complex (Nematoda) show differential resource use and have distinct microbiomes with high intraspecific variability. *Mol. Ecol.* 25, 2093–2110. <https://doi.org/10.1111/mec.13597>

Donázar-Aramendía, Sánchez-Moyano, J.E., García-Asencio, I., Miró, J. M., Megina, C., García-Gómez, J.C., (2019). Human pressures on two estuaries of the iberian peninsula are reflected in food web structure. *Scientific Reports* (2019) 9:11495. <https://doi.org/10.1038/s41598-019-47793-2>.

Francis, B., Urich, T., Mikolasch, A. et al. North Sea spring bloom-associated *Gammaproteobacteria* fill diverse heterotrophic niches. *Environmental Microbiome* 16, 15 (2021). <https://doi.org/10.1186/s40793-021-00385-y>

Gallucci F., Moens T., Vanreusel A., Fonseca G., 2008. Active colonization of disturbed sediments by deep-sea nematodes: evidence for the patch mosaic model. *Mar Ecol Prog Ser* 367:173–183

Giere, O. (2009) *Meiobenthology: the microscopic motile fauna of aquatic sediments*. Springer Science & Business Media, Berlin.

Jessen, G.L., Lichtschlag, A., Ramette, A., Pantoja, S., Rossel, P.E., Schubert, C.J., Struck, U., Boetius, A., 2017. Hypoxia causes preservation of labile organic matter and changes seafloor microbial community composition (Black Sea). *Sci. Adv.* 3, e1601897. <https://doi.org/10.1126/sciadv.1601897>

Kolda, A., Ljubešić, Z., Gavrilović, A., Jug-Dujaković, J., Pikelj, K., Kapetanović, D., 2020. Metabarcoding Cyanobacteria in coastal waters and sediment in central and southern Adriatic Sea. *hrcak.srce.hr* 79, 157–169. <https://doi.org/10.37427/botcro-2020-021>.

Laiolo E, Alam I, Uludag M, Jamil T, Agusti S, Gojobori T, Acinas SG, Gasol JM, Duarte CM. 2024. Metagenomic probing toward an atlas of the taxonomic and metabolic foundations of the global ocean genome. *Front Sci* (2024) 1:1038696. doi: 10.3389/fsci.2023.1038696

Mahamoud A., Lyautey E., Bonnneau C., Dabrin A., Pesce S., 2018. Environmental concentrations of Copper, alone or in mixture with Arsenic, can impact river sediment microbial community structure and functions. *Sec. Microbiotechnology*, Volume 9 – 2018. <https://doi.org/10.3389/fmicb.2018.01852>

Materatski, P., Vafeiadou, A.-M.M., Ribeiro, R., Moens, T., Adão, H., 2015. A comparative analysis of benthic nematode assemblages from *Zostera noltii* beds

before and after a major vegetation collapse. *Estuar. Coast Shelf Sci.* 167, 256–268. <https://doi.org/10.1016/j.ecss.2015.07.001>

Moens, T., Bouillon, S., Gallucci, F., 2005. Dual stable isotope abundances unravel trophic position of estuarine nematodes. *J. Mar. Biol. Assoc. U. K.* 85, 1401–1407. <https://doi.org/10.1017/S0025315405012580>

Nawaz A., Purahong W., Lehmann R., Herrmann M., Totsche K.U., Küsel K., Wubet T., Buscot F., 2018. First insights into the living groundwater mycobiome of the terrestrial biogeosphere *Water Res.*, 145, pp. 50-61, <https://doi.org/10.1016/j.watres.2018.07.067>

Ruppert M.K., Kline J.R., Rahman Md. S., Past, present, and future perspectives of environmental DNA (eDNA) metabarcoding: A systematic review in methods, monitoring, and applications of global eDNA. *Global Ecology and Conservation* 17 (2019) e00547. <https://doi.org/10.1016/j.gecco.2019.e00547>

Sahraean, N., Bezerra, T.C., Ejlali Khanaghah, K., Mosallanejad, H., Ranst, V.E., Moens, T., 2017. Effects of pollution on nematode assemblage structure and diversity on beaches of the northern Persian Gulf. *Hydrobiologia* 799, 349–369. <https://doi.org/10.1007/s10750-017-3234-z>.

Stoeck T., Frühe L., Forster D., Cordier T., Martins C.I., Pawlowski J., 2018. Environmental DNA metabarcoding of benthic bacterial communities indicates the benthic footprint of salmon aquaculture *Mar. Pollut. Bull.*, 127, pp. 139-149

Szczepanek, M., Silberberger, M.J., Koziorowska-Makuch, K., Nobili, E., Kedra, M., 2021. The response of coastal macrobenthic food-web structure to seasonal and regional variability in organic matter properties. *Ecol. Ind.* 132 (2021), 108326 <https://doi.org/10.1016/j.ecolind.2021.108326>.

Vafeiadou, A.-M.M., Materatski, P., Adão, H., De Troch, M., Moens, T., 2013. Food sources of macrobenthos in an estuarine seagrass habitat (*Zostera noltii*) as revealed by dual stable isotope signatures. *Mar. Biol.* 160, 2517–2523. <https://doi.org/10.1007/s00227-013-2238-0>.

Vieira, S., Maurer A-F., Dias C.B., Neves J., Martins M., Lobo-Arteaga J., Adão H., Sroczyńska K., (2024a). “Food web attributes to assess spatial–temporal

dynamics in estuarine benthic ecosystem", Ecological Indicators, Volume 166, 2024, 112243. <https://doi.org/10.1016/j.ecolind.2024.112243>

Wasmund K., Mußmann M., & Loy A., 2017. The life sulfuric: microbial ecology of sulfur cycling in marine sediments. Environmental Microbiology Reports 9(4), 323–344, doi:10.1111/1758-2229.12538

Xu, W., Shin, K.S.P., Sun, J., 2022. Organic Enrichment Induces Shifts in the Trophic Position of Infauna in a Subtropical Benthic Food Web, Hong Kong. *Front. Mar. Sci.* 9, | 937477. <https://doi.org/10.3389/fmars.2022.937477>

Young, M., Howe, E., O'Rear, T., Berridge, K., Moyle, P., 2021. Food Web Fuel Differs Across Habitats and Seasons of a Tidal Freshwater Estuary. *Estuar. Coasts* 44, 286–301. <https://doi.org/10.1007/s12237-020-00762-9>.

Zheng, X., Como, S., Huang, L., Magni, P., 2020. Temporal Changes of a Food Web Structure Driven by Different Primary Producers in a Subtropical Eutrophic Lagoon. *Mar. Environ. Res.* 161, 105128  
<https://doi.org/10.1016/j.marenvres.2020.105128>.